UNIVERSITAT POLITÈCNICA DE VALÈNCIA

FINAL MASTER THESIS

Master's Degree in Geomatics and Geo-information

GNSS Open Service Case Study: Development of SW Tools for Assessing GPS and GALILEO Positioning Performances by Means of Post-Processing Single-Frequency Pseudorange Observations

A contribution to available open source tools

Author: **Pablo Pinto Santos**

pabpinsa@topo.upv.es

ESCUELA TÉCNICA SUPERIOR DE INGENIERÍA GEODÉSICA CARTOGRÁFICA Y TOPOGRÁFICA

Mentor: **Ángel Esteban Martín Furones**

aemartin@upvnet.upv.es

Valencia, July of 2019

State of commitment:

The presented document has been fully edited by the author; not being delivered as a previous academical work. All other external items have been properly referenced either on the text or in the bibliography section.

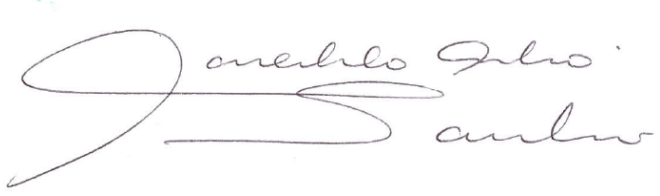

Sin duda alguna este trabajo es la historia de un fracaso y un éxito. Un fracaso, porque me acuerdo perfectamente de que al terminar mi trabajo de final de grado de 134 páginas, allá en el 2016, me prometí que no me volvería a castigar de semejante manera. Con unas orgullosas 163 razones puedo concluir que siempre incumplo este tipo de promesas. Pero no puedo evitar sentirme orgulloso al mismo tiempo y considerar este trabajo también un éxito.

Mañana justo se cumplirán dos años desde que empecé a trabajar como ingeniero en Madrid, y por decirlo de la manera más correcta posible, no es que haya sido precisamente de mi particular gozo (al menos de manera global y relativa). Esto se aplica especialmente a compaginar el trabajo con un máster. Ya las cosas iban justas solo teniendo una asignatura en el primer semestre, no me quería ni imaginar como sería con el trabajo final. No me equivocaba, trabajar 40 horas semanales y dedicarte hacer lo mismo otras 22 más es… bueno, hacerlo durante 1 añito y me decís que tal ;)

Nunca he presumido de conocerme a mi mismo lo suficientemente bien -de hecho, seguramente ahora mismo conozca mejor la teoría de GNSS- pero si que tengo clara una cosa y es que yo saco lo mejor de mi cuando me empleo en algo que me apasiona, hasta el punto en el que no puedo hacer otra cosa (deberíais verme hacer algo que detesto o me aburre). Por lo que tuve que añadir esa pizca de "pasión" a este trabajo, ese ingrediente común que me acompañó y me motivó a estudiar Geomática y Topografía. Es entonces cuando decidí que había que hacer algo al respecto. Es entonces cuando decidí que nada me haría más feliz que mi trabajo tuviera algún tipo de trascendencia. Y es entonces cuando decidí que mi herramienta GNSS sería publicada de forma abierta para que otras personas pudieran aprovecharlo. Sinceramente creo que esto ha sido el corazón del éxito del que tan orgulloso me siento hoy… y también la razón de que se me haya ido la pinza y haya hecho un código yo solito de casi 13K líneas.

¿Y a quién agradezco este resultado? Por supuesto a mi familia por apoyarme y aconsejarme tan sabiamente durante el proceso: "Acaba esto antes de ponerte a otra cosa" me decían mis padres, posiblemente esta frase es mi salvación de que mis ambiciones me conduzcan del relativo orden al más inmediato caos. A mi hermano, porque existe este mutuo acuerdo no escrito en que yo aguante sus tonterías y él la mías, es sencillamente perfecto. Mención de honor para mi tutor, Ángel que ha aguantado mis correos kilométricos y hemos compartido la esperada revelación de que, a día de hoy, preferimos ir en un coche autónomo controlado por GPS que por GALILEO :) (aunque yo no me montaría en ninguno de los dos y él seguramente tampoco). Agradecer también a los profesores del máster y su insistencia en desarrollar aplicaciones con una orientación al usuario, porque esto ha contribuido en gran parte a la pizca de "pasión" que os estaba contando. Y gracias a mis personas más cercanas de siempre: Alexey, Pepe, Lluis, Sol, Reda, compis de GMV (y sus consejos para que GALILEO funcione) y a los que me estoy dejando por el camino.

¿Y después de esto qué? Es invertible preguntárselo. Pero acabo de entender que es completamente normal responder con un "no lo sé". La ciencia siempre mantiene desconocidas las respuestas a sus grandes preguntas. Parece que esta es una de ellas. Los últimos acontecimientos me han demostrado que hay que estar listo para el fracaso y que el futuro es caprichoso e incierto. Así que será mejor que disfrutemos del proceso, porque será lo último que recordemos al final del camino. "Busca lo que es relevante, no lo que es fácil o conveniente", esta frase de Jordan B. Peterson no puede venir mejor para el caso. Tengo la sensación de que se cierra una etapa y comienza otra nueva con una incertidumbre cuanto menos atractiva. No sé exactamente que vendrá después de esto, pero no será más de lo mismo…

Table of Contents

List of Figures

List of Tables

Abstract

English

Nowadays, as the number of GNSS services are increasing, it is necessary to study and evaluate with real data the enhanced capabilities which these positioning products can provide, and how they are evolving compared with their legacy services and its competitors.

Among the emerging positioning services, it is noteworthy Europe's GALILEO system, which is close to reach its full operational capability, and is willing to fulfill competitive user level performances which can be used through its open service signals: E1, E5a and E5b. On the legacy side, the most remarkable constellation is USA's GPS, which has been achieving a positioning standard service with the C/A signal and a precise positioning service for military purposes with the P signal. In addition, GPS evolutions will provide a civilian service through more robust signals, such as the L5.

The objective of this work is to compare open positioning services from GPS and GALILEO constellations by analyzing their accuracy and integrity performances obtained from a pre-planned campaign, taking as reference-data the IGS station network. The positioning methodology to be used is post-processing single-frequency pseudorange observations in static mode.

For committing this purpose, the main workload is focused on developing a configurable and flexible SW tool which is able to batch the pseudorange observations provided by the spatial frame of the GPS and GALILEO satellites, in order to estimate the receiver's position by means of a Least Squares routine. Lately, these data will be inputted in other analysis tools, which will also be developed in the framework of this project, in order to summarize and display the obtained performances. Consequently, and supported by the obtained results, the conclusions regarding the evolution of the studied services will be drawn.

Castellano

Actualmente, mientras el número de servicios GNSS disponibles aumenta, resulta necesario evaluar con datos reales las mejoras que ofrecen los nuevos productos de posicionamiento, y cuál es su desempeño y evolución respecto de sus servicios antecesores y el de sus competidores.

Entre los servicios de posicionamiento emergentes, resulta de especial interés el proporcionado por la constelación Europea de GALILEO, la cual está cerca de alcanzar su completa capacidad operacional, y que resulta prometedora en cuanto a sus requisitos de prestaciones a nivel usuario, que pueden obtenerse mediante el uso de las señales de su servicio abierto: E1, E5a y E5b. De entre los sistemas ya existentes, el más destacado es el proporcionado por la constelación Estadounidense de GPS, el cual ha estado permitiendo con la señal C/A un servicio de posicionamiento estándar y un servicio de posicionamiento preciso con la seña P para fines militares. Adicionalmente las evoluciones del sistema GPS planean transmitir un servicio civil con señales más robustas, como puede ser la L5.

El objetivo de este trabajo es comparar los servicios abiertos de posicionamiento de las constelaciones de GPS y GALILEO, mediante el análisis de sus prestaciones de precisión e integridad obtenidas de una campaña de observación, dónde los datos de referencia a usar son la red de estaciones del IGS. La metodología de posicionamiento a implementar es el post-procesado de observables de pseudo-rango mono-frecuencia en modo estático.

Para alcanzar este objetivo, el esfuerzo principal estará enfocado en el desarrollo de una herramienta SW totalmente configurable por el usuario, que sea capaz de procesar los observables de pseudorango

proporcionados por el marco de referencia espacial que forman los satélites de GPS y GALILEO, para posteriormente obtener las posiciones del receptor por medio de un algoritmo de estimación por mínimos cuadrados. Los resultados que se obtengan de este procesamiento serán transmitidos a otras herramientas de análisis, las cuales se desarrollarán también en el marco de este proyecto, con la finalidad de resumir y presentar de manera gráfica las prestaciones obtenidas de la campaña. Finalmente, con el soporte de estos resultados, se expondrán las conclusiones sobre el desempeño y la evolución de los servicios anteriormente comentados.

Valencià

Actualment, mentre el nombre de serveis GNSS disponibles augmenta, cal avaluar amb dades reals les millores que ofereixen els nous productes de posicionament, i quin és el seu acompliment i evolució respecte dels seus serveis antecessors i el dels seus competidors.

Entre els serveis de posicionament emergents, resulta d'especial interès el proporcionat per la constel·lació Europea de GALILEO, la qual està a prop d'arribar a la seva completa capacitat operacional, i que resulta prometedora quant als seus requisits de prestacions a nivell usuari, que poden obtenir-se mitjançant l'ús dels senyals del seu servei obert: E1, E5a i E5b. D'entre els sistemes ja existents, el més destacat és el proporcionat per la constel·lació Nord-americana de GPS, el qual ha estat permetent amb el senyal C / A un servei de posicionament estàndard i un servei de posicionament precís amb el senyal P per a fins militars. A més a les evolucions del sistema GPS planegen transmetre un servei civil amb senyals més robustes, com pot ser la L5.

L'objectiu d'aquest treball és comparar els serveis oberts de posicionament de les constel·lacions de GPS i GALILEO, mitjançant l'anàlisi de les seves prestacions de precisió i integritat obtingudes d'una campanya d'observació, on les dades de referència a utilitzar són la xarxa d'estacions del IGS. La metodologia de posicionament a implementar és el post-processat d'observables de pseudo-rang mono-freqüència en manera estàtica.

Per assolir aquest objectiu, l'esforç principal estarà enfocat en el desenvolupament d'una eina SW totalment configura-ble per l'usuari, que sigui capaç de processar els observables de pseudo-rang proporcionats pel marc de referència espacial que formen els satèl·lits de GPS i GALILEO, per posteriorment obtenir les posicions del receptor per mitjà d'un algoritme d'estimació per mínims quadrats. Els resultats que s'obtinguin d'aquest processament seran transmesos a altres eines d'anàlisi, les quals es desenvoluparan també en el marc d'aquest projecte, amb la finalitat de resumir i presentar de manera gràfica les prestacions obtingudes de la campanya. Finalment, amb el suport d'aquests resultats, s'exposaran les conclusions sobre l'acompliment i l'evolució dels serveis anteriorment comentats.

Chapter 1: Introduction

1 Introduction

The current document presents the memorandum of the Final Master's Degree Thesis in Geomatics and Geo-information belonging to the student Pablo Pinto Santos of the Superior Technical School in Geodesy, Cartography and Land Surveying Engineering (ETSIGCT) of the Polytechnic University of Valencia (UPV). The thesis has been mentored by Professor Ángel Esteban Martín Furones, belonging to the Department of Cartography, Geodesy and Photogrammetry Engineering of the UPV.

The memorandum is divided in 8 chapters where each contains a major aspect e.g. methodology, analysis, references, conclusions etc. The chapters are not independent, but they maintain a relation. At the beginning of each chapter, a general contextualization will be detailed in order to enclose this work as a whole.

This first chapter is devoted to introduce the master thesis conducted by the student, its scope/motivation and its main objectives to be achieved; as well as to provide a document outline which summarizes the project phases.

1.1 Thesis Scope

This master thesis is under the scope of Geomatics engineering. Geomatics involves all the disciplines which deal with data subjected to be geo-referenced by applying new information technologies. It could be said that geo-positioning is the common feature which determines the quality of the geospatial information. In other words, location determination is at stake when enabling geo-information applications such as GIS, mapping or surveying data collection.

Traditionally, coordinate determination was performed by land surveying techniques thanks to the local reference frames supported by the nations. However, with the raise of space exploration, other positioning methods were born. This is the case of Global Navigation Satellite Systems (GNSS) which provide global and continuous navigation services to the users. Nowadays, GNSS has practically replaced classical positioning methods and is the main technology used for geo-referencing data, either by direct methods i.e. GNSS surveying antenna; or by indirect means e.g. GNSS locates a sensor which gathers metric data.

According to the master's disciplines, this master thesis will be focused in the Spatial Geodesy field. More specifically, Geodesy is the science which is devoted to determining the earth's shape and the position of its nearby objects. The "spatial" word is added for indicating that these purposes are achieved by space-based techniques. Currently, there are several spatial geodesy techniques but, GNSS is indisputably among the most relevant due to its application, economic and social outreach.

GNSS State of the Art

The GNSS field has suffered from an exponential growth in the last years. From technological solutions based on single-service and single-frequency (with intended civilian positioning degradation by the system e.g. GPS Anti-Spoofing), to the current multi-GNSS and multi-frequency implementations, thanks to the latest global systems i.e.: GALILEO and BEIDOU; and the modernization of the existing ones i.e.: GPS and GLONASS.

Unquestionably, the tendency in the GNSS sector is focused on developing multi-GNSS/frequency products since they allow for higher accuracy services which, not only fulfill traditional professional applications, but they also have allocated their benefits in the mass market. For instance: driverless cars or augmented reality products (see GNSS User Technology Report: [BR.13]).

On the professional side, non-absolute techniques such as Real Time Kinematic (RTK) are used for centimetric positioning, whilst absolute and real-time Precise Point Positioning (PPP) has increased and is the most sounded technology under the GNSS scientific research.

On the mass market side, a division is observed. Sigle-Frequency combined with Standard Point Positioning (SPP) offers economical and energy low-cost advantages, meanwhile dual-frequency, plus multi-GNSS, plus sensor fusion implementation enables the highest accuracy but at a greater expense. Either way, both methods are proven to meet user accuracy requirements. However, the arise of security and safety standards which must be guaranteed in Safety of Life applications (SoL) still requires further work in order to accomplish other performances, mainly: integrity, continuity and availability. These performances may seem achievable on paper with simulations, but reality shows that very few experiments have been performed with real data scenarios.

Under the pragmatic nature of the GNSS state of the art review, this thesis will be focused in assessing accuracy and integrity performances with real data, using mass-market single-frequency SPP, for both legacy and new generation systems i.e. GPS and GALILEO. Besides, the individual performance assessment of each system is also an essential background in order to combine and produce multi-GNSS or multi-frequency solutions as it will be concluded.

Academical Implications

Moreover, and since this thesis is also framed under the termination of the aforementioned master's degree, it is expected that the student will demonstrate the knowledge and technical skills gained through this academic stage. The master is intended not only in expanding the geomatic fields but also in the student's ability to produce dedicated applications for their social, scientific and economic exploitation.

Henceforth, across this memorandum the theoretical basis regarding the GNSS positioning techniques used will be settled. Then, the methodology for implementing the dedicated algorithms will be explained i.e. software developed tool. Afterwards, a practical analysis application using the exposed methodology will be carried out i.e. the positioning performance study campaign. And finally, the conclusions regarding all the work phases and the project as whole will be enumerated.

Added Values

In addition, it should be mentioned that this thesis is also devoted to present an open-source GNSS tool contribution to the user community (hence, the thesis subtitle). The tool's preliminary intention was to fulfill the needs for the analysis stage. However, its design was taken in advantage and adapted for a user-end usage. It is expected that this approach will add more value and transcendence to the work performed.

As a final point, it is noteworthy to mention that the SW tool and many other features of this project are also due to the student's gained know-how of his professional experience in the GNSS technological sector. This has led to combine other skills producing better results and work methods, as it will be shown in the following pages of this work.

1.1 Thesis Purpose

Having introduced the scope of this work, its purpose can be defined accordingly. For the sake of simplicity, this is divided in a sequence of main objectives. Each objective encloses a major work feature i.e.: methodology, analysis and synthesis of the master's degree aptitudes. The following three main objectives are listed:

- **Development of GNSS Software (SW) tools**. The tools will be focusing on single-frequency SPP algorithms by means of processing GNSS pseudoranges measurements and navigation data in post-processing mode with the receiver being in static mode.

- **Positioning performance assessment of GPS Standard Positioning Service (SPS) and GALILEO Open Service (OS) with real data**. The target performances to measure will be user-domain accuracy and integrity.

- **Demonstrate the knowledge and skills gained during the master's degree** are properly applied. This will be illustrated emulating a professional application. The end-objective is to perform an individual and original work in order to present it in a university courtroom.

The first two objectives are covered in dedicated thesis chapters: Chapter 2 and Chapter 3 respectively. The third objective is assessed in all the phases, from the writing of this introduction until the conclusion enumeration.

Performance Specification

Further performance specification is needed at this stage. GNSS, as any other technique, is not free of error. Several phenomena affect the uncertainty of the solution, as it will be explained in the theory framework (chapter 2). By now, it is enough to understand that GNSS positioning always involves an error which its magnitude varies randomly (at least in theory). Commonly, the performances measured in the user domain are related with the real positioning error. This is the case for accuracy and integrity:

- **Accuracy** is the performance which provides the positioning error magnitude by taking advantage of the redundancy during the GNSS observation (more measurements than parameters to be estimated).

- **Integrity** is the correctness or the trust which can be placed in the system position solution for being representative of the real error.

Both performances are deeply explained in sections 2.6.1 and 2.6.2. The reader is encouraged to read these sections is he/she is not familiar with the terminology (especially for integrity performance).

GPS-SPS and GALILEO-OS stipulate its system user domain requirements. This is done in its definition documents: GPS-SPS-PD [BR.18] and GALILEO-OS-SDD [BR.16]. These requirements are presented in Table 2.6 for GPS, and in Table 2.7 for GALILEO.

Table 1.1 – Stipulated Positioning Error Requirements for GPS-SPS and GALILEO-OS.

Single-Frequency SPP Service	GPS-SPS and GALILEO-OS	
Coverage	Global	
Accuracy (95%)	Horizontal	Vertical
	7 m	**11 m**

However, the student's academical experience has showed that these values are kept very conservative since better performances are usually obtained. **Thus, a more optimistic criteria for this thesis will be set according to the student's judgement.** The error requirements for both GPS-SPA and GALILEO-OS are presented in Table 1.1. Eventually, the conclusions will remark if these requirements are properly accomplished, and in case they are not, which shall be used.

Complementary Objectives

Last but not the least, it is important to highlight a complementary objective to keep in mind regarding the added value of creating an open-source SW tool.

Preliminarily, the first alternative was not to develop any SW but to take advantage of the already available free-of-charge GNSS processing tools. However, these tools did not fit the thesis expectations. As a result, it was decided to develop a dedicated SW with the motivation of fulfilling the specific project needs. But thanks to the encouragement provided by the master's degree in developing geomatic applications, and following with the GNSS open-service approach, the SW tool adopted a user-end motivation.

Therefore, a complementary objective regarding the SW development process was born during the thesis development. This objective can be defined as **the developed SW shall be available as an open-source tool for any user willing to make use of it**. It is important to keep this objective in mind since all the stages of the thesis will somehow prove that this is being accomplished, as it will be detailed in each chapter.

1.2 Document Outline

As previously mentioned, the memorandum is divided in 8 chapters attending to the main thesis stages:

- **Chapter 1** encompass the thesis introduction. It explains broadly the scope, motivation, main objectives and provides the specification of the expected positioning performances for GPS and GALILEO systems.

- **Chapter 2** serves as the theoretical framework. GNSS systems and algorithms used for the methodology and analysis phases are detailed in order to support the developed solutions for this project.

- **Chapter 3** presents the methodology used for the thesis, i.e. developed SW tool. It emphasizes the followed lifecycle approach for its specification, implementation and validation; rather than being a deep source code explanation.

- **Chapter 4** is devoted to explain the project analysis stage. This is the campaign for assessing GPS and GALILEO positioning performances. The scope, data arrangement and its results are presented and commented in this chapter.

- **Chapter 5** enumerates the conclusions based on the thesis purposes. In addition, enhancements and planned evolutions regarding the developed SW tool are also included for future work lines.

- **Chapter 6** lists the acronyms used through the document.

- **Chapter 7** includes the references which encompass the bibliography and media links used for the thesis development.

- **Chapter 8** holds the annexes. More specifically:

  - SW tool items such as source code repository, budget estimation and internal interface examples.

  - Analysis Campaign items like results repository and selected stations world map.

Chapter 2: Theory Framework

2 Theory Framework

A Global Navigation Satellite System (GNSS) is defined as a system composed of a satellite constellation which enables a 3D navigation service anywhere in the globe. For committing this purpose, the satellites are constantly emitting signals, so dedicated GNSS receivers can acquire them and determine their position by solving a triangulation geometric problem which involves the distances retrieved from the satellite's signals.

The GNSS term can also be referred as all the different systems which provide global navigation services. The oldest and most known is U.S. Global Positioning System (GPS). But there are several others such as the Russian GLObal Navigation Satellite System (GLONASS), Europe's own system GALILEO or the Chinese system COMPASS/BEIDOU.

The following sections of this chapter are devoted to explain the GNSS systems and positioning techniques for establishing the knowledge basis used through this work. Beware that if the reader is familiar with GNSS terminology, this chapter can be skipped. The rest of the chapters will usually refer to this framework, so the reader can review the theory concepts whenever needed.

2.1 GNSS Based Positioning

For an intuitive approach on GNSS positioning, it shall be pointed that for any position determination two concepts must be defined:

- Reference System.
- Reference Frame.

A reference system is a theoretical concept which establishes a universal reference by defining parameters, hypothesis and constants. In geodesy, a Terrestrial Reference System (TRS) is commonly defined as 3 perpendicular right-hand axes where their intersection is centered on the earth's center of masses and their movement is fixed relative to the earth's rotation, denoting an ECEF (Earth Centered, Earth Fixed) reference system. In addition, approximate models of the earth are defined as part of the reference system as well. On the one hand a revolution ellipsoid is defined for a geometric approximation as shown in Figure 2.1. On the other hand, a Geoid is defined as a physical approximation since it represents a constant geopotential surface.

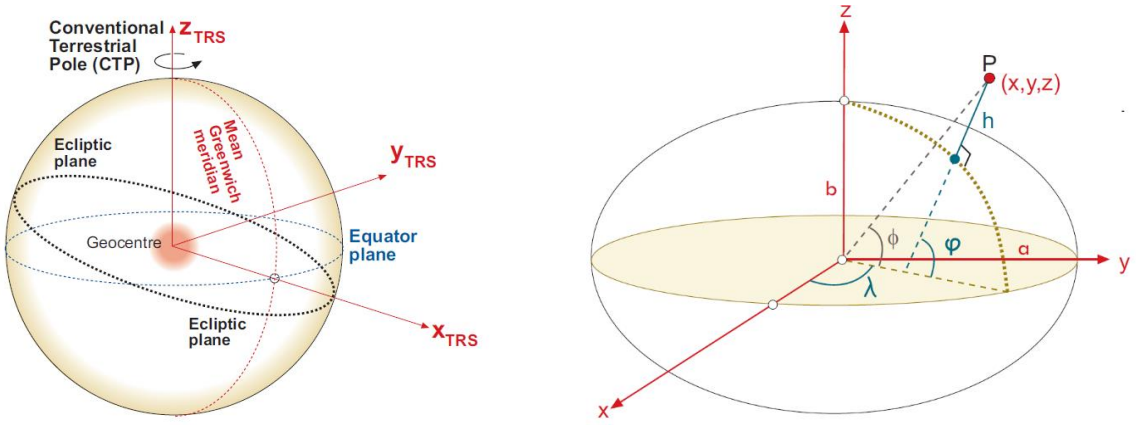

Figure 2.1 – ECEF reference system definition and geodetic ellipsoid. Source: Sanz Subirana et al. 2013.

The different TRS are defined with continuous GNSS observations and other geodesy techniques such as VLBI, SLR or gravitational measures. A reference system could be enough to determine the three

coordinates of any point: X, Y and Z; which are the perpendicular distances to the axes (or geodetic coordinates: latitude φ, longitude λ and ellipsoidal height h). However, in a practical sense is hard to achieve such thing, since the reference system is just a theoretical definition and not a physical materialization. Therefore, a reference frame which provides reference coordinates is needed, so any other point can be placed on the reference system by observing this frame.

Classically, the reference frames were a network of monuments build up on the earth's surface (see Figure 2.2). These points were defined with very precise coordinates by astronomical observations and network adjustments, meaning that fair precision could only be achieved locally and not globally. With the rise of space exploration in the 1970's and the launch of satellites orbiting the earth, a new reference frame concept is borne, and this is the primary characterization of a GNSS: the satellite constellation acts as the reference frame.

Figure 2.2 – Geodetic monument and geodetic network example. Source: Wikipedia.org.

So, satellite coordinates are known, and any user can measure the distance to the satellites in order to triangulate its position. Unfortunately, this is a complex matter because:

- A precise ranging satellite-user determination of at-least 3 satellites is essential.
- A precise method is needed for knowing the satellite coordinates at any time, since they are moving relative to the earth at a high speed (approximately 5 km/s).

The satellite's signal is intended to solve these issues. The signal is an electromagnetic wave that is being generated by an atomic clock onboard the satellites. The signal is allocated on the L band of the microwave spectrum with a nominal frequency of 10.23 MHz. This also allows to modulate information onto the signal itself. The information transmitted by the GNSS signals is the navigation message (the so-called ephemerids) which contain the Keplerian parameters, so the satellite coordinates can be computed by applying orbital mechanics.

GNSS users make use of receivers in order to decode the information transmitted by the signal. In addition, the signal travels at the speed of light, thus the travel time among the satellites and the user is directly derived into a range measurement for the receiver. This enables a precise notion of the reference frame and the range measurements to it.

However, the signal transmission time requires a very precise timing system. Note that the signal travels at the speed of light (299800 km/h), meaning that an ambiguity of 10^{-5} seconds is translated into an

uncertainty of 300 meters in the position solution. As previously mentioned, satellites are equipped with high precision atomic clocks. These clocks rely on the frequency needed for transitioning energy levels in the atoms of a stable element such as Hydrogen.

Nevertheless, for a fair timing synchronization, user receivers should be equipped with atomic clock as well. But this is not cost-effective. Instead, the receivers use quartz clocks, which are much cheaper, and take advantage of observing an additional satellite in order to estimate the offset among the receiver's clock and the reference time system defined by the constellation. This leads to have at least 4 satellites in view as shown in Figure 2.3 in order to obtain a position solution. This constraint is essential for the constellation design as it will be specified in section 2.2.1.

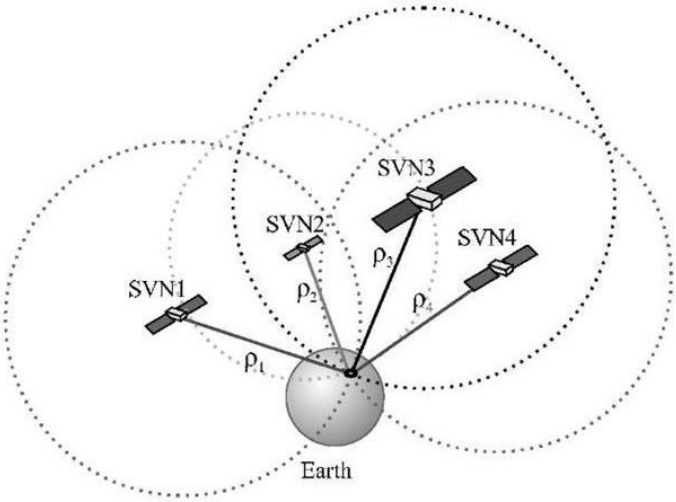

Figure 2.3 – Minimum GNSS satellite configuration for positioning. Source: mobacommunity.com

Summing up, the GNSS basic positioning principles have been covered by an intuitive approach. The following key points are highlighted:

- For any positioning method a reference system and a reference frame need to be precisely defined.
- For GNSS positioning, the satellite constellation defines the reference frame.
- Satellite coordinates are precisely determined thanks to the orbital information broadcasted in the signal.
- In addition, the signal's time of travel is used as the primary range measurement, but this needs high timing accuracy.
- Precise timing is achieved by the atomic clocks onboard the satellites which in addition generate the signal.
- GNSS receivers can estimate its position X, Y, Z and its receiver clock offset by observing at least four satellites.

No to mention that GNSS positioning is far more complex when achieving metric precision. But this will be issued in the upcoming sections of this chapter.

2.2 GNSS Architecture

A GNSS is primarily composed of the satellite constellation, the space segment and their broadcasted signals, but this is not enough for maintaining a reliable and continuous service. A GNSS generally consist of two more segments: the control (or ground) segment and the user segment.

2.2.1 Space Segment

As previously mentioned, the GNSS space segment is the satellite constellation composed of the different Space Vehicles (SV). The main goal of the SV is to transmit the signals and to store and broadcast their navigation message uplinked from the control segment. In addition, the constellation must ensure that at least 4 satellites are in view from anywhere on the earth to maintain global coverage.

GNSS SV are placed in Medium Earth Orbit (MEO) at about 20000 km over the earth. They have an approximate revolution period of 12 hours, meaning that a SV is in view two times per sidereal day. Their inclination over the equator's plane oscillates among 60º and 50º, and their orbits are nearly circular. With this orbital configuration, a GNSS constellation needs of at least 21 satellites for ensuring global coverage, although it is common for systems to maintain more than 24 satellites which are used as backup SV.

Figure 2.4 – GNSS satellite constellation. Source: Navipedia.net.

SV by themselves are complex engineering pieces and have various mechanisms which allow them to be in orbit, communicate with the control segment and broadcast their signals. Nevertheless, their most critical component is the atomic clock which is the signal generator and precise time instrument. As pointed in section 2.1, these clocks are made of a stable element such as Rubidium, Cesium or Hydrogen.

2.2.2 Signal in Space

Atomic clocks onboard the SV, generate the Signal In Space (SIS) service. This is done by inducing atomic jumps in the stable element which generates an electromagnetic wave with a very precise nominal frequency. This frequency is allocated in the L band of the microwave spectrum. As all the electromagnetic waves, the signal travels at the speed of light in the void.

The SIS is just an energy propagation and does not provide any information. However, the signal can be easily modulated in order to carry the SV's navigation message and ranging code. Consequently, the main signal components are:

- **Carrier wave** is defined as the wave which "carries" the information.

- **Ranging code** is also referred as the Pseudo-Random Noise (PRN) which is a sequence of zeros and ones for the receiver to determine the travel time of the signal.

- **Navigation data** is the binary coded message which contains the orbital parameters of the SV, its clock corrections, almanacs and other useful information.

The Ranging code and navigation data are modulated over the carrier wave with a lower frequency rate. This creates a certain bandwidth which is used for multiplexing the signal and take advantage of broadcasting different data at the same time. There are three types of modulation based on the wave property to vary as shown in Figure 2.5:

- Amplitude Modulation (AM)
- Frequency Modulation (FM)
- Phase Modulation (PM)

The common way for modulating GNSS SIS is the phase modulation. Except for GLONASS, which uses frequency modulation.

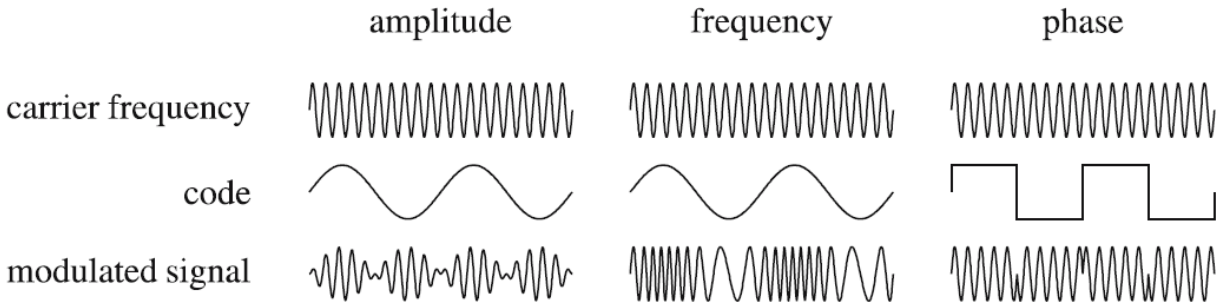

Figure 2.5 – Carrier wave modulation methods. Source: Hoffman et al. 2008.

2.2.3 Control Segment

The control segment is comprised of the facilities, systems and operators which are constantly monitoring the space segment. It is also referred as the ground segment and its main objectives are:

- Control SV health status and configuration.
- Compute, predict and validate the SV ephemeris (navigation message).
- Maintain the time reference with the SV's clocks and ground atomic clocks.
- Uplink the ephemerids to each SV.
- Resolve SV anomalies.

Usually control segments are composed of master control centers and remote tracking stations but the architecture differs on each system (GPS, GALILEO…). For more information about ground control segments, refer to [BR.1] or [BR.2].

2.2.4 User Segment

The user segment encompasses all the GNSS receivers which provide positioning and accurate timing. This is achieved by receiving the carrier signal and demodulating its information, so they can estimate the

pseudoranges (and other observables) and compute the SV position, to finally determine the user position by solving navigation equations.

Nowadays there is a wide variety of GNSS receivers which can range from complex surveying antennas with up to 400 channels, to minimalistic receivers which are usually allocated on smartphones and watches. In any case a GNSS receiver is composed of:

- Antenna with preamplification.
- Radio frequency section.
- Micro-processor and memory data for storage.
- An intermediate-precision oscillator e.g. quartz clock.

2.3 GNSS Systems

It was early mentioned that GNSS can also be referred as the different systems which deliver navigation services. At the issue date of this document, the fully operational and autonomous systems are the U.S. GPS and the Russian GLONASS. There are several others in development, such as the Chinese system BEIDOU or Europe's own system GALILEO, which are expected to reach their Full Operational Capability (FOC) phase in the upcoming years. In addition, GNSS also englobes the Space Based Augmentation Services (SBAS) such as U.S Wide Area Augmentation System (WAAS) and the European Navigation Overlay System (EGNOS). Although these systems do not provide an autonomous and global positioning service but enhance precision and integrity broadcasting wide area corrections.

The following sections describe the GNSS segments and services used for this master thesis purpose i.e. GPS and GALILEO. For other GNSS specifications such as GLONASS, BEIDOU or SBAS, refer to [BR.1].

2.3.1 GPS

"The NAVSTAR Global Positioning System (GPS) is an all-weather, space based navigation system under development by the Department of Defense (DoD) to satisfy the requirements for the military forces to accurately determine their position, velocity, and time in a common reference system, anywhere on or near the earth on a continuous basis" (Hoffman et al 2008, [BR.2]).

"Since the DoD is the initiator of GPS, the primary goals were military ones. But the US Congress, with guidance from the President, directed the DoD to promote its civil use […]. However, the real impact of the originally military GPS occurred in 1983, when the US President offered free civilian access after the incident of the Korean Airlines Flight 007" (Hoffman et al. 2008, [BR.2]). Furthermore, On May of 2000, U.S president Bill Clinton announced the de-activation of Selective-Availability (S/A), a feature that was causing a positioning precision degradation of ten times.

GPS program was started in the 1960's and after several tests, the Initial Operational Capability (IOC) was announced in 1993 when 24 SV were available for navigation. Later, on 1995, FOC was declared after validating the systems for military performances.

GPS Space Segment

NAVSTAR (Navigation System With Ranging and Timing) is the GPS satellite constellation. NAVSTAR is arranged with 24 SV slots divided in 6 orbital planes with 55º of inclination at an approximate altitude of 20200km with an eccentricity of 0.02.

NAVSTAR satellites are divided into different blocks based on the time they were launched and its evolutions:

- **Block I** was formed by 11 development satellites launched between 1978 and 1985.
- **Block II and IIA** were formed by 28 operational satellites launched from 1989 and some of them are still operating nowadays.
- **Block IIR, IIR-M and IIF** were formed by replacement operational satellites. "Block IIR satellites are capable of autonomously determining their orbits and generating their own navigation messages" (Sanz Subirana et al. 2013, [BR.1]). Block IIR-M included some modernizations such as new military code and a more robust civilian signals (L2C and L5).

- **Block III** will be formed by future satellites which will include enhancements such as interoperability with other GNSS and jamming protection. This block will broadcast the fourth civilian signal (L1C).

GPS Services and Signals

GPS has a SIS legacy service which is based on two carrier waves in the L band denoted as L1 and L2. They both are derived from a nominal frequency of 10.23MHz:

$$L1 = 154\ x\ 10.23\ MHz = 1575.420\ MHz$$

$$L2 = 120\ x\ 10.23\ MHz = 1227.600\ MHz$$

On these two carrier waves, two codes and one navigation message are modulated using Binary Shift Keying Technique (BPSK):

- **Coarse/Acquisition** (C/A) code has a chipping rate of 1.023 Mbps which is translated in on a chip length of 293.1 m. C/A code is only modulated over L1 and purposely omitted from L2 in order to deny full precision to civilian users.

- **Precise Code** (P) is dedicated to military means and other authorized users. Its chipping rate is 10 Mbps (chip width of 29.31 m). Unlike C/A, P code is modulated over both carrier waves, L1 and L2, thus enabling military receivers to take advantage of dual-frequency solutions.

- **Navigation message**: is modulated on L1 and L2 as well, carrying the SV ephemerids as specified in section 2.2.2.

The main legacy services provided by GPS are derived from the aforementioned codes:

- **Standard Positioning Service** (SPS) is based on C/A code which is only provided on L1. Is open service and free of charge. Although S/A was applied in C/A, it was completely removed on 2008 and it will not be included in the next GPS evolutions.

- **Precise Positioning Service** (PPS) provides a more precise service than SPS with P code modulated over L1 and L2. P code is subjected to Anti-Spoofing, resulting in the Y code, in order to restrict system availability to nonmilitary users. Additionally, GPS has a service modernization which includes new civilian and an additional military signal (the M code).

- **L2C** is open use and was introduced in block IIR-M. The code is modulated using BPSK on L2 carrier and broadcasted at a higher power, "making reception easier under trees and even indoors" (Saenz Subirana et al. 2013, [BR.1]).

- **L5C** is open service and was introduced in block IIF. This signal is provided onto the new carrier frequency, the L5 ($1173.45\ \text{MHz} = 115\ \text{x}\ 10.23\ \text{MHz}$), and has a modulation that meets Safety of Life (SoL) requirements, a better multipath performance and robustness against interferences.

- **L1C** will enter service with block III. It will be open service and its main purpose is to provide interoperability with other GNSS such as GALILEO and to improve positioning in urban areas thanks to its MBOC modulation.

Figure 2.6 depicts GPS signal spectra meanwhile Table 2.1 provides a technical summary of the mentioned services.

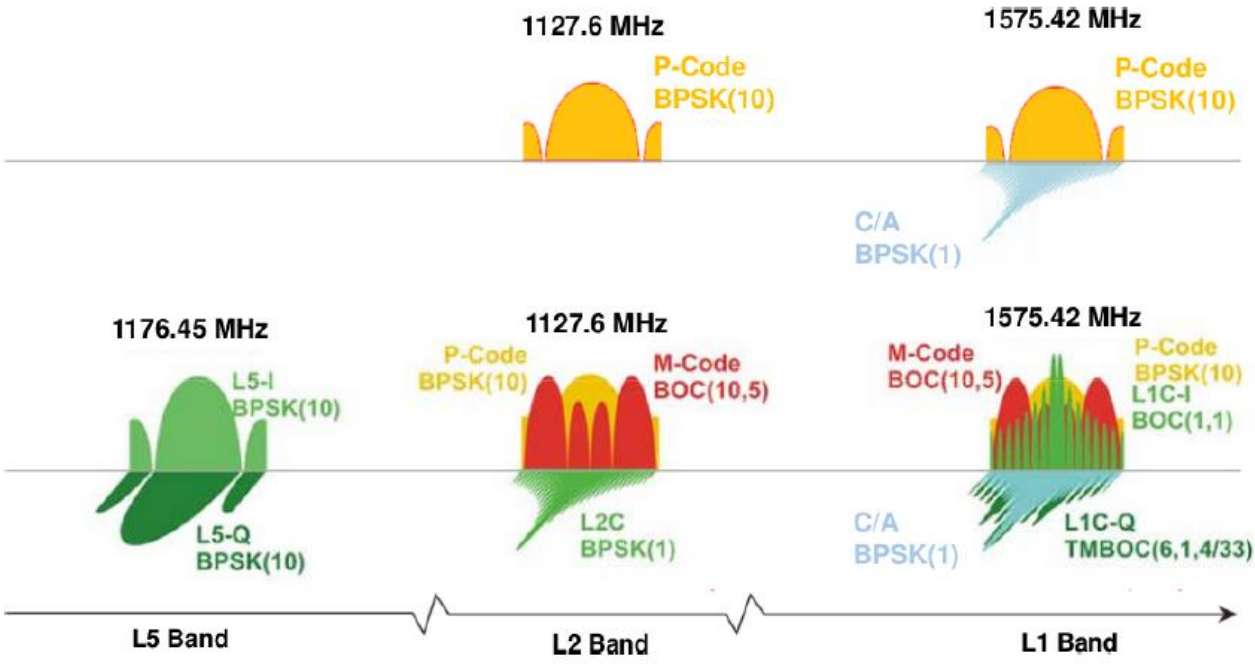

Figure 2.6 – GPS signal spectra allocation before and after modernization. Source: Sanz Subirana et al. 2013.

Table 2.1 – GPS signal service specifications.

Link	Carrier Freq. [MHz]	Code	Modulation	Code Rate [Mcps]	Data Rate [bps]	Service
L1	1575.420	C/A	BPSK	1.023	50	Civil
		P		10.23	50	Military
		M	BOC	5.115	N/A	Military
		L1C-I data	MBOC	1.023	50	Civil
		L1C-Q pilot			-	
L2	1227.600	P	BPSK	10.23	50	Military
		L2C		1.023	25	Civil
		M	BOC		N/A	Military
L5	1176.450	L5-I data	BPSK	1.023	50	Civil
		L5-Q pilot			-	

2.3.2 GALILEO

In the 1980's the European Union understood the economic, social and technologic importance of satellite-based navigation. On 1999, they started to develop its own and independent GNSS called GALILEO. Unlike GPS, GALILEO's primary premise is to be civil-use oriented and it will ensure interoperability with other GNSS: "In its paper concerning the involvement of Europe in a new generation of satellite navigation service, the European Commission (1999) recommended Galileo to be an open, global system, fully compatible with GPS but independent from it. The key parameters of Galileo have been identified to be the independence of any other system while maintaining interoperability, global availability, and high level of service reliability, thus implementing integrity information." (Hoffman et al. 2008, [BR.2]).

The main reasons for European Union countries to start its own GNSS rely on GPS (and other systems) lack of compliance with the following requirements:

- Other GNSS do not satisfy aviation standards for accuracy, integrity and continuity.
- GPS and GLONASS are under military control and their availability can be trimmed in case of conflict.
- They do not provide a legal guarantee nor a legal frame in case of a system failure.

GALILEO system is still under development by the European Space Agency (ESA) and managed through the European Commission (EC). Nonetheless, GALILEO is not the only European satellite-navigation project. As mentioned earlier, EGNOS is the European SBAS which was developed in the frame of GALILEO and has acted as its cornerstone. EGNOS's is nowadays operative and it will be a key system in the future for providing maximum integrity to airborne users along with GALILEO.

It is noteworthy to point out that GALILEO is a promising system to the GNSS ecosystem. On the one hand, each satellite is equipped with two maser hydrogen passive atomic clocks, with better long-term and short-term stability, which provide a better accuracy and timing than other GNSS. On the other hand, GALILEO will have the capability of transmitting real-time integrity information. This is achieved by broadcasting maximum error in the SIS domain: SISE (Signal In Space Error).

GALILEO Space Segment

The GALILEO constellation in FOC, will consist in 27 SV allocated on MEO (23 222 km), arranged in 3 orbital planes with 56º of inclination and with an orbit eccentricity of 0.002. The satellites will have a period of 14 hours, repeating their geometry every 10 days. "This constellation guarantees, under nominal operation, a maximum of six satellites in view from any point on the Earth's surface at any time, with an elevation above the horizon of more than 10º" (Sanz Subirana et al. 2013, [BR.1]). In addition, "this satellite disposition will ensure a better coverage in northern latitudes" (Berné Valero et al. 2014, [BR.5]).

The GALILEO space segment has been evolving as specified in the following milestones:

- **Experimental Phase.** Two experimental SV were launched between 2005 and 2008: GIOVE-A and GIOVE-B (GIOVE stands for GALILEO In Orbit Validation). They served several purposes such as: ensuring GALILEO frequency fillings, validate the technologies to be used in the operational SV and develop user equipment.

- **In Orbit Validation Phase**. Four more SV were launched (2 on October 2011 and other 2 on October 2012) for qualifying the control and user segments through validation tests and operations. These four satellites were allocated in the first and second orbital planes and were the first operational GALILEO SV.

- **Full Operational Capability Phase**. On the issue date of this document, there are 26 GALILEO SV in orbit: 22 of them marked as USABLE and the other 4 mark as NOT USABLE for testing or maintenance reasons. Consequently, FOC is unlikely to be reached as expected by 2020, although is viable to be declared in the upcoming years with 30 SV (27 operational plus 3 backup).

GALILEO Services and Signals

"Europe has chosen a service-oriented approach for the design of GALILEO" (Hoffman et al. 2008, [BR.2]). GALILEO will transmit 10 navigation signals in the same frequency bands as GPS, denoted: E1, E5a, E5b and E6. The signals were designed to serve the different services which are based in a variety of needs:

- **Open Service** (OS). It is free of charge to users worldwide and it is provided by three different signals (E1, E5a and E5b). Is the equivalent to GPS's SPS as "Single-frequency receivers will provide similar performances as GPS C/A" (Sanz Subirana et al. 2013, [BR.1]).

- **Public Regulated Service** (PRS). This service is provided with two signals and two navigation messages, which allows for higher continuity performance and introduces robustness against jamming and spoofing. However, it is only available to security authorities e.g.: police or military, with a controlled access and under governmental control.

- **Commercial Service** (CS). It is reserved for commercial purposes. It is broadcasted with two additional signals protected with encryption and two higher rate navigation messages.

- **Search and Rescue Service** (SAR). This service complements the COSPAS-SARSAT rescue service by adding an up-link signal in order to inform users that its emergency situation has been notified.

- **Safety of Life Service** (SoL). The service is already offered by EGNOS to airborne users which require critical safety standards. On FOC, GALILEO will improve this service along with the future versions of EGNOS.

These services are provided through 4 dedicated signals:

- **E1** is allocated on the E1 (homologous of L1) band and supports the OS, PRS, CS and SoL with three signal components:
  - E1-A is dedicated to PRS and hence is encrypted.
  - E1-B is open service and stands for the data channel which contains unencrypted integrity information and encrypted commercial data.
  - E1-C is the pilot or data less of the open service component.

- **E6** is encrypted in the E6 band and dedicated exclusively to the CS and PRS. As E1 signal, it is composed of three components:
  - E6-A is only accessible to PRS users.
  - E6-B is the data channel for the CS. The higher E6 data rate (500 bps) allows for the modulation additional commercial information.
  - E6-C is the pilot channel for the CS broadcasting the ranging code.

- **E5a** is allocated on the E5 band (homologous of L5) and only supports GALILEO's OS. The signal allows basic navigation and timing. It is composed of:
  - E5a-I, the data channel which includes navigation data.

- E5a-Q, the pilot channel which encompass unencrypted ranging code.

- **E5b**, like E5a, is allocated on the E5 band. However, it supports SoL and CS besides of OS. It is also comprised of two components:
  - E5b-I, the data channel, includes unencrypted integrity data and encrypted commercial information.
  - E5b-Q, the pilot channel, includes ranging code available to all users.

An additional signal can be created as a result of combining E5a and E5b using the Alternate Binary Offset Carrier (AltBOC) modulation technique. The resulting signal is denoted as E5 and can be processed as a whole with a proper user implementation. This signal is encouraging for many applications since it has proved, at least with simulated data, a very enhanced positioning accuracy with low multi-path and tracking noise performances (see [BR.7]).

Figure 2.7 depicts the GALILEO's signal spectra and Table 2.2 summarizes the signal specification and supported services.

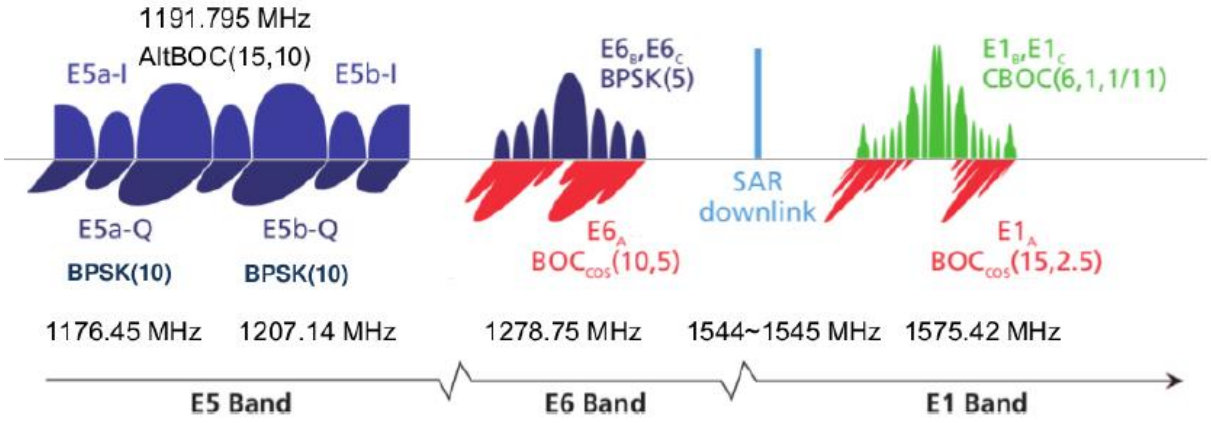

Figure 2.7 – GALILEO signal spectra allocation. Source: San Subirana et al. 2013.

Table 2.2 – GALILEO signal service specifications.

Band	Carrier Freq. [MHz]	Channel	Modulation	Code Rate [Mcps]	Data Rate [bps]	Service
E1	1575.420	E1-A data	BOC	2.5575	N/A	PRS
		E1-B data	MBOC	1.023	125	OS, CS, SoL
		E1-C pilot			-	
E6	1278.750	E6-A data	BOC	5.115	N/A	PRS
		E6-B data	BPSK		500	CS
		E6-C pilot			-	
E5a	1176.450	E5a-I data	BPSK	10.23	25	OS
		E5a-Q pilot			-	
E5b	1207.140	E5b-I data	BPSK	10.23	125	OS, CS, SoL
		E5b-Q pilot			-	

2.4 GNSS Reference Frames

GNSS positioning relies on the accurate definition of the spatial reference frame formed by the satellite constellation and the synchronization against the time scale. In the following sections, the theory regarding the time and coordinates frames will be exposed and detailed for GPS and GALILEO systems.

2.4.1 Time Scales

Time scales have been always defined upon periodic cycles. Therefore, the first systems used natural phenomena as the earth's rotation or celestial mechanics in order to stablish time frames. These are known as Universal Time (UT) and Sidereal Time. Both use the earth's rotation as a reference, UT sets the reference against the Sun and the Sidereal Time against the Aries Point (vernal equinox).

However, these references are not uniform and accurate enough for achieving high synchronization demands. As technology evolved, more accurate time frames could be defined. International Atomic Time (TAI) was introduced and it is based on the transitions between atomic energy levels.

TAI and UT accumulate drift over time. Eventually, Universal Time Coordinated (UTC) was defined in order to be aligned within a certain margin from UT. UTC is based on an atomic reference composed of 250 Caesium and Hydrogen clocks distributed in 65 laboratories around the world. The following relations between TAI, UTC and UT are met:

$$TAI = UTC + 1s \times n; \tag{2.1}$$

$$UTC = UT + dUT;\ |dUT| < 0.9s \tag{2.2}$$

As deduced from equation (2.1), UTC is maintained from TAI plus a number of leap seconds denoted as n. The number of leap seconds is not constant and is provided periodically by the International Earth Rotation and Reference System Service (IERS); e.g. 1 Jan 1999 n = 32 seconds. Equation (2.2), points that UT and UTC realizations are kept within 0.9 seconds.

GPS Time

Simplified as GPST, is a continuous atomic time scale with no leap seconds. GPST is constantly maintained by the GPS control segment by means of its atomic clocks onboard the GPS SV and those on the ground segment. The GPST's origin started at 0 hours UTC, January the 6th of 1980, meaning that at that time GPST = 0 seconds. Since the number of leap seconds at GPST's origin was 19 seconds, the following relation among UTC and GPST can be deduced:

$$GPST - UTC = n - 19s; \tag{2.3}$$

GALILEO Time

Like GPST, GALILEO System Time (GST) is a continuous time scale based on the atomic references from the GALILEO's space and ground segments. In addition, GST is kept synchronized with TAI below 50ns. GST origin was set at 0 hours UTC August the 22th of 1999.

2.4.2 Spatial Reference Systems

As explained in section 2.1, the usual reference system used for framing a GNSS navigation solution is a TRS, also referred as an ECEF. More specifically, and as showed at the beginning of this chapter in Figure 2.1, the TRS:

- Has its origin on the Earth's center of masses.
- Its Z-axis is aligned with the Earth's rotation movement as defined by the Conventional Terrestial Pole.
- Its X-axis is aligned with the intersection among the equatorial plane and the Greenwich meridian (perpendicular to the Z-axis)
- Its Y-axis is right hand perpendicularly defined against the Z and X axes.

The international definition of the TRS is known as the International Reference System (ITRS). Along the mentioned TRS characteristics, ITRS's ellipsoid is the GRS80 model (Geocentric Reference System 1980). ITRS realization is the International Terrestrial Reference Frame (ITRF), a set of ground stations around the globe which its coordinates are precisely and periodically determined by spatial geodesy techniques such as VLBI, SLR or GNSS. These realizations are denoted as $ITRF_{yy}$, where *yy* stands for the last two-year digits of the data used to determine the solution. Usually, GNSS reference systems and frames tend to be closely aligned with ITRS and ITRF respectively.

GPS Reference System

Since NAVSTAR origins, GPS has used its own World Geodetic System, the so-called WGS-84, developed by the U.S. DoD. Its initial implementation was derived from a set of observations from first GPS satellites (Transit SV). However, further WGS-84 refinements have used ITRF solutions like $ITRF_{92}$ and $ITRF_{94}$. WGS-84 uses its own ellipsoid definition.

Since WGS-84 was defined as GPS reference system: "GPS broadcast ephemerids are linked to the position of the satellite antenna phase center in the WGS84 reference frame. Thus, the user's receiver coordinates will be expressed in the same ECEF frame." (Sanz Subirana et al. 2013, [BR.1]).

GALILEO Reference System

The GALILEO Terrestial Reference Frame (GTRF) was established by the GALILEO Geodetic Service Provider (GGSP). Its first realization was produced from GPS observation since it was needed for the GALILEO satellite IOV phase. Consequently, future GTRF versions will use both GALILEO and GPS measurements. Like GPS system, the user coordinates will be provided against GTRF if GALILEO ephemerids are used.

GTRF is required to be maintained against ITRF with no more than 3 cm of difference. Therefore, the difference among GTRF, WGS84 or ITRF are not significant for applications which require metric precision: "For navigation purposes and most user requirements, the agreement between ITRF, GTRF, and WGS-84 is sufficient and no coordinate transformations have to be applied. For geosciences, surveying, and other high-accuracy applications, an appropriate transformation has to be applied." (Hoffman et al. 2008, [BR.2]).

2.5 GNSS Standard Point Positioning

The GNSS single-frequency pseudorange positioning method, commonly referred as Standard Point Positioning (SPP), has been intuitionally introduced in section 2.1. However, this technique requires several modelling techniques since there are a lot of error sources affecting the positioning accuracy such as atmospheric disturbance, instrumental delays, clock synchronization or satellite orbits uncertainty determination among the most relevant.

In the upcoming subsections, a more detailed explanation of the techniques concerning pseudorange positioning will be covered. In addition, algorithms used in this project will be detailed. Note that the subsections were written for GPS and GALILEO systems. For other GNSS and further processing techniques, refer to the bibliography references: [BR.4], [BR.6] or [BR.3].

2.5.1 Geometric Range Modelling

GNSS signal contains a ranging code pseudo-randomly generated which is referred as the PRN. This is just a bit sequence different for each operational SV. Recalling section 2.2.2, the primary GNSS raw measurement is the signal's time of transmission between the SV's antenna and the receiver's antenna, denoted as ΔT. This observation is obtained by correlating the PRN broadcasted by the SV and the replica generated in the receiver. The maximum correlation peak is the observed ΔT as shown in Figure 2.8.

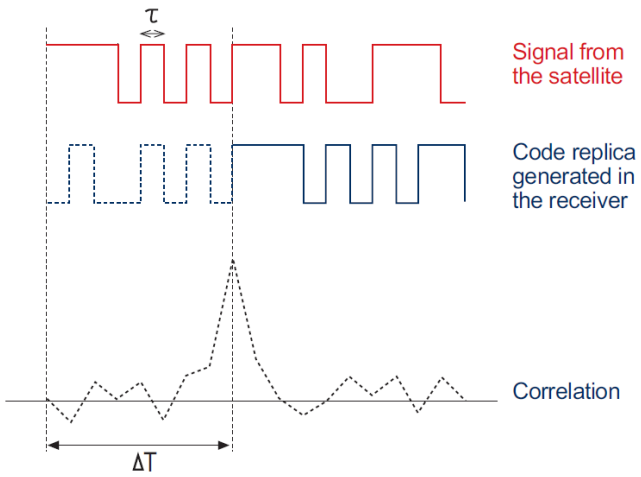

Figure 2.8 – PRN correlation among SV and Receiver. Source: Sanz Subirana et al. 2013.

If ΔT is multiplied by the signal's speed propagation, the speed of light ($c = 299792458\ m/s$), the pseudorange (R) is obtained as shown in the following equation:

$$R_{Rec}^{SV} = c \times \Delta T; \tag{2.4}$$

The pseudorange is the apparent range between the SV and the receiver. Nonetheless, this range is critically affected by several error sources. The most significant is the disagreement among satellite's time scale t^{SV}, receiver's time scale t_{Rec} and the time reference scale T (e.g. GPST). The pseudorange obtained from a ranging code S (e.g. GPS C/A) at a given carrier frequency f (e.g. GPS L1) can be expressed accounting for the different time scales as:

$$R_{S_f} = c \times (T_{Rec}(t_r) - T^{SV}(t_e)); \tag{2.5}$$

Where t_r is the pseudorange reception time expressed in the receiver's time scale and t_e is the pseudorange emission time expressed in the SV's time scale. Referring this expression to the reference time scale T, equation (2.6) is adopted:

$$R_{S_f} = \rho + c \times (\delta_{T_{Rec}} - \delta_{T}{}^{sv}); \quad (2.6)$$

ρ denotes the actual range between the SV and the receiver. $\delta_{T_{Rec}}$ and $\delta_{T}{}^{sv}$ denote respectively the receiver and satellite clock offsets (or clock biases) against the time reference scale T. Common SPP algorithms, compute from satellite ephemerids the SV's clock bias and estimate the receiver's clock bias along with its position solution.

The following most significant error sources in the pseudorange measurements account for signal's propagation though the atmosphere. In GNSS, the atmospheric errors are split in two types:

- **Ionosphere delay**. This delay occurs at approximately 350 km over the earth's surface caused by the Total Electron Content (TEC) re-distribution on the upper atmosphere due to the ionization by several phenomena like Sun's rays. This is translated in a positive delay on the pseudorange directly related to the signal's carrier frequency (dispersive medium). This delay can vary between 5 m and even 30 m, but fortunately, most of it can be easily modelled with deterministic algorithms for single-frequency GNSS users.

- **Troposphere delay**. This delay occurs at approximately 60 km from the earth's surface. It is mainly caused by the temperature, pressure and water vapor variations in the first layers of the atmosphere and usually split in the hydrostatic and wet components. Unlike Ionosphere delay, the troposphere delay is a non-dispersive medium and cannot be related to any of the signal's properties. This causes troposphere effect to be difficultly estimated. Nevertheless, 90% of the delay comes from the hydrostatic component which causes an approximate positive delay of 10 m in the positioning solution.

Dedicated algorithms used in this project for ionosphere and troposphere delays are detailed in section 2.5.3. Ionosphere delay, troposphere delay and other error sources affecting the range observation (ε_S) can be added to equation (2.6) resulting in the basic pseudorange expression:

$$R_{S_f} = \rho + c \times \left(\delta_{T_{Rec}} - \delta_{T}{}^{sv}\right) + \Delta_{iono}^{S_f} + \Delta_{trop} + \varepsilon_S \; ; \quad (2.7)$$

Equation (2.7) shows the best possible range observation between the SV and the receiver. Therefore, this equation will be combined, with at least other four equations, in order to estimate the receiver's position by an algorithm which minimizes the positioning error i.e. the Least Squares (LSQ) method. This will be mathematically assessed in section 2.5.4.

Several other error sources can be added to this expression such as instrumental delays or multipath effects. However, for metric precision, which is achieved in SPP, the pointed error sources are enough, and the rest affect fewer to have a significant impact on positioning performances. Nonetheless, further information about pseudorange measurement modelling can be consulted in [BR.1].

2.5.2 Satellite Orbit and Clock Modelling

Recalling section 2.2.1, SV constitute the reference frame of a GNSS solution and therefore their coordinates must be precisely estimated for an accurate positioning service. Orbital and satellite's clock correction parameters are transmitted in the navigation message. The orbital parameters are the Keplerian

elements derived from classical orbital mechanics. According to Newton's theory, the movement between two bodies can be defined by their gravity attractive forces:

$$\ddot{r} + \frac{G(m_1 + m_2)}{r^3} \times r = 0; \tag{2.8}$$

Where r is the relative position vector, m terms denote the two object masses and G is the universal gravity constant ($G = 6.674 \times 10^{-11}\ \frac{Nm^2}{Kg^2}$).

The satellite's orbit can be expressed as follows by integrating equation (2.8):

$$r(t) = r(t_0, a, e, i, \Omega, \omega, \tau); \tag{2.9}$$

Arguments: $t, a, e, i, \Omega, \omega, \tau$ are the Keplerian elements illustrated in Figure 2.9. More specifically:

- Ω is the ascending node, the geocentric angle between the ascending node direction and the Aries point direction.
- i is the inclination of the orbit against the equatorial plane.
- ω is the perigee's argument, which is the angle between the ascending node and perigee directions measured along the orbital plane.
- a is the orbit's semi-major axis.
- e is the orbit eccentricity, the ratio between its semi-major axis and semi-minor axis.
- t_0 is the perigee passing time, when the satellite is closest to the earth.

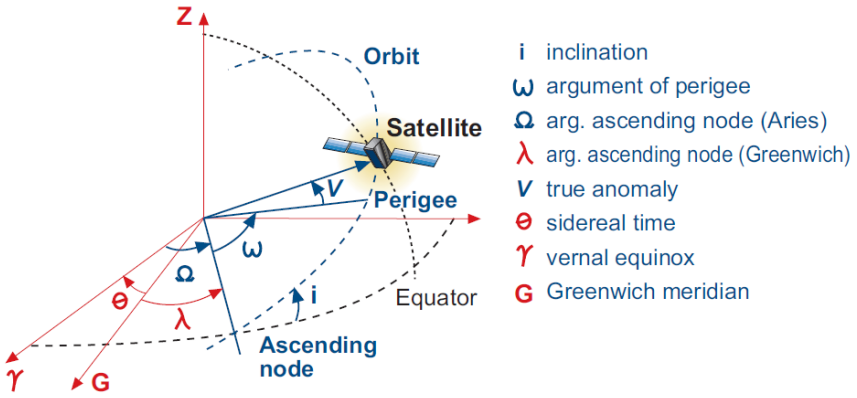

Figure 2.9 – SV Orbital Parameters (Keplerian Elements). Source: San Subirana et al. 2013.

The orbital position of a satellite can be obtained at any epoch (t), using the so-called orbital anomalies (see Figure 2.10):

- **True Anomaly $V(t)$** is the geocentric angle between the perigee direction and the satellite direction.

- **Eccentric Anomaly $E(t)$** is the angle among the perigee and an imaginary point obtained from drawing a line which is normal to the major axis and crosses through the satellite, intersecting a circle with a radius.

- **Mean Anomaly $M(t)$** is a mathematical abstraction related to mean angular motion (areolar velocity).

For satellite's clock correction, the ephemerids provide this information with three coefficients (a_0, a_1, a_2), modelling a second-degree polynomial at a given reference epoch. This reference epoch is

denoted as Time Of Ephemerids (ToE), which is transmitted in the ephemerids as well. Therefore, for computing the satellite's clock correction at any epoch t, the following expression shall be applied:

$$t_c = a_0 + a_1(t - ToE) + a_2(t - ToE)^2; \quad (2.10)$$

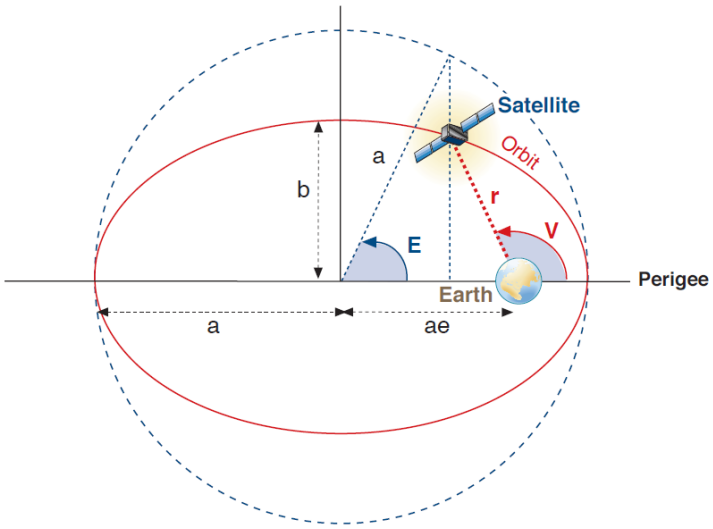

Figure 2.10 – Orbital Anomalies. Source: Sanz Subirana et al. 2013.

Satellite Position and Clock Correction at Emission Time

Table 2.3, shows the Keplerian elements and the satellite clock parameters broadcasted in the navigation message of any GPS or GALILEO SV.

Table 2.3 – Navigation message. Broadcasted parameters.

Parameter	Definition
Satellite Clock Parameters	
$\boldsymbol{ToE}$	Time of ephemerids. Reference epoch in seconds within the week (ToW format).
$\boldsymbol{a_0}$	SV clock offset against system's reference time scale (e.g. GPST)
$\boldsymbol{a_1}$	SV clock rate
$\boldsymbol{a_2}$	SV clock drift rate
Orbital Parameters	
$\boldsymbol{\sqrt{a}}$	Square root of the semi-major axis
$\boldsymbol{e}$	Orbital plane eccentricity
$\boldsymbol{\Delta_n}$	Mean motion difference
$\boldsymbol{M_0}$	Mean anomaly at ToE
$\boldsymbol{\omega}$	Argument of perigee
$\boldsymbol{i_0}$	SV inclination at ToE
$\boldsymbol{\Omega_0}$	Longitude of the ascending node at the beginning of the week
$\boldsymbol{\dot{i}}$	Rate of inclination
$\boldsymbol{\dot{\Omega}}$	Rate of node's right ascension
$\boldsymbol{Cuc, Cus}$	Cosine and sine Latitude argument corrections
$\boldsymbol{Crc, Crs}$	Cosine and sine orbital radius corrections
$\boldsymbol{Cic, Cis}$	Cosine and sine inclination correction

In order to compute the SV coordinates using the broadcast ephemerids, the following algorithm based on GAL-OS-SIS-ICD/2016 ([BR.17]) and IS-GPS-200J/2018 ([BR.15]) is presented. "An accuracy of about 5 m (RMS) is achieved for GPS satellites with S/A off" (Sanz Subirana et al. 2013, [BR.1]).

1. Solve by two iterations the emission time t_e, by applying the following expression:

$$t_e = t_r - \left(\frac{R}{c}\right) - t_c - ToE; \tag{2.11}$$

2. Where t_r is the reception time by the receiver in ToW format, R is the SV-Receiver pseudorange measurement, c denotes the speed of light and t_c stands for SV's clock correction. t_c is set to 0 in the first iteration and is computed by applying equation (2.10), where $t_e = t - ToE$. In addition, Emission time (computed in ToW format) must be protected against interpolation jumps by applying:

$$\begin{aligned} t_e &= t_e - 604800s; \ \ if\ t_e > 302400s; \\ t_e &= t_e + 604800s; \ \ if\ t_e < -302400s; \end{aligned} \tag{2.12}$$

3. Having computed the time parameters, the satellite's coordinates are computed from the Keplerian elements. Firstly, compute SV's orbit mean motion parameter:

$$n = \sqrt{\frac{\mu}{a}} + \Delta_n; \tag{2.13}$$

4. Where $\mu = 3.986004418 \times 10^{14}$, is the geocentric gravitational constant. The mean anomaly is found as:

$$M = M_0 + n \times t_e; \tag{2.14}$$

5. Eccentric anomaly can be iteratively computed (e.g. 10 iterations), where $E = M$,in the first iteration:

$$E = M + e \times \sin(E); \tag{2.15}$$

6. And true anomaly is:

$$v = \operatorname{atan}\left(\frac{\sqrt{1 - e^2} \times \sin(E)}{\cos(E) - e}\right); \tag{2.16}$$

7. The argument of latitude is found as:

$$\phi_0 = v + w; \tag{2.17}$$

8. The orbital correction terms are computed as follows:

$$\begin{aligned} \delta_u &= Cus \times \sin(2\phi_0) + Cuc * \cos(2\phi_0); \\ \delta_r &= Crs \times \sin(2\phi_0) + Crc * \cos(2\phi_0); \end{aligned} \tag{2.18}$$

$$\delta_i = Cis \times \sin(2\phi_0) + Cic * \cos(2\phi_0);$$

9. Argument of latitude, orbit radius and inclination are corrected by the following expressions:

$$\begin{gathered} \phi = \phi_0 + \delta_u; \\ r = a(1 - e \times \cos(E)) + \delta_r; \\ i = i_0 + \delta_i + \dot{i} \times t_e; \end{gathered} \tag{2.19}$$

10. The corrected longitude of the ascending node along the orbital plane parameters are defined:

$$\begin{gathered} \Omega = \Omega_0 + (\dot{\Omega} - \Omega_e) \times t_e - \Omega_e \times ToE; \\ x_{op} = r \times \cos(\phi); y_{op} = r \times \sin(\phi); \end{gathered} \tag{2.20}$$

11. Where $\Omega_e = 7.2921151467 \times 10^{-5}$ is the earth's angular speed (earth's rotation speed). Finally, satellite ECEF coordinates are obtained as:

$$\begin{gathered} X_{sat} = x_{op} - \cos(\Omega) - y_{op} \times \cos(\mathrm{i}) \times \sin(\Omega); \\ Y_{sat} = x_{op} - \sin(\Omega) - y_{op} \times \cos(\mathrm{i}) \times \cos(\Omega); \\ Z_{sat} = x_{op} \times \sin(i); \end{gathered} \tag{2.21}$$

12. Last but not the least, two additional corrections are necessary in order to obtain SV's clock bias. The first one stands for the relativistic effect correction. The second one should only be applied to single-frequency users and accounts for the group delay:

$$\begin{gathered} \delta_{TSV} = t_c + \Delta_{Trel} - \Delta_{GD}^{f2}; \\ \Delta_{Trel} = -2 \times \frac{\sqrt{\mu \times a}}{c^2} \times e \times \sin(E); \Delta_{GD}^{f2} = \left(\frac{f1}{f2}\right)^2 \times \Delta_{GD}^{f1}; \end{gathered} \tag{2.22}$$

Where $f1$ is the carrier frequency for the signal which the group delay is broadcasted and $f2$ the carrier frequency for the signal which the group delay correction is computed. GPS broadcast its group delay in the navigation message for L1 carrier frequency. GALILEO, with OS navigation data, broadcast the group delay for E1-E5a and E1-E5b frequency combinations (refer to [BR.17]).

Satellite Position at Reception Time

The previous method has introduced the algorithm for computing the SV coordinates at the time when the satellite's antenna produces the signal. However, for the user is not useful to have these coordinates at emission time but at reception time because it is a common reference for all other SV measurement. Therefore, SV coordinates must be propagated at reception time knowing the signal transmission time.

Moreover, the coordinates are tied to an ECEF frame (fixed to earth's rotation). Thus, the SV coordinate propagation will be translated in a rotation over the Z axis which lasts as much as the signal transmission time. The following algorithm retrieved from Sanz Subirana et al. 2013 ([BR.1]) is presented for this work:

1. SV ECEF coordinates are provided at emission time as:

$$r_e^{SV} = \begin{pmatrix} X_e^{SV} \\ Y_e^{SV} \\ Z_e^{SV} \end{pmatrix}; \tag{2.23}$$

2. In addition, an approximate receiver position must be provided in order to compute the transmission time:

$$r_{0_{Rec}} = \begin{pmatrix} X_{0_{Rec}} \\ Y_{0_{Rec}} \\ Z_{0_{Rec}} \end{pmatrix}; \tag{2.24}$$

3. Compute the signal's transmission time using a geometric approach (no pseudorange measurement is needed):

$$\Delta T_{Rec}^{SV} = \frac{\left\| r_e^{SV} - r_{0_{Rec}} \right\|}{c}; \tag{2.25}$$

4. Propagate the earth fixed SV coordinates at emission time (t_e) to reception time (t_r) using the transmission time. Firstly, compute the earth's rotation angle lapsed during the transmission time:

$$\theta_{t_e}^{t_r} = \Delta T_{Rec}^{SV} \times \Omega_e; \tag{2.26}$$

5. Where $\Omega_e = 7.2921151467 \times 10^{-5}$ is the earth's angular speed. Finally, apply a Z-axis rotation matrix with $\theta_{t_e}^{t_r}$ over the SV coordinates at emission time:

$$r_r^{SV} = R_Z\left(\theta_{t_e}^{t_r}\right) \cdot r_e^{SV} = \begin{pmatrix} X_r^{SV} \\ Y_r^{SV} \\ Z_r^{SV} \end{pmatrix}; \; R_Z\left(\theta_{t_e}^{t_r}\right) = \begin{pmatrix} \cos(\theta_{t_e}^{t_r}) & \sin(\theta_{t_e}^{t_r}) & 0 \\ -\sin(\theta_{t_e}^{t_r}) & \cos(\theta_{t_e}^{t_r}) & 0 \\ 0 & 0 & 1 \end{pmatrix}; \tag{2.27}$$

2.5.3 Atmospheric Effects Modelling

As previously explained, atmospheric effects on GNSS positioning are divided in two major components, the Ionosphere delay and the Troposphere delay. Is not the intention of this project to present a detailed explanation of this phenomena on GNSS measurements but to present the algorithms used to mitigate them. In order to find out more about Ionosphere and Troposphere effects, please refer to the following references: [BR.1] and [BR.5].

Several ionosphere and troposphere models for error estimation are developed in the GNSS bibliography for single-frequency users. Ionosphere models usually rely on the provision of ionosphere coefficients for modelling the delay. The coefficients are used to estimate the Slant TEC contained in the SV-Receiver

Line Of Sight (LoS) and then mapped to Vertical TEC in the receiver's zenith. These coefficients are provided through the navigation messages. Both GPS and GALILEO broadcast their own ionosphere coefficients. Nominally, GPS coefficients are used in the Klobuchar model and GALILEO coefficients in the NeQuick model.

- **Klobuchar Model**. This model was dedicated for GPS receivers and assumes that the highest TEC is located at an altitude of 350 km and it presents a daily periodicity with a maximum peak at midday and a lowest peak at midnight. The highest amplitude is represented as a cosine function of the geo-magnetic latitude and the GPS α and β coefficients; modelled by a third-degree polynomial function as illustrated in Figure 2.11. "Klobuchar's model does not remove completely the ionosphere delay and several authors point that the model compensates for the 60% to 70% during night time and 70% and 90% during day time" (Berné Valero et al. 2014, [BR.5]).

- **NeQuick Model**. This model was dedicated for GALILEO single-frequency receivers using the broadcasted GALILEO ionosphere coefficients in the navigation message. NeQuick is far more complex than Klobuchar's model, but more accurate in return. NeQuick is based on the numerical integration of the TEC in the signal's propagation along the LoS, based on the local time and the solar activity in the receiver's latitude. The detailed NeQuick algorithm is completely described in [BR.14].

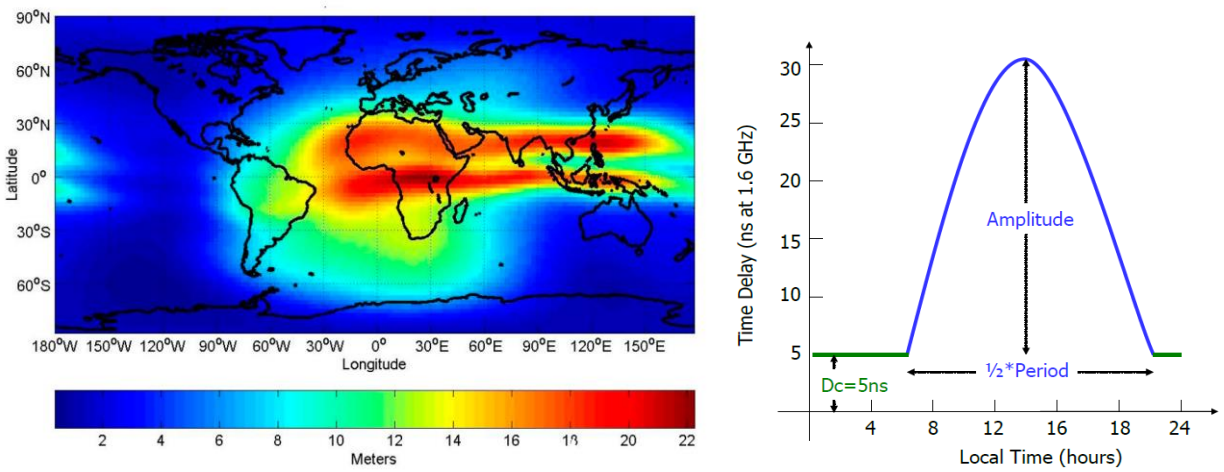

Figure 2.11 – World Ionosphere delay map extracted from TEC measurements and Klobuchar's model ionosphere amplitude modelling. Source: Sanz Subirana et al. 2013.

Troposphere delay relies on the angle in which the signal is received respect the user's horizon, (satellite elevation). Then, the slant delay is mapped in the zenithal direction of the receiver position. Troposphere delay also depends on the receiver's altitude and weather parameters. These weather parameters are normally modelled, since it is difficult to derive them from ground measurements. The most used models are Hopfield and Saastamoinen:

- **Hopfield Model**. This model was developed using experimental data obtained from long-term observations on the troposphere. The model splits the root cause of the delay in two components: a wet component and a dry one. Dry component can be easily derived from dry gas laws meanwhile wet component is much more difficult to model.

- **Saastamoinen Model**. This model establishes that the delay can be derived from the gas laws. The empiric formulae require the atmospheric pressure, the water vapor content and the temperature as inputs. Saastamoinen model provides the functions to estimate these three parameters based on the user's height. Moreover, a mapping function is introduced for a more refined model which depends on the height and the SV elevation.

For this project, Klobuchar and Saastamoinen models have been used for estimating the ionosphere and troposphere delay on the developed single-frequency positioning solution. The algorithms for both models are presented hereafter.

Klobuchar Ionosphere Model

Klobuchar's model for estimating ionosphere delay of a specific signal S carried in the frequency f, needs the following inputs:

- $\alpha_0, \alpha_1, \alpha_2$ and α_3: ionosphere coefficients retrieved from GPS navigation message.
- $\beta_0, \beta_1, \beta_2$ and β_3: ionosphere coefficients retrieved from GPS navigation message.
- φ_{Rec} and λ_{Rec}: approximate receiver geodetic coordinates both in semicircles (1 semicircle = π radians).
- Ev_{Rec}^{SV} and Az_{Rec}^{SV} : the SV-Receiver elevation over the receiver's horizon in semicircles and azimuth in radians.
- t_w: epoch seconds within GPS time of week.

The following algorithm has been extracted from [LR.1]:

1. Calculate the Earth-center angle:

$$\psi = \frac{0.0137}{Ev_{Rec}^{SV} + 0.11} - 0.22; \tag{2.28}$$

2. Compute the latitude and longitude of the Ionospheric Pierce Point (IPP):

$$\begin{gathered} \phi_i = \varphi_{Rec} + \psi \times \cos(Az_{Rec}^{SV}) \,; \phi_i = \begin{cases} 0.416; \; if \; \phi_i > 0.416 \\ -0.416; \; if \; \phi_i < -0.416 \end{cases}; \\ \lambda_i = \lambda_{Rec} + \frac{\psi \times \sin(Az_{Rec}^{SV})}{\cos(\phi_i)}; \end{gathered} \tag{2.29}$$

3. Find the geomagnetic latitude of the IPP:

$$\phi_m = \phi_i + 0.064 \times \cos(\lambda_i - 1.617) \,; \tag{2.30}$$

4. Find the local time at the IPP:

$$t_{IPP} = 43200 \times \lambda_i + t_w; t_{IPP} = \begin{cases} t_{IPP} - 86400; \; if \; t \geq 86400 \\ t_{IPP} + 86400; \; if \; t < 0 \end{cases}; \tag{2.31}$$

5. Compute the ionosphere delay amplitude, period and phase:

$$\begin{gathered} A_i = \sum_{n=0}^{3} \alpha_n \times \phi_m^n \,; \; A_i = 0 \; if \; A_i < 0; \\ P_i = \sum_{n=0}^{3} \beta_n \times \phi_m^n \,; \; P_i = 72000 \; if \; P_i < 72000; \end{gathered} \tag{2.32}$$

$$X_i = \frac{2\pi \times (t - 50400)}{P_i};$$

6. Compute the slant factor:

$$F = 1 + 16 \times (0.53 - Ev_{Rec}^{SV})^3; \quad (2.33)$$

7. Compute the ionosphere time delay and transform it to meters:

$$\Delta_{iono}^{S_{f1}} = \begin{cases} \left[5 \times 10^{-9} + A_i \times \left(1 - \frac{X_i^2}{2} + \frac{X_i^4}{24}\right)\right] \times F; if\ |X_i| \leq 1.57 \\ 5 \times 10^{-9} \times F; if\ |X_i| < 1.57 \end{cases}; \ \Delta_{iono}^{S_{f1}}[m] = \Delta_{iono}^{S_{f1}}[s] * c; \quad (2.34)$$

8. Finally, ionosphere delay is given on frequency f_1 (i.e. GPS L1). Transformation between the target carrier frequency $f = f_2$ is given by:

$$\Delta_{iono}^{S_{f2}} = \left(\frac{f_1}{f_2}\right)^2 \times \Delta_{iono}^{S_{f1}}; \quad (2.35)$$

Saastamoinen Troposphere Model

The following algorithm has been retrieved from Moreno Monge 2011 ([BR.9]). Saastamoinen's troposphere model only needs as inputs the approximate receiver's height and the SV-Receiver zenital angle:

- h_{Rec}: approximate receiver height in kilometers.
- Ze_{Rec}^{SV}: the SV-Receiver zenital angle respect to the receiver's zenith in radians.

In addition, Table 2.4 gives the interpolation table for the height dependent B mapping parameter to be applied in the model's basic correction. The saastamoinen delay is computed as follows:

$$\Delta_{trop} = \frac{0.002277}{\cos(Ze_{Rec}^{SV})} \times \left[p + \left(\frac{1255}{T} + 0.05\right) \times e_{wp} - B \times \tan^2(Ze_{Rec}^{SV})\right] + dR; \quad (2.36)$$

Where T stands for temperature in Kelvin degrees, p denotes pressure in millibars, e_{wp} is the partial pressure of water vapor, B is interpolated from Table 2.4 based on the input height and dR shall be extracted from Table 5.5 of Hoffman et.al 2008 ([BR.2]). T, p and e_{wp} are found as:

- $p = 1013.25 \times (1 - 0.000065 \times h_{Rec})^{5.225}$;
- $T = 291.15 - 0.0065 \times h_{Rec}$;
- $H = 50 \times e^{-0.0006396 \times h_{Rec}}$;
- $e_{wp} = (H \times 0.01) \times e^{-37.2465 + 0.213166 - (0.000256908 \times T^2)}$;

(2.37)

Table 2.4 – Saastamoinen B mapping parameter interpolation table.

Height (km)	B (mb)
0.0	1.156

0.5	1.079
1.0	1.006
1.5	0.938
2.0	0.874
2.5	0.813
3.0	0.757
4.0	0.654
5.0	0.563

2.5.4 Least Squares Estimation for Standard Point Positioning

The aim of single-frequency code based-based point positioning, hereafter SPP, is to determine the receiver ECEF coordinates: $(X, Y, Z)_{Rec}$ and its clock bias: $\delta_{T_{Rec}}$. Recalling section 2.1, this involves a triangulation geometric problem involving at least four SV in view with known coordinates (computed from the broadcasted ephemerids as specified in section 2.5.2): $(X, Y, Z)^{SV_j}$ and the pseudoranges retrieved from them: $R_{S_{Rec}}^{SV_j}$.

Linear Equation System

Since the pseudoranges are noisy, the corrections must account for several error sources as postulated in equation (2.7). ρ is the actual range between the SV and the receiver expressed as:

$$\rho_{Rec}^{SV_j} = \sqrt{(X^{SV_j} - X_{Rec})^2 + (Y^{SV_j} - Y_{Rec})^2 + (Z^{SV_j} - Z_{Rec})^2}; \tag{2.38}$$

This induces a non-linear system whose actual resolution is based on linearizing (2.38) from an approximate position of the receiver: $(X_0, Y_0, Z_0)_{Rec}$. The approximate SV-Receiver range is denoted as $p_{0_{Rec}}^{SV_j}$.

From the arrangement of equation (2.7) the following one is derived:

$$R_{S_{Rec}}^{SV_j} - D_{Rec}^{SV_j} \cong \rho_{Rec}^{SV_j} + c \times \delta_{T_{Rec}}; \tag{2.39}$$

Where $D_{Rec}^{SV_j} = c \times \delta_{T^{SV_j}} + \Delta_{iono}^{S_f} + \Delta_{trop}$; and the linearization of (2.38) introducing $p_{0_{Rec}}^{SV_j}$ gives:

$$\rho_{Rec}^{SV_j} = p_{0_{Rec}}^{SV_j} + \frac{X_{0_{Rec}} - X^{SV_j}}{p_{0_{Rec}}^{SV_j}} dx + \frac{Y_{0_{Rec}} - Y^{SV_j}}{p_{0_{Rec}}^{SV_j}} dy + \frac{Z_{0_{Rec}} - Z^{SV_j}}{p_{0_{Rec}}^{SV_j}} dz; \tag{2.40}$$

With $dx = X_{Rec} - X_{0_{Rec}}$, $dy = Y_{Rec} - Y_{0_{Rec}}$ and $dz = Z_{Rec} - Z_{0_{Rec}}$. And substituting (2.40) in (2.39), finally gives:

$$R_{S_{Rec}}^{SV_j} - D_{Rec}^{SV_j} - p_{0_{Rec}}^{SV_j} = \frac{X_{0_{Rec}} - X^{SV_j}}{p_{0_{Rec}}^{SV_j}} dx + \frac{Y_{0_{Rec}} - Y^{SV_j}}{p_{0_{Rec}}^{SV_j}} dy + \frac{Z_{0_{Rec}} - Z^{SV_j}}{p_{0_{Rec}}^{SV_j}} dz\ c \times \delta_{T_{Rec}}; \quad (2.41)$$

Which is the desired linear expression of equation (2.39). Equation (2.41) can be expressed in matrix notation with n observed satellites as:

$$\begin{pmatrix} R_{S_{Rec}}^{SV_1} - D_{Rec}^{SV_1} - p_{0_{Rec}}^{SV_1} \\ \cdots \\ R_{S_{Rec}}^{SV_n} - D_{Rec}^{SV_n} - p_{0_{Rec}}^{SV_n} \end{pmatrix} = \begin{pmatrix} \frac{X_{0_{Rec}} - X^{SV_1}}{p_{0_{Rec}}^{SV_1}} & \frac{Y_{0_{Rec}} - Y^{SV_1}}{p_{0_{Rec}}^{SV_1}} & \frac{Z_{0_{Rec}} - Z^{SV_1}}{p_{0_{Rec}}^{SV_1}} & c \\ \cdots & \cdots & \cdots & \\ \frac{X_{0_{Rec}} - X^{SV_n}}{p_{0_{Rec}}^{SV_n}} & \frac{Y_{0_{Rec}} - Y^{SV_n}}{p_{0_{Rec}}^{SV_n}} & \frac{Z_{0_{Rec}} - Z^{SV_n}}{p_{0_{Rec}}^{SV_n}} & c \end{pmatrix} \begin{pmatrix} dx \\ dy \\ dz \\ d\delta_{T_{Rec}} \end{pmatrix}; \quad (2.42)$$

Once dx, dy, dz and $d\delta_{T_{Rec}}$ are obtained, the receiver position is obtained along with its clock bias $\delta_{T_{Rec}}$:

$$\begin{pmatrix} X_{Rec} \\ Y_{Rec} \\ Z_{Rec} \\ \delta_{T_{Rec}} \end{pmatrix} = \begin{pmatrix} X_{0_{Rec}} \\ Y_{0_{Rec}} \\ Z_{0_{Rec}} \\ \delta_{0_{T_{Rec}}} \end{pmatrix} + \begin{pmatrix} dx \\ dy \\ dz \\ d\delta_{T_{Rec}} \end{pmatrix}; \quad (2.43)$$

This procedure could be done iteratively on each epoch, thus having a more precise approximate position on each iteration. This will improve the final receiver solution till a certain threshold is accomplished or a maximum number of iterations is reached. "In a GNSS static observation a fair estimation has converged in the third iteration. More than 4 or 5 iterations induce the risk of losing statistical reliability." (Berné Valero et al. 2014, [BR.5]).

Weighted Least Squares Estimation

The equation system presented in (2.42) with 4 SV ($n = 4$), will define a compatible system where only one possible parameter solution could be computed. However, this is not the optimal case since more SV pseudorange observations will provide redundancy to the solution. Furthermore, previous linear models have been presented neglecting the measurement residuals encompassed in ε_S from equation (2.7). In the case of $n = 4$, the solution could not give any accuracy estimation and no positioning performances could be assessed.

Consequently, the minimum SPP case is when $n \geq 5$, creating a un-determined compatible system, where the best solution possible is the one which minimizes ε_S (the observation residuals). This scenario leads to adopt a Least Squares method. More specifically, a Weighted Least Squares method (WLSQ) since the pseudorange measurement quality vary as function of the SV elevation.

Several bibliography references deeply explain the WLSQ algorithm. However, a brief introduction is presented hereafter based on Berné Valero et al. 2014 ([BR.5]), using its mathematical notation:

- The WLSQ algorithm is evolved from the one developed by Gauss-Makarov. This enumerates the following assumptions:

- Stochastic model: the observations, for this issue the pseudoranges, follow a normal distribution free of systematic errors. Where O_T denotes the observations and s_0^2 the a priori variance estimator, typically set as 1:

$$O \sim N(O_T, s_0^2); \tag{2.44}$$

- Functional model: establishes the mathematical relations between the observations and the parameters to be retrieved:

$$F(X, C) = 0; \tag{2.45}$$

- X are the parameters to be estimated through WLSQ and C the corrected observations. Following with the LSQ definition:

$$\begin{aligned} X &= X_a + dX; \\ C &= O_T + v; \end{aligned} \tag{2.46}$$

- From the previous expression it can be pointed, firstly, that the parameters are expressed as the sum of the approximate parameters (X_a) plus the estimated parameter corrections (dX). Secondly, the corrected observations are expressed as the sum of the raw observation (O_T) plus its associated residual (v).

- Expressing equation (2.45) as a linear system:

$$F(X, C) = F(X_a, O_T) + \frac{\partial F}{\partial X} dX + \frac{\partial F}{\partial C} dC = 0; \tag{2.47}$$

  - $F(X_a, O_T)$ is denoted as the independent term vector: W.
  - $\frac{\partial F}{\partial X}$ is denoted as the parameter design matrix: A.
  - $\frac{\partial F}{\partial C}$ is denoted as the observation design matrix: B.
  - $dC = v$ is the vector containing the observation residuals.

- The residual vector accomplishes a normal distribution with 0 mean and a theoretical variance (s^2):

$$\begin{aligned} v &\sim N(0, {s_0}^2 Q); \\ Q &= P^{-1}; \end{aligned} \tag{2.48}$$

- Q stands for the cofactor matrix, P the weight matrix which details the expected variance of the observations.

- Equation (2.47) can be expressed in matrix notation as:

$$F(X, C) = AX + Bv - W = 0; \tag{2.49}$$

- This model solution implies the WLSQ basic assumption of minimizing the residuals:

$$\Omega = v^T P v = minimum; \tag{2.50}$$

Now that WLSQ has been introduced, the algorithm will be specified for the GNSS SPP case exposed at the beginning:

- By taking the indirect observation reduction ($B = -I$), expression (2.49) is equivalent to equation (2.42) adding the observations residuals ($v = \varepsilon_S$):

- $W = AX - v;$

- $$W = \begin{pmatrix} R_{S_{Rec}}^{SV_1} - D_{Rec}^{SV_1} - p_{0_{Rec}}^{SV_1} \\ \cdots \\ R_{S_{Rec}}^{SV_n} - D_{Rec}^{SV_n} - p_{0_{Rec}}^{SV_n} \end{pmatrix};$$

- $$A = \begin{pmatrix} \frac{X_{0_{Rec}} - X^{SV_1}}{p_{0_{Rec}}^{SV_1}} & \frac{Y_{0_{Rec}} - Y^{SV_1}}{p_{0_{Rec}}^{SV_1}} & \frac{Z_{0_{Rec}} - Z^{SV_1}}{p_{0_{Rec}}^{SV_1}} & c \\ \cdots & \cdots & \cdots & \\ \frac{X_{0_{Rec}} - X^{SV_n}}{p_{0_{Rec}}^{SV_n}} & \frac{Y_{0_{Rec}} - Y^{SV_n}}{p_{0_{Rec}}^{SV_n}} & \frac{Z_{0_{Rec}} - Z^{SV_n}}{p_{0_{Rec}}^{SV_n}} & c \end{pmatrix}; \quad (2.51)$$

- $$X = \begin{pmatrix} dx \\ dy \\ dz \\ d\delta_{T_{Rec}} \end{pmatrix};$$

- $$v = \begin{pmatrix} \varepsilon_{S_1} \\ \cdots \\ \varepsilon_{S_n} \end{pmatrix};$$

- For the weight matrix (P), the diagonal terms are arranged according to the following expression extracted from Moreno Monge 2011 ([BR.9]). Ev is the satellite observation elevation and e_S is the expected mean error of signal S. This allows for a better fit when processing different GNSS signals:

$$P_i = \frac{\sin^2\left(Ev_{Rec}^{SV_i}\right)}{e_S^2}; \quad (2.52)$$

- If the minimum condition (2.50) is applied to the system in (2.51), the following expression is obtained:

$$(A^T \cdot P \cdot A) \cdot x = A^T \cdot P \cdot W; \quad (2.53)$$

- The steps to reach the aforementioned expression are detailed in Berné Valero et al. 2014 ([BR.5]).

- Specified for our SPP case, of 4 parameters ($m = 4$) to be estimated and n SV retrieved pseudoranges, the matrixes are dimensioned as:

- $A\ [n \times 4]$, holding the design terms for each observation and parameter: e.g. $\frac{X_{0_{Rec}} - X^{SV_j}}{p_{0_{Rec}}^{SV_j}}$
- $X\ [4 \times 1]$, holding the parameters to be estimated: dx, dy , dz and $d\delta_{T_{Rec}}$

- $W\ [n \times 1]$, holding the independent terms: $R_{S_{Rec}}^{SV_1} - D_{Rec}^{SV_1} - p_{0_{Rec}}^{SV_1}$
- $v\ [n \times 1]$, holding the residuals for each SV observed pseudorange: ε_{S_1}
- $P\ [n \times n]$, holding the weights of each observation: $P^{SV_j} = \frac{1}{\sigma_{SV_j}^2}$

- From expression (2.53), the parameter solution, the residual vector, the ex-post covariance matrix (σ_{xx}) and ex-post variance estimator (σ_0^2) can be deduced:

- $X = (A^T \cdot P \cdot A)^{-1} \cdot P \cdot W;$ (2.54)
- $Q = (A^T \cdot P \cdot A)^{-1};$ (2.55)
- $v = A \cdot X - W;$ (2.56)
- $\sigma_0^2 = \frac{v^T P v}{n-m}; m = 4;$ (2.57)
- $\sigma_{xx} = \sigma_0^2 \times Q;$ (2.58)

Finally, equations (2.54) to (2.58) shall be applied in every observation epoch t. Consequently, the position parameters and its associated errors can be postulated as:

- $X(t)_{Rec} = [X_{0_{Rec}} + dx](t) \pm \sigma(t)_x \rightarrow 68\%;$
- $Y(t)_{Rec} = [Y_{0_{Rec}} + dy](t) \pm \sigma(t)_y \rightarrow 68\%;$
- $Z(t)_{Rec} = [Z_{0_{Rec}} + dz](t) \pm \sigma(t)_z \rightarrow 68\%;$
- $\delta(t)_{TRec} = [\delta_{0_{TRec}} + d\delta_{TRec}](t) \pm \sigma(t)_{\delta_{TRec}} \rightarrow 68\%$

(2.59)

Note that sigma parameters σ_x, σ_y, σ_z and σ_{δ_T} are extracted from square-rooting the diagonal elements in σ_{xx}. Since these uncertainties follow a normal distribution, the sigma values will be representative in the 68% of the cases when a new measurement is done over the population. This is the also the area covered by $\pm 1 \times \sigma$ as shown in Figure 2.12. If more reliability is needed, sigma values shall be multiplied by a scaling factor e.g. $\pm 3 \times \sigma$ for a 99.7%.

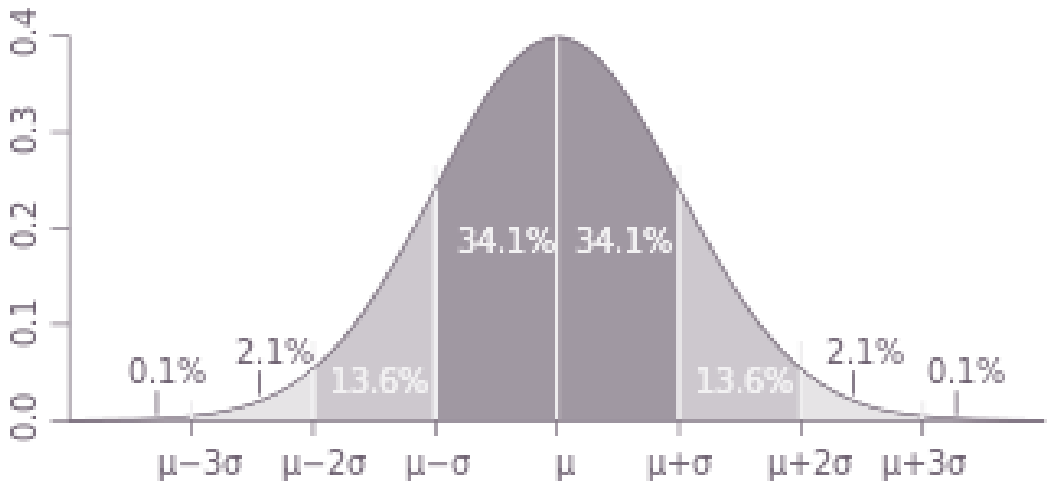

Figure 2.12 – Gaussian distribution area covered by sigma critical values. Source: Wikipedia.org.

Furthermore, since the priori variance estimator was set to 1 ($s_0^2 = 1$), the ex-post value shall be close to it ($\sigma_0^2 \cong 1$) for a good-natured WLSQ estimation:

- If $\sigma_0^2 > 1$, the actual errors are greater than those postulated in P (weight terms).
- If $\sigma_0^2 < 1$, the actual errors are smaller than those postulated in P (weight terms).
- If $\sigma_0^2 \gg 1$, this is an indicator of a bad-fitted estimation. Most likely root causes for this behavior are:
  - Bad error source mitigation (systematic errors not removed).
  - Bad a-priori variance observation estimation.
  - Wrong functional model.

2.5.5 Receiver Position Solution and Precision

So far, GNSS positions have been referred to an ECEF frame with three coordinates: X, Y and Z. However, from a user's perspective this is not intuitive because is hard for him to determine where the positioning error is located. Therefore, it is more proper to express the receiver position in a local reference system centered on a reference position close to the user. Easting e_i, Northing n_i and Upping u_i are the new components (hereafter denoted as ENU) which stand for the local increment of the receiver position solution $(X_i, Y_i, Z_i) \rightarrow (\varphi_i, \lambda_i, h_i)$ and its reference $(X_R, Y_R, Z_R) \rightarrow (\varphi_R, \lambda_R, h_R)$. The method for transforming among ECEF and ENU coordinates is by applying a rotation matrix R_{ECEF}^{ENU} over the user's geodetic position (φ, λ):

$$R_{ECEF}^{ENU}(\varphi,\lambda) = \begin{pmatrix} -\sin(\varphi) & -\sin(\varphi)\cos(\lambda) & \cos(\varphi)\cos(\lambda) \\ \cos(\lambda) & -\sin(\varphi)\sin(\lambda) & \cos(\varphi)\sin(\lambda) \\ 0 & \cos(\varphi) & sin(\varphi) \end{pmatrix}; \tag{2.60}$$

In order to obtain the ENU increments against the reference on the receiver solution, the following formula shall be applied:

$$\begin{pmatrix} e_i \\ n_i \\ u_i \end{pmatrix} = R_{ECEF}^{ENU}(\varphi_R, \lambda_R) \cdot \begin{pmatrix} X_i - X_R \\ Y_i - Y_R \\ Z_i - Z_R \end{pmatrix}; \tag{2.61}$$

Note that expression (2.61) could be applied on the accuracy indicators, the sigma parameters estimated on equation (2.59), in order to translate them in the ENU frame:

$$\begin{pmatrix} \sigma_{e_i} \\ \sigma_{n_i} \\ \sigma_{u_i} \end{pmatrix} = R_{ECEF}^{ENU}(\varphi_i, \lambda_i) \cdot \begin{pmatrix} \sigma_{X_i} \\ \sigma_{Y_i} \\ \sigma_{Z_i} \end{pmatrix}; \tag{2.62}$$

The sigma values obtained from WSLQ solution on equation (2.59) and those on equation (2.62), can be adopted in order to obtain the following precision indicators:

- $\sigma_G = \sqrt{\sigma_{X_i}^2 + \sigma_{Y_i}^2 + \sigma_{Z_i}^2 + c \times \sigma_{\delta_{Rec}}^2}$; (2.63)
- $\sigma_P = \sqrt{\sigma_{X_i}^2 + \sigma_{Y_i}^2 + \sigma_{Z_i}^2} = \sqrt{\sigma_{e_i}^2 + \sigma_{n_i}^2 + \sigma_{u_i}^2}$; (2.64)

- $\sigma_T = \sqrt{c \times \sigma^2_{\delta_{Rec}}}$; (2.65)
- $\sigma_H = \sqrt{\sigma^2_{e_i} + \sigma^2_{n_i}}$; (2.66)
- $\sigma_V = \sqrt{\sigma^2_{u_i}}$; (2.67)

Respectively, these terms denote the geometric, position, time, horizontal and vertical accuracies at 1 sigma level (reliability of 68%). As previously specified, the most significant precision indicators from a user perspective are σ_H, σ_V and sometimes σ_T along with its ENU components e_i, n_i and u_i.

2.6 GNSS Positioning Performances

The services provided by GNSS are usually assessed through navigation or positioning performances which measure the service's quality in a certain aspect, commonly based on the service's provided overall accuracy. However, the growth of GNSS applications in several demanding fields has caused new performances to be defined. This is the case for maritime and civil aviation fields where an unwarned large solution error can seriously increase the risk of an accident possibly causing injuries, large economic losses or even deaths. Furthermore, aviation users for instance, require the system to ensure fair performances during a large period of time with no interruption e.g. in the approach to landing phase. Consequently, and in addition to accuracy performance, integrity, continuity and availability performances are introduced:

- **Accuracy (or Precision)** is the error bound provided by the system's algorithms for the estimated position at a given epoch. The precision is a statistical value meaning that the navigation or position solution must have enough redundancy to provide this information fairly.

- **Integrity** is the reliability which can be placed on the system's solution. In the positioning paradigm, integrity measures if the position accuracy is representative of the actual error. Integrity is also referred as the probability of a system to provide misleading solutions e.g. phenomena which can lead to aircraft accidents.

- **Continuity** is the system's ability to perform under a certain accuracy and integrity without interruption. It is measured as the probability in which the system performances will be maintained for the duration of an operation.

- **Availability**: is the percentage of time in which the system accomplishes accuracy, integrity and continuity performances. It also represents the probability of finding a system to be available for a certain time period.

In the following subsections a deeper explanation about accuracy and integrity concepts related to GNSS positioning is done along with the specifications on these for both GPS-SPS and GALILEO-OS. On the one hand, continuity will be out of the scope of this project since it is more related with real time systems rather than post-processing ones. On the other hand, availability will not be strictly defined in this work. In return, availability will denote the percentage of time in which stipulated GPS and GALILEO precision does not over-bound the user's required accuracy.

2.6.1 GNSS Positioning Accuracy Performance

In GNSS, the measured accuracy stands for the uncertainty on the parameter estimation provided by a redundant system solution. The obtained accuracy is highly dependent on the following terms:

- **Statistical nature of the measurement errors**. As explained in equation (2.48) , these errors should follow a white noise patter (random gaussian distribution) with 0 mean and expected $s_0{}^2Q$ variance.

- **Satellite geometry**. This is a critical effect which can cause a bad precision performance as intuitively show in Figure 2.13, where a bad geometric arrangement can lead to a wider positioning error.

The SV geometry is usually denoted as Dilution Of Precission (DOP). In most of the cases, a GNSS observation with more than 8 SV is more than enough for ensuring a good DOP whereas an observation with 5 SV is potentially dangerous of having a weaker geometry. Eventually, a fair SV geometry will depend on the SV disposition over the user's sky at the observation epoch. The more the SV are uniformly spread, the better for the accuracy performance as illustrated in Figure 2.14. The satellite geometry issue is also

the cause of why the GNSS navigation solutions account for a higher error in the vertical domain than in the horizontal, since a better vertical solution will involve SV to be located beneath the ground.

As adopted in section 2.5.5, equation (2.64) to (2.67), present the accuracy parameters from the user's perspective in the horizontal and vertical components. These sigma values are given for 1 sigma of reliance level, meaning that in the case of the vertical component, the accuracy is reliable at the 68%, but for the horizontal component this will be the 39% of the cases, since it is a two-dimension measurement. This percentage is the statistical probability, or the area covered by the gaussian distribution at $\pm 1\sigma$ critical values as it was shown in Figure 2.12. In order to have a higher reliability, horizontal and vertical sigma components shall be multiplied by a scale factor to cover a higher area (probability) on the normal distribution. Table 2.5 presents these scale factors for the of one-dimension and two-dimension distributions. For instance, to obtain an accuracy performance on both vertical and horizontal components with the 95% of reliability, their sigma values should be multiplied by 1.96 and 2.45 respectively.

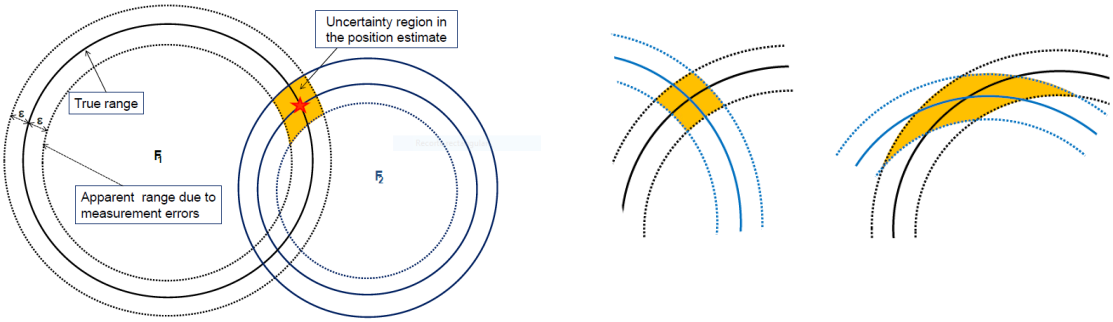

Figure 2.13 – Geometry range disposition affecting the solution precision. Source: Sanz Subirana et al. 2013.

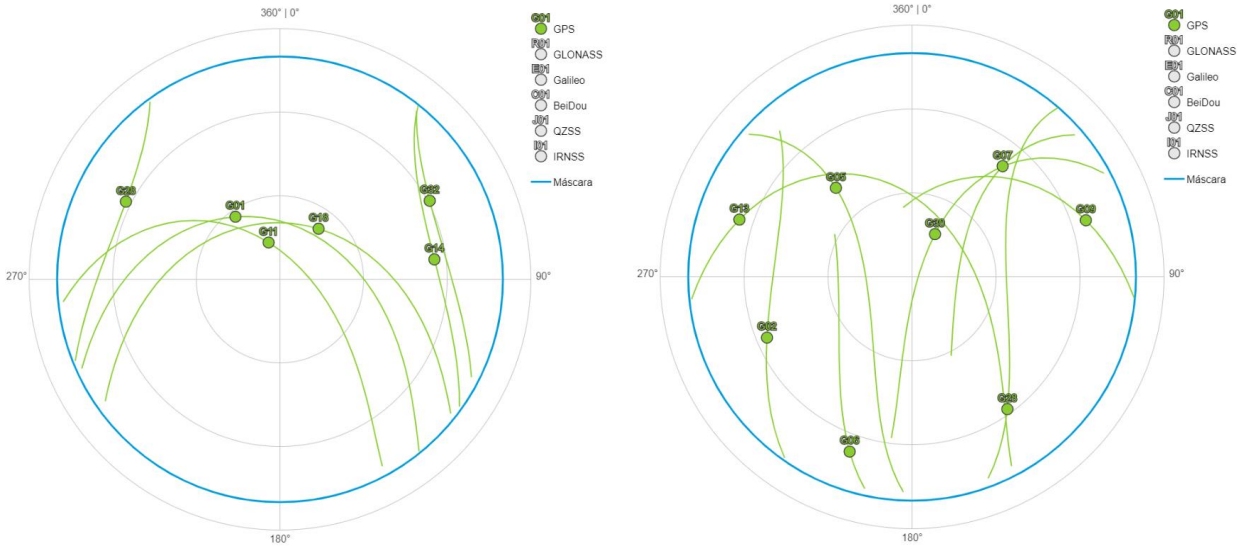

Figure 2.14 – Left: poor SV geometry configuration. Right: a much better SV geometry configuration. Source: Trimble GNSS Planner.

Finally, a fine numerical indicator for the accuracy performance obtained through n observation epochs is the so-called Root Mean Squared (RMS) trace. Accuracy RMS can be computed for both horizontal and vertical components as well as for the 3D position component from ENU sigma parameters:

- $RMS_V = \sqrt{\frac{1}{n}\sum_{i=1}^{n}\sigma_{u_i}^2} = \sqrt{\frac{1}{n}\sum_{i=1}^{n}{\sigma_V}^2}$; (2.68)
- $RMS_H = \sqrt{\frac{1}{n}\sum_{i=1}^{n}(\sigma_{e_i}^2 + \sigma_{n_i}^2)} = \sqrt{\frac{1}{n}\sum_{i=1}^{n}{\sigma_H}^2}$; (2.69)
- $RMS_P = \sqrt{\frac{1}{n}\sum_{i=1}^{n}(\sigma_{e_i}^2 + \sigma_{n_i}^2 + \sigma_{u_i}^2)} = \sqrt{\frac{1}{n}\sum_{i=1}^{n}{\sigma_P}^2}$; (2.70)

Table 2.5 – Sigma scale factors for gaussian distributions.

Scale Factor	Probability (%) for 1-D	Probability (%) for 2-D
1	68.3	39.3
1.96	95.00	TBD
2.00	95.40	86.50
2.45	98.57	95.00
3.00	99.70	98.90

GPS and GALILEO Accuracy Requirements

Table 2.6 displays the accuracy requirements for GPS SPS, using SPP techniques with C/A signal. The values based on the 95% of probability level and extracted from Hoffman et al. 2013. The values presented are very conservative since they are assuming the worst-case positioning scenario. "Furthermore, the SPS performance is usually much better than the specification. "Conley et al. (2006: p. 362) mention average values for a 20-site network of 7.1m horizontal error and 11.4m vertical error but stress the large number of possible GPS receiver configurations and integrations and the various environmental conditions" (Hoffman et al 2008, [BR.2]). In contrast, some other authors set other accuracy values (Kelly 2006): 8 and 60 meters on the horizontal and vertical components respectively for 95% of probability. For any other concerns regarding GPS SPS accuracy performance, please refer to [BR.1].

Table 2.6 – GPS Standard Positioning Service accuracy requirements.

Satellite-Only Service	GPS Standard Positioning Service	
Coverage	Global	
Accuracy (95%) for single-frequency SPP	Horizontal	Vertical
	13m	22m
Timing accuracy (95%)	40ns	

For GALILEO system, Table 2.7 shows the Open Service accuracy performances obtained with E1 signal. The accuracy requirements have been extracted as well from Hoffman et al. 2008 ([BR.2]). "Since always

the worst-case situation is considered, the service availability has to be considered the critical parameter in the performance definition […]. Galileo single-frequency receivers will provide a performance comparable to GPS C/A-code receivers." (Hoffman et al. 2008, [BR.2]). Refer to this reference for the exact definition of this parameters for GALILEO system.

Table 2.7 – GALILEO Open Service accuracy requirements.

Satellite-Only Service	GALILEO Open Service	
Coverage	Global	
Accuracy (95%) for single-frequency SPP	Horizontal	Vertical
	15m/24m	35m
Timing accuracy (95%)	30ns	

2.6.2 GNSS Positioning Integrity Performance

Under the scope of GNSS positioning, "Integrity is the measure of the trust that can be placed in the correctness of the information supplied by a navigation system" (Navipedia, [LR.2]). Some real time GNSS like SBAS are able broadcast their own integrity messages by providing alarms to users whenever the system is not suitable for navigation. This requires an Alert Limit (AL) definition.

For the GNSS static positioning case, integrity compliance can be measured by having the receiver's reference coordinates so the actual error can be determined and compared with the solution's accuracy. If the accuracy (also called Protection Limit) over-bounds the AL threshold, the system shall warn the user, hence providing integrity. Note that the tradeoff between the AL definition and the nominal accuracy is essential to define a system which accomplishes integrity performance.

Several scenarios can raise among different integrity phenomena. Firstly, true negative and false positives integrity events can occur, being the second ones the most feared. These are also known as Misleading Information events. Meanwhile, true negative phenomena will only flag the system as not available and thus losing availability performance on the way. In order to illustrate these concepts, Figure 2.15 shows the integrity events for the vertical component through time and Figure 2.16 presents the same for the horizontal component on 4 different situations.

Summing up, the following integrity events can be defined:

- **Misleading Information (MI)** events occur when the system's accuracy is passed by the actual position error, but this is kept within AL.

- **Hazardous Misleading Information (HMI)** events occur when the AL is exceeded without the system being able to notice this to the user. In other words, system's accuracy is below the AL but not the position error.

- **System Availability (SA)** is flagged as valid whenever the accuracy is within the AL and vice-versa.

As a conclusion, ideal cases will occur whenever the actual positioning error is covered by the system's accuracy, providing fair SA. The worst-case scenario would be when a high number of HMI events are taken place.

As an advance for the integrity assessment on this work, horizontal and vertical AL (HAL and VAL) can be placed by adopting the required system's accuracy performances (e.g. Table 2.6 for GPS case and Table 2.7 for GALILEO case). Consequently, and if the reference receiver coordinates are known, the

percentage of MI, HMI and SA epochs could be computed through an observation campaign. Finally, note that if the assumed statistical nature of the measurement errors is met, the measured SA should be very similar to the gaussian reliance level stipulated. For instance, if GPS horizontal accuracy is 13 meters at the 95%, SA shall be close to 95% for a reliable solution estimation.

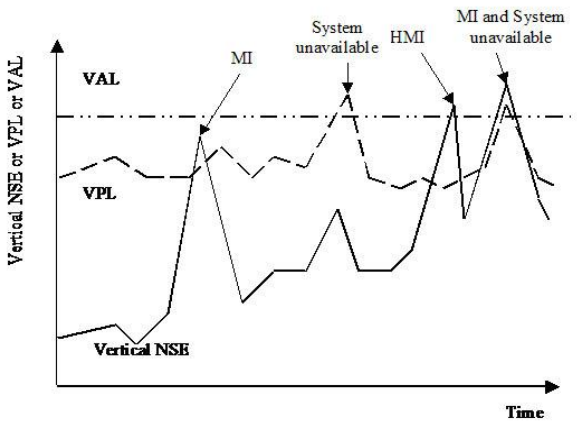

Figure 2.15 – Integrity events on vertical domain. Source: Navipedia.net.

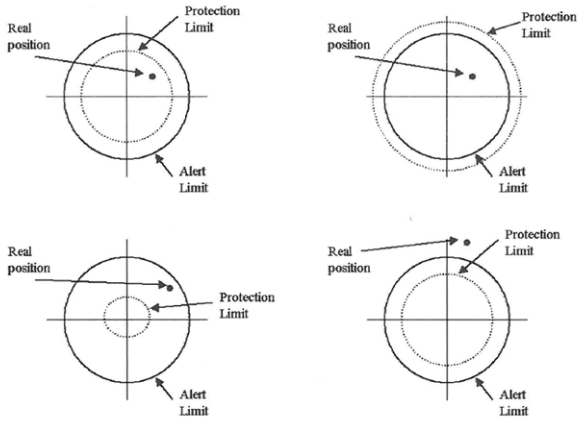

Figure 2.16 – Integrity events on horizontal domain. Source: Navipedia.net

GPS and GALILEO Integrity Requirements

On the one hand, GPS does not provide integrity performance requirements, at least on its SPS. On the other hand, one the reasons that brought GALILEO to be developed was the provision of integrity against the legacy GNSS. Unfortunately, at the time being, the integrity GALILEO service is being redefined and therefore no integrity requirements can be stipulated for its OS. Nonetheless, integrity on GNSS solutions can be measured and relatively compared between different services.

2.7 GNSS Data Formats

Even though it has been discussed the necessary data for GNSS SPP single frequency algorithms, it has not been pointed yet in which format this information can be provided.

Real time pseudoranges and navigation data are transmitted through the SV's signal, and with the proper receiver implementation, they can be decoded. Eventually, the receiver stores the data with the manufacturer's format. However, under the scope of this project, since several data sources from different receivers will be treated; it is imperative for the GNSS data to be receiver independent. In addition, the analysis study will be done in post-processing mode, meaning that no real-time implementations are needed. In this context the RINEX (Receiver INdependent Exchange) format is introduced.

The RINEX format was originally designed by the University of Bern for a better exchange of GPS data during the first large European Reference Frame (EUREF 89) realization. This was assessed with a plain text (or ASCCI) structured file which gathered the pseudoranges and carrier frequency observations related to a common timestamp (observation epoch). Due to the useful nature of this format, RINEX evolutions were translated in several file types which enclose different GNSS information as follows:

- **Observation file** contains all the GNSS measurements sources (not only pseudoranges but carrier phase or doppler) referred to the epochs in which the receiver has observed them.

- **Navigation file** gathers the broadcasted ephemerids data as transmitted by the SV navigation channel. They can also contain useful information like coefficients for ionosphere modelling.

- **Meteorological file** contains the station's atmospheric data like pressure, temperature or relative humidity.

In addition to the aforementioned types, several other spin-off standards are based on RINEX concept as well, such as SINEX (station precise coordinate information), IONEX (ionosphere accurate data) or SP3 (SV precise position).

Legacy RINEX encompass version 1 and version 2. Version 2 has been widely used and many SW products only accept this format. However, a more modern RINEX version 3 is available and enables several benefits like a better signal source identification and the enhanced use of the latest GNSS like GALILEO.

The RINEX data exchange versatility is also based on a name convention format. Tough RINEX files can be named without this convention, it is highly recommended. This is especially relevant in RINEX version 3 in order to access useful information, like RINEX file type, source constellation, receiver marker name, etc. The naming convention is deeply explained in RINEX documents [BR.8].

Since RINEX are plain text based format (.rnx extension for RINEX version 3), large observation files can occupy high portions of disk space. Thus, it is usual to encounter RINEX files compressed in Hatanaka format, denoting CRINEX files (.crx extension). The decompression of this format can be done straight forward with the binaries provided by Yuri Hatanaka in [LR.3].

In general terms RINEX files are arranged in a file header and a file body. They both are fixed structured form, meaning that no length dependents fields are allowed. This enables RINEX parsers to take advantage of template reading formats. Examples of observation and navigation RINEX files are presented in the hereafter file extracts. Further information about RINEX standard can be consulted in [BR.8].

- **RINEX V3 Observation file extract:**

```
     3.02           OBSERVATION DATA    M (MIXED)           RINEX VERSION / TYPE
NetR9 5.22          Receiver Operator   20190115 000000 UTC COMMENT
gfzrnx-1.05-6775    HEADER EDIT         20190116 012648 UTC PGM / RUN BY / DATE
YEBE                                                        MARKER NAME
13420M001                                                   MARKER NUMBER
GEODETIC                                                    MARKER TYPE
Area de Geodesia    Instituto Geografico Nacional           OBSERVER / AGENCY
5536R50061          TRIMBLE NETR9       5.22                REC # / TYPE / VERS
0180418             TRM29659.00     NONE                    ANT # / TYPE
  4848724.9050  -261632.4930  4123093.9010                  APPROX POSITION XYZ
        0.0000        0.0000        0.0000                  ANTENNA: DELTA H/E/N
G   12 C1C L1C S1C C2W L2W S2W C2L L2L S2L C5X L5X S5X      SYS / # / OBS TYPES
R   12 C1C L1C S1C C1P L1P S1P C2C L2C S2C C2P L2P S2P      SYS / # / OBS TYPES
    30.000                                                  INTERVAL
  2019     1    15     0     0    0.0000000     GPS         TIME OF FIRST OBS
G L2X -0.25000                                              SYS / PHASE SHIFT
R L1P  0.25000                                              SYS / PHASE SHIFT
R L2C -0.25000                                              SYS / PHASE SHIFT
DBHZ                                                        SIGNAL STRENGTH UNIT
 24 R01  1 R02 -4 R03  5 R04  6 R05  1 R06 -4 R07  5 R08  6 GLONASS SLOT / FRQ #
    R09 -2 R10 -7 R11  0 R12 -1 R13 -2 R14 -7 R15  0 R16 -1 GLONASS SLOT / FRQ #
    R17  4 R18 -3 R19  3 R20  2 R21  4 R22 -3 R23  3 R24  2 GLONASS SLOT / FRQ #
                                                            GLONASS COD/PHS/BIS
                                                            END OF HEADER
> 2019  1 15  0  0  0.0000000  0 13        .000000002000
R2  22650554.75805 120867759.49215       30.800                                                  22650564.92206
94008232.29106        38.500    22650564.81306
 94008233.28006        39.700
G10   22654444.02307 119050059.30307           44.900      22654450.29705   92766187.39705           33.900
22654450.08206  92766169.40406        41.600    22654445.18005
 88900871.14605        33.800
```

- **RINEX V3 Navigation file extract:**

```
     3.02           N: GNSS NAV DATA    G: GPS NAV DATA     RINEX VERSION / TYPE
NetR9 5.22          Receiver Operator   20190115 000000 UTC PGM / RUN BY / DATE
GPSA    .7451D-08  -.1490D-07  -.5960D-07   .1192D-06       IONOSPHERIC CORR
GPSB    .8806D+05  -.4915D+05  -.1966D+06   .3277D+06       IONOSPHERIC CORR
GPUT   .0000000000D+00  .355271368D-14 319488 2036          TIME SYSTEM CORR
    18    18  1929     7                                    LEAP SECONDS
                                                            END OF HEADER
G10 2019 01 15 00 00 00  .135467387736D-03 -.648014975013D-11  .000000000000D+00
      .260000000000D+02 -.340625000000D+02  .460840624433D-08  .282394335255D+01
     -.169314444065D-05  .422777992208D-02  .690296292305D-05  .515366102409D+04
      .172800000000D+06 -.670552253723D-07  .440579833061D+00 -.521540641785D-07
      .962418025762D+00  .247093750000D+03 -.278465880730D+01 -.806105006081D-08
      .392873507616D-10  .100000000000D+01  .203600000000D+04  .000000000000D+00
      .240000000000D+01  .000000000000D+00  .186264514923D-08  .260000000000D+02
      .168966000000D+06  .400000000000D+01
```

Chapter 3: Methodology

3 Methodology: Software Tool development

For committing the work purposes defined in chapter 1, it has been decided to develop a dedicated Software tool (hereafter simplified as SW) flexible enough for processing different GNSS pseudorange measurements in post-processing mode and using single-frequency SPP algorithms introduced in chapter 2.

Currently, there are already several open source tools for GNSS measurement processing, such as RTKLIB, gLAB or GAMP. As a matter of fact, the first alternative for this work was to use them to measure the target GPS and GALILEO performances. However, our own experience with these tools demonstrated a lack of flexibility and completeness from a user perspective. Some of them did not support all GPS-SPS and GALILEO-OS signals, whereas some others required of an extensive input and output treatment in order to assess integrity performance or process only E5b signal. On topo of that, the black-box nature of these tools made difficult to know the specific processing details which were taking place, like the ionosphere model.

Consequently, the feasibility of this approach was considered not to be as time-consuming as developing our own SW solution, which in return has produced a fair and flexible tool. Taking advantage of this alternative, it was then decided that the developed SW will establish a preliminary version of a new open source tool which, apart from contributing to the GNSS community, will hopefully fill the gap that was initially encountered with the other tools.

Nonetheless, the added value of making a user-oriented product implied to carry out a premeditated SW development process for producing a quality solution which will satisfy the different user needs. Note that this situation is very different from developing a single script, where is user-limited and solves one specific problem. In contrast, this case requires a precise definition of functional, performance and user necessities; along with a warranty that the SW works accordingly. As a result, it was necessary to adopt a SW engineering process for its development.

The SW engineering paradigm is based on a lifecycle workflow which implies the definition, design, implementation, verification, documentation and bug-fixing of a SW product. In the context of this project, the lifecycle adopted has been the waterfall kind (see [LR.4]), a logic ordered sequence of steps. Tough the settled waterfall model has not been strictly followed, the main steps of the SW development have been:

- **SW tool specification and definition**. This phase is intended to explain the nature and the high-level concept of the solution to be developed.

- **SW tool architecture and algorithm design**. This accounts for the detailed architecture and algorithm decomposition adopted in order to accomplish the SW specifications.

- **SW tool performance verification**. This phase verifies that the SW is compliant with the specifications by defining test cases which validate the SW features.

The upcoming sections of this chapter are dedicated to explain more deeply these steps in order to reveal the functional nature but also the complexity encompassed in the SW tool. Please, note that it is not the intention of this chapter to completely assess the SW lifecycle or to be a user manual, but to illustrate and summarize it for a better understanding of the thesis methodology.

***Note**: In spite of the fact that the developed SW tool is open-source and free of charge, a budget estimation is available in annex A.3 emulating the production cost in a commercial contract scenario.*

3.1 Specification and Definition

The first logic step when developing a SW solution is to define what the SW shall do, to whom is oriented, in which context is to be used and many other aspects. Once the main goal of the SW has been settled, this is abstracted in high level diagrams and a set of preliminary design items. These features are then decomposed in low level SW features, such as requirements and detailed design diagrams; so the detailed architecture and algorithm implementation can be performed.

The Preliminary Item Design Specifications (PIDS) adopted for this project SW are summarized in Table 3.1. In a real commercial scenario, these items would be provided by the costumer in order to specify its needs on the SW contract.

Table 3.1 – Preliminary Item Design Specifications for the SW tool.

Code	Preliminary Item Design Specification
PIDS-01	The SW shall post-process GNSS pseudorange measurements and navigation data for single-frequency SPP services.
PIDS-02	The SW shall support GPS Standard Positioning Service and GALILEO Open Services.
PIDS-03	The SW shall measure both accuracy and integrity performances whenever the receiver is in static mode.
PIDS-04	The pseudoranges and navigation data shall be provided as inputs with a GNSS-receiver independent format.
PIDS-05	The accuracy and integrity performance results shall be provided in both numerical and graphical formats.
PIDS-06	The SW shall be open source, free of charge and user oriented.
PIDS-07	The SW shall enable different processing configurations which are specified by the user.

3.1.1 High Level Architecture

From Table 3.1, a high-level architecture diagram can be drawn in order to illustrate the SW main batch sequence. This is displayed on Figure 3.1.

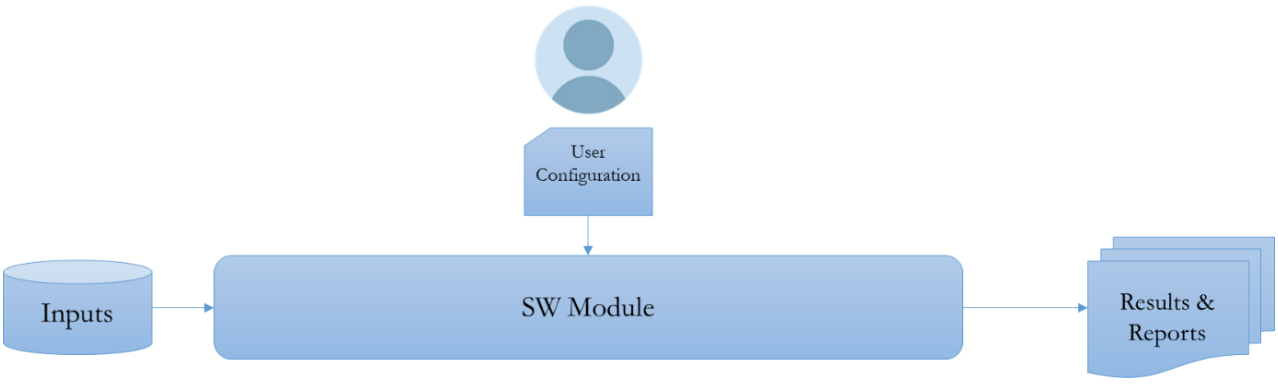

Figure 3.1 – SW tool high level architecture, first decomposition.

Figure 3.1, represents the SW highest architecture possible. However, from PIDS a lower SW architecture can be decomposed as illustrated in Figure 3.2.

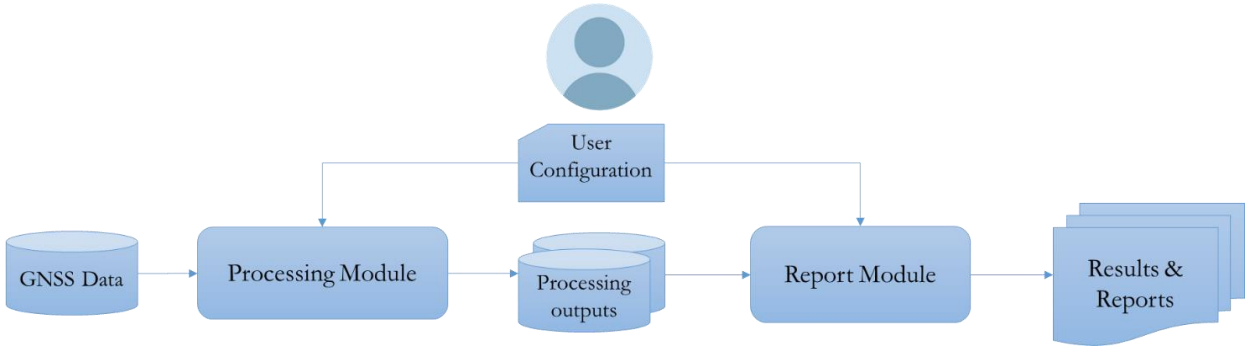

Figure 3.2 – SW tool high level architecture, second decomposition.

On the one hand, the processing module will oversee the GNSS data processing and will measure the accuracy and integrity performances. On the other hand, the report module will use the processing module outputs to show and summarize them with a proper display method. On top of that, processing and report modules will have a user configuration-dependent behavior and this configuration will be common for both modules.

Note that the architecture presented encompass all the specified PIDS. Furthermore, it is already adopting a modulated solution by splitting the SW in a processing and report modules, allowing for a more flexible and independent implementation. Further decomposition of both modules is done in section 3.2.

Lastly, both processing and report modules will be eventually maintained and executed as separated tools. This will allow more flexibility since, for instance, the user may only want to run the processing module and treat by his own the processing outputs.

Expected Inputs and Outputs

The high-level architecture has been defined. However, the definition phase should account as well for the input and output specification. From the high-level architecture presented, the following inputs and outputs can be enumerated:

- Inputs
  - **User-Configuration** encompass the user-specified processing parameters. These parameters will be specified in the SW's requirements, but they account for the different settings of the GNSS SPP algorithms, like pseudorange signal or the satellite mask. The configuration will be inserted as a plain text file and will allow the tool for a more flexible nature.

  - **GNSS Data** stands for the raw pseudoranges, the navigation data and any other necessary inputs. Since the SW is not real-time and must accept measurements from any receiver, the best possible standard to adopt is the settled RINEX version 3 format (refer to section 2.7).

- Outputs
  - **Processing outputs** will be raw numeric outputs from the SPP algorithms implemented in the processing module. For instance, they will cover satellite positions computed from the broadcasted ephemeris, Receiver-SV ionospheric correction, observations residuals from WLSQ estimation, etc. These outputs will be arranged in delimited plain text files with a column and row arrangement. For instance, rows could hold the observation epochs and columns the accuracy indicators.

- **Results and Reports** will summarize the processing outputs in numerical and graphical formats in order to display the obtained positioning performances. Besides accuracy and integrity indicators, they should also provide useful processing information like satellite availability or LSQ routine estimation results, although this has not been specified in PIDS. Results and reports will be provided in plain text file format (ASCII coded) and image plots (e.g. .png extension).

3.1.2 Requirements

The SW requirements are a detailed abstraction of the PIDS and therefore can be traced to them. They are not user demands but engineering criteria which shall be accomplish by the SW. These criteria must be precisely and unambiguously defined, not allowing for assumption presumption. Eventually, requirements are the SW baseline or main reference for all its lifecycle.

Due to the nature of this project commitment, it has been decided to split the SW requirements in three kinds for a better understanding:

- **Environment Requirements**. They refer to SW and even Hardware (HW) external components specification for the development, maintenance and execution support.

- **User Configuration Requirements**. They encompass the required parameters customization by the user which allow for a different SW processing configuration.

- **Functional Requirements**. They depict the several functionalities which the SW shall fulfill. They are subdivided for each module:
  - Processing Module Functional Requirements
  - Report Module Functional Requirements

Environment Requirements

This requirement type stands for the environments specifications where the tool is going to be developed and executed. Since our SW tool has an open-source and free of charge approach, its programming language and target Operative System (OS) should have these characteristics as well. On the HW side, the SW is expected to be executed on a common user machine e.g. personal laptop. Environment requirements are arranged in Table 3.2.

Table 3.2 – SW environment requirements.

Requirement ID	Description	Related PID
REQ-ENV-1	The SW shall be developed by open source and free of charge programming languages.	PIDS-06
REQ-ENV-2	The SW shall be developed and supported on an open source and free of charge operating system.	PIDS-06
REQ-ENV-3	The SW execution shall be supported on a computer machine with the following minimum specifications: ▪ Processor - dual core @ 2.4 GHz (i5 or i7 Intel processor or equivalent AMD)	PIDS-06

	▪ RAM - 4 GB ▪ Hard Drive - 320 GB 5400 RPM hard drive ▪ Wireless (for laptops) - 802.11g/n (WPA2 support required) ▪ Monitor - 19" LCD - desktop only ▪ Operating System – Open Source Linux Distro (Ubuntu, Fedora, RedHat, …) ▪ Backup Device - External hard drive and/or USB Flash Drive	

User Configuration Requirements

The user configuration requirements specify all the parameters which can be changed manually by the user in order to allow for different processing customization. The needed parameters have been identified thanks to the theorical framework presented in chapter 2. Nonetheless some tests during the SW development revealed that further configuration was needed. The configuration requirements are detailed in Table 3.3.

Table 3.3 – SW user configuration requirements.

Requirement ID	Description	PID Trace
	Main Configuration	
REQ-CFG-4	The SW shall require as input the GNSS system configuration among GPS or GALILEO systems.	PIDS-07
REQ-CFG-5	The SW shall require as input the receiver static mode configuration among activated or de-activated.	PIDS-07
REQ-CFG-6	The SW shall require as input the receiver integrity mode configuration among activated or de-activated if the receiver static mode has been set as "activated".	PIDS-07
	Input/Output Configuration	
REQ-CFG-7	The SW shall require as input the path of a RINEX version 3 observation file.	PIDS-07
REQ-CFG-8	The SW shall require as input the path of a RINEX version 3 GPS navigation file if GPS system has been selected or if Klobuchar ionospheric model has been selected.	PIDS-07
REQ-CFG-9	The SW shall require as input the path of a RINEX version 3 GALILEO navigation file if GALILEO system has been selected.	PIDS-07
REQ-CFG-10	The SW shall require as input the processing output path configuration.	PIDS-07
	Processing Configuration	
REQ-CFG-11	The SW shall require as input the initial and end epoch configuration.	PIDS-07
REQ-CFG-12	The SW shall require as input the interval time stamp configuration.	PIDS-07

REQ-CFG-13	The SW shall require as input the RINEX version 3 GPS pseudorange observation code among C/A or L2C signals if GPS has been selected.	PIDS-07
REQ-CFG-14	The SW shall require as input the RINEX version 3 GALILEO pseudorange observation code among E1, E5a or E5b signals, if GALILEO system has been selected.	PIDS-07
REQ-CFG-15	The SW shall require as input the Receiver-SV mask configuration.	PIDS-07
REQ-CFG-16	The SW shall require as input the excluded PRN configuration for GPS and GALILEO systems.	PIDS-07
REQ-CFG-17	The SW shall require as input the ephemerids time-out threshold configuration.	PIDS-07
	Atmosphere Modelling Configuration	
REQ-CFG-18	The SW shall require as input the ionosphere model configuration among Klobuchar or Null (no correction) models for each GPS and GALILEO systems.	PIDS-07
REQ-CFG-19	The SW shall require as input the troposphere model configuration among Saastamoinen or Null (no correction) models.	PIDS-07
	Position Estimation Configuration	
REQ-CFG-20	The SW shall require as input the mean expected measurement error configuration for GPS observations weighting, if GPS system has been selected.	PIDS-07
REQ-CFG-21	The SW shall require as input the mean expected measurement error configuration for GALILEO observation weighting, if GALILEO system has been selected.	PIDS-07
REQ-CFG-22	The SW shall require as input the delta displacement convergence threshold configuration for WLSQ estimation.	PIDS-07
REQ-CFG-23	The SW shall require as input the maximum allowed number of iterations configuration for WLSQ estimation.	PIDS-07
	Integrity Mode Configuration	
REQ-CFG-24	The SW shall require as input the receiver static reference position in WGS84 ECEF coordinates when both static and integrity modes have been activated.	PIDS-07
REQ-CFG-25	The SW shall require as input the horizontal AL and sigma scale factor configuration if integrity mode has been activated.	PIDS-07
REQ-CFG-26	The SW shall require as input the vertical AL and sigma scale factor configuration if integrity mode has been activated.	PIDS-07

Functional Processing Requirements

These requirements depict the functionality features of the processing module. They mostly account for the algorithms to be implemented but also on how the different user configuration must be allocated from a processing perspective. Processing module functional requirements are listed in Table 3.4.

Table 3.4 – SW processing module functional requirements.

Requirement ID	Description	PID Trace
	Generic Features	
REQ-FUN-27	The SW processing module shall support pseudorange measurements and navigation data for GPS and GALILEO systems.	PIDS-02
REQ-FUN-28	The SW processing module shall support WGS84 and GRS80 ellipsoid models.	PIDS-01
	Supported Inputs	
REQ-FUN-29	The SW processing module shall support and read a user-specified single RINEX version 3 multi-GNSS observation file.	PIDS-04 PIDS-07
REQ-FUN-30	The SW processing module shall support and read a user-specified single RINEX version 3 GPS navigation file.	PIDS-04 PIDS-07
REQ-FUN-31	The SW processing module shall support and read a user-specified single RINEX version 3 GALILEO navigation file.	PIDS-04 PIDS-07
	Output Formatting	
REQ-FUN-32	The SW processing module shall provide its processing information, warnings and errors in a dedicated plain text log file and in the terminal STDOUT.	PIDS-06 PIDS-07
REQ-FUN-33	The SW processing module shall provide its processing outputs on a user-specified directory.	PIDS-05 PIDS-07
	Measurement Processing	
REQ-FUN-34	The SW processing module shall process only the pseudorange measurements which fall between a user-specified initial and end epochs.	PIDS-01 PIDS-07
REQ-FUN-35	The SW processing module shall process the pseudorange measurements every user-specified interval stamp.	PIDS-01 PIDS-07
REQ-FUN-36	The SW processing module shall process the user-specified GPS-SPS pseudorange measurements among C/A or L2C signals.	PIDS-01 PIDS-02 PIDS-07
REQ-FUN-37	The SW processing module shall process the user-specified GALILEO-OS pseudorange measurements among E1, E5a or E5b signals.	PIDS-01 PIDS-02 PIDS-07

REQ-FUN-38	The SW processing module shall not process measurements from observed SV which are below a user-specified elevation mask.	PIDS-01 PIDS-07
REQ-FUN-39	The SW processing module shall not process measurements from user-specified GPS PRN numbers.	PIDS-01 PIDS-07
REQ-FUN-40	The SW processing module shall not process measurements from user-specified GALILEO PRN numbers.	PIDS-01 PIDS-07
	Ephemerids Processing	
REQ-FUN-41	The SW processing module shall accept the satellite system PRN ephemerids, coming from the RINEX navigation file, which do not exceed a user-specified time-out threshold on each observed SV.	PIDS-01 PIDS-07
REQ-FUN-42	The SW processing module shall compute for every observed SV its ECEF coordinates in WGS84 at the time reception of each processing epoch by implementing the broadcast ephemerids satellite coordinate computation algorithms specified in section 2.5.2.	PIDS-01
REQ-FUN-43	The SW processing module shall compute for every observed SV its clock bias against GPST at the emission time of each processing epoch, by implementing the broadcast ephemerids satellite clock correction computation algorithm specified in section 2.5.2, taking into account the selected signal carrier frequency.	PIDS-01
	Atmosphere Error Modelling	
REQ-FUN-44	The SW processing module shall implement Klobuchar's ionosphere correction model specified in section 2.5.3, taking into account selected signal carrier frequency, for every processing epoch and on each SV-Receiver LoS, using the alpha and beta ionospheric coefficients provided by GPS navigation message.	PIDS-01
REQ-FUN-45	The SW processing module shall be able of not applying ionosphere correction model in every processing epoch.	PIDS-01
REQ-FUN-46	The SW processing module shall implement Saastamoinen's troposphere correction model specified in section 2.5.3, for every processing epoch and for each SV-Receiver LoS.	PIDS-01
REQ-FUN-47	The SW processing module shall be able of not applying troposphere correction model in every processing epoch.	PIDS-01
	Receiver Parameter Estimation	
REQ-FUN-48	The SW processing module shall estimate the receiver position ECEF coordinates in WGS84 and its clock bias against GPST time scale for every processing epoch by implementing the algorithms specified in section 2.5.4.	PIDS-01
REQ-FUN-49	The SW processing module shall set the weight terms for GPS measurements with the user-specified observation mean error as indicated in equation (2.52).	PIDS-01 PIDS-07

REQ-FUN-50	The SW processing module shall set the weight terms for GALILEO measurements with the user-specified observation mean error as indicated in equation (2.52).	PIDS-01 PIDS-07
REQ-FUN-51	The SW processing module shall stop estimating the receiver position solution, on every processing epoch, if a user-specified delta displacement threshold is reached respect to the previous iteration of the same processing epoch.	PIDS-01 PIDS-07
REQ-FUN-52	The SW processing module shall stop estimating the receiver position solution, on every processing epoch, if a user-specified maximum number of iterations is reached in the same processing epoch.	PIDS-01 PIDS-07
	Performance Indicators	
REQ-FUN-53	The SW processing module shall estimate the positioning accuracy indicators from WLSQ routine and provide them as specified in section 2.5.5 for each processing epoch.	PIDS-01 PIDS-03
REQ-FUN-54	The SW processing module shall flag for the horizontal domain the integrity MI, HMI and SA events on each processing epoch if the integrity mode is activated.	PIDS-03
REQ-FUN-55	The SW processing module shall flag for the vertical domain the integrity MI, HMI and SA events on each processing epoch if the integrity mode is activated.	PIDS-03

Functional Report Requirements

Finally, report module requirements listed in Table 3.5 specify the functional aspects of the user-end results and plots. Although from PIDS decomposition, only positioning performance reports are needed, the report module will also provide further information depicted from processing outputs, such as observation residuals or satellite availability among many others. This has been worthy for illustrating GNSS processing concepts and for many other reasons like bug detection and mitigation during the SW development.

Table 3.5 – SW report module functional requirements.

Requirement ID	Description	PID Trace
	Output Formatting	
REQ-FUN-56	The SW report module shall provide its report results on a user-specified directory.	PIDS-05
REQ-FUN-57	The SW processing module shall provide its processing information, warnings and errors in a dedicated plain text log file and in the terminal STDOUT.	PIDS-05
	Numeric Reports	
REQ-FUN-58	The SW report module shall provide in a plain text format the measured accuracy RMSE for horizontal, vertical and position domains as specified in section 2.6.1.	PIDS-05

REQ-FUN-59	The SW report module shall provide in a plain text format the mean position error against its reference for horizontal, vertical and position domains (ENU components) if static mode is activated.	PIDS-05
REQ-FUN-60	The SW report module shall provide in a plain text format the integrity performance indicators: MI, HMI and SA cases; for the horizontal and vertical domains if both static and integrity modes are activated.	PIDS-05
	Graphical Reports	
REQ-FUN-61	The SW report module shall display in a 2D plot the horizontal receiver positions errors against its reference, Easting and Northing components, of each processing epoch if static mode is activated.	PIDS-05
REQ-FUN-62	The SW report module shall display in a 2D plot the vertical receiver position errors against its reference, Upping component, of each processing epoch if static mode is activated.	PIDS-05
REQ-FUN-63	The SW report module shall display in a 2D plot the measured accuracies in the horizontal, vertical and position domains (ENU components) of each processing epoch.	PIDS-05
REQ-FUN-64	The SW report module shall display in a 2D plot the integrity performance information: system accuracy, system error, AL, MI, HMI and SA; of each processing epoch, for the horizontal and vertical domains and if both static and integrity modes are activated.	PIDS-05

3.2 Architecture and Algorithm Design

Once the SW features have been precisely defined, the detailed design regarding the architecture and algorithm composition can be assessed.

But first, some detailed technical implementations need to be specified. These generic details stand for the Operative System (OS) and the programming language used for developing and executing the SW. Note that these two features will be conditioned from the environment requirements specified in the previous section of this chapter.

- **Operative System**. The free of charge and open source paradigm is indisputably the Linux kernel-based OS. Therefore, the SW has been developed under Ubuntu MATE distro, Long Term Support version 16.04 (more information on Ubuntu MATE official website [LR.5]). Nonetheless, the SW could be run on any Linux distro OS as far it has the required programming language environments.

- **Programming Language**. The chosen programming language for the SW development has been the Practical Extraction and Reporting Language, or Perl for short, version 5.26 (more information on Perl official website [LR.6]). In addition, the processing module will use the Perl Data Language (PDL) extension for matrix algebra and other math operations, and the report module will take advantage of Gnuplot language, version 5.2 (see web link [LR.9]) in order to produce the graphical displays.

Figure 3.3 – Ubuntu MATE distro icon. Source: ubuntu-mate.org

Figure 3.4 – Perl programming language icon. Source: perl.org

The many advantages of choosing Ubuntu and Perl environments counteract the fewer drawbacks which came along in this project's context:

- On the one hand, Ubuntu and Perl are compliant with the environment requirements specified in section 3.1.2, since they are both open source and free of charge. In addition, Ubuntu MATE OS HW requirements cover the ones specified in REQ-ENV-3.

- On the other hand, Perl programming language is an interpreted programming language which allows dynamic memory treatment. Thus, tedious memory initialization is not needed but can be done "on the run" while the algorithm is executing. This combined with its hash data structure, makes Perl a very appealing choice for an efficient SW interface modulation.

In the computer science context, a hash is a structure which builds a direct relation among two variables. A Perl hash is composed as a list of keys-value pairs which can only be scalar variable types: characters, string or numbers. However, scalars can also hold variable and code references (memory addresses) allowing Perl hashes to build complex structures which can contain arrays or subsequent hashes (see [LR.7]).

Indeed, extrapolating the hash concept to the SW paradigm, a hash can act as input/output interface in order to be used by the SW modules. This also allows for accessing data "on-the-fly" and not depending of a long-list of input/output interface. However, a hash-based SW requires of a detailed definition of the

interfaces for the algorithms to access the data homogeneously. The Perl hash-interfaces of the SW are exemplified in annex A.4.

By having specified this implementation approach, the high-level architecture presented in section 3.1.1 can be further depicted with the aforementioned hash-interface elements as shown in Figure 3.5. Note that an extra SW item has been added, the Configuration Parser module. This will be in charge of reading the user configuration and translate it into a generic configuration interface which can be used by the processing and report modules.

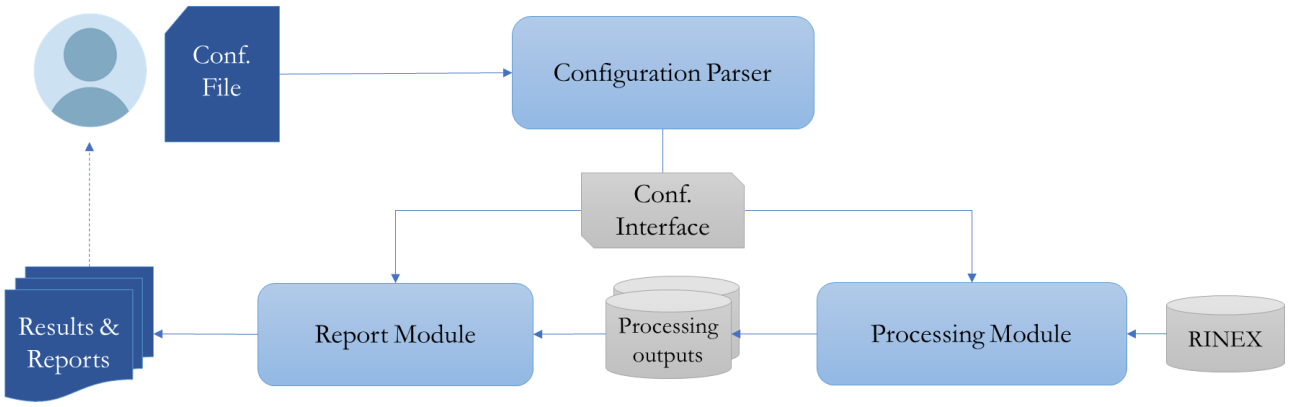

Figure 3.5 – Processing flow diagram.

Furthermore, Perl programs can be composed of package modules (.pm extension) or script files (.pl extension). Packages are divided in Perl functions or subroutines, meanwhile Perl scripts can contain subroutines, but they execute a main routine. The packages can be loaded in a Perl scripts in order to execute its subroutines. However not all subroutines are imported by default, in the package exportation properties, a list of exported subroutines must be specified. These exported features are known as public subroutines whereas package items which are not exported are the private subroutines.

The following subsections contain each of the SW Perl modules architecture and public subroutine specification. Please note that not all SW features are covered in this section since deeper SW specification is out of scope of the project's methodology explanation. Nevertheless, SW details can be explored by source code inspection (refer to annex A.1).

3.2.1 User Configuration Module

It can be deduced from Figure 3.5 that a user configuration parser is needed in order to create a common configuration interface.

This module is available in the source code as a single Perl package named *GeneralConfiguration.pm*. The module's purpose is to read the user's configuration file (see example in annex A.2) with the processing parameters specified in section 3.1.2, and translate them into a hash which follows the common-configuration hash-interface. In addition, configuration module also exports constant information such as GNSS signal frequencies or satellite system RINEX codes.

Module Architecture

The Configuration modules is made of a single Perl package and therefore no detailed architecture diagram is presented.

Public Subroutine Specification

The configuration module exports the following public subroutines:

- **LoadConfiguration** is in charge of reading the configuration file provided by the user and build the common-configuration hash-interface (see an interface example in annex A.4). The subroutine basically loads the input file in memory and parses it by taking advantage of the Perl built-in regular expression functionalities. The parsed parameters are then saved in the configuration hash. The subroutine also makes consistency checks while reading the parameters e.g. checks that the configured satellite mask is a numeric parameter. If the parameters are not properly set, the subroutine will raise an error indicating the erroneous configured parameter and its cause (see Terminal Demo 1). This subroutine implements all the User Configuration Requirements (REQ-CFG-4 to REQ-CFG-26).

Terminal Demo 1 – Wrong user configuration example.

```
# Troposphere model has been configured wrong in the following configuration file:
ppinto@ppinto-UbuntuVM:~/WorkArea/cfg$ grep Troposphere tst/wrong_parameters.cfg
Troposphere Model     :  Jaastamoinen

# When LoadConfiguration subroutine is called, it raises a configuration error and the execution is aborted:
ppinto@ppinto-UbuntuVM:~/WorkArea/cfg$ $GRPP tst/wrong_parameters.cfg
*** 2019/06/05 18:54:56 *** ERROR:30405 ***
***     - Troposphere model 'Jaastamoinen' is not supported
***     - Supported models are: none, saastamoinen

*** 2019/06/05 18:54:56 *** ERROR:30405 *** at /home/ppinto/WorkArea/src/GeneralConfiguration.pm line 659.
Configuration file loading error at /home/ppinto/WorkArea/src/GNSS_RINEX_Post-Processing//MainRoutine.pl line
85.
```

- **CheckConfigurationFile** this subroutine makes simple checks on the provided configuration file. The checks are not made over the configured parameters but on the file itself. It checks that the file exists, has plain text format and has user reading permissions. This subroutine is called when the processing or report modules receive a raw configuration file before parsing it.

3.2.2 Processing Module: GNSS RINEX Post-Processing

The processing module constitutes the core element of the SW since it processes the RINEX data using single-frequency pseudorange SPP algorithms presented in chapter 2. Consequently, the module has been named: GNSS RINEX Post-Processing, hereafter GRPP.

Module Architecture

It can be deduced from functional processing requirements in section 3.1.2 that GRPP is likely to present a certain complexity. Therefore, SW decomposition is essential in order to depict its architecture into simpler elements. GRPP architecture approach is package-oriented which encompass the following Perl packages:

- **RinexReader.pm** encompass the subroutines which read the RINEX files and store their information in internal GRPP observation and navigation hash-interfaces.

- **SatPosition.pm** holds the implemented algorithms for estimating the satellite position and clock bias using the navigation data retrieved from RinexReader package.

- **RecPosition.pm** encompass the algorithms for estimating the user's receiver position and clock bias at the processing epochs using the observation data retrieved from RinexReader package and the satellite positions from SatPosition package.

- **ErrorSource.pm** constitutes the subroutines for modeling the error sources in the pseudorange observations. So far, the package only supports atmosphere error modelling since satellite clock modelling is done in SatPosition package.

- **DataDumper.pm** holds the subroutines for dumping the computed data through all the other modules. The processing data is passed through a GRPP internal observation-data hash-interface.

The package hierarchy is presented in Figure 3.6. Note that not all packages are independent, but they maintain a hierarchical relation. For instance, RecPosition needs to import ErrorSource for estimating the atmosphere corrections in each LoS when building the pseudorange equations for the WLSQ algorithm. Also note that all GRPP packages load the GeneralConfiguration module and a Library Perl Module.

This library stands for a recopilation of common subroutines and constants used throughout all SW modules. It consists of several individual packages: MyUtil.pm, MyPrint.pm, MyMath.pm, TimeGNSS.pm and Geodetic.pm. For instance, MyMath package includes the WLSQ algorithm whilst TimeGNSS encapsulates all the conversion time functions for GNSS time scale management. More details about library module can be found by code inspection (refer to annex A.1).

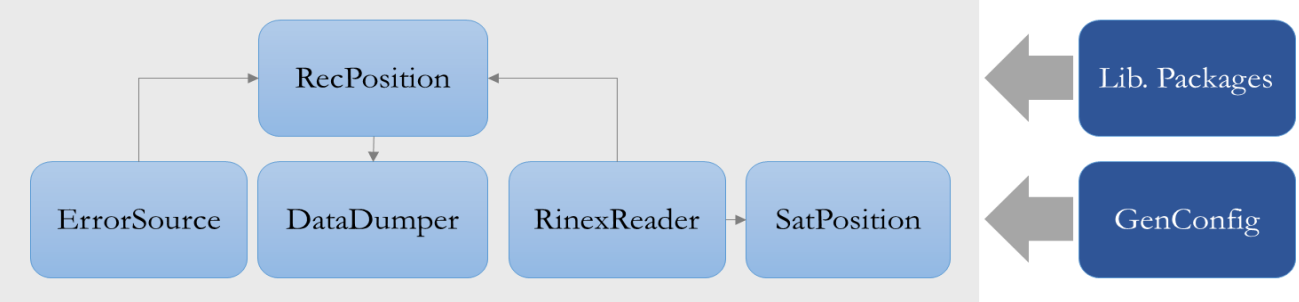

Figure 3.6 – GRPP architecture hierarchy diagram.

Public Subroutine Specification

GRPP tool uses the following public subroutines exported by each of the packages. For the sake of clarity, not all subroutines have been included, only the most relevant:

- RinexReader:
  - **ReadObservationRinexV3** reads a RINEX version 3 observation file, as specified in REQ-FUN-29. The retrieved data is stored in a hash which follows the observation-data hash-interface (exemplified in annex A.4). The subroutine also checks that the configured observations are present on the file and only stores the observations which fall in the time configuration specified by the user (see REQ-FUN-34 and REQ-FUN-35).

  - **ReadNavigationRinex** reads a RINEX version 2 or 3 navigation file as specified in REQ-FUN-30 and REQ-FUN-31. The navigation data is stored as well in hash which follows a navigation-data hash-interface. Technically, the sub can only read GPS and GALILEO navigation files since the data is arranged differently for each system (for instance, GLONASS has its own arrangement). In order to solve this, the ephemerids block subroutines are called by reference depending on the treated satellite. In addition, the reading takes in consideration the navigation data sources. For

GPS this is always the same but for GALILEO it can vary depending on the signal service (see [BR.8]).

- SatPosition:
  - **ComputeSatPosition** computes the position and clock bias of each observed SV on each processing epoch by implementing the algorithms specified in REQ-FUN-42 and REQ-FUN-43. Nonetheless, the SV must select valid ephemerids from the navigation-data hash before proceeding to the computation. The ephemerid selection criteria is based on REQ-FUN-41. Furthermore, since navigation data reading for GPS and GALILEO was different, the SV position computation and ephemerids selection take this into account. Specifically, they account for the GALILEO data source when selecting the ephemerids, and the different ephemerid arrangement when computing the SV clock bias correction.

- RecPosition:
  - **ComputeRecPosition** estimates the receiver position and its clock bias along with its associated accuracy by implementing the functional requirements: from REQ-FUN-48 to REQ-FUN-52. This involves that the WLSQ routine stops iterating when it reaches a maximum number of iterations or when the position solution has converged. Moreover, the subroutine also discards those observed SV which fall below the configured mask as indicated in REQ-FUN-38. Finally, and if both static and integrity modes have been activated, the integrity performance indicators are computed as specified in REQ-FUN-54 and REQ-FUN-55.

- ErrorSource:
  - **NullIonoDelay** and **NullTropoDelay** they return zero delay estimation for ionosphere and troposphere corrections. These subroutines fulfill REQ-FUN-45 and REQ-FUN-47.

  - **ComputeIonoKlobucharDelay** estimates the ionosphere delay through Klobuchar's model for the selected signal carrier frequency. This subroutine fulfills REQ-FUN-44.

  - **ComputeTropoSaastamoinenDelay** estimates the troposphere delay through Saastamoinen's model. The subroutine fulfills REQ-FUN-46.

- DataDumper:
  - **DumpRecPosition** writes the receiver position solution and clock bias for each observation epoch. The receiver position is outputted in ECEF and geodetic coordinates along with its sigma values. In addition, and if the static mode has been activated, the receiver ENU components and its accuracy indicators are also outputted.

Table 3.6 – Receiver position raw output.

# > Receiver marker 'CEBR' adjusted coordinates.												
# > Reference system for ECEF coordinates : WGS84												
# > Reference coordinates from static mode 'igs'												
#ECEF_X	ECEF_Y	ECEF_Z	GEO_Lat	GEO_Lon								
4846664.92	-370195.201	4116929.52	40.45342914	-4.36785259								
EpochGPS	Status	NumObs	ECEF_X	…	Sigma_X	…	Sigma_E	…	GEO_Lat	…	REF_IE	…
1241740800	1	9	4846665.771	…	0.858	…	0.669	…	40.4534217	…	0.355	…
1241740830	1	9	4846666.002	…	0.793	…	0.619	…	40.4534213	…	0.333	…
…	…	…	…	…	…	…	…	…	…	…	…	…

- **DumpSatPosition** writes the satellite positions and its clock bias computed from its navigation data for each observation epoch. The satellite coordinates are given in both ECEF and geodetic formats.

- **DumpNumValidSat** outputs the satellite availability metrics on each observation epoch. These metrics are: number of observed satellites, number of satellites with no-null observation, number of satellites with valid navigation position and number of satellites to enter in WLSQ routine.

Table 3.7 – Number of valid SV raw output.

# > Satellite system 'G' number of valid satellites.				
# > Selected observation for G -> C1C				
EpochGPS	AvailSat	ValidObs	ValidNav	ValidLSQ
1241740800	10	9	9	9
1241740830	10	9	9	9
…	…	…	…	…

- **DumpInfoBySat** outputs satellite related information such its estimated residuals from WLSQ algorithm, or its computed ionosphere delay. It also outputs the satellite observed azimuth and elevation.

Table 3.8 – Residuals per SV raw output.

# > Receiver-Satellite 'G' LSQ residuals.									
# > Configured mean_obs_err for 'G' -> 3.000									
# > Resiudals are refered to last LSQ iteration									
EpochGPS	Status	NumIterLSQ	G01	G02	…	G19	G22	…	G32
1241740800	1	3	0.991	-0.747	…	-0.657	-1.191	…	NaN
1241740830	1	3	0.568	-0.293	…	-0.759	-0.845	…	NaN
…	…	…	…	…	…	…	…	…	…

- **DumpLSQReportByEpoch** writes the WLSQ information per observation epoch. This is: number of parameters, number of observations, degrees of freedom, ex-post standard deviation estimator, convergence status and, the approximate and estimated parameters.

Table 3.9 – WLSQ report raw output.

# > Least Squares Report by observation epoch.											
EpochGPS	Iter	Status	Convergence	NumObs	Parameter	DegOfFree	StdDevEstimator	ApxX	…	dX	…
1241740800	3	1	0	9	4	5	0.1	4846664.918	…	0.448	…
1241740830	3	1	0	9	4	5	0.1	4846665.771	…	-0.174	…
…	…	…	…	…	…	…	…	…	…	…	…

- **DumpEpochSigma** writes the accuracy indicators specified in section 2.6.1 per observation epoch. The sigma values are in essence the accuracy indicators. By default, no sigma scale factor is applied.

Table 3.10 – Accuracy report raw output.

# > Accuracy (sigma) report.						
# > Reference ECEF frame : WGS84						
# > Reference ENU frame : Local receiver position						
EpochGPS	Status	SigmaG	SigmaP	SigmaT	SigmaH	SigmaV

1241740800	1	1.378	1.164	0.736	0.894	0.916
1241740830	1	1.273	1.076	0.680	0.827	0.845
…	…	…	…	…	…	…

- **DumpIntergrityInfo** writes the integrity indicators specified in section 2.6.2 along with their precision (with the configured sigma scale factor) and actual error. The information is split for vertical and horizontal domains. The outputs are only available when both static and integrity modes have been activated.

Table 3.11 – Vertical integrity report raw output.

# > Vertical integrity information.								
# > 'Status' refers to receiver position estimation								
# > Created : 2019/06/14 19:56:08								
EpochGPS	Status	SigmaScaleFactor	AlertLimit	Error	Precision	MI	HMI	Available
1241740800	1	1.96	30	0.374	1.796	0	0	1
1241740830	1	1.96	30	0.643	1.658	0	0	1
…	…	…	…	…	…	…	…	…

Module Execution

In order to maintain GRPP as a single tool and with a user-friendly usage, GRPP is orchestrated by a single Perl script, which is called in order to run the module as a whole:

- **MainRoutine.pl** manages GRPP public subroutines in order to run the tool with the user configuration. The main routine is subdivided in three steps:
  - **Configuration Loading** imports GeneralConfiguration package, check and loads the user configuration parameters.
  - **Data Processing** manages the processing routine by reading the RINEX data, computing the satellite positions and finally computing the receiver positions.
  - **Data Dumping** creates the GRPP outputs by dumping the processed data pushed in the GRPP internal hashes. In addition, it dumps in binary format the common-configuration and observation-data hashes for other Perl scripts to recover them if needed.

GRPP package and public subroutine arrangement by MainRoutine can be illustrated by its processing flow diagram in Figure 3.7.

In Figure 3.7, the GRPP hash-interface flow is better understood. Note that:

- RinexReader package is in charge of initializing the observation data hash and then this is received and updated by SatPosition and RecPosition.
- SatPosition also initializes and fills navigation data hash which contains all the SV ephemerids.
- Navigation data hash is transmitted to RecPosition in order to retrieve the ionosphere coefficients if needed by the input configuration.
- ErrorSource is plugged into RecPosition for importing the ionosphere and troposphere correction subroutines.

- All packages make use of the configuration hash-interface and thus, the user cannot execute their public subroutines without it.

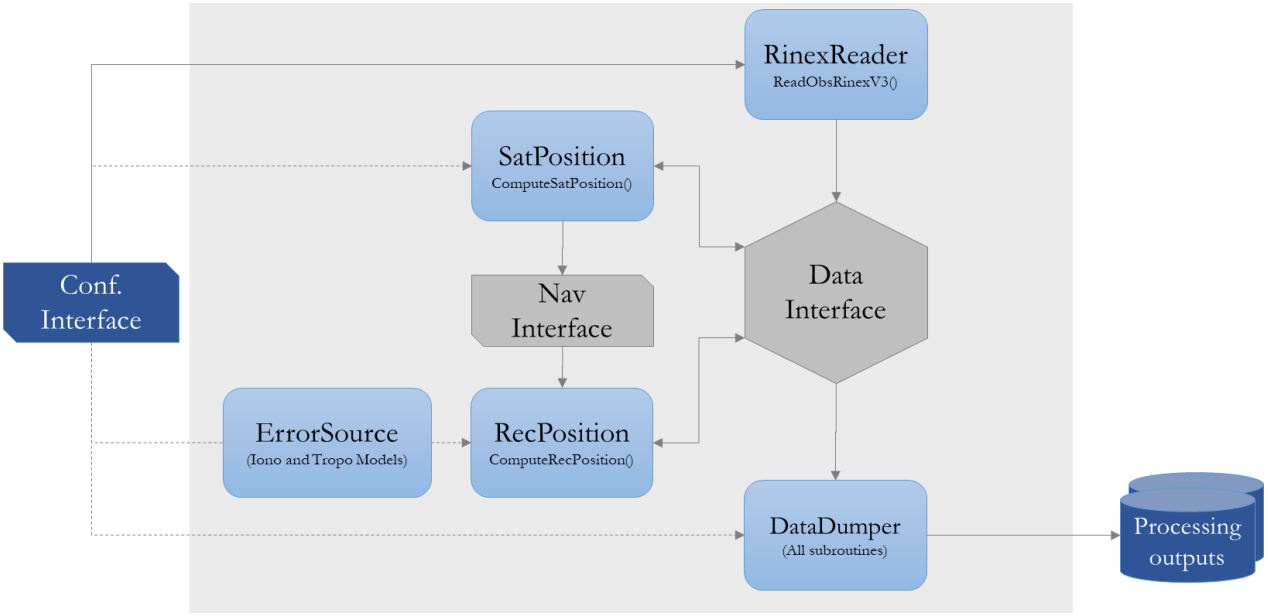

Figure 3.7 – GRPP architecture flow diagram.

Finally, to illustrate how a user would run GRPP, a Linux terminal example is contained in Terminal Demo 2. This example launches GRPP for GALILEO-OS E1 verification case (see section 3.3.2). The only input received by GRPP is the user configuration file (see annex A.2). When launching GRPP MainRoutine, the scripts starts to print useful information to the user like:

- Configuration brief.
- Which part of the tool is being executed.
- Any processing warnings such as a processing epoch with invalid solution status or a SV with no selected ephemerids.
- Receiver position summary containing ECEF coordinates and its standard deviation accuracies, along with the percentage of valid and invalid solution status.
- Where the outputs have been allocated.
- The time which took to execute the public subroutines and the entire GRPP processing.

Terminal Demo 2 – GRPP launching example for GALILEO-OS E1 on KOKV IGS station.

```
ppinto@ppinto-UbuntuVM:~/WorkArea/demo$ $GRPP cfg/KOKV_GAL-E1.cfg

# ########################################################################## #
# > Welcome to GNSS Rinex Post-Processing tool                               #
# ########################################################################## #

# Script was called from  : '/home/ppinto/Drive/tmp/MASTER/TFM/src/GNSS_RINEX_Post-Processing/MainRoutine.pl'
# Configuration file used : '/home/ppinto/Drive/tmp/MASTER/TFM/demo/cfg/KOKV_GAL-E1.cfg'

# ========================================================================== #
# > Configuration brief of 'KOKV Demo'                                       #
# ========================================================================== #
# > Selected Satellyte Systems and Observation                               #
# .......................................................................... #
#       - GALILEO (E) -> E1 (C1X)

# > Satellite Mask configuration                                             #
# .......................................................................... #
```

```
#       - Elevation threshold = 10 [deg]
#       - Discarded GALILEO satellites : E14, E18

# > Error Source Models                                                    #
# ........................................................................ #
#       - Troposphere model : Saastamoinen
#       - GALILEO Ionosphere model : Klobuchar

# > Rinex Input files                                                      #
# ........................................................................ #
#       - Observation Rinex : KOKV00USA_R_20183520000_01D_30S_MO.rnx
#       - GALILEO Navigation Rinex : KOKV00USA_R_20183520000_01D_EN.rnx

# > Processing time window                                                 #
# ........................................................................ #
#       - Start time = 2018/12/18 00:00:01 (GPS time = 1229126401)
#       - End time   = 2018/12/18 07:00:00 (GPS time = 1229151600)
#       - Interval   = 30 [sec]
#       - Number of epochs = 840

# > Static Mode Configuration                                              #
# ........................................................................ #
#       - Static mode : IGS
#       - IGS station : KOKV
#       - Reference ECEF (X, Y, Z) = -5543838.239 -2054586.439  2387810.121
#       - Reference Geodetic (lat, lon, h) = 22.1262643 -159.6649309 1167.360

# ======================================================================== #
# > Data Processing routine has started                                    #
# ======================================================================== #

# > Reading Observation Rinex...                                           #
# ........................................................................ #

# > Computing satellite positions...                                       #
# ........................................................................ #

# > Computing receiver positions...                                        #
# ........................................................................ #
***   2019/06/16   18:57:32   ***   WARNING:90305   ***   at   /home/ppinto/WorkArea/src/GNSS_RINEX_Post-
Processing/RecPosition.pm line 275.

# > Receiver position summary:                                             #
#       Observation epoch : 2018/12/18 00:00:30 -> Status = OK
#       |  X |  Y |  Z = -5543833.009 | -2054584.615 |  2387809.444 |
#       | sX | sY | sZ =       16.535 |        4.522 |        4.848 |

#       Observation epoch : 2018/12/18 00:01:00 -> Status = OK
#       |  X |  Y |  Z = -5543837.207 | -2054585.560 |  2387810.140 |
#       | sX | sY | sZ =       15.490 |        4.251 |        4.557 |

#       Observation epoch : 2018/12/18 00:01:30 -> Status = OK
#       |  X |  Y |  Z = -5543836.577 | -2054585.698 |  2387810.395 |
#       | sX | sY | sZ =       15.583 |        4.291 |        4.601 |

#       Observation epoch : 2018/12/18 00:02:00 -> Status = OK
#       |  X |  Y |  Z = -5543836.364 | -2054585.624 |  2387809.881 |
#       | sX | sY | sZ =       15.583 |        4.307 |        4.618 |

#       [...]

#       Observation epoch : 2018/12/18 06:58:30 -> Status = OK
#       |  X |  Y |  Z = -5543834.811 | -2054581.220 |  2387809.224 |
#       | sX | sY | sZ =        6.166 |        2.664 |        2.253 |

#       Observation epoch : 2018/12/18 06:59:00 -> Status = OK
#       |  X |  Y |  Z = -5543834.128 | -2054581.138 |  2387808.424 |
```

```
#       | sX | sY | sZ =        5.206 |        2.250 |        1.898 |

#       Observation epoch : 2018/12/18 06:59:30 -> Status = OK
#       |  X |  Y |  Z = -5543836.136 | -2054582.119 |  2387809.629 |
#       | sX | sY | sZ =        7.895 |        3.415 |        2.871 |

#       Observation epoch : 2018/12/18 07:00:00 -> Status = OK
#       |  X |  Y |  Z = -5543835.016 | -2054581.957 |  2387809.450 |
#       | sX | sY | sZ =        7.576 |        3.279 |        2.749 |

# > Receiver position status summary:                                          #
#       >        840 (100%) epochs processed
#       >        839 ( 99%) epochs with valid status
#       >          1 (  0%) epochs with invalid status

# > Data processing time lapses:                                               #
# ..................................................................... #
# > Elapsed time for reading observation RINEX     =  1.90 seconds             #
# > Elapsed time for computing satellite positions =  0.72 seconds             #
# > Elapsed time for computing receiver positions  =  8.66 seconds             #

# ============================================================================ #
# > Data Dumping routine has started                                           #
# ============================================================================ #

# > Dumping satellite observation data...                                      #
# ..................................................................... #
#       - Gathered satellite observations
#       - Number of valid satellites
#       - Satellite navigation positions

# > Dumping satellite line of sight related data...                            #
# ..................................................................... #
#       - Elevation by satellite
#       - Azimut by satellite
#       - Line of sight information

# > Dumping satellite error modelling related data...                          #
# ..................................................................... #
#       - Ionosphere delay by satellite
#       - Troposphere delay by satellite
#       - LSQ residuals by satellite

# > Dumping LSQ related data...                                                #
# ..................................................................... #
#       - LSQ report by performed iteration per epoch
#       - LSQ report per observation epoch (last performed iteration)

# > Dumping receiver position related data...                                  #
# ..................................................................... #
#       - Receiver position solutions in ECEF and ENU frames per epoch
#       - Dilution Of Precision in ECEF and ENU frames per epoch

# > Dumping integrity related data...                                          #
# ..................................................................... #
#       - Vertical integrity information
#       - Horizontal integrity information

# > Dumping raw configuration and data hashes...                               #
# ..................................................................... #
#       - Raw general configuration perl hash : "$ref_gen_conf"
#       - Raw observation data perl hash : "$ref_obs_data"

# > Data dumping time lapses:                                                  #
# ..................................................................... #
# > Elapsed time for dumping satellite observation data      =  0.52 seconds   #
# > Elapsed time for dumping line of sight related data      =  0.35 seconds   #
```

```
# > Elapsed time for dumping satellite error modeling data   =  0.32 seconds   #
# > Elapsed time for dumping least squares related data      =  0.16 seconds   #
# > Elapsed time for dumping receiver position related data  =  0.11 seconds   #
# > Elapsed time for dumping integrity related data          =  0.05 seconds   #
# > Elapsed time for dumping raw configuration and data hash =  0.48 seconds   #

# ============================================================================ #
# > GNSS Rinex Post-Processing routine is over for 'KOKV Demo'                 #
# ============================================================================ #

# Results are available at : /home/ppinto/WorkArea/demo/grpp/GAL-E1/
# Log file is available at : /home/ppinto/WorkArea/demo/gal_e1_grpp+gspa.log

# > Elapsed time for GRPP script =  13.30 seconds                              #
# ############################################################################ #
```

3.2.3 Report Module: GNSS Service Performance Analyzer

Although GRPP outputs can be interpreted by the user, the amount of information produced by the module is such that it requires significant time and effort to summarize it. Furthermore, GRPP only produces numeric information, and for instance, performance analysis is much easier assessed with plots. Therefore, the report module purpose is two-fold, in order to fill GRPP gaps.

Since the end objective of this work is to analyze the different GNSS service positioning performances, the report module has been named as: GNSS Service Performance Analyzer, hereafter donated as GSPA.

Still, GSPA not only provides accuracy and integrity performance information but reports most of the data produced by GRPP. Consequently, the GSPA architecture is arranged with the same logic as the GRPP DataDumper package, meaning at the same time that GSPA is dependent from GRPP outputs.

Module Architecture

The Perl packages which encompass GSPA are showed in Figure 3.8:

- **ReportPerformances.pm** is in charge of providing the positioning performances numeric results as specified in REQ-FUN-58, REQ-FUN-59 and REQ-FUN-60.
- **PlotSatObservation.pm** generates the plots which illustrate satellite availability, elevation and geometry during the observation time window.
- **PlotSatErrorSource.pm** shows the modelled error for each SV at each observation epoch like the ionosphere delay or the residual error from WLSQ.
- **PlotLSQInformation.pm** reports in graphical format the WLSQ routine information.
- **PlotPosPerformance.pm** outputs the plots which account for the positioning accuracy and integrity performances. Furthermore, it displays the positioning solution and the receiver clock bias estimation.
- **CommonUtil.pm** is a package imported by all other GSPA packages. It contains generic functionalities which widely account for the treatment of the data extracted from GRPP outputs.

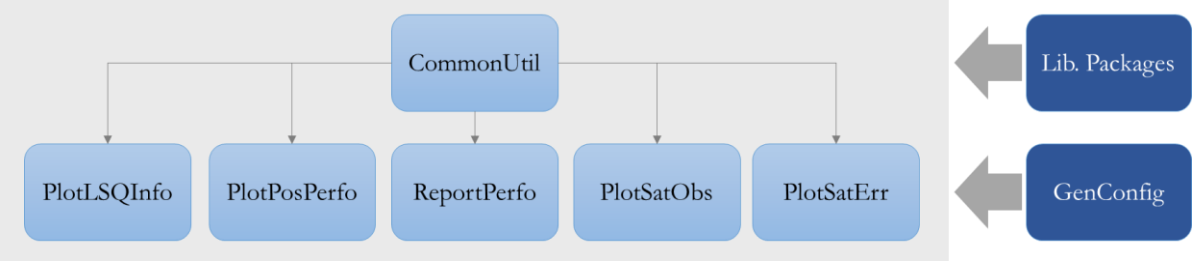

Figure 3.8 – GSPA architecture hierarchy diagram.

As previously mentioned, plot packages take advantage of an external library, since Perl built-in features do not offer graphical displays. This Perl library is the Chart::Gnuplot (version 2.23) and its basic functionality relies on arranging chart and dataset objects in order to build Gnuplot scripts, which are then called to generate the plots. The library is part of the Comprehensive Perl Archive Network (CPAN) project, a large collection or Perl SW and documentation that has grown over 24 years. For more information regarding Chart::Gnuplot or CPAN project, visit the following links: [LR.8] and [LR.10].

Public Subroutine Specification

GSPA encapsulates the following public subroutines arranged by package (except for CommonUtil). An output file/figure comes along with each subroutine to illustrate the user-end result:

- ReportPerformances.pm:
  - **ReportPostionAccuracy** writes in a dedicated file the maximum, minimum and RMS statistics for the receiver vertical, horizontal, position and time domains as indicated in REQ-FUN-58. The file also reports the number of observations and how many of them have a valid position solution.

```
# ------------------------------------------------------------------------ #
# > Position accuracy report from CEBR on 2019/05/13 using GPS-C/A         #
# ------------------------------------------------------------------------ #
#  Component NumEpochs NumOkEpochs     % SigmaFactor    MinAcc    RMSAcc    MaxAcc
>   Vertical      2880        2880 100.0        1.96      0.05      3.05     13.00
> Horizontal      2880        2880 100.0        2.45      0.04      3.25      9.50
>   Position      2880        2880 100.0        3.14      0.06      4.46     16.10
>       Time      2880        2880 100.0        1.96      0.04      2.39      9.96
```

  - **ReportPositionError** provides the same information as the accuracy report using the real receiver local errors (ENU increments) against the configured reference, fulfilling REQ-FUN-59.

```
# ------------------------------------------------------------------------ #
# > Position actual error report from CEBR on 2019/05/13 using GPS-C/A     #
# ------------------------------------------------------------------------ #
#  Component NumEpochs NumOkEpochs     %    MinErr    RMSErr    MaxErr
>   Vertical      2880        2880 100.0     -5.62      1.80      4.30
> Horizontal      2880        2880 100.0      0.03      1.04      2.90
>   Position      2880        2880 100.0      0.09      2.08      5.73
```

  - **ReportPositionIntegrity** reports in a dedicated file the number of observations epochs which were flagged with an integrity event for the receiver vertical and horizontal domains as indicated in REQ-FUN-60.

```
# ------------------------------------------------------------------------ #
# > Position integrity report from CEBR on 2019/05/13 using GPS-C/A        #
# ------------------------------------------------------------------------ #
#  Component NumEpochs NumOkEpochs     % SigmaFactor AlertLimit     MI     %    HMI     %     SA     %
>   Vertical      2880        2880 100.0        1.96      30.00    660  22.9      0   0.0   2880 100.0
> Horizontal      2880        2880 100.0        2.45      15.00     67   2.3      0   0.0   2880 100.0
```

- PlotSatObservation.pm:
  - **PlotSatelliteAvailability** shows the information dumped by DumpNumValidSat (GRPP DataDumper subroutine).

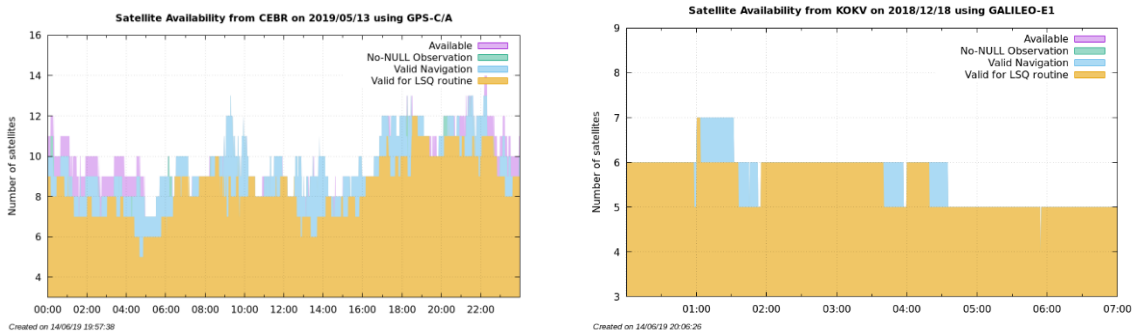

Figure 3.9 – SV Availability plots for GPS and GALILEO.

  - **PlotSatelliteElevation** illustrates for each SV its observed elevation against the receiver's horizon. The configured mask is presented as shaded grey area. One plot is generated for each GNSS (GPS/GALILEO).

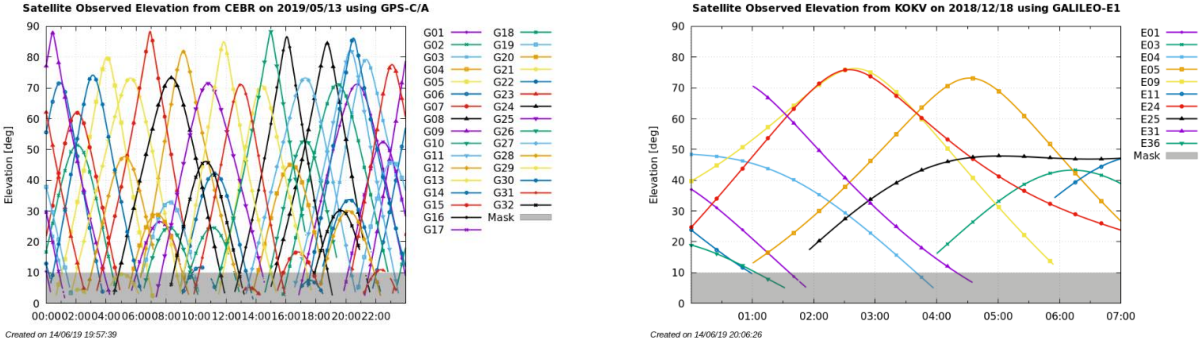

Figure 3.10 – SV elevation plots for GPS and GALILEO.

  - **PlotSatelliteSkyPath** displays the SV paths as if the trails were drawn from the receiver's zenith perspective. The paths are colored to represent the observation epoch, thus depicting the SV geometry evolution. In addition, the configured satellite mask is drawn as a shaded grey area. SV falling below the mask, do not account for the receiver position estimation.

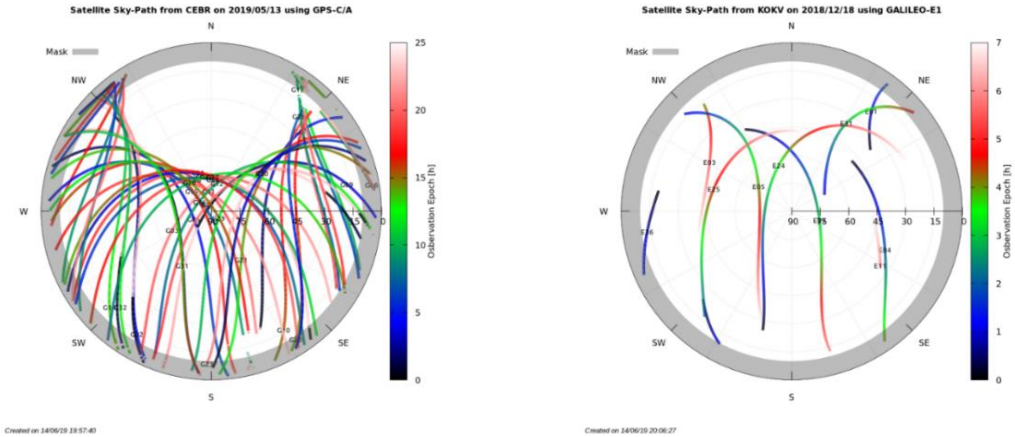

Figure 3.11 – SV sky-path plots for GPS and GALILEO.

- PlotSatErrorSource.pm:
  - **PlotSatelliteResiduals** shows the estimated residuals from WLSQ algorithm of each SV (arranged in the Y axis). The residuals are colored with a bi-polar palette. The highest residuals are colored as either blue or red, whereas small residuals (the optimal situation) are colored with a lighter beige color. This illustrates where the errors are mainly focused. An optimal estimation should equally distribute the residuals among LoS.

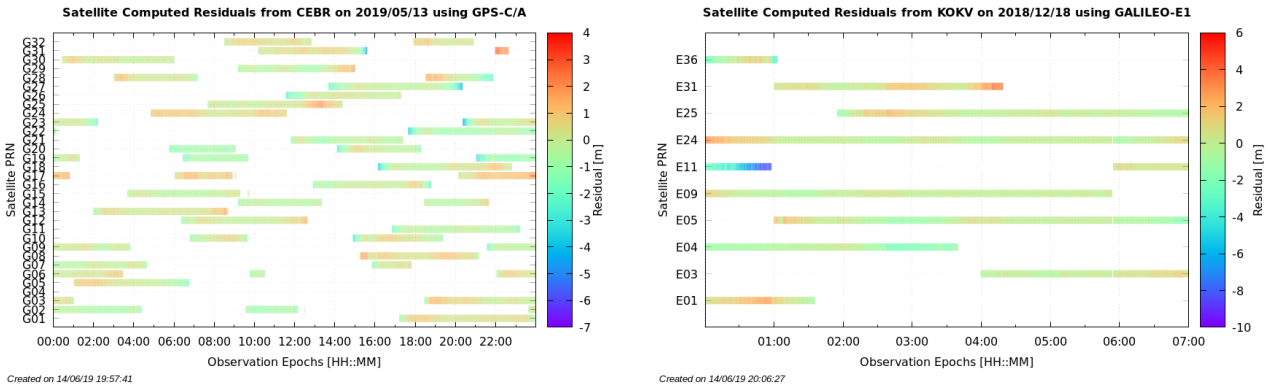

Figure 3.12 – SV residuals plot for GPS and GALILEO.

  - **PlotSatelliteIonosphereDelay** the plot arrangement is similar as PlotSatelliteResidual differing in the palette type, being a color-value increase for a higher ionosphere delay. This plot should show that higher delays are encountered when the SV have lower elevation, because the slant signal path is greater than its zenital projection.

  - **PlotSatelliteTroposphereDelay** displays the troposphere delay with the same format specified in PlotSatelliteIonosphereDelay.

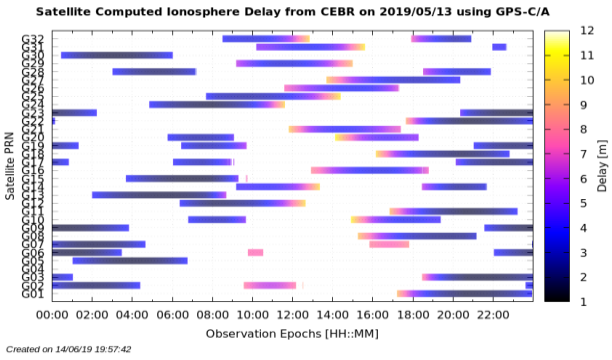

Figure 3.13 – SV ionosphere delay plot.

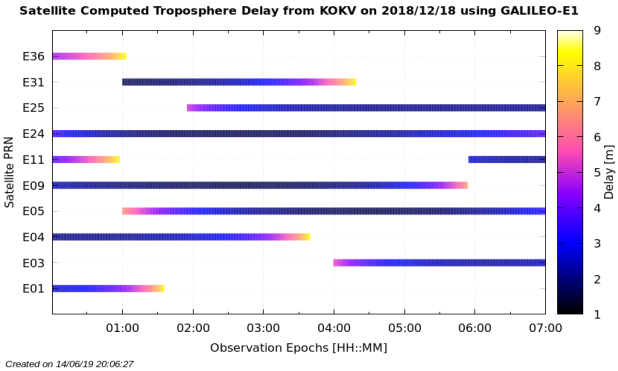

Figure 3.14 – SV troposphere delay plot.

- PlotLSQInformation.pm:
  - **PlotLSQEpochEstiamton** generates two types of plots:

    - The first one summarizes the basic WLSQ information such as the number of iterations performed or the ex-post standard deviation indicator.

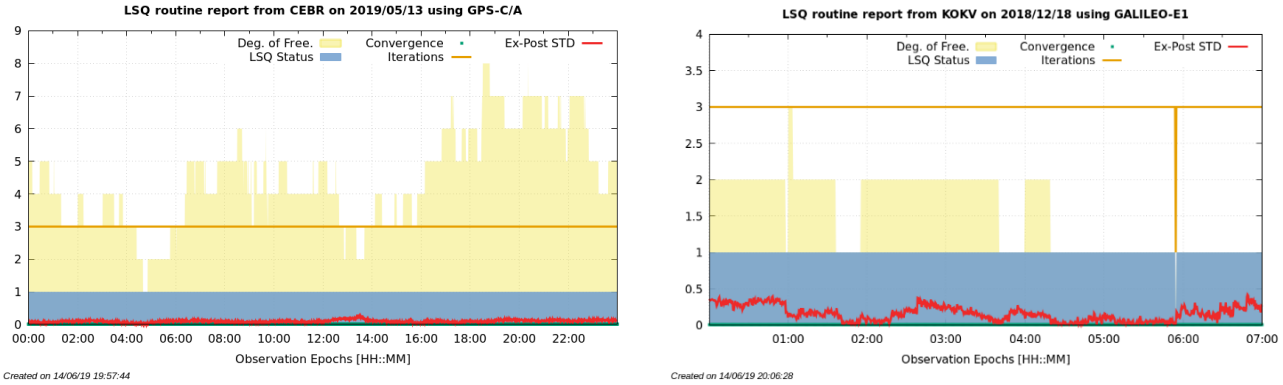

Figure 3.15 – WLSQ overall report plots.

- The second plot type encompass 4 different plots which illustrate each of the receiver parameters (X, Y, Z and clock bias) estimation evolution. The approximate and estimated values are showed in the first subplot. Besides, delta accumulated corrections for all iterations are displayed in the bottom subplot.

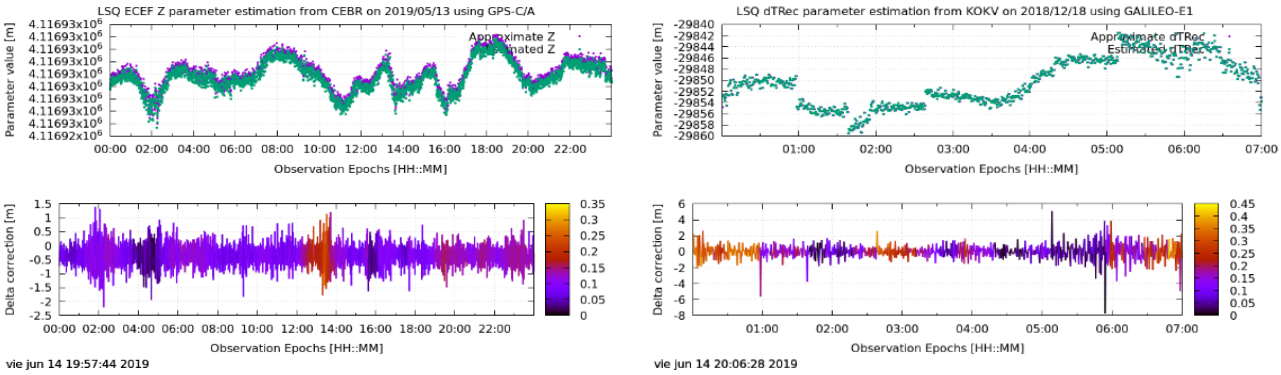

Figure 3.16 – WLSQ specific parameter estimation report plots.

- PlotPosPerformance.pm:
  - **PlotReceiverPosition**: outputs three types of plots.

    - The first plot type emulates a bullseye diagram where the hits are the obtained receiver positions in the horizontal domain. The position origin (0, 0) represents the configured reference position, therefore, the plot is representing the positioning errors committed. Three plots are generated where the positions are colored with its Upping component, horizontal accuracy and observation epoch.

    - The second plot type is a single chart with a multiplot arrangement in where the ENU components have individually plotted along with a grey line that represents the static reference. Each line is colored with its associated accuracy. In the optimal case, the highest deviations from the reference should be yellow-colored for a better integrity performance.

    - The last plot type shows the receiver clock bias evolution. The points are colored with the clock bias sigma as in the previous plot.

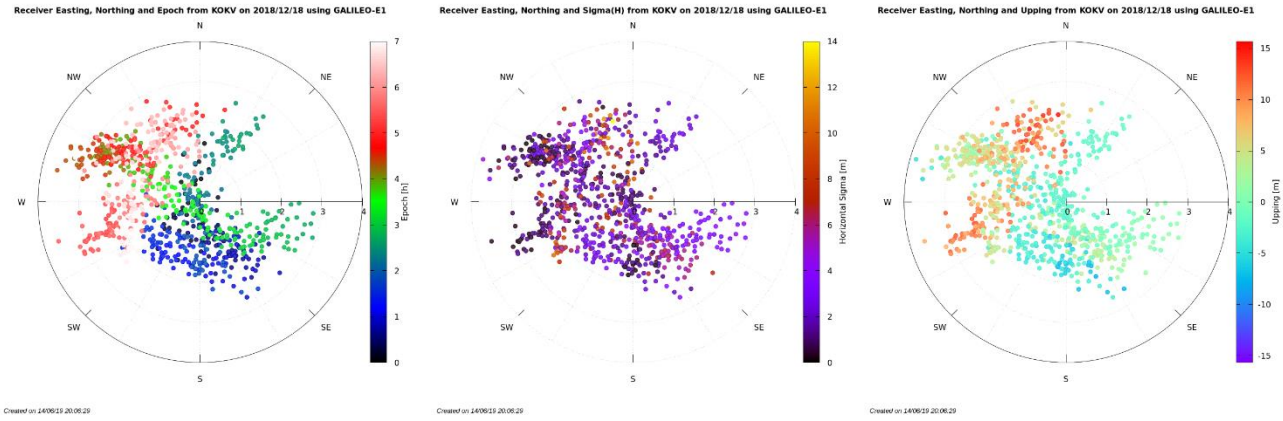

Figure 3.17 – Receiver EN position plots.

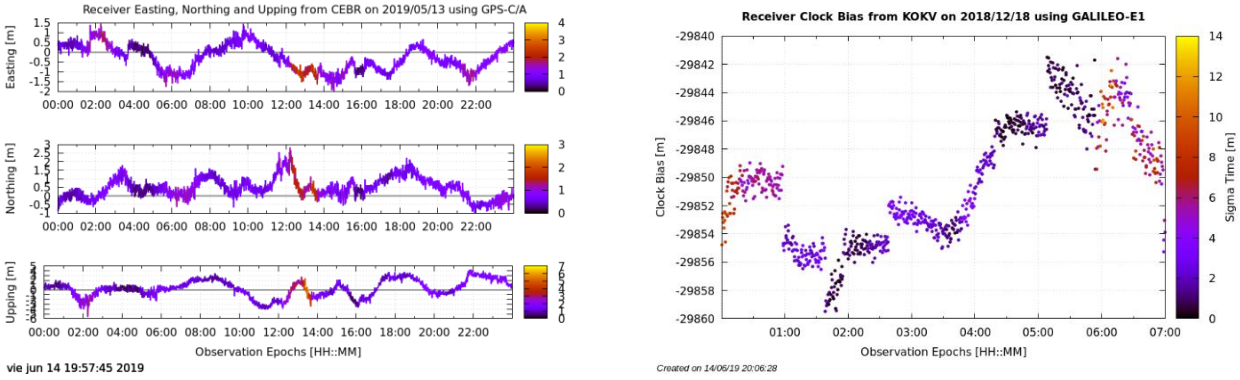

Figure 3.18 – Receiver ENU position and clock bias solution plots.

- **PlotAccuracyPerformance** displays the accuracy indicators as specified in REQ-FUN-63. The sigma values are split in two plots, one for the ECEF frame and other one for the ENU frame.

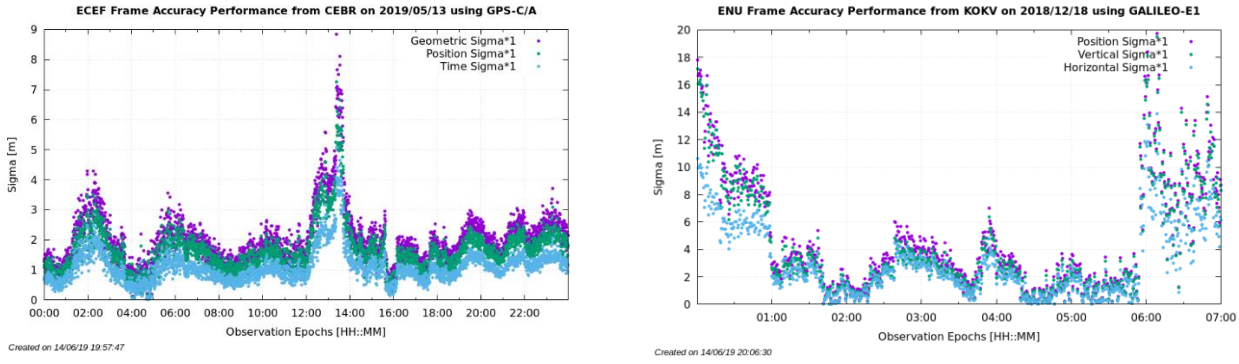

Figure 3.19 – Accuracy report plots on ECEF and ENU frames.

- **PlotIntegrityPerformance** shows the integrity phenomena for the vertical and horizontal domains (arranged in two different plots). The plots were inspired in Figure 2.15 and colors have

been added to them for a more intuitive information extraction. An desired integrity position solution occurs when the scaled precision does not over-pass the real error and the alert limit, having SA over most of the observation window.

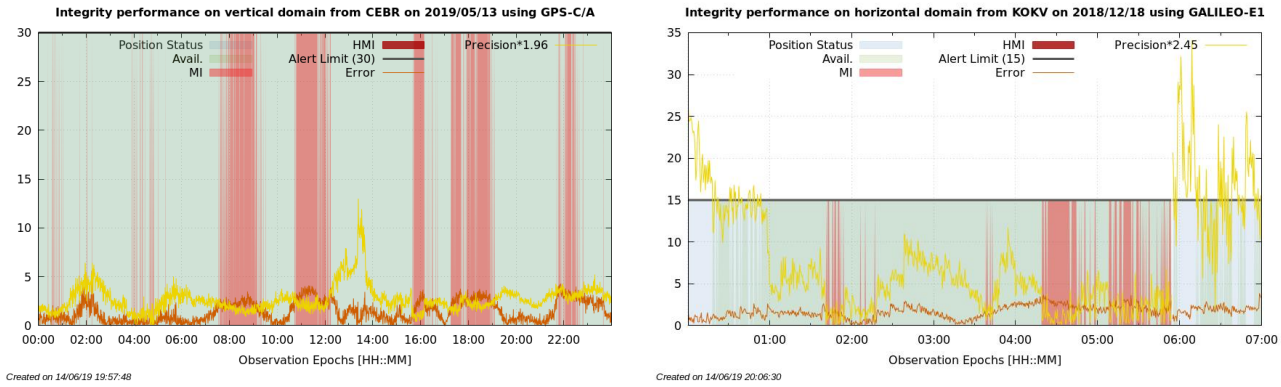

Figure 3.20 – Vertical and horizontal integrity report plots.

Module Execution

As adopted in GRPP, GSPA is orchestrated by a main Perl script, which is called in order to run GSPA module:

- **MainSoleService.pl** organizes the public GSPA subroutines for running the module as a whole. Moreover, it also loads the user configuration by importing GeneralConfiguration package. The main routine is basically divided in the following steps:
  - **Plot reporting routine** calls the public subroutines allocated in the plotting packages in order to generate the plot images.
  - **Performance reporting routine** calls the subroutines exported by ReportPerformances package to provide the numeric results.

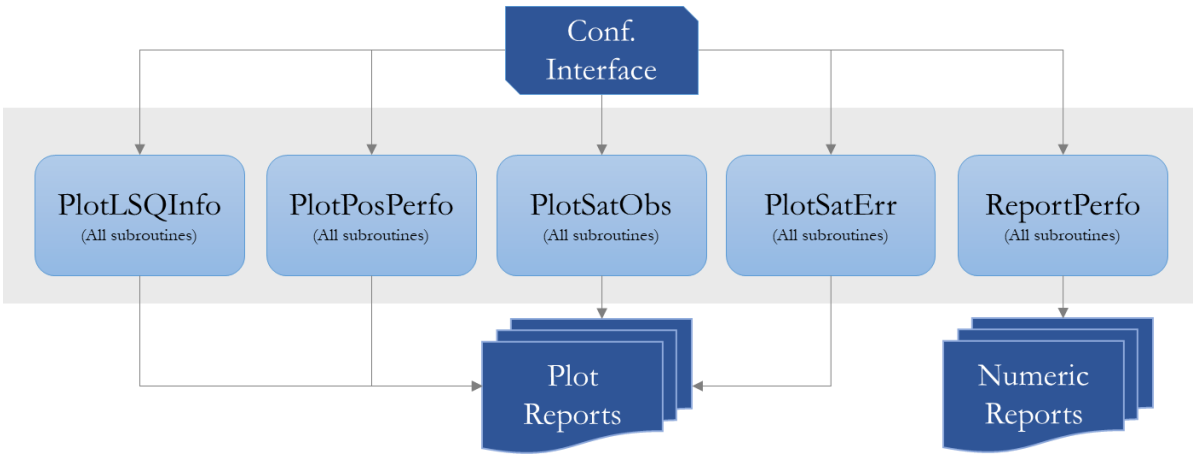

Figure 3.21 – GSPA architecture flow diagram.

As it can be seen in Figure 3.21, the execution flow of GSPA is simpler than GRPP. Each GPSA package uses the hash-interface configuration for running their subroutines and, unlike GRPP, no internal interfaces are needed.

GSPA is launched calling the same user configuration file used for running GRPP previously. Otherwise, GRPP outputs will not be available and GSPA will run raising an execution error. GSPA execution is presented in Terminal Demo 3. The execution example is the one used for validating GRPP under GPS-SPS signals (see section 3.3.2). Like GRPP, GSPA also informs the user about which module is currently running and where the outputs will be located.

Terminal Demo 3 – GSPA launching example for GPS-SPS C/A on CEBR station.

```
ppinto@ppinto-UbuntuVM:~/WorkArea/demo$ $GSPA cfg/CEBR_GPS-CA.cfg

# ############################################################################ #
# > Welcome to GNSS Service Performance Analyzer tool                          #
# ############################################################################ #

#    Script    was    called    from               :    '/home/ppinto/WorkArea/src/GNSS_Service-Performance-
Analyzer//MainSoleService.pl'
# GRPP data loaded from     : '/home/ppinto/Drive/tmp/MASTER/TFM/demo/grpp/GPS-CA'
# Configuration loaded from : '/home/ppinto/Drive/tmp/MASTER/TFM/demo/cfg/CEBR_GPS-CA.cfg'


# ============================================================================ #
# > Plot reporting routine has started                                         #
# ============================================================================ #

# > Ploting GPS satellite availability                                         #
# ···------------------------------------------------------------------------ #

# > Ploting GPS observed elevation                                             #
# ···------------------------------------------------------------------------ #

# > Ploting GPS sky-path                                                       #
# ···------------------------------------------------------------------------ #

# > Ploting GPS satellite residuals                                            #
# ···------------------------------------------------------------------------ #

# > Ploting GPS satellite ionosphere delay                                     #
# ···------------------------------------------------------------------------ #

# > Ploting GPS satellite troposphere delay                                    #
# ···------------------------------------------------------------------------ #

# > Ploting LSQ estimation iformation                                          #
# ···------------------------------------------------------------------------ #

# > Ploting receiver position solutions                                        #
# ···------------------------------------------------------------------------ #

# > Ploting accuracy performance results                                       #
# ···------------------------------------------------------------------------ #

# > Ploting integrity performance results                                      #
# ···------------------------------------------------------------------------ #

# > Graphical report time lapses:                                              #
# ···------------------------------------------------------------------------ #
# > Elapsed time for ploting satellite observation data   =  1.87 seconds      #
# > Elapsed time for ploting satellite error source data  =  2.55 seconds      #
# > Elapsed time for ploting LSQ estimation information   =  1.15 seconds      #
# > Elapsed time for ploting positioning performance data =  3.61 seconds      #


# ============================================================================ #
# > Performance reporting routine has started                                  #
# ============================================================================ #
```

```
# > Reporting position accuracy performance                                  #
# ······························································ #

# > Reporting position error performance                                     #
# ······························································ #

# > Reporting position integrity performance                                 #
# ······························································ #

# > Numerical report time lapses:                                            #
# ······························································ #
# > Elapsed time for reporting accuracy performance   =  0.06 seconds        #
# > Elapsed time for reporting error performance      =  0.10 seconds        #
# > Elapsed time for reporting integrity performance  =  0.08 seconds        #

# ============================================================================ #
# > GNSS Service Performance Analyzer routine is over                        #
# ============================================================================ #

# Plots and reports are available at : '/home/ppinto/WorkArea/demo/gspa/GPS-CA/'
# Log file is available at           : '/home/ppinto/WorkArea/demo/gps_ca_grpp+gspa.log'

# > Elapsed time for GSPA script =  9.44 seconds                             #
# ############################################################################ #
```

3.3 Performance Verification

Verification in the context of a SW lifecycle is intended to demonstrate that the SW is compliant with its specification by means of testing. In other words, Verification designs, executes and checks that the SW fulfills its baseline requirements.

In the technological industry, the Verification and Validation (V&V) phase depends on the SW complexity. Nonetheless in most cases, V&V is depicted in a Unitary Test phase, e.g. Perl subroutines are executed individually with controlled inputs and theirs outputs are cross-checked with those expected; and a System Test phase i.e. the entire SW is tested as a whole with different nominal and robustness scenarios. Eventually, the SW performances are also assessed by these verification methods. It can be remarked that performance criteria accomplishment is one of the best indicators (if not the best) of a SW being ready and validated.

3.3.1 Verification Scope

The verification phase of a project can be very expensive and time-consuming. For SoL systems, V&V is crucial and mandatory in their contracts. However, considering the scope of this project, the developed SW is neither critical nor real-time, so no Unitary Test are really needed to demonstrate that each feature of GRPP and GSPA works accordingly. As instead, the positioning performance results are much more interesting from the academic perspective, since they will be used to study GPS and GALILEO navigation services.

Note that GSPA will not be verified since GSPA does not compute performance indicators by itself. It only arranges those retrieved from GRPP outputs. Consequently, the verification of GRPP would be focused on assess the performances obtained with the SW tool. But, in order to compare GRPP performances, reference data must be stipulated from an outer source. As a result, it was decided to compare GRPP positioning results with those obtained with other GNSS post-processing tool. The discrepancies among both results will then determine if GRPP is successfully verified.

The selected tool on where the trust of reference data is relying, has been RTKLIB, which is an open source program developed by T. Takasu for SPP with GNSS. It also includes several enhanced capabilities such as PPP algorithms for both real time and post-processing. It also supports RINEX data format, apart from other protocols. The program consists on a collection of application programs, one per tool functionality. The one which it has been used for the verification of this project has been *RTKPOST – Post-Processing Analysis*. For more information regarding RTKLIB, please refer to the following link [LR.11].

From both RTKLIB and GRPP, station receiver coordinates are computed in WGS-84 ECEF format. The vector difference can be computed straight forward with a simple subtraction and a root square trace:

$$d_{XYZ} = \sqrt{d_X^2 + d_Y^2 + d_Z^2};$$
$$(d_X, d_Y, d_Z) = (X_{GRPP}, Y_{GRPP}, Z_{GRPP}) - (X_{RTKLIB}, Y_{RTKLIB}, Z_{RTKLIB}); \quad (3.1)$$

Since this difference is obtained for several observation epochs, the RMS, maximum and minimum differences can be computed as representative statistical values:

$$Max_{d_{XYZ}} = \max(d_{XYZ});\ Min_{d_{XYZ}} = \min(d_{XYZ});\ RMS_{d_{XYZ}} = \sqrt{\frac{1}{n}\sum_{i=0}^{n} di_{XYZ}^2};\qquad (3.2)$$

These values will be used as verification indicators which must fulfill the upcoming criterion for GRPP to be successfully validated. Otherwise, GRPP specification and implementation should be reviewed and modified.

3.3.2 Verification Cases and Criteria

Once the high-level scope of the verification has been set, the case specification and criteria are the next items to be detailed. Since the upcoming performance study campaign will be centered on GPS-SPS and GALILEO-OS, two verification cases can be created accordingly:

- **GPS-SPS Verification Case.** RTKLIB and GRPP will be executed with RINEX data from the same station using only GPS C/A pseudorange signal.

- **GALILEO-OS Verification Case**. RTKLIB and GRP will be executed with RINEX data from the same station using only GALILEO E1 pseudorange signal.

Note that GPS-SPS or GALILEO-OS broadcast other free-access signals like L2C. However, RTKLIB does not support the processing of all of them and it was decided that C/A and E1 would represent fairly the verification performances.

For both cases, it has been decided to use RINEX from IGS institution (International GNSS Service), who publishes daily data of their associated stations under a free-access repository. After a constellation availability study for GALILEO case, the selected stations have been CEBR and KOKV, located in the Iberia peninsula and Hawaii archipelago as showed in Figure 3.22.

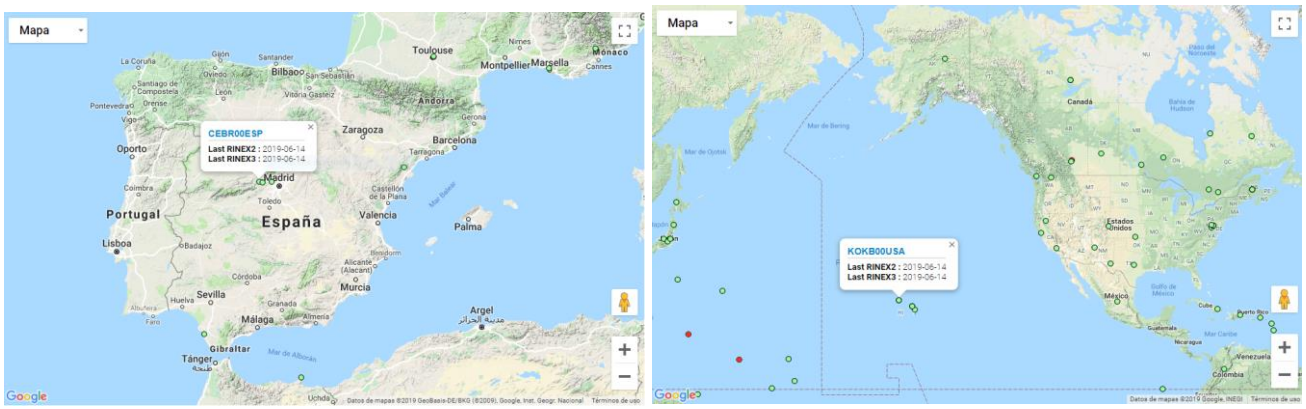

Figure 3.22 – IGS reference stations used for the performance verification.

Regarding configuration of both tools:

- **RTKLIB** has been configured in single mode, with a 10º mask, using broadcasted ephemerids (RINEX navigation files) for satellite position determination, Saastamonien troposphere correction and broadcasted ionosphere model (which it turned out to be Klobuchar's for both GPS and GALILEO executions). Observation RINEX files needed to be trimmed for the selected constellation and signal observation since RTKLIB does not allow the user to specifically select a single observation source.

- **GRPP** was configured similarly as RTKLIB but setting directly the observation codes (C1C) for C/A and E1 pseudorange observations. Furthermore, some SV needed to be discarded (G04, E14 and E18) due to processing anomalies.

Finally, the criterion was set accordingly to the accuracy performance requirements of GPS and GALILEO presented in section 2.6.1. As a remainder, these are the positioning error tolerances for the 95% of the cases. Since verification process is being assessed under nominal conditions, the tolerance threshold criteria will be defined as:

- The maximum and minimum difference indicators presented in equation (3.2), shall not exceed 0.5 times the GNSS 3D position accuracy requirement for 95% confidence level.

- The RMS difference indicator presented in equation (3.2), shall not exceed 0.2 times the GNSS 3D position accuracy requirement for 95% confidence level.

Note that these values are arbitrary and may be further discussed. However, they are acting as a verification tolerance indicator. Beware that there will always be differences among GRPP and RTKLIB, the magnitude on these should be around the GNSS system's precision but, assuming fair system performances, they should never be higher than the worst-case accuracy threshold. In this case, the thresholds have been lowered to the 50% and 20% in order to account for the nominal conditions presented in the verification cases.

As a summary, the verification information for both services is detailed in Table 3.12.

Table 3.12 – Verification case specification and criteria.

	GPS-SPS	GALILEO-OS
Measurement Source	C/A pseudorange	E1 pseudorange
Station	CEBR (Iberia Peninsula)	KOKV (Hawaii Archipelago)
Date	13/05/2019	18/12/2018
Processing Window	Whole day	From 00:00 to 07:00
Difference Threshold Criteria	5 meters for RMS ±13 m for max/min	8 m for RMS ±19 m for max/min

3.3.3 Verification Results and Reports

For producing the verification results, ECEF coordinates obtained with RTKLIB and GRPP were arranged in a spreadsheet and then, their differences were computed as specified in equation (3.1). In addition, plots representing the differences for each coordinate component were drawn. Lastly, the reference position for each station was also incorporated to the plots in order to discard possible gross-singular errors produced by RTKLIB or GRPP.

GPS-SPS using C/A signal

For GPS-SPS C/A verification case, differences range to a maximum of 5 meters which is the most-known precision when using GPS C/A signal with SPP algorithms. In addition, Figure 3.23 shows a kind-of random pattern in the coordinate differences, probably due to the SV-ephemerid different criteria selection

among GRPP and RTKLIB. Therefore, and since verification indicators in Table 3.13 are compliant whit those postulated in section 3.3.2, **GRPP can be successfully verified when processing GPS-SPS pseudorange signals**.

Table 3.13 – Verification difference indicators for GPS-SPS C/A case.

Comparison Statistics for GPS-SPS C/A (GRPP – RTKLIB)				
	Diff. X	**Diff. Y**	**Diff. Z**	**Diff. XYZ (3D)**
Min	-0.9	-1.4	-0.9	0.2
RMS	1.5	0.4	1.2	2.0
Max	4.1	0.9	3.9	4.9

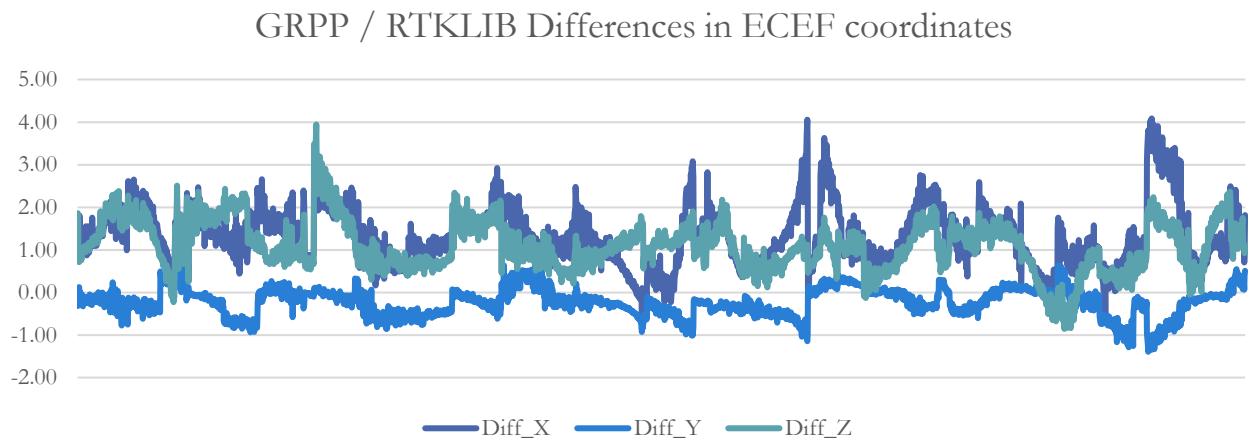

Figure 3.23 – GRPP vs RTKLIB differences using GPS-SPS C/A.

GALILEO-OS using E1 signal

Unfortunately, for GALILEO verification case, the difference indicator values presented in Table 3.14 do not accomplish the threshold criteria, especially on the maximum difference. By looking at the differences in the ECEF coordinates displayed in Figure 3.24, it can be seen how the discrepancy among GRPP and RTKLIB is concentrated on a few epochs in the ECEF X component. A closer look to this coordinate obtained with both tools, and displaying its station (KOKV) static reference, is showed in Figure 3.25.

Table 3.14 – Verification difference indicators for GALILEO-OS E1 case.

Comparison Statistics for GALILEO-E1 (GRPP – RTKLIB)				
	Diff. X	**Diff. Y**	**Diff. Z**	**Diff. XYZ (3D)**
Min	-15.2	-5.2	-5.4	0.5
RMS	7.1	2.6	3.2	8.2
Max	23.4	5.1	6.3	24.2

Figure 3.25 is illustrating that the highest difference seems to be due by an RTKLIB outlier. Note that RTKLIB result is uneven with the real station X coordinate. Also, note that in the remaining observations epochs, the differences are within the expected range. At this point, it can be assured that these

discrepancies are caused by an unexpected behavior in RTKLIB. We could think of a GALILEO system failure as well, but GRPP results are fairly aligned to the reference using the same processing data and no GALILEO issues were published for that date. Eventually, it was decided to re-compute the verification indicators excluding the observation epochs presenting this anomaly.

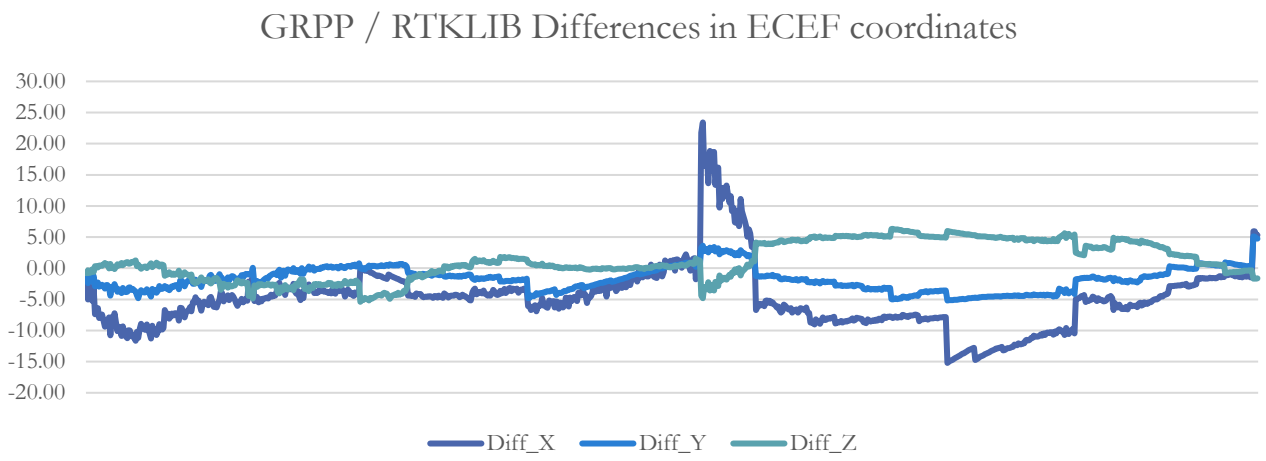

Figure 3.24 – GRPP vs RTKLIB differences using GALILEO-OS E1.

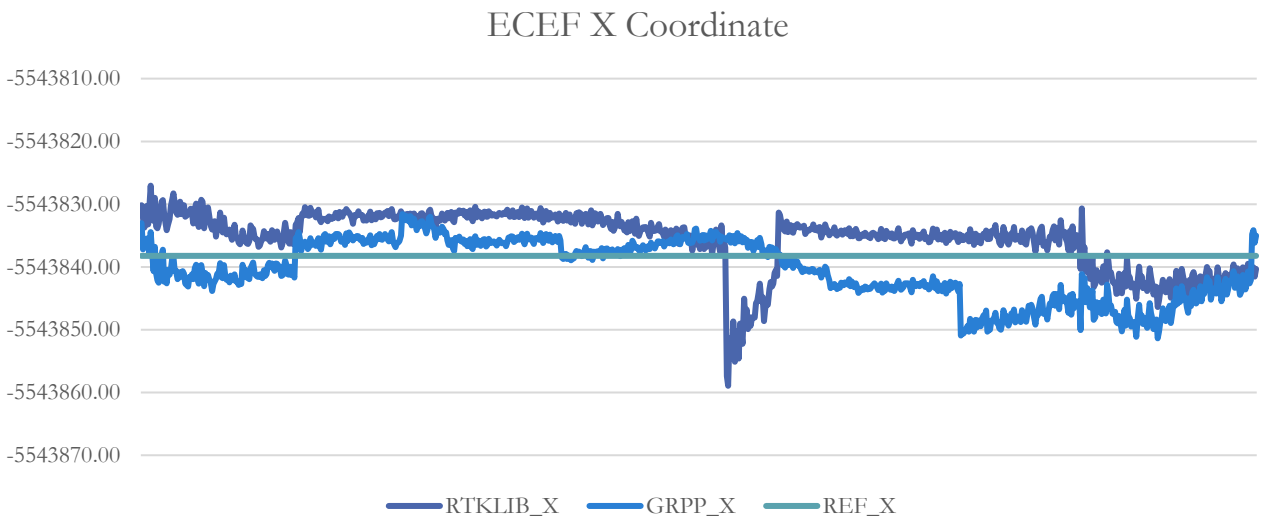

Figure 3.25 – ECEF X coordinate against its real value, obtained with RTKLIB and GRPP using GALILEO-OS E1.

Difference indicators in Table 3.15 are now compliant with the threshold criteria defined in section 3.3.2. Moreover, the differences observed in the ECEF coordinates are also within the expected GALILEO precision. Thus, it can be conluded that **GRPP is also successfully verified for GALILEO-OS pseudorange signal processing**.

However, it must be remarked that indicators are compliant with a very narrow margin, beign almost at the threshold value. This is probably caused by a poor GALILEO SV geometry, causing a worse accuracy performance as disscussed in section 2.6.1. Note that at that time (18/12/2018) GALILEO constellation was not in FOC, having 20 SV which were operating with a reliable status.

As a metter of fact, the RTKLIB anomaly previously observed was located on a time window when only the minum number of SV were observed (this is 5 SV). GSPA satellite availability plots for this execution were presented in section 3.2.3 (Figure 3.9 and Figure 3.11). Also note in Figure 3.15, where GPS and

GALILEO WLSQ estimations can be comapred, the difference among degrees of freedom: GPS has in most epochs at least 3 DoF whereas this situation in GALILEO is exceptional. This leaves no doubt about GPS and GALILEO verification performance differences, as it will be concluded too in the upcoming analysis chapter.

Table 3.15 – Verification difference indicators for GALILEO-OS E1 without RTKLIB outlier.

Comparison Statistics for GALILEO-E1 (GRPP – RTKLIB)				
	Diff. X	**Diff. Y**	**Diff. Z**	**Diff. XYZ (3D)**
Min	-15.2	-5.2	-5.4	0.5
RMS	6.7	2.6	3.3	7.9
Max	5.9	5.1	6.3	17.1

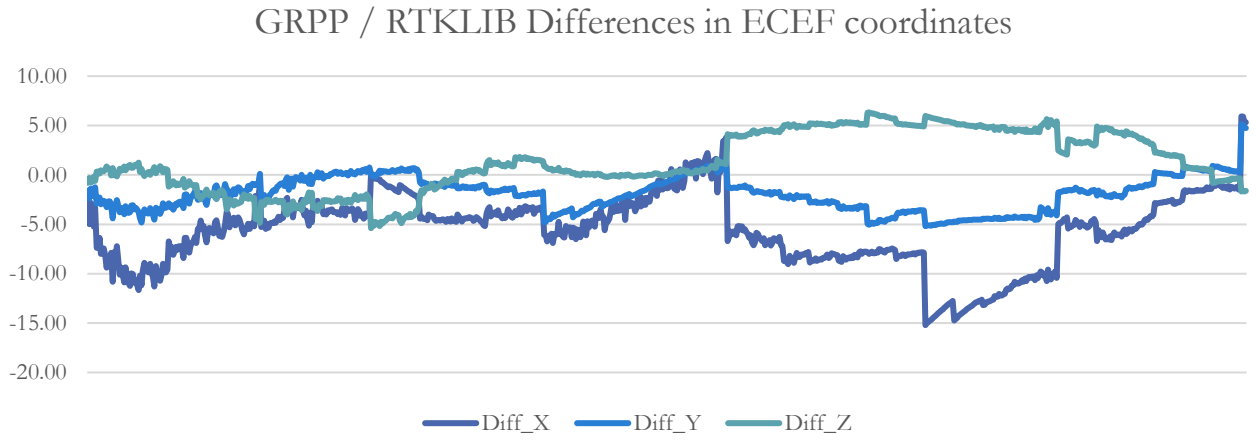

Figure 3.26 – GRPP vs RTKLIB differences using GALILEO-OS E1 without RTKLIB outlier.

Chapter 4: Analysis

4 Analysis: Positioning Performance Study Campaign

As introduced in chapter 1, the main academic objective is to apply the knowledge acquired in chapter 2 and the methodology developed in chapter 3 in a GNSS study-case. This is encompassed in this forth analysis chapter, where the effort is focused on the positioning performance assessment of GPS-SPS and GALILEO-OS with real data. In other words, the analysis chapter presents the committed positioning performance campaign with GRPP and GSPA SW.

Along this chapter, the major campaign features and results will be detailed and commented in order to later assess the project conclusions (refer to chapter 5). The following sections are focused in the most relevant campaign items: starting by its purpose and scope, passing through the planification and ending up with the performance results obtained.

For the sake of clarity, not all detailed campaign results are available in the document (like every single GSPA plot). If any detailed campaign result is wished to be consulted, a dedicated free-access repository is available for this purpose. Please refer to annex 0.

4.1 Motivation and Description

The importance of GNSS products, from a civilian-end perspective, rely on their economic potential and their market reach. Over 8 million of devices are expected to incorporate GNSS antennas and navigation solutions by 2020 (see European GNSS market report [BR.12]). This potential relies in the provision of an enough-accurate position with a global and continuous service. Therefore, the positioning performances are directly related with the GNSS solutions benefit and the investment for a GNSS to be improved and evolved.

Moreover, the GNSS ecosystem has evolved from a single/dual constellation usage (traditionally GPS and GLONASS) to a multi-GNSS constellation environment with the rise of BEIDOU, GALILEO and the rest of local navigation services such as EGNOS or WAAS (see section 2.3). Although nowadays the GNSS receiver market tendency is indisputably focused on a multi-frequency solution, is still of interest to develop single-frequency SPP algorithms. Needless to point that these have the easiest implementation and lowest cost approach (hence a huge market reach, as mentioned in section 1.1), but they also lead to study single-constellation and single-service performances.

Eventually, it does not matter how complex is the GNSS and service combination if a sole service or constellation is not performing as expected in the reality. This is the core interest of studying performances individually and the reason being for using real data in the assessment.

Seeing that navigation accuracy is the most valuable performance from a user perspective, this performance will be assessed in the campaign by presenting the accuracy results obtained with GRPP and reported by GSPA. As a reminder of section 2.6.1, accuracy is the error bound of a solution which is provided thanks to the observation redundancy.

Normally the user trusts the navigation algorithm's accuracy, not even wondering if the solution is being representative of its actual error. In order to fill this gap, not only accuracy is considered but also its solution integrity. Recalling section 2.6.2, integrity indicates how reliable a systems navigation solution is. Integrity will also be measured from GSPA reports.

Finally, and as stated in the project's title, accuracy and integrity positioning performances will be study for both GPS-SPS and GALILEO-OS (under nominal and singular conditions) using single-frequency SPP methodology presented in chapter 3.

4.1.1 Main Objectives

As previously mentioned, this master thesis work had initially a main objective which it turned out to be complemented by an additional one. The main settled objective was to study the positioning performances of GNSS free-access services. But on the run, a dedicated GNSS processing SW was borne for committing this intention, forming then a baseline version for a new open-source tool contribution to the GNSS user community.

Consequently, it can be said that the campaign's reason being serves the preliminary objective, but it goes beyond that. The actual campaign purpose is two-fold:

- **Assess accuracy and integrity performances** for both GPS-SPS and GALILEO-OS signal services, by means of processing its data with GRPP+GSPA SW.

- **Demonstrate GRPP+GSPA potential** in a real study-case in order to further validate it as a user-oriented tool.

The first objective will be assessed numerically by comparing the performances obtained with GPS and GALILEO services on both receiver vertical and horizontal domains. The second objective will be assessed with a more subjective approach by illustrating GRPP+GSPA results along the campaign presentation (section 4.3).

4.1.2 Expected Results

In order to introduce the expected campaign results, it is noteworthy to have a clear picture of the status of both GPS and GALILEO systems. The campaign has been performed over observation dates between August 2018 to April 2019. At that time, GPS satellite constellation was operating in FOC with over 30 SV in healthy conditions. Therefore GPS-SPS status can be expected to be nominal with very few and ground-segment notified anomalies.

However, GALILEO has not acquired at the time being FOC. On August 2018, 20 SV were orbiting the earth, 3 of them with an unhealthy status: E14 and E18 (due orbit eccentricity); and E22, which was removed from active service until further notice. On November 2018, 4 new SV entered service accounting for a total of 21 SV operating in nominal conditions. The incompletion of GALILEO satellite constellation is a key fact to consider since not as many satellites as GPS-SV would be available. Obviously, this will be affecting the SV-observation geometry, degrading at the same time GALILEO performances.

Having stated the aforementioned conditions, the following campaign expected results can be listed according to each target performance:

- **Accuracy** is expected to meet the requirements stipulated in section 1.1, with worse vertical domain performance. Although these requirements are in fact more demanding compared to those in section 2.6.1, the expectations are kept optimistic since it is usual to obtain better performances under nominal conditions. Nonetheless, GALILEO status will lead to worse accuracy performances compared to those in GPS; but in any case, they should not be worse than those stipulated by its own system definition document (refer to [BR.16]).

- **Integrity** cannot possibly be compared with any reference criteria. However, it can be presumed that better integrity results are expected in the horizontal domain rather than in the vertical one. In addition, GPS-SPS integrity outcomes will be better than those on GALILEO, demonstrating that fair integrity performance requires a good SV observation geometry. Finally, if accuracy performances have been

accomplished as expected, SA should be close to the 95% and MI should not overpass the 30% whereas HMI shall be very few (less than 7%), unless in special scenario conditions.

Expected campaign positioning performances are schematically presented in Table 4.1.

Table 4.1 – Expected performance campaign results.

Performance	Domain	GPS-SPS	GALILEO-OS
Accuracy	**Horizontal**	Meet criteria of Table 1.1. Expected even better results.	Meet criteria of Table 1.1. If not, at least meet worst case requirements in Table 2.7.
	Vertical	Meet criteria of Table 1.1. Assumed worse performance than horizontal domain.	Meet criteria of Table 1.1. If not, meet at least the worst-case requirements in Table 2.7. Assumed a worse performance than horizontal domain.
Integrity	**Horizontal**	Expect more than 95% of SA with a maximum of 20% MI and 5% HMI under nominal conditions.	Expect in most cases SA dropped under 95% (70% minimum) with more than 20% MI and 5% HMI under nominal conditions.
	Vertical	Expect around 95% of SA with a maximum of 30% of MI and 5% HMI under nominal conditions.	Expect in most cases SA dropped under 95% (50% minimum) with slightly more than 30% of MI and 5% of HMI under nominal conditions.

Apart from assess performances in nominal conditions, the campaign will also include scenarios where non-nominal conditions are taken place. These will be ionosphere critical phenomena (refer to section 4.2.2).

Positioning performances will also be measured in these cases, but since the behavior under abnormal phenomena is non-deterministic, no expected results will be stipulated. As instead, the obtained results will serve as comparison among normal and abnormal situations. This will add further vale to the analysis phase and will also illustrate how accuracy and integrity unfold under critical circumstances.

4.2 Data Arrangement

For committing the proposed performance study campaign, a data-source and a preliminary planification was essential.

Regarding the data source, it was already used in section 3.3 the IGS station network for the GRPP+GSPA performance verification. For the campaign it has not been different since IGS provides the widest free-of-charge GNSS data collection. More specifically, it has been taken in advantage the Multi-GNSS Experimental Service (hereafter denoted as MGEX) which is a pilot project of IGS institution.

The IGS-MGEX is a dedicated service to track, collect and analyze all possible GNSS signal services. Of course, this includes the legacy and non-legacy GNSS like GPS and GALILEO. Over a four-year period, MGEX has been gathering GNSS data from their tracking stations and publishing them in open repositories, along with processed GNSS products such as precise SV positions. For more information regarding MGEX, please refer to the bibliography references: [BR.10] and [BR.11].

From MGEX service, a set of stations will be selected, and then different observation dates will also be determined in order to gather a data archive in where to study the positioning performances. This will be detailed in the upcoming sections: 4.2.1 and 4.2.2. The downloaded data has been GRPP inputs: RINEX observation and navigation files.

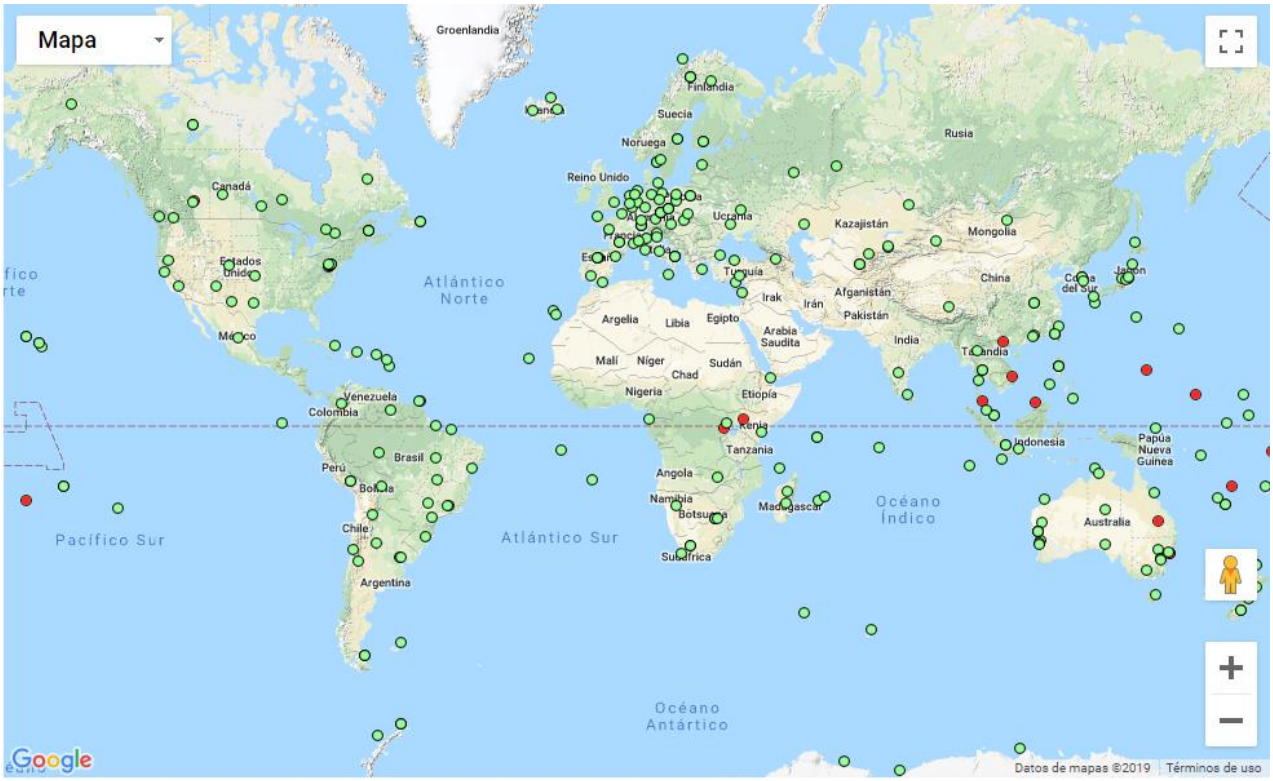

Figure 4.1 – IGS MGEX available tracking stations. Source: igs.org

Regarding preliminary planification and prior to the data download, it was necessary to select those stations and dates with a fair GPS and GALILEO constellation availability. For committing this purpose Trimble GNSS Planner was used (see [LR.12]). This planner is web-based and uses the almanac data of the GNSS constellations for building an observation report. In addition, it also displays the SV anomalies and even the ionosphere TEC and critical phenomena like scintillation. The Trimble GNSS planner was especially helpful for planning GALILEO processing windows since without this tool, more tedious approaches would have been necessary, turning the campaign in a much more time-consuming process.

4.2.1 Selected Stations

The IGS MGEX stations selected for the performance campaign are identified by its four-letter combination and listed in Table 4.2. The location of these stations can be geographically consulted in the world map of annex A.6.

Table 4.2 – Detailed information of selected stations for campaign.

Station	City	Country	Agency	Lat	Long	Height (m)	Receiver
ABMF	Les Abymes	Guadeloupe	IGN	16.26231 N	61.52753 W	-25.0	LEICA GR25
FAIR	Fairbanks	USA	JPL	64.97800 N	147.49924 W	319.2	JAVAD TRE_G3TH DELTA
KIRU	Kiruna	Sweden	ESOC	67.85730 N	20.96840 E	391.1	SEPT POLARX4
KOKV	Kokee Park	USA	JPL	22.12626 N	159.66493 W	1167.5	JAVAD TRE_G3TH DELTA
KOUG	Kourou	French Guiana	CNES	5.09847 N	52.63975 W	107.2	SEPT POLARX5TR
MAJU	Rita, Majuro	Marshall Islands	GA	7.11914 N	171.36453 E	33.9	SEPT POLARX4TR
OWMG	Owenga	New Zealand	CNES	44.02430 S	176.36880 W	21.6	TRIMBLE NETR9
TASH	Tashkent	Uzbekistan	GFZ	41.32805 N	69.29557 E	439.7	JAVAD TRE_G3TH DELTA

Eight stations have been selected according to five different geographical areas. These areas were not randomly selected. As contrary, they were carefully chosen in order to study the GPS and GALILEO performances over different locations. Note that the stations are spread in different latitudes and longitudes for accounting different phenomena which may affect the GNSS measurement processing.

Station Precise Reference

It was already explained in section 2.5.4 that in order to measure integrity performance the reference station coordinates shall be precisely defined. The precise coordinates of the aforementioned stations were extracted from the ITRF realizations (refer to section 2.4.2 for ITRF definition). The campaign station precise coordinates are presented in Table 4.3.

Note that the these ECEF coordinates are given in ITRS whereas GRPP results are outputted in WGS84. However, both references are so closely aligned that the difference between them is insignificant, considering the accuracy magnitude expected in the campaign, as so it happens with the different ITRF realizations.

Last but not the least, GRPP SW loads the precise coordinates defined in Table 4.3 by reading a dedicated data file containing all the stations coordinates. Afterwards, GRPP loads the reference of the configured station for the static and integrity modes. The data file is stored under a *dat* directory in the GRPP+GSPA repository (refer to annex A.1).

Table 4.3 – Campaign stations precise ITRF coordinates.

Station	ECEF X [m]	ECEF Y [m]	ECEF Z [m]	ITRF realization
ABMF	2919785.720	-5383745.056	1774604.712	ITRF14
KIRU	2251420.712	862817.279	5885476.769	ITRF14
KOKV	-5543838.239	-2054586.439	2387810.121	ITRF14
OWMG	-4584393.742	-290932.452	-4410048.404	ITRF96
TASH	1695945.059	4487138.593	4190140.719	ITRF14
FAIR	-2281621.697	-1453595.838	5756961.799	ITRF14
KOUG	3855263.343	-5049731.993	563040.402	ITRF14
MAJU	-6257572.259	950332.805	785215.297	ITRF14

4.2.2 Selected Dates

Once target IGS stations were defined, the next step was to select the observation dates of each location. By making different date arrangements. It was concluded that three dates would be enough to cover the positioning performance analysis.

These three dates are dedicated to study different scenarios which may affect differently to the GNSS measurement processing and SV availability:

- **Date #1** will be set as the same UTC time processing window for all stations. Since the stations are world-wide spread, this date will test if the GNSS has indeed global coverage.

- **Date #2** sets a different time in each campaign station in order to encounter good SV availability. This date will test both GPS and GALILEO free-access services with the best possible constellation availability.

- **Date #3** also sets a different UTC dates for each station. But unlike Date #2, the dates have been selected according to ionosphere critical events such as high TEC or scintillation phenomena.

Summing up, it could be stated that Date #1 and Date #2 test the performances under nominal conditions and Date #3 under singular conditions. The detailed time setting for each station-date pair is listed in Table 4.4.

Note in Table 4.4 that stations for Date #1 and Date #2 are the same whereas Date #3 includes different ones. The initial objective was to maintain the same stations for all dates. However, issues for selecting time windows with critical ionosphere conditions were found and hence, different stations were set.

Once again, for selecting the dates presented in Table 4.4 Trimble GNSS planner was quite useful (as a matter of fact, several GSPA plots were inspired by those found in this tool). On the one hand, the SV availability plots helped to determine those dates with fair GALILEO constellation availability for Date #2. On the other hand, ionosphere information displayed in this tool was essential in order to identify the time windows for Date #3 as showed in Figure 4.2.

Table 4.4 – Selected station-date pair for campaign.

Station	Date ID	Date	Day of year	Processing start time	Processing end time
ABMF	Date #1	20/02/2019	51	6:00	10:00
KIRU		20/02/2019	51	6:00	10:00
KOKV		20/02/2019	51	6:00	10:00
OWMG		20/02/2019	51	6:00	10:00
TASH		20/02/2019	51	6:00	10:00
ABMF	Date #2	20/02/2019	51	6:00	10:00
KIRU		29/04/2019	119	13:00	21:00
KOKV		18/12/2018	352	0:00	9:00
OWMG		26/04/2019	116	8:00	18:00
TASH		07/04/2019	97	7:20	17:20
FAIR	Date #3	26/08/2018	238	6:20	9:40
KIRU		07/03/2019	66	20:00	23:59
KOKV		16/04/2019	106	18:00	23:59
KOUG		22/11/2018	326	14:00	22:00
MAJU		10/04/2019	100	1:00	11:00

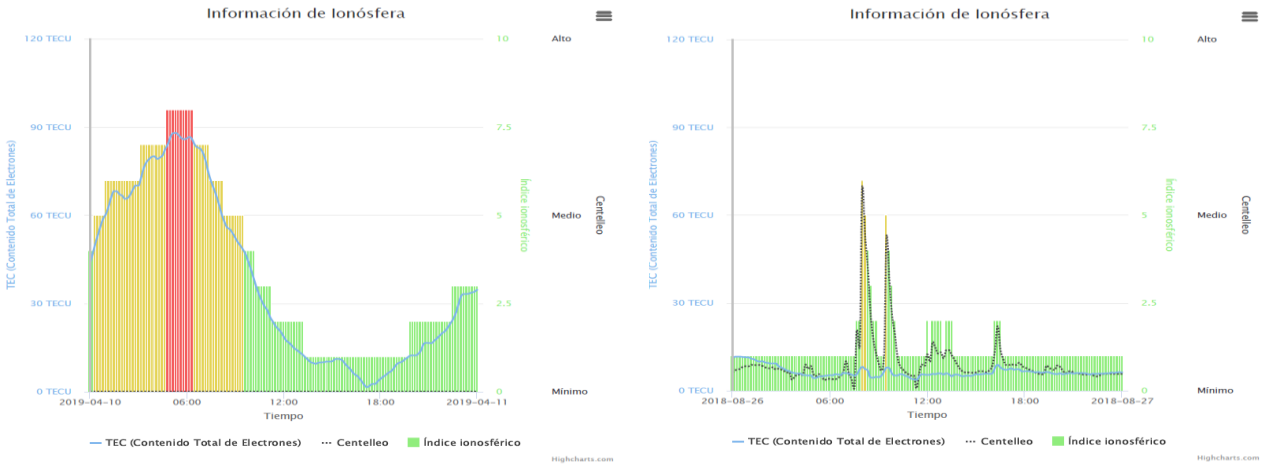

Figure 4.2 – Ionosphere conditions over MAJU and FAIR stations for Date #3 analysis.

Each critical ionosphere phenomena for each station is listed in Table 4.5. High TEC values are usually found in equatorial latitudes, not as scintillation events, which are more singular and located in high latitudes. Scintillation is known for being a rapid electron density change in the ionosphere layers which affects electro-magnetic waves severely. Find more information about this phenomenon on [LR.13].

Table 4.5 – Date #3 critical ionosphere phenomena on each station.

Station	Critical Ionosphere Phenomenon	Observations
FAIR	Moderate-Severe Scintillation	Between 8:00 and 10:00 UTC
KIRU	Moderate Scintillation	At around 22:00 UTC
KOKV	Moderate TEC	Maximum of 40 TECU
KOUG	Moderate TEC	Maximum of 35 TECU
MAJU	High TEC	Maximum of 95 TECU

4.2.3 Selected Signals

As a recap of GNSS systems services explained in section 2.3, GPS and GALILEO encompass different free-access service which are provided by different carrier frequencies, ranging codes and navigation data.

For GPS-SPS, the signals offered nowadays are C/A, L2C, L5C and L1C (refer to theory section 2.3.1 for a deeper specification). For the campaign realization, it has been selected:

- Legacy **C/A** signal.
- New-generation **L2C** signal.

L5C and L1C wanted to be incorporated but eventually were discarded due to the few SV available broadcasting these signals. Also note that worse performances may be obtained with L2C since not all SV incorporate this ranging code.

Regarding GALILEO, available signals encompassing the OS are E1, E5a and E5b (refer to section 2.3.2 for a more detailed explanation). For the campaign study, it has been decided to process GRPP with:

- **E1** signal
- **E5a/E5b** signals (depending on station receiver signal disposition).

It would have been very interesting to incorporate E5 signal (combination of E5a and E5b through AltBOC modulation) since this signal-service seems to offer very promising performances in the simulations (refer to [BR.7]). However, the algorithm implementation was far-too complex and finally it was decided to leave this signal out of the campaign's scope.

Eventually, it was concluded to launch the campaign processing with 4 different free-access GNSS signals. These are listed in Table 4.6 along with its expected pseudorange domain errors.

A relevant technical detail related with the expected errors in Table 4.6 needs to be highlighted. Remember from GRPP specification (see REQ-FUN-49 and REQ-FUN-50) that the expected observation error is configured by the user and used by GRPP in order to account for the ponderation performed when estimating the receiver position parameters. The criteria followed for the campaign GRPP configuration has been to configure the 1% of the chip length of each signal observation.

The chip length is defined as the longitude of each ranging code bit as shown in Figure 4.3. The chip length can be directly computed knowing the number of bits which form the code sequence and its chipping rate (refer to [BR.2] for formulae definition). Consequently, signal's chipping rate is indirectly proportional to the expected pseudorange error e.g. E1 against E5a/E5b specifications. Note that, the higher the chipping rate, the more precise ranging code correlation is achieved but wider bandwidths are needed.

Table 4.6 – Selected signal-service observations and expected error in the pseudorange domain.

System	Service	Signal	Carrier Frequency [MHz]	Chipping rate [Mbps]	Chip length [m]	Expected precision [m]
GPS	SPS	C/A	1575.42	1.023	293.05	3.0
GPS	SPS	L2C	1227.6	1.023	293.05	3.0
GALILEO	OS	E1	1575.42	1.023	293.05	3.0
GALILEO	OS	E5a/E5b	1176.45 / 1207.14	10.23	29.30	0.3

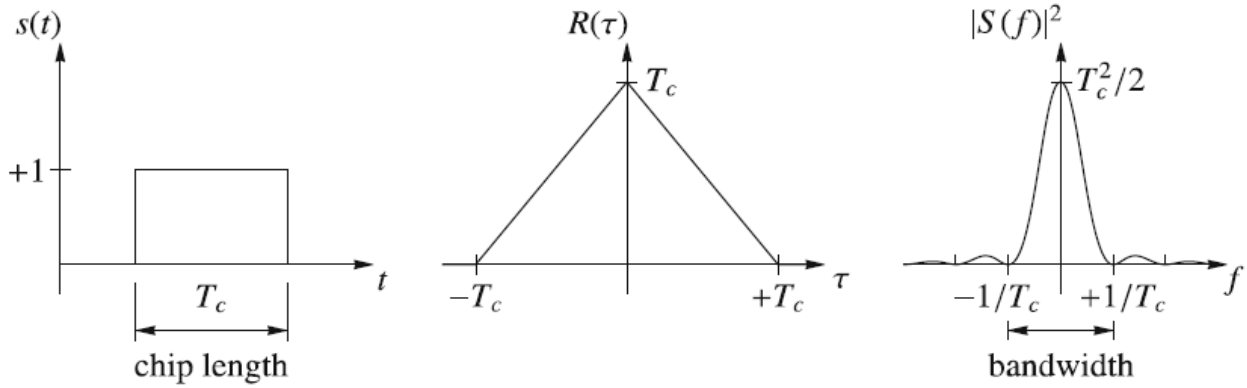

Figure 4.3 – Chip length illustration along with signal's bandwidth. Source: Hoffman et al. 2008.

4.3 Obtained Results

Having stated the data arrangement for the campaign analysis, the observation and navigation RINEX files were downloaded and archived in an Ubuntu MATE virtual machine. Then the whole campaign launch process was assessed by automatizing its routine with Perl and Bash scripts (these can be consulted in the dedicated campaign repository of annex 0).

The campaign is formed by 5 stations on 3 observation dates and 4 signal executions. This is translated in 60 GRPP+GSPA executions to be carried out for the campaign. Once again, script automatization came in handy for its management.

Configuration Brief

A small mention about GRPP+GSPA configuration needs to be added before presenting the campaign results. Since 60 executions were needed, 60 configuration files were necessary too. It would have been very tedious to configure each of them individually. Therefore, the configuration for the campaign was assessed by using 4 configurations templates (one for each signal). These are available in the campaign repository.

The configuration was kept with a basic profile. For both GPS-SPS and GALILEO-OS:

- Satellite mask of 10º.
- Klobuchar model for ionosphere correction.
- Saastamoinen model for troposphere correction.
- Expected observation error according to Table 4.6.
- Maximum of 4 iterations on LSQ routine and a convergence threshold of 0.0001 m.
- Accuracy scale factors to account for the 95% of reliability in both vertical and horizontal domains.
- Static mode with station references set according to the precise coordinates defined in Table 4.3.
- Integrity mode with stipulated alert limits according to our own accuracy requirements in Table 1.1.

The configuration differing among GPS and GALILEO was the ephemerids time-out threshold and the discarded SV:

- Ephemerid time threshold:
  - For GPS 1.5 hours
  - For GALILEO 0.5 hours

This is due to different navigation data layout in the RINEX format. On GPS side, the ephemerids block among each SV are spaced more or less by two hours, whereas on GALILEO case they are normally separated 10 minutes (though it can be more). Eventually, this specific configuration was needed in order to do not use timed-out navigation data.

- Discarded SV:
  - None for GPS
  - E14, E18 and E24 (not in all scenarios) for GALILEO

As previously commented, E14 and E18 are the two SV with a higher eccentricity due to launching issues. In addition, E24 was ripped of some E5a/E5b processing since residual plots showed significant noise in the first campaign iterations for this SV.

4.3.1 Campaign Processing Status

For successfully launching the whole campaign, one iteration was not enough. As a matter of fact, 6 trials were necessary due to input data processing issues, such as GPS navigation files which did not include Klobuchar ionosphere coefficients. Nevertheless, 97% of the executions were successfully launched.

Among all campaign executions, not all epochs had a valid position status. The campaign scenario status is exemplified in Table 4.7 and completely included in annex 0 (Table 8.6). Is not a surprise that GALILEO scenarios account for fewer valid processing status than GPS cases due to the announced lack of SV availability. Additionally, it can be observed that GPS C/A status for Date #1 and Date #2 are very similar, but this is not the case for GALILEO. When the same processing time window is set (as in Date 1) for an incomplete constellation, availability lacks in a global network are logically encountered.

Table 4.7 – Campaign executions status extract.

Station	Date	System	Signal	Epochs	Valid Epochs	Invalid Epochs	Valid %	Invalid %
ABMF	DATE_1	GPS	C/A	481	481	0	100.0	0.0
OWMG	DATE_2	GPS	L2C	1201	1201	0	100.0	0.0
KOUG	DATE_3	GAL	E1	961	954	7	99.3	0.7
KIRU	DATE_2	GAL	E5b	721	698	23	96.8	3.2
MAJU	DATE_3	GPS	L2C	1201	1152	49	95.9	4.1
TASH	DATE_2	GPS	L2C	1201	846	355	70.4	29.6
KOKV	DATE_1	GAL	E1	481	318	163	66.1	33.9
TASH	DATE_1	GAL	E5b	481	308	173	64.0	36.0
FAIR	DATE_3	GAL	E1	401	203	198	50.6	49.4
TASH	DATE_2	GAL	E5b	1201	587	614	48.9	51.1

Unfortunately, two executions out of the 60 performed needed to be discarded. These two are the GALILEO scenarios in MAJU station on Date #3. Available GSPA plots seem to show a total lack of observed SV. Nonetheless, the root cause should be further investigated. Henceforth, these executions will not be included in the campaign results.

4.3.2 Accuracy Results

Regarding accuracy performance campaign results, these have been arranged by campaign date. On each date, two figures are available which account for each GPS-SPS and GALILEO-OS. Inside each figure, the accuracy RMS indicators are available for each station, horizontal/vertical domain and system signal combination.

Minor comments for each graph will be included. More important, accuracy issues and expected performance results will be highlighted and later discussed in section 4.3.4.

Date #1

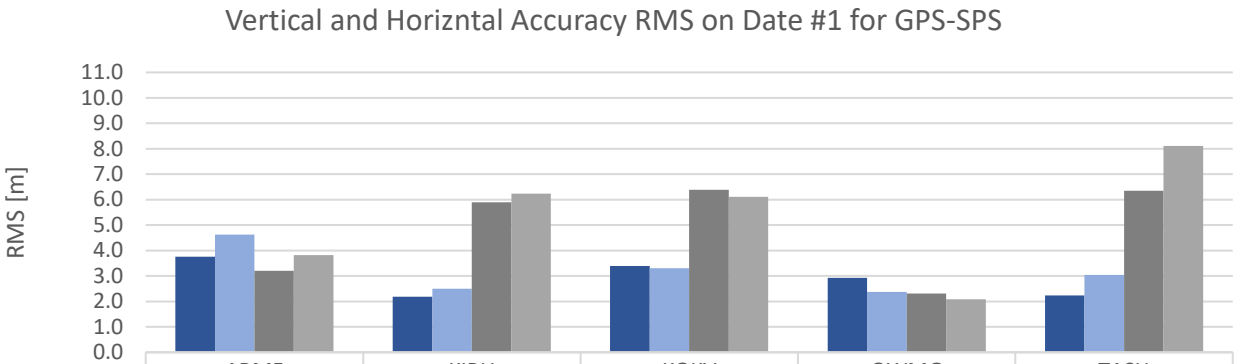

	ABMF	KIRU	KOKV	OWMG	TASH
HRMS C/A	3.8	2.2	3.4	2.9	2.2
VRMS C/A	4.6	2.5	3.3	2.4	3.0
HRMS L2C	3.2	5.9	6.4	2.3	6.4
VRMS L2C	3.8	6.2	6.1	2.1	8.1

Figure 4.4 – Campaign accuracy results on Date #1 for GPS-SPS.

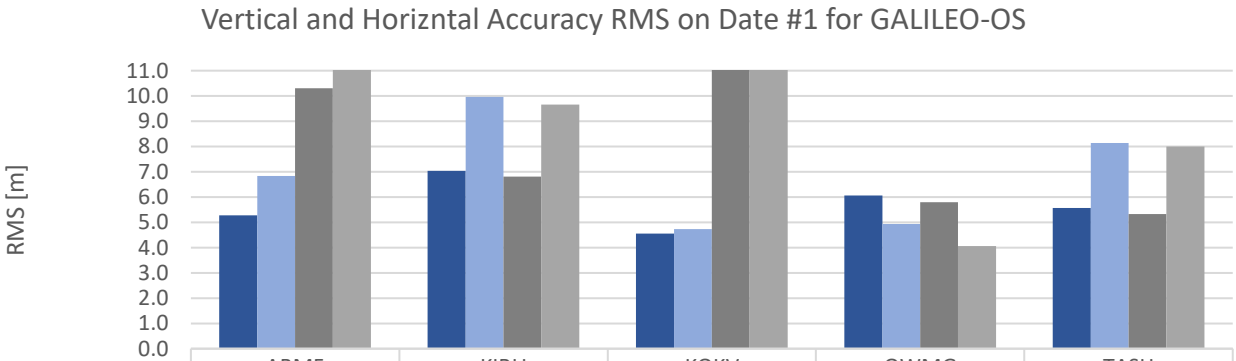

	ABMF	KIRU	KOKV	OWMG	TASH
HRMS E1	5.3	7.0	4.6	6.1	5.6
VRMS E1	6.8	10.0	4.7	4.9	8.1
HRMS E5a/E5b	10.3	6.8	29.2	5.8	5.3
VRMS E5a/E5b	12.9	9.7	29.7	4.1	8.0

Figure 4.5 – Campaign accuracy results on Date #1 for GALILEO-OS.

From Figure 4.4 and Figure 4.5 a better performance on the GPS side is immediately deduced. In fact, GPS accuracy performance is quite good specially for C/A signal not as for L2C due to the fewer SV available broadcasting this signal. All GPS performances fall within the expected results from section 4.1.2. Some GSPA plots examples with fair performances are sowed in page 120.

For GALILEO results, a worse performance than in GPS cases is observed but this was expected due to the constellation incompletion. However, the performances of both signals meet the expected results criteria except for KOKV case. KOKV accuracy results can only be accepted with the requirements listed in Table 2.7. The KOKV issue is later assessed in page 123. Also note that performance among GALILEO in each station is more heterogenous. This is caused by the stations and time window selection. Since GALILEO has less than 24 SV, global coverage cannot be reached, hence having an impact in the accuracy performance.

Date #2

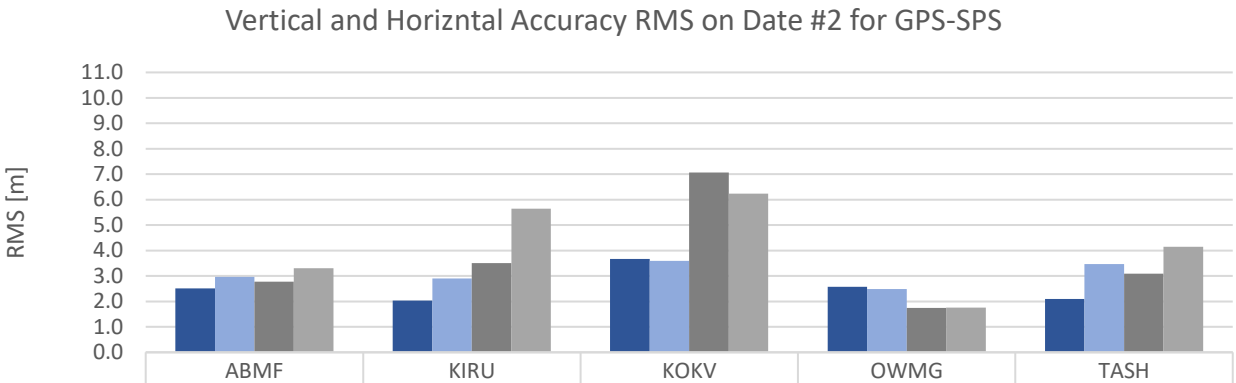

	ABMF	KIRU	KOKV	OWMG	TASH
HRMS C/A	2.5	2.0	3.7	2.6	2.1
VRMS C/A	3.0	2.9	3.6	2.5	3.5
HRMS L2C	2.8	3.5	7.1	1.8	3.1
VRMS L2C	3.3	5.7	6.2	1.8	4.2

Figure 4.6 – Campaign accuracy results on Date #2 for GPS-SPS.

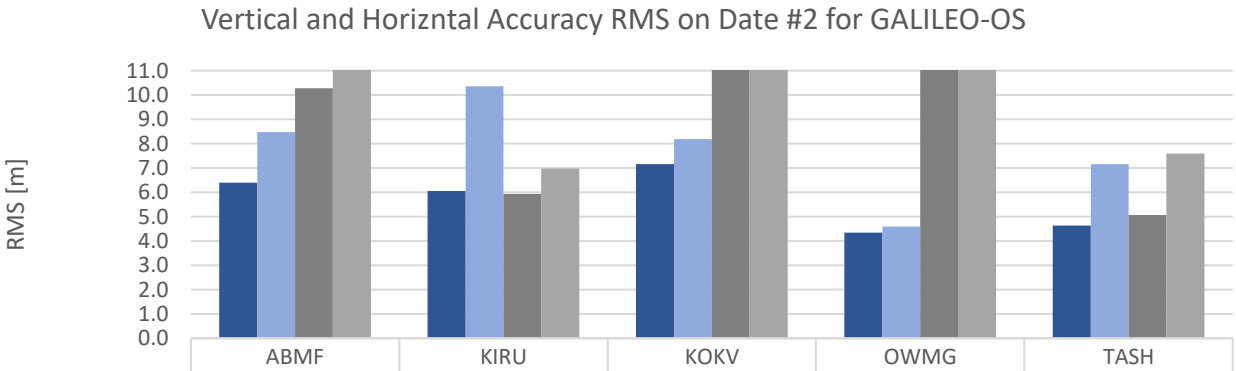

	ABMF	KIRU	KOKV	OWMG	TASH
HRMS E1	6.4	6.1	7.2	4.3	4.6
VRMS E1	8.5	10.4	8.2	4.6	7.2
HRMS E5a/E5b	10.3	5.9	28.9	12.7	5.1
VRMS E5a/E5b	13.4	7.0	28.1	11.6	7.6

Figure 4.7 – Campaign accuracy results on Date #2 for GALILEO-OS.

Again and as expected, a better performance is accomplished in GPS side by looking at Figure 4.6 and Figure 4.7. GPS-SPS accuracies accomplish the expected results exceeding expectations in most cases.

Date #2 was supposed to have fair constellation availability conditions. Consequently, better performances compared to those in Date #1 should be encountered. This seems to be the case for GPS (by a very narrow margin) but for GALILEO only a few instances of signal E1 present a significant improvement while some others are even worse. Most probably, the E14, E18 and E24 SV were included in the preliminary planning and then discarded for the campaign processing, eventually resulting in a worse observation geometry than the one predicted.

GALILEO E1 scenarios are accomplish (tough in the limit) the expected results. However, some E5a/E5b executions seem to be problematic (again, especially in KOKV).

Date #3

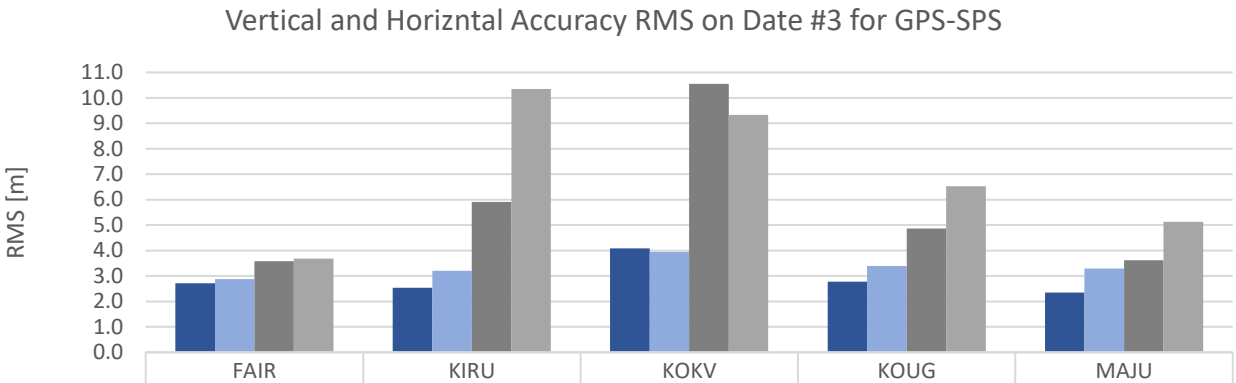

	FAIR	KIRU	KOKV	KOUG	MAJU
HRMS C/A	2.7	2.5	4.1	2.8	2.4
VRMS C/A	2.9	3.2	4.0	3.4	3.3
HRMS L2C	3.6	5.9	10.6	4.9	3.6
VRMS L2C	3.7	10.4	9.3	6.5	5.1

Figure 4.8 – Campaign accuracy results on Date #3 for GPS-SPS.

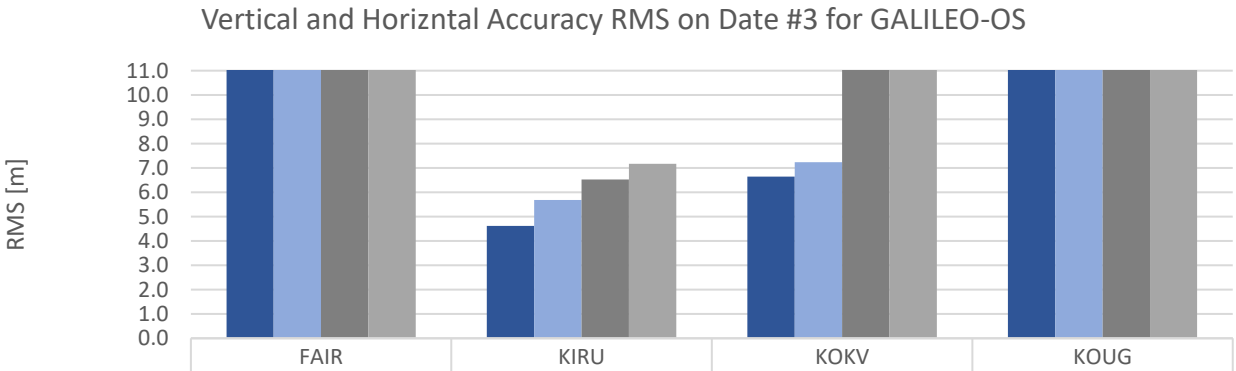

	FAIR	KIRU	KOKV	KOUG
HRMS E1	14.7	4.6	6.6	17.2
VRMS E1	11.4	5.7	7.2	22.6
HRMS E5a/E5b	14.8	6.5	44.9	17.9
VRMS E5a/E5b	11.5	7.2	49.1	23.0

Figure 4.9 – Campaign accuracy results on Date #3 for GALILEO-OS.

In the scenarios where non-nominal conditions are encountered, performances suffer from degradation as expected (see Figure 4.8 and Figure 4.9). Beware that for Date #3 is not as important meeting the expected results but to compare them with the ones obtained under nominal conditions.

Nonetheless, GPS services are fulfilling the expected results even in critical conditions, especially for C/A signal where performances stay the same. Nonetheless, significant performance degradation does happen for L2C signal, meaning that ionosphere phenomena effects are projected through weaker SV constellation geometries.

This statement is confirmed too by observing GALILEO performances where FAIR and KOUG cases seem to have a very bad constellation disposition. Is quite surprising that GALILEO performances stay nominal on KIRU and KOKV-E1 cases performing even better than in L2C homologous occurrences.

4.3.3 Integrity Results

For integrity performance, results have also been arranged by processing date. For each date, percentages regarding integrity events (MI, HMI and SA) are represented on four figures. Each figure stands for the combination among the signals and the receiver local components (vertical and horizontal domains).

Like accuracy results, minor comments are included for each date and most relevant results are highlighted and then detailed in section 4.3.4.

Date #1

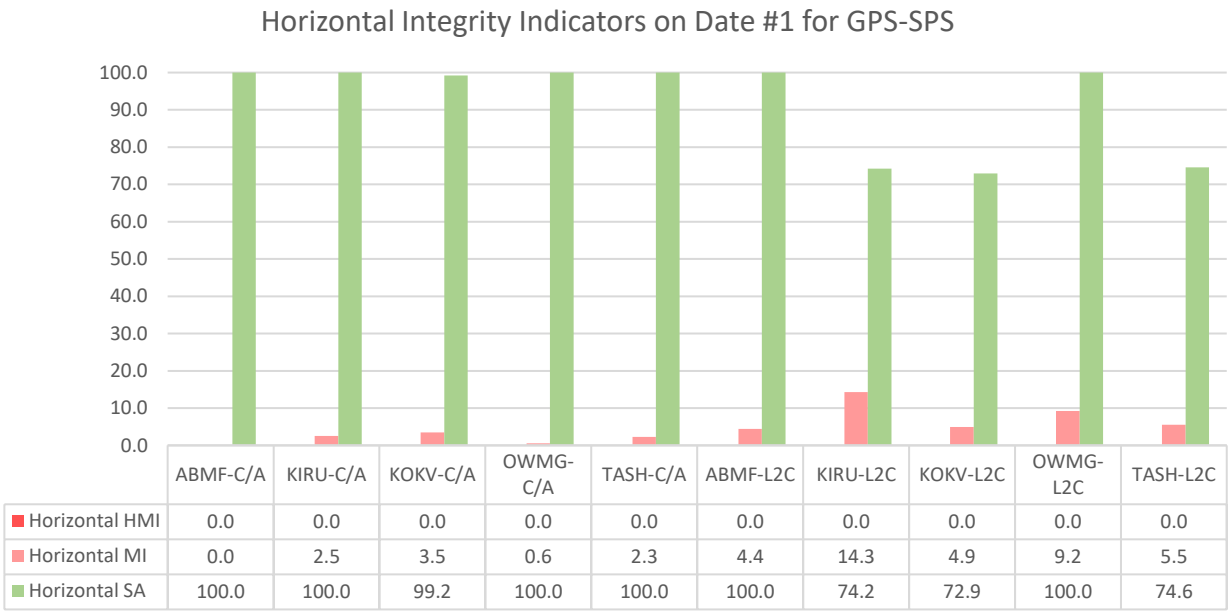

	ABMF-C/A	KIRU-C/A	KOKV-C/A	OWMG-C/A	TASH-C/A	ABMF-L2C	KIRU-L2C	KOKV-L2C	OWMG-L2C	TASH-L2C
Horizontal HMI	0.0	0.0	0.0	0.0	0.0	0.0	0.0	0.0	0.0	0.0
Horizontal MI	0.0	2.5	3.5	0.6	2.3	4.4	14.3	4.9	9.2	5.5
Horizontal SA	100.0	100.0	99.2	100.0	100.0	100.0	74.2	72.9	100.0	74.6

Figure 4.10 – Campaign horizontal integrity results on Date #1 for GPS-SPS.

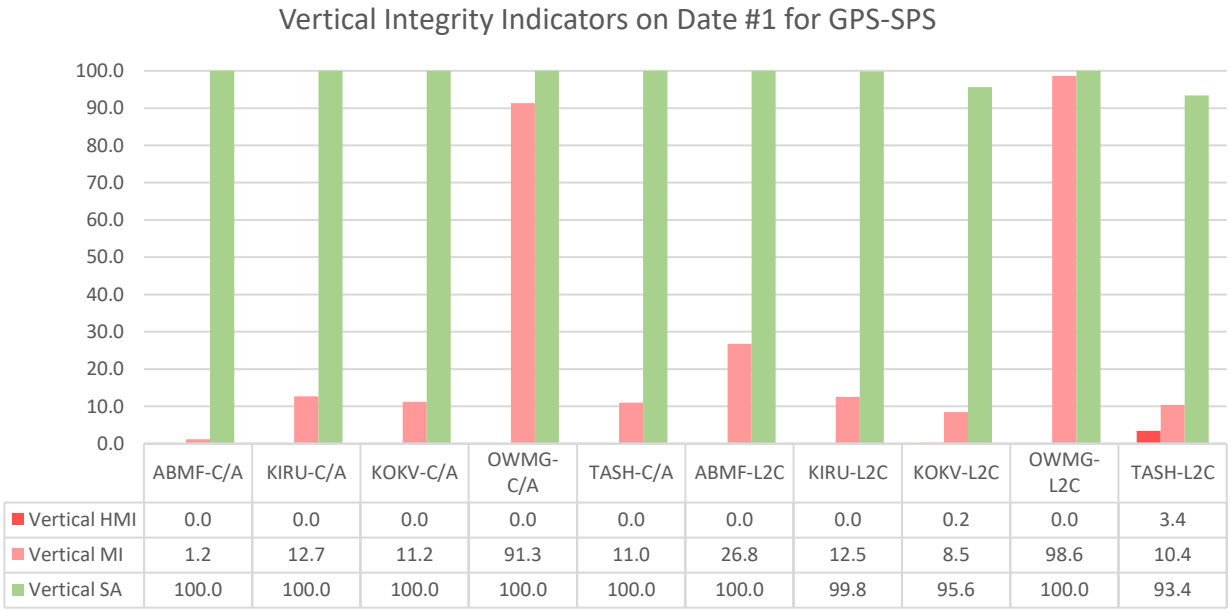

	ABMF-C/A	KIRU-C/A	KOKV-C/A	OWMG-C/A	TASH-C/A	ABMF-L2C	KIRU-L2C	KOKV-L2C	OWMG-L2C	TASH-L2C
Vertical HMI	0.0	0.0	0.0	0.0	0.0	0.0	0.0	0.2	0.0	3.4
Vertical MI	1.2	12.7	11.2	91.3	11.0	26.8	12.5	8.5	98.6	10.4
Vertical SA	100.0	100.0	100.0	100.0	100.0	100.0	99.8	95.6	100.0	93.4

Figure 4.11 – Campaign vertical integrity results on Date #1 for GPS-SPS.

For GPS integrity performance under Date #1 nominal conditions (Figure 4.10 and Figure 4.11), C/A integrity performances on both vertical and horizontal domains are outstanding and exceed the expected results, except for OWMG. In fact, seems like OWMG has vertical integrity issues for both signal-services, meaning that the root cause may be related with the site instead of the signal. The most suspicious fact for this is OWMG precise coordinates ITRF realization which it turns to be the oldest (see Table 4.3).

For L2C integrity performances these are bit odd and do not perform as well as C/A. Nonetheless this is due to the fewer SV available. Surprisingly, L2C vertical performances accomplish more SA trading off higher MI cases (compare L2C KOKV and TASH cases among vertical and horizontal components).

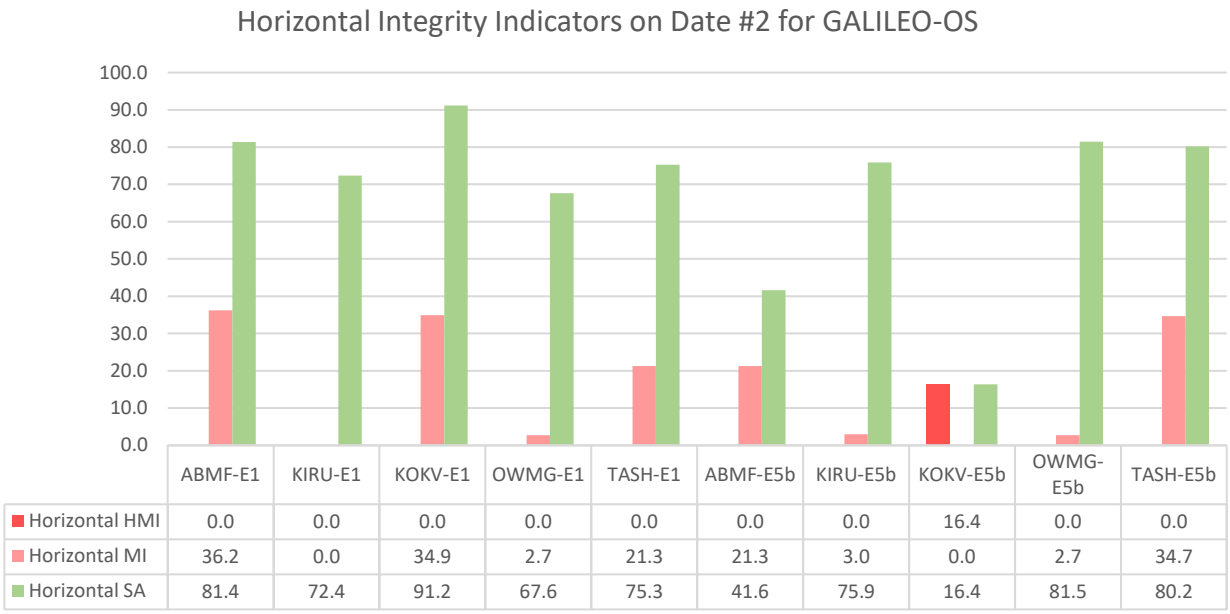

	ABMF-E1	KIRU-E1	KOKV-E1	OWMG-E1	TASH-E1	ABMF-E5b	KIRU-E5b	KOKV-E5b	OWMG-E5b	TASH-E5b
Horizontal HMI	0.0	0.0	0.0	0.0	0.0	0.0	0.0	16.4	0.0	0.0
Horizontal MI	36.2	0.0	34.9	2.7	21.3	21.3	3.0	0.0	2.7	34.7
Horizontal SA	81.4	72.4	91.2	67.6	75.3	41.6	75.9	16.4	81.5	80.2

Figure 4.12 – Campaign horizontal integrity results on Date #1 for GALILEO-OS.

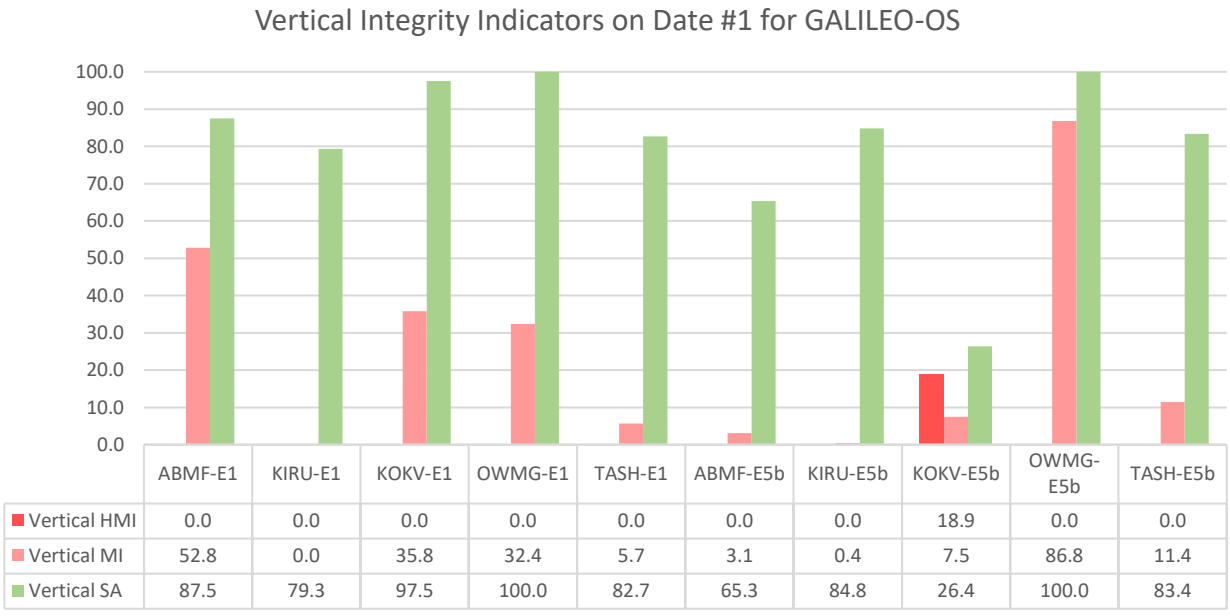

	ABMF-E1	KIRU-E1	KOKV-E1	OWMG-E1	TASH-E1	ABMF-E5b	KIRU-E5b	KOKV-E5b	OWMG-E5b	TASH-E5b
Vertical HMI	0.0	0.0	0.0	0.0	0.0	0.0	0.0	18.9	0.0	0.0
Vertical MI	52.8	0.0	35.8	32.4	5.7	3.1	0.4	7.5	86.8	11.4
Vertical SA	87.5	79.3	97.5	100.0	82.7	65.3	84.8	26.4	100.0	83.4

Figure 4.13 – Campaign vertical integrity results on Date #1 for GALILEO-OS

For GALILEO, integrity performances are much more degraded compare to those obtained with GPS as expected (Figure 4.12 and Figure 4.13). It can be deduced a severe SA lost specially in the horizontal domain. High MI events (higher than 20%) are more often encounter in the vertical than in the horizontal domain. Also note that KOKV is manifesting its processing issue with high HMI cases.

It can be stated that expected performances are accomplished by a very narrow margin, except for ABMF and KOKV E5b executions. In addition, note again the OWMG precise coordinate definition issue.

Date #2

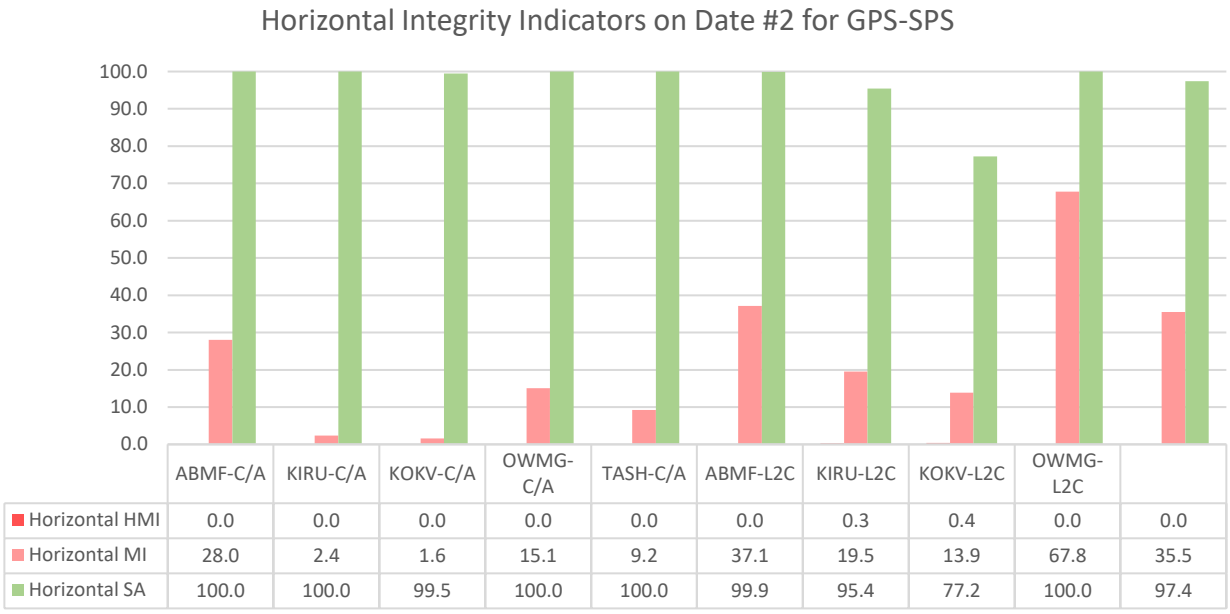

	ABMF-C/A	KIRU-C/A	KOKV-C/A	OWMG-C/A	TASH-C/A	ABMF-L2C	KIRU-L2C	KOKV-L2C	OWMG-L2C	
Horizontal HMI	0.0	0.0	0.0	0.0	0.0	0.0	0.3	0.4	0.0	0.0
Horizontal MI	28.0	2.4	1.6	15.1	9.2	37.1	19.5	13.9	67.8	35.5
Horizontal SA	100.0	100.0	99.5	100.0	100.0	99.9	95.4	77.2	100.0	97.4

Figure 4.14 – Campaign horizontal integrity results on Date #2 for GPS-SPS.

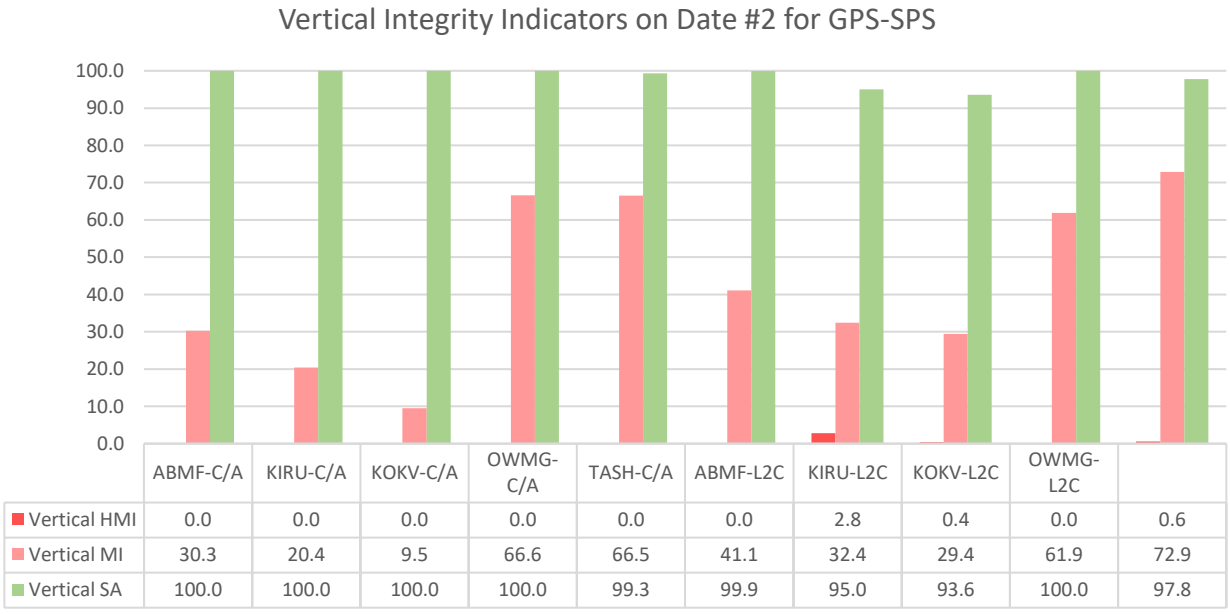

	ABMF-C/A	KIRU-C/A	KOKV-C/A	OWMG-C/A	TASH-C/A	ABMF-L2C	KIRU-L2C	KOKV-L2C	OWMG-L2C	
Vertical HMI	0.0	0.0	0.0	0.0	0.0	0.0	2.8	0.4	0.0	0.6
Vertical MI	30.3	20.4	9.5	66.6	66.5	41.1	32.4	29.4	61.9	72.9
Vertical SA	100.0	100.0	100.0	100.0	99.3	99.9	95.0	93.6	100.0	97.8

Figure 4.15 – Campaign vertical integrity results on Date #2 for GPS-SPS.

On Date #2 for GPS-SPS (Figure 4.14 and Figure 4.15), similar results as those obtained previously under nominal conditions in Date #1 are obtained. At least for SA and HMI indicators but not for MI where expected results are not met in most cases even with C/A signal. This situation is especially relevant in ABMF, KIRU and TASH stations. Regarding OWMG this is not relevant since we have already commented the potential issue with this station.

Furthermore, KOKV seems to present a horizontal L2C SA lost, probably due to the SV observation availability. The SA is improved in the vertical domain but at the expense of increasing MI cases over 20%.

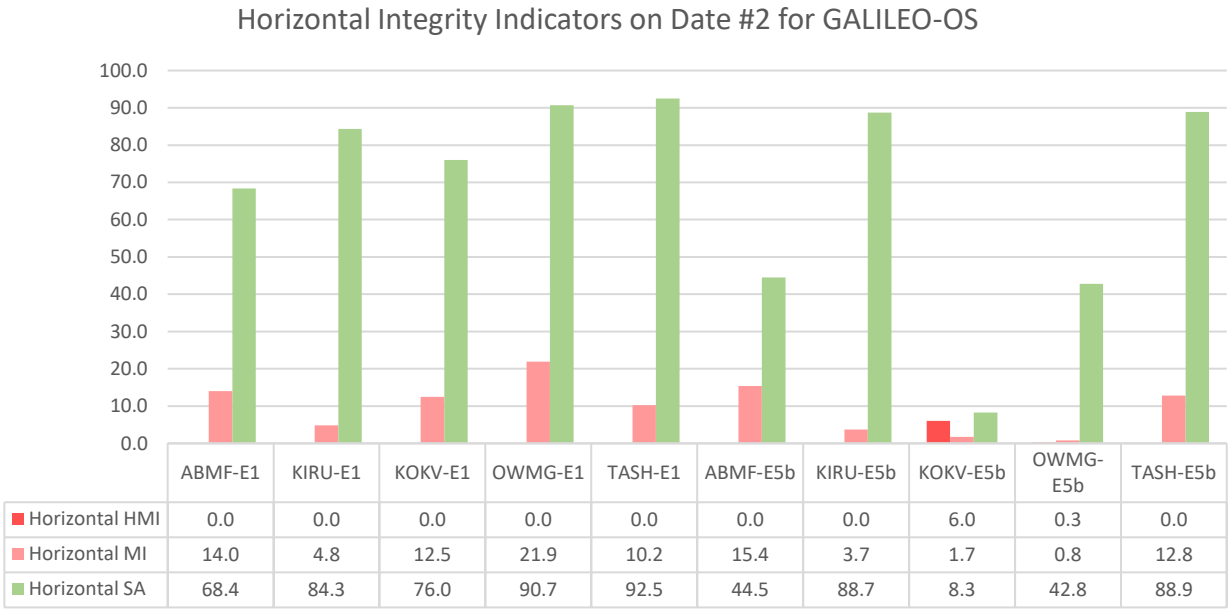

	ABMF-E1	KIRU-E1	KOKV-E1	OWMG-E1	TASH-E1	ABMF-E5b	KIRU-E5b	KOKV-E5b	OWMG-E5b	TASH-E5b
Horizontal HMI	0.0	0.0	0.0	0.0	0.0	0.0	0.0	6.0	0.3	0.0
Horizontal MI	14.0	4.8	12.5	21.9	10.2	15.4	3.7	1.7	0.8	12.8
Horizontal SA	68.4	84.3	76.0	90.7	92.5	44.5	88.7	8.3	42.8	88.9

Figure 4.16 – Campaign horizontal integrity results on Date #2 for GALILEO-OS.

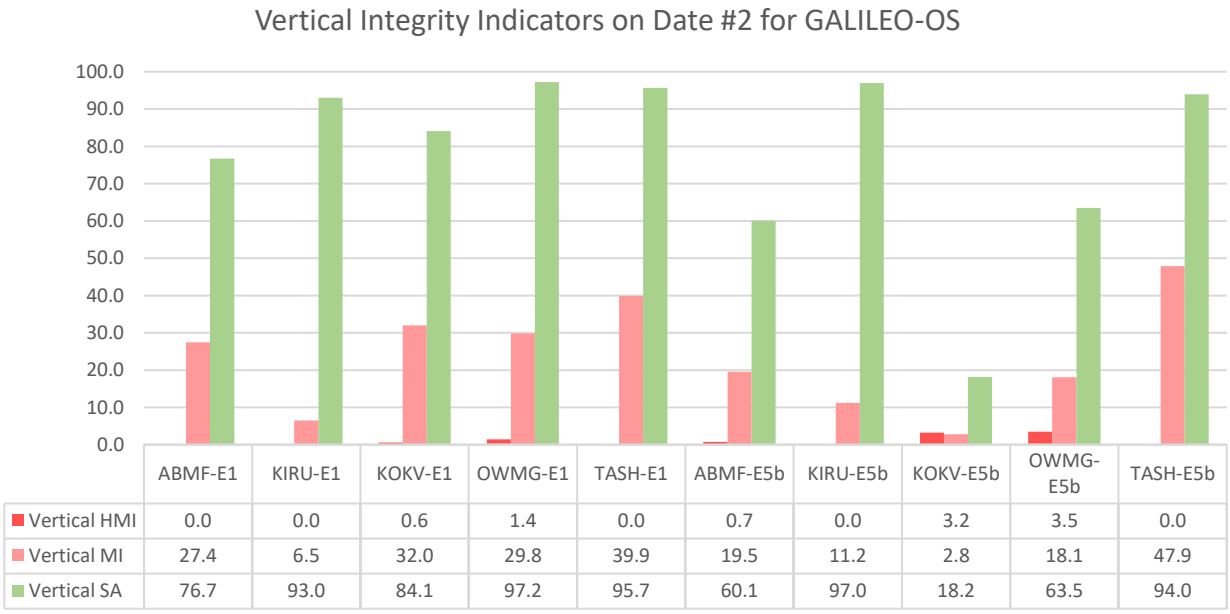

	ABMF-E1	KIRU-E1	KOKV-E1	OWMG-E1	TASH-E1	ABMF-E5b	KIRU-E5b	KOKV-E5b	OWMG-E5b	TASH-E5b
Vertical HMI	0.0	0.0	0.6	1.4	0.0	0.7	0.0	3.2	3.5	0.0
Vertical MI	27.4	6.5	32.0	29.8	39.9	19.5	11.2	2.8	18.1	47.9
Vertical SA	76.7	93.0	84.1	97.2	95.7	60.1	97.0	18.2	63.5	94.0

Figure 4.17 – Campaign vertical integrity results on Date #2 for GALILEO-OS.

For GALILEO integrity results on Date #2, it can be deduced that expected performances are met specially for SA indicator (Figure 4.16 and Figure 4.17). Once again KOKV and OWMG present processing issues.

Obviously, GPS performances are far better, but for Date #2 the difference is not as big as in Date #1. This may be due to the date selection nature: Date #1 was set as the same UTC processing window for both GPS and GALILEO whereas Date #2 epochs were selected based on the best SV availability scenario.

Date #3

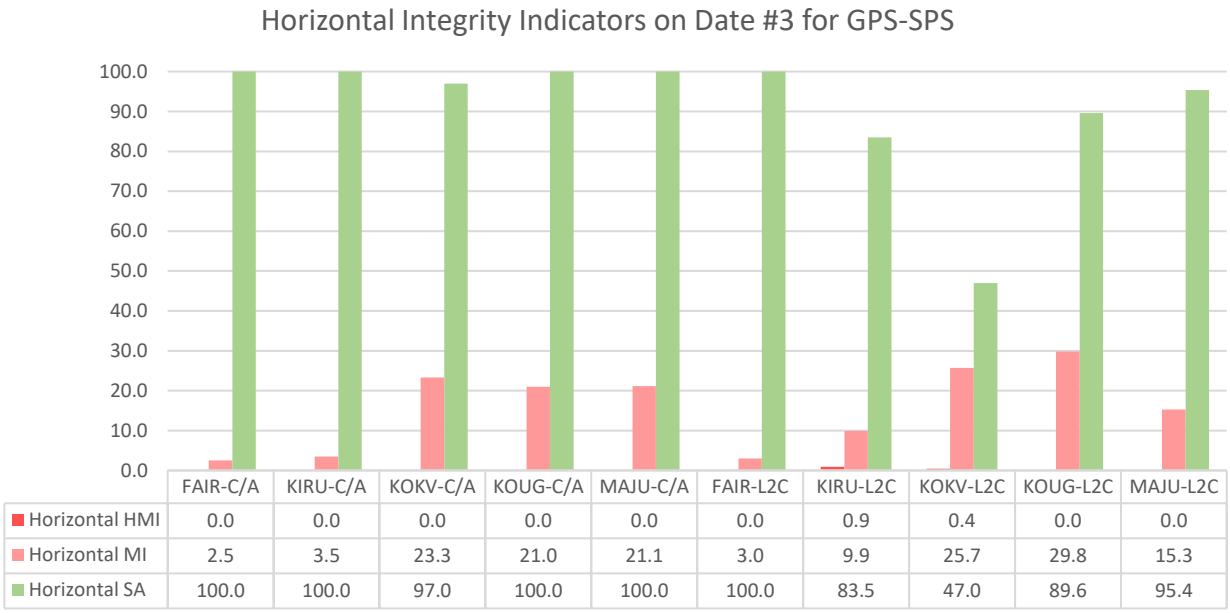

	FAIR-C/A	KIRU-C/A	KOKV-C/A	KOUG-C/A	MAJU-C/A	FAIR-L2C	KIRU-L2C	KOKV-L2C	KOUG-L2C	MAJU-L2C
Horizontal HMI	0.0	0.0	0.0	0.0	0.0	0.0	0.9	0.4	0.0	0.0
Horizontal MI	2.5	3.5	23.3	21.0	21.1	3.0	9.9	25.7	29.8	15.3
Horizontal SA	100.0	100.0	97.0	100.0	100.0	100.0	83.5	47.0	89.6	95.4

Figure 4.18 – Campaign horizontal integrity results on Date #3 for GPS-SPS.

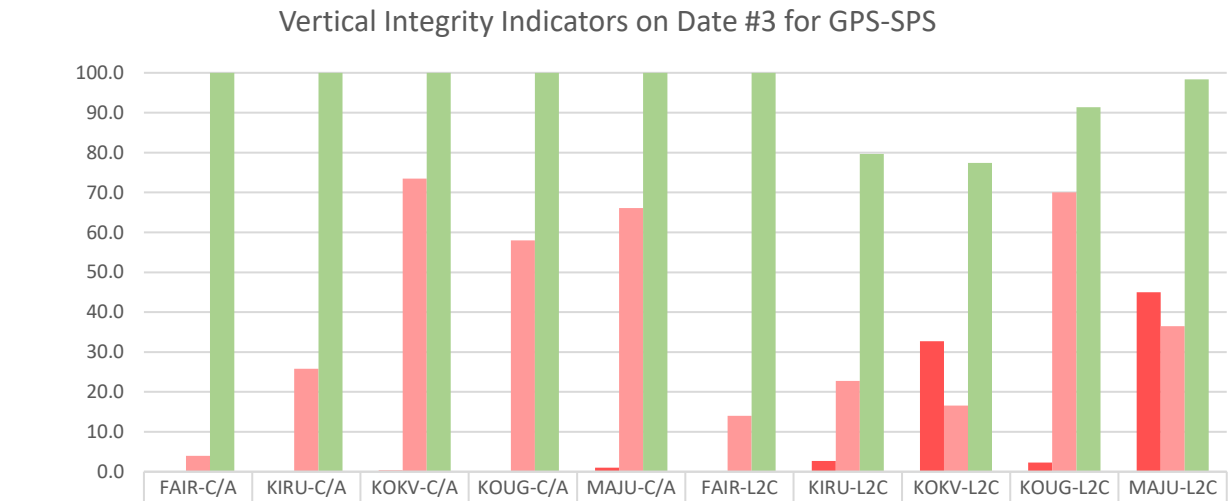

	FAIR-C/A	KIRU-C/A	KOKV-C/A	KOUG-C/A	MAJU-C/A	FAIR-L2C	KIRU-L2C	KOKV-L2C	KOUG-L2C	MAJU-L2C
Vertical HMI	0.0	0.0	0.3	0.0	1.0	0.0	2.7	32.7	2.3	45.0
Vertical MI	4.0	25.8	73.5	58.0	66.1	14.0	22.8	16.6	70.0	36.5
Vertical SA	100.0	100.0	100.0	100.0	100.0	100.0	79.7	77.4	91.4	98.4

Figure 4.19 – Campaign vertical integrity results on Date #3 for GPS-SPS.

As expected, Figure 4.18 and Figure 4.19 demonstrate that integrity performances are severely affected when facing abnormal ionosphere conditions. Despite that for GPS horizontal performances stay more or less the same, for the vertical domain these suffer from dramatic increase in either MI or HMI. Obviously, this is the expected behavior since ionosphere delay affects the receiver's zenithal component. The only remarkable exception is FAIR station which is not so affected by the scintillation.

It shall be remarked that the vertical MI cases are significant in C/A signal while HMI cases for L2C are extreme for KOKV and MAJU executions. As in accuracy, seems like integrity performance degradation is largely projected through weaker SV geometries (differences in SV observation availability among C/A and L2C).

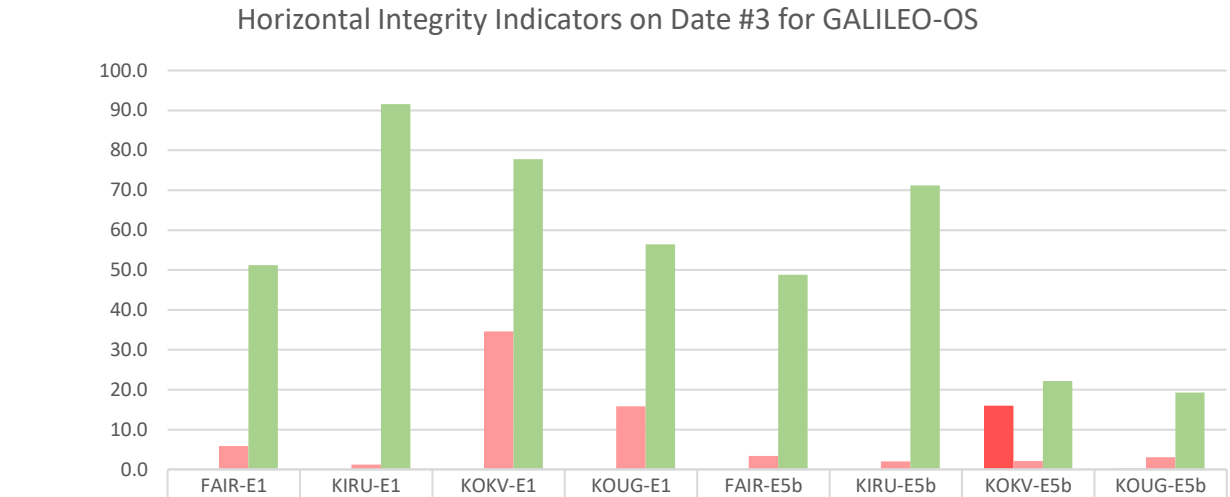

	FAIR-E1	KIRU-E1	KOKV-E1	KOUG-E1	FAIR-E5b	KIRU-E5b	KOKV-E5b	KOUG-E5b
Horizontal HMI	0.0	0.0	0.0	0.0	0.0	0.0	16.0	0.2
Horizontal MI	5.9	1.2	34.6	15.8	3.4	2.0	2.1	3.1
Horizontal SA	51.2	91.6	77.8	56.4	48.8	71.2	22.2	19.3

Figure 4.20 – Campaign horizontal integrity results on Date #3 for GALILEO-OS.

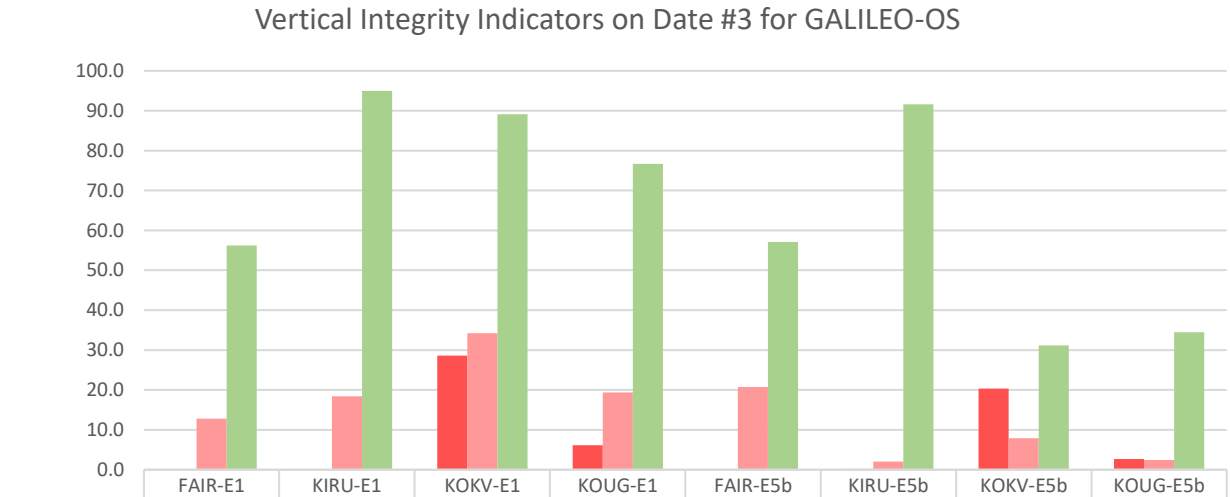

	FAIR-E1	KIRU-E1	KOKV-E1	KOUG-E1	FAIR-E5b	KIRU-E5b	KOKV-E5b	KOUG-E5b
Vertical HMI	0.0	0.0	28.6	6.1	0.0	0.2	20.3	2.7
Vertical MI	12.8	18.4	34.2	19.4	20.7	2.0	7.9	2.4
Vertical SA	56.2	95.0	89.1	76.7	57.1	91.6	31.2	34.5

Figure 4.21 – Campaign vertical integrity results on Date #3 for GALILEO-OS.

For GALILEO integrity outcomes on non-nominal conditions (Figure 4.20 and Figure 4.21), when comparing them to those obtained in the other dates (discarding pesky KOKV case), the performances are degraded specially in the vertical domain as expected.

But compared to those obtained on the same date with GPS, a few interesting facts can be enumerated. Firstly, a worse SA indicator is clearly observed in GALILEO side most probably due to the fewer SV availability. Secondly, MI and HMI indicators are much better than those in GPS. It can be assumed that even with the lack of observed SV, GALILEO presents better alarming performances which are achieved by trading-off SA on the way.

Finally, it is important to recall that MAJU station was discarded due to GALILEO processing issues. It would have been very interesting these results sine MAJU station seems to hold the worst integrity outcome in the whole campaign.

4.3.4 Detailed Results

For this section, major campaign results aspects commented on section 4.3.2 and 4.3.3 are presented and detailed with GSPA output plots in order to better depict the performance analysis. If any further detailed results need to be consulted these are accessible through the campaign repository (refer to annex 0).

Fair Performances Status

Figure 4.22 shows the positioning errors and the horizontal integrity performance obtained with C/A signal. This is a clear example of GPS-SPS exceeding the expected performances under nominal conditions. A random position pattern can be observed in the polar plot with a slightly biased upping component estimation, but only reaching 4 m as maximum, which is quite good for this service. Furthermore, the error white noise patter corresponds to the LSQ hypothesis detailed in equation (2.44), therefore is not a surprise that horizontal integrity is accomplished with 100% of SA and only a few MI cases.

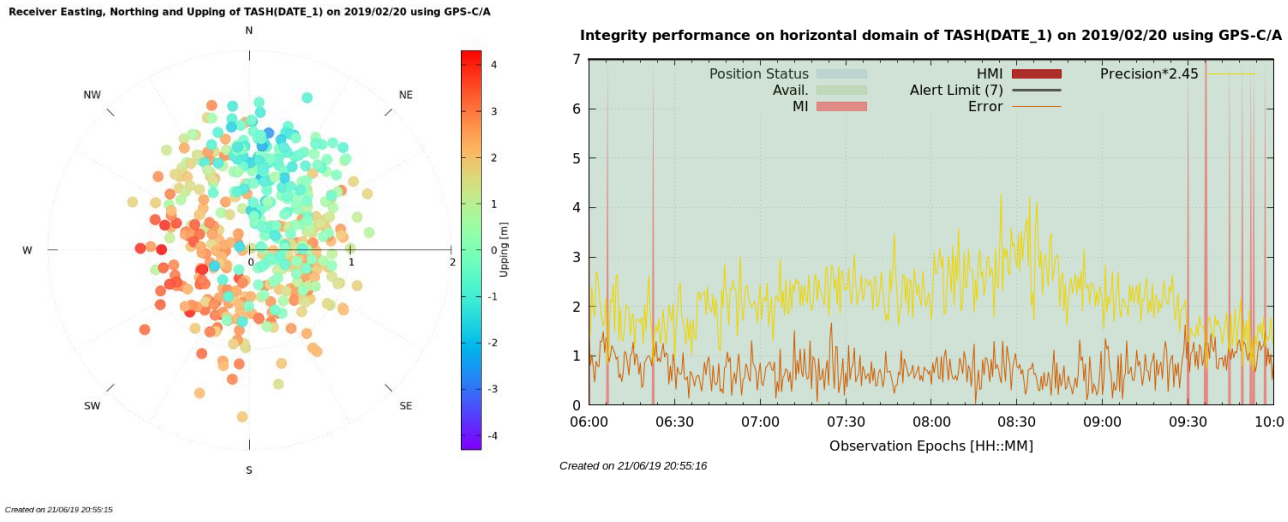

Figure 4.22 – GPS C/A expected performances under nominal conditions.

On Figure 4.23 and Figure 4.24, positioning performances obtained with GALILEO-OS signals are displayed. They key aspect on both graphs is that most of the solutions are centered and do follow a

random pattern distribution around the reference, but some positions are far away from it. However, it can be deduced that these anomalous solutions are mainly due to the SV availability. Figure 4.23 comes along the WLSQ report which indicates a very few DoF. Figure 4.24 is complemented with the SV availability plot which in most cases, the number of valid SV is not greater than 7.

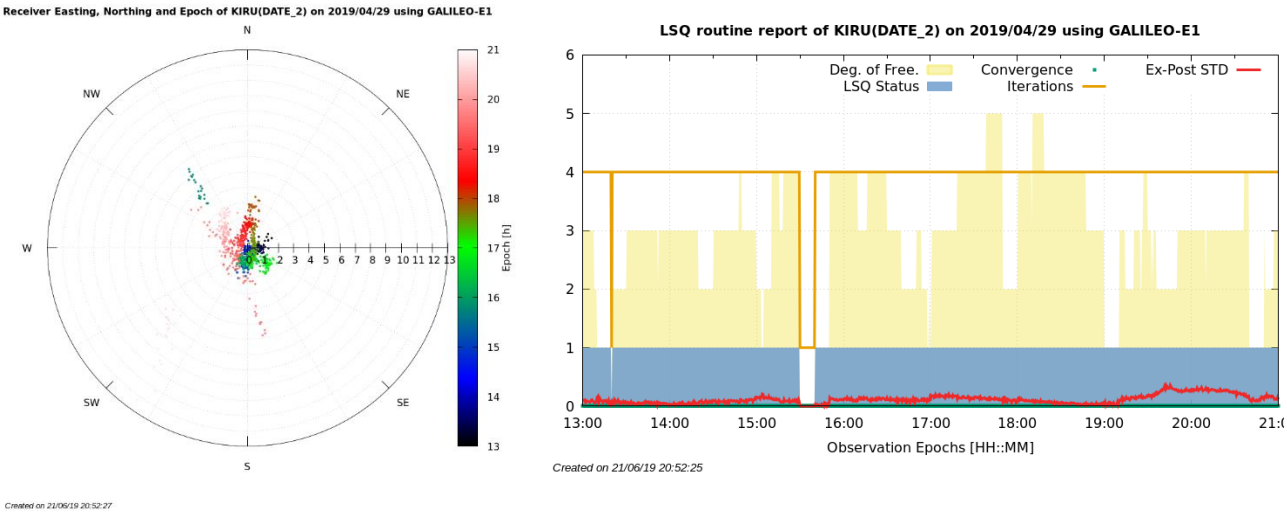

Figure 4.23 – GALILEO E1 expected performances under nominal conditions (accounting for fewer SV).

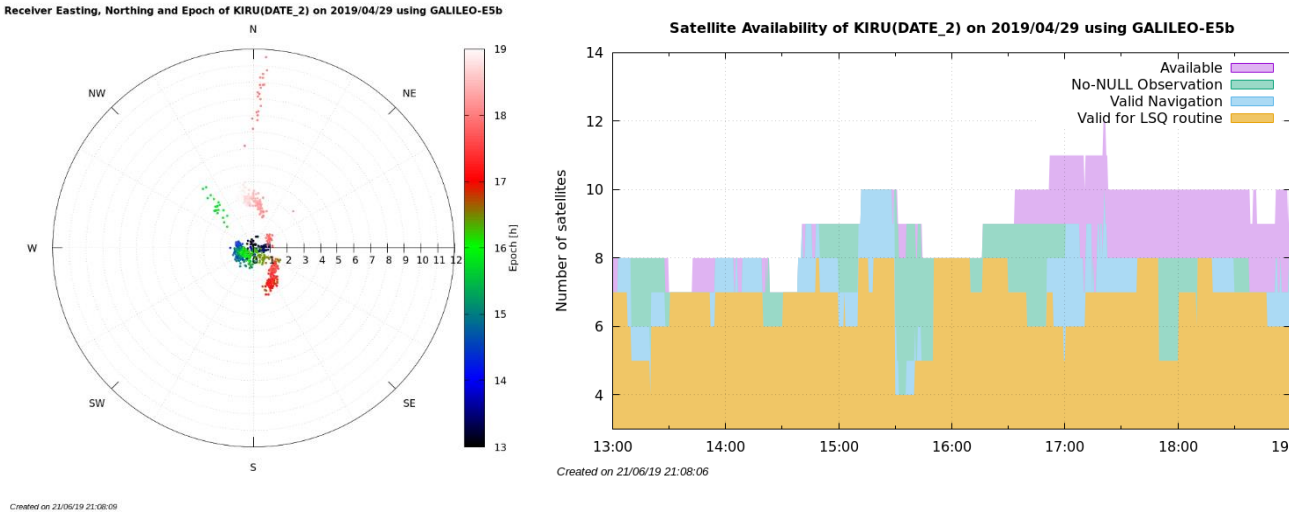

Figure 4.24 – GALILEO E5b expected performances under nominal conditions (accounting for fewer SV).

Last but not the least, Figure 4.25 is a good example of fair performances, but this time obtained under non-nominal circumstances. Seems like L2C signal is not affected by the scintillation event in FAIR on Date #2. However, a few MI cases in the vertical domain occur just when the abnormal event was reported (see Table 4.5). This means that eventually L2C signal is affected but probably due to its fair SV geometry disposition its performances are not severely degraded.

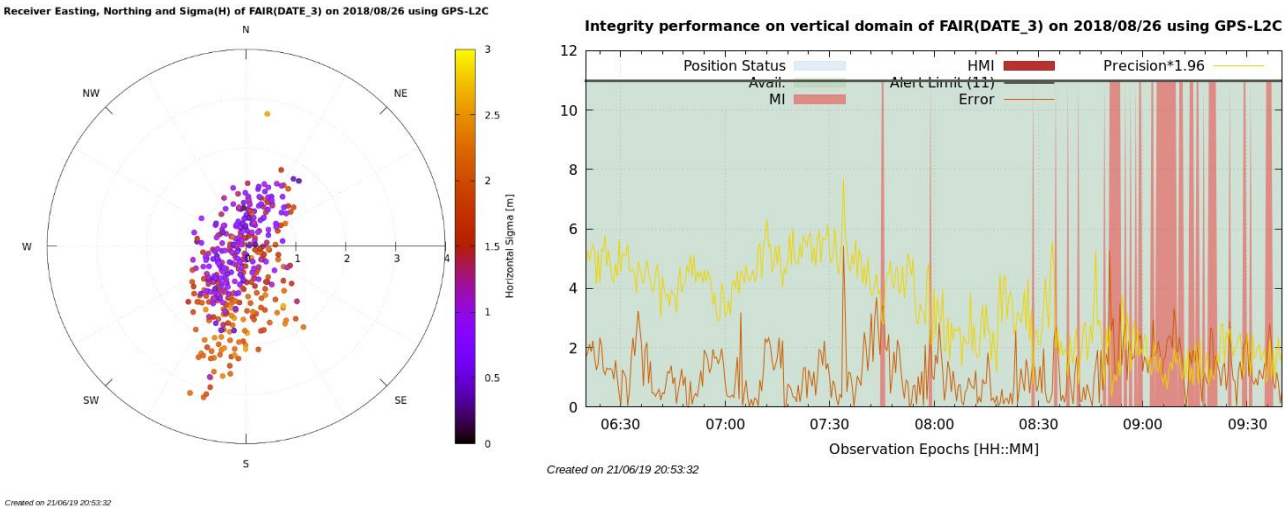

Figure 4.25 – GPS L2C fair performances under non-nominal conditions.

Constellation Geometry Disposition

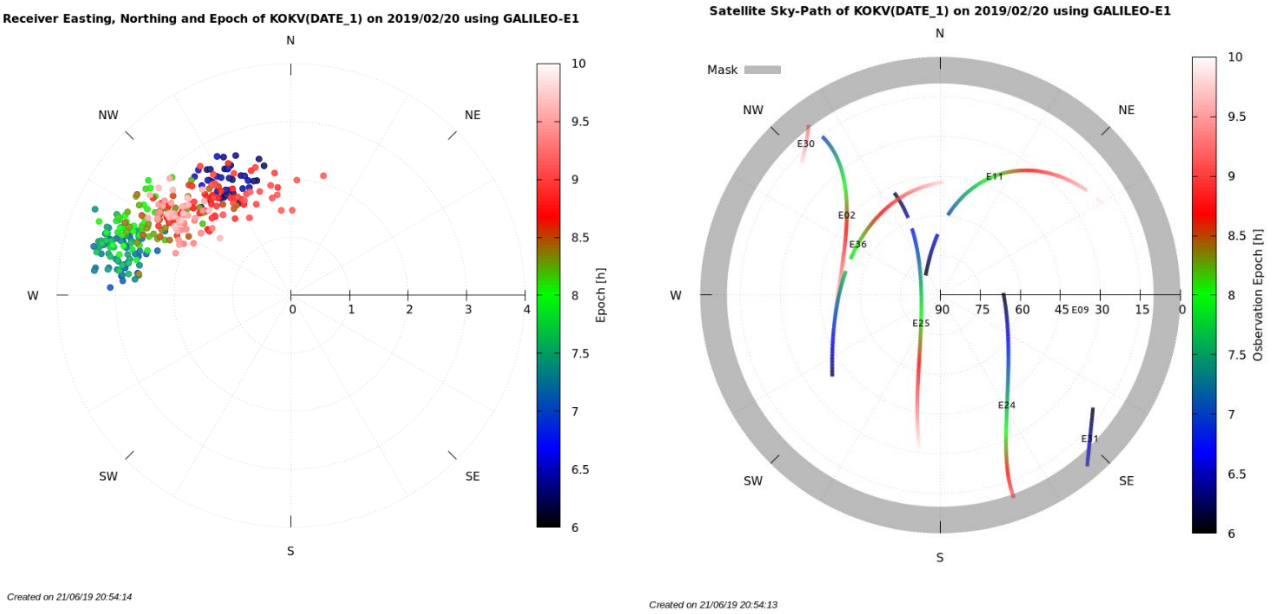

Figure 4.26 – SV geometry affecting GALILEO-E1 positioning results.

GSPA sky plot and its color palette applied to the observation epoch have turned to be very useful for analyzing the SV geometry impact on the positioning performances as showed in Figure 4.26 and Figure 4.27.

On Figure 4.26, apart from a NW bias in the position solution, it can be seen how the cloud is also spread in the SW to NE direction. This is due to the SV geometry observed next to it. Note that the SV geometry is mainly aligned in all processing epochs in the NW-SE direction, thus "letting the solution to be free" in the complementary direction (SW-NE).

This behavior is better depicted in Figure 4.27. Note that, for instance, solutions around 8:00 AM (colored in green) have a fair SV geometry and thus a centered and non-biased solution at the reference is obtained. As opposite, solution obtained at 9:00 AM (colored in red) has a SV geometry aligned in the E-W direction, thus producing a North-biased positioning estimation.

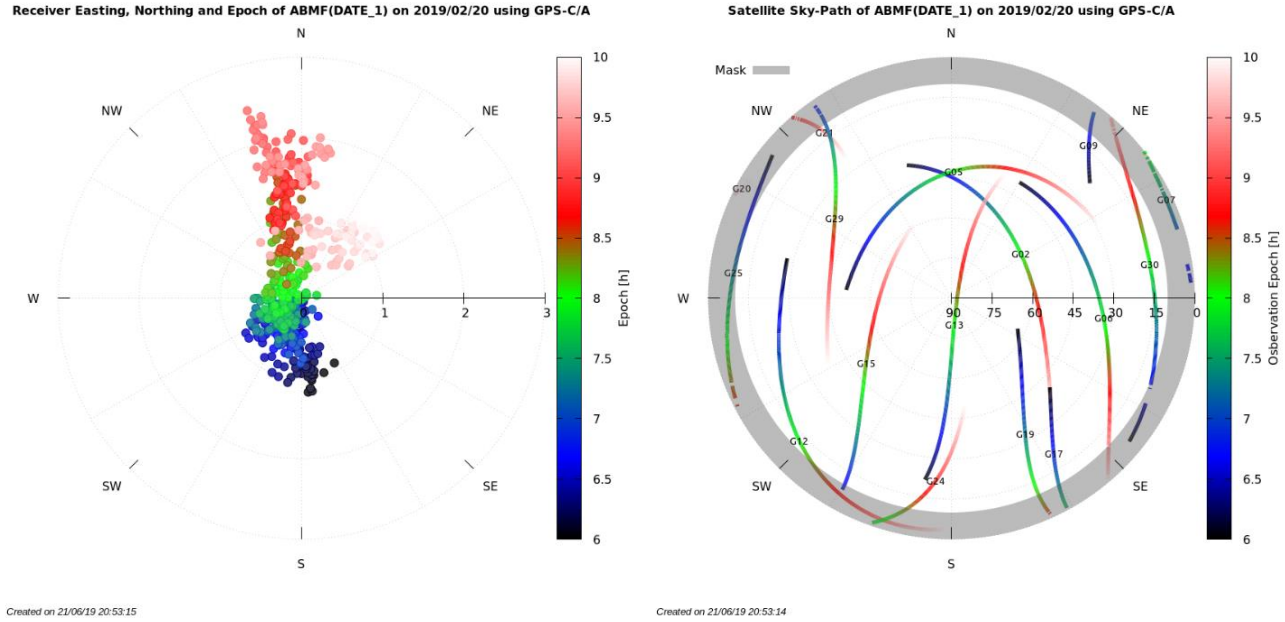

Figure 4.27 – SV geometry affection on GPS-C/A positioning results.

Unexpected Processing Issues

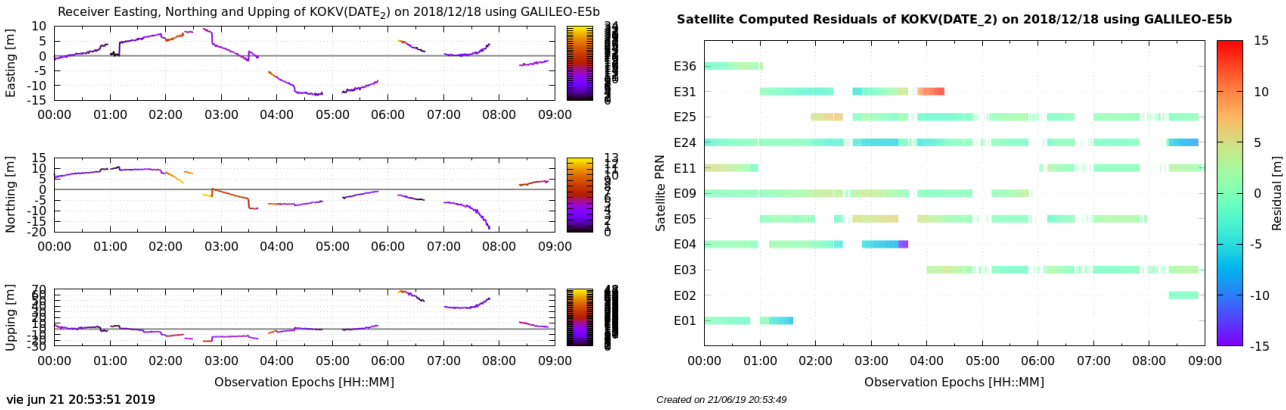

Figure 4.28 – GALILEO-E5b KOKV processing issue illustration.

Figure 4.28 illustrates the so commented issues encountered in KOKV when processing GALILEO E5b signal. It can be immediately deduced some kind of error correlated with time, not presenting a random pattern as expected and exemplified previously in the fair performances instances. Also note that the residuals are especially high (15 meters) for E31 and E04, but with such a few SV it could not be possible to discard them. Possible explanations for this behavior could be:

- KOKV receiver issues. This is assumed since all issues are always encountered in this station. However, reviewing receiver models in Table 4.2, this is the same than TASH station. Nonetheless other phenomena like multipath could be taken place.

- GRPP bug when processing E5b signal. This cause is also suspicious since GRPP has not been validated using this signal. It is believed that the root cause may be located at the navigation data selection since the errors showed in Figure 4.28 were obtained in other processing tests and they were due to incorrect clock parameters selection. However, this behavior is not observed in any other campaign scenario.

Eventually, KOKV root cause issue should be further investigated and assessed in future campaign versions.

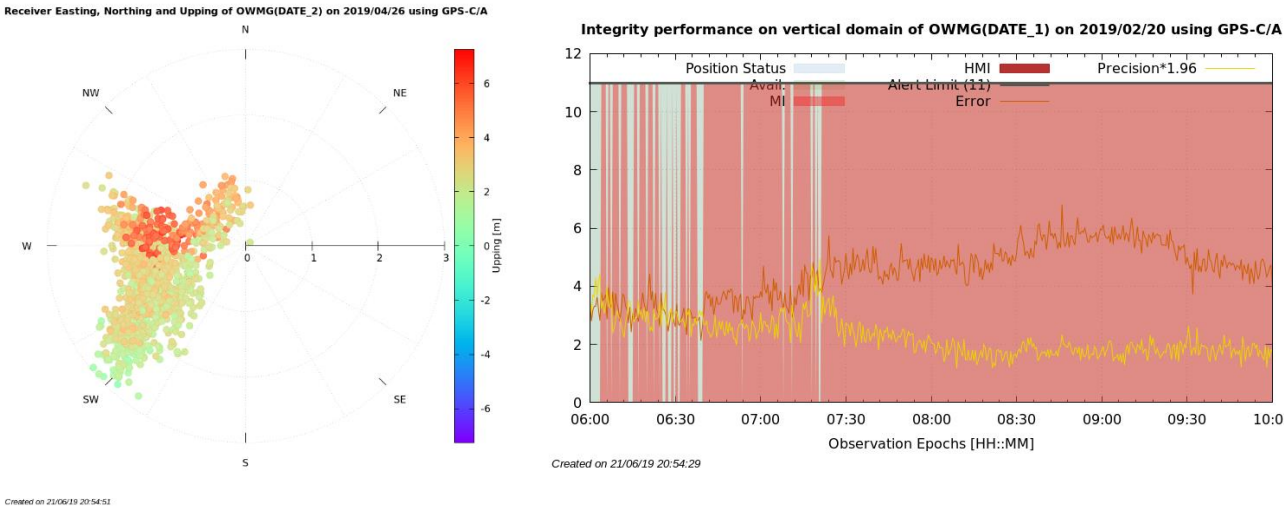

Figure 4.29 – OWMG systematic positioning error and vertical integrity issue.

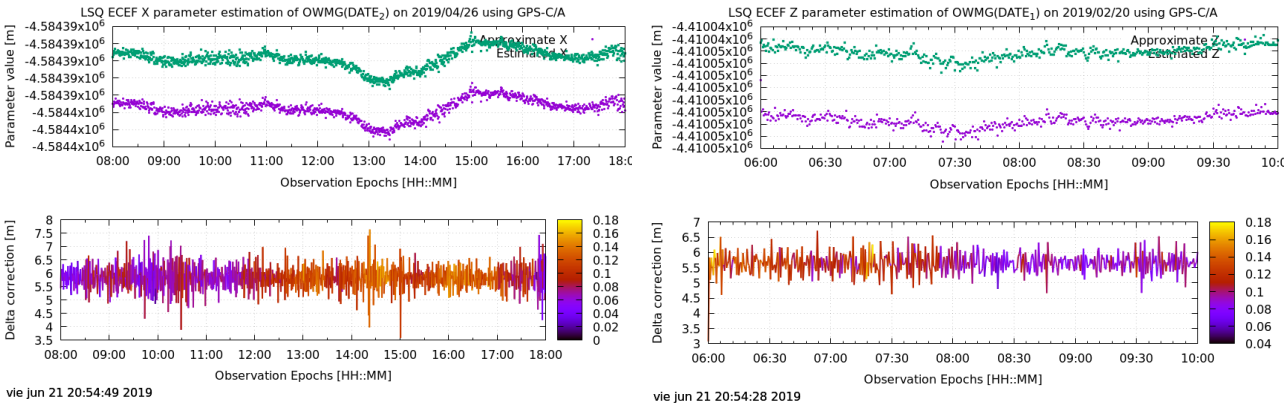

Figure 4.30 – OWMG parameter estimation showing high correction over approximate position.

Regarding OWMG issue mentioned in 4.3.3, Figure 4.29 and Figure 4.30 illustrate more information regarding the root cause problem. By looking at Figure 4.29, it can be pointed that integrity MI cases are due to a continuous precision against error overflow. The polar plot is also showing a biased positioning estimation, which do not seem to be due to signal anomalies but to the station reference coordinates. Indeed, by observing Figure 4.30, the approximate position is corrected in both X and Z ECEF components by around 6 meters. In conclusion, all these evidences seem to point that OWMG precise

ITRF station coordinates need to be updated. Note that the time between the ITRF 1996 realization used as a reference (see Table 4.3) and the campaign processing year, is 23 years, which it turns to be a significant period of time for coordinates to have suffered from tectonic plate displacement, especially in the pacific area.

Ionosphere Abnormal Phenomena Impacts

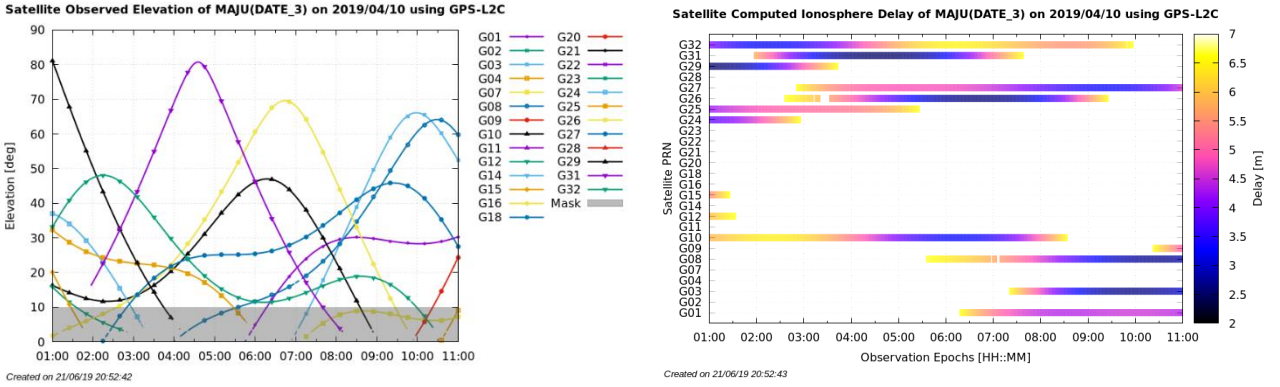

Figure 4.31 – MAJU SV elevation and ionosphere correction under critical events.

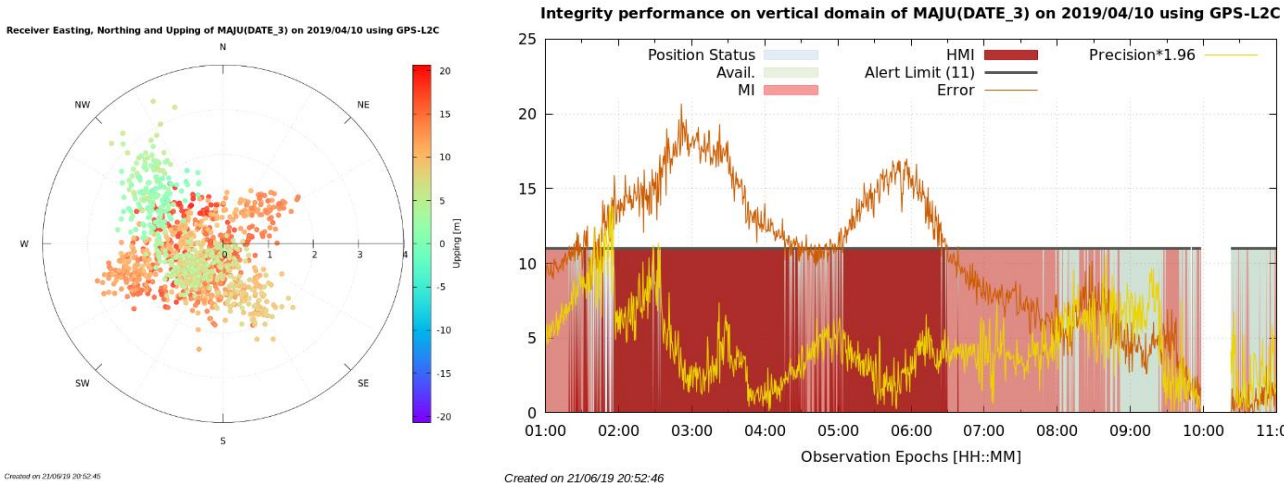

Figure 4.32 – MAJU positioning results and integrity performance under high TECU events.

Figure 4.32 and Figure 4.33 show C/A performances over MAJU station under abnormal ionosphere conditions. It can be concluded from both figures that a total lack of integrity is encountered when SV have a lower elevation which is translated in a high ionosphere correction provided by Klobuchar's model, but not effectively mitigated. This was expected since Klobuchar estimates a complex mean such as the ionosphere by a cosine amplitude function (recall section 2.5.3). Note also in the polar plot on Figure 4.32 how the ionosphere is affecting the horizontal domain "spreading" the position solutions.

Finally, an interesting phenomenon which has taken place over KIRU station during scintillation phenomena is depicted in Figure 4.33. Note that the "peak" in the polar plot is caused by a progressively augmentation of the accuracy (which by the way accomplishes integrity performance quite well). This peak can be placed when the scintillation event occurred (see Table 4.5, approximately at 22:00), thus evidencing that the event had a symbolic impact on the positioning solution.

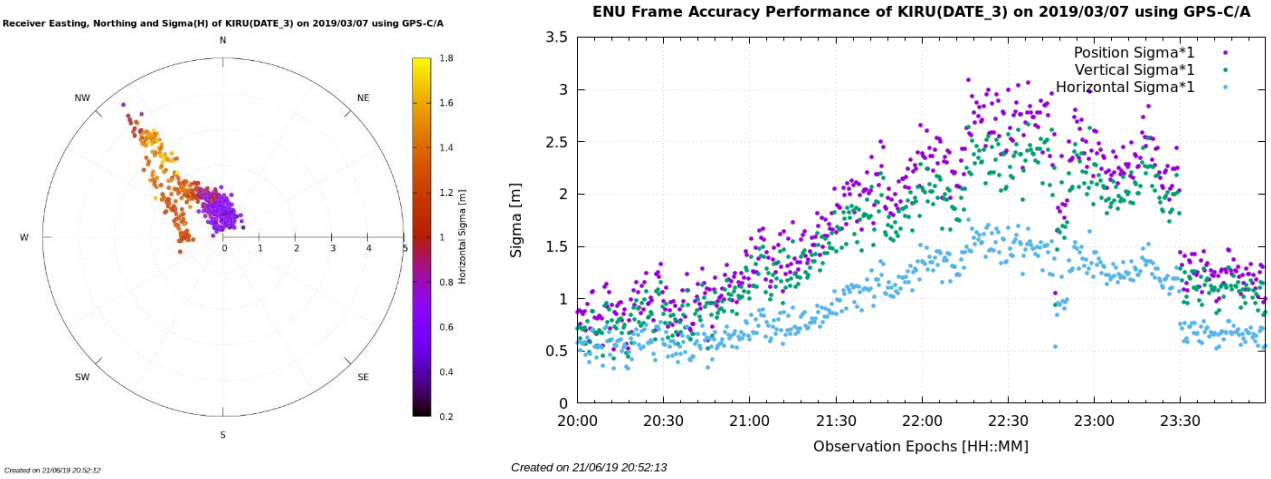

Figure 4.33 – FAIR ionosphere scintillation event and accuracy performance impact.

Chapter 5: Conclusions

5 Conclusions

Chapter 4 has presented the analysis campaign performed with the methodology explained in chapter 3. Both chapters were introduced by chapter 1 and supported by the theory frame in chapter 2. Consequently, the thesis conclusions are ready to be enumerated in this chapter.

The conclusions cover the main aspects of the thesis which are not just a few. Therefore, this chapter has been divided in three main sections as follows:

- **Section 5.1** comprises the conclusions regarding the methodology techniques used, i.e. the SW tool development.
- **Section 5.2** lists the conclusions about the analysis phase i.e. the positioning performance study campaign.
- **Section 5.3** relates the main objectives presented in section 1.1 with the final thesis conclusions in order to determine their grade of accomplishment.

These sections start with a brief recap of the procedures followed through-out the work and then the conclusions are enumerated. The conclusions may be also grouped in different subsections attending to their complexity.

Finally, section 5.4 has been added in order to account for future work lines which may arise from this thesis. They are mainly focused in improvements and additions to the SW tool developed which will hopefully be implemented in future versions.

5.1 Regarding Methodology Techniques

As a recap, the followed methodology has been to produce a dedicated SW tool for processing GNSS pseudorange measurements using single-frequency SPP algorithms in order to report accuracy and integrity performances for GPS-SPS and GALILEO-OS.

Since it was decided that the SW will constitute an open source tool contribution to the GNSS community, the development approach adopted was contextualized in a SW lifecycle waterfall model with three differentiated phases: specification, implementation and validation. This was necessary in order to produce a controlled user-oriented solution.

Specification was defined by the SW PIDS and their abstraction into high-level concepts diagrams and baseline requirements to be implemented in the SW algorithms.

Implementation was carried out by selecting Ubuntu MATE, and Perl as programming language. Perl hash data structure was used in advantage of settling common interfaces for connecting SW modules and packages. Eventually two main tools were produced: GRPP and GSPA.

Finally, verification phase was assessed by performance comparison among GRPP and RTKLIB. The positioning results of both tools were compared and then analyzed against stipulated pass/fail criteria based on the GPS and GALILEO positioning requirements. GRPP finally showed to be compliant for processing GPS-SPS and GALILEO-OS signals.

About SW lifecycle adopted

- Lifecycles are essential for SW development. They guarantee an organized approach and a traced environment for documenting, evolving, maintaining and bug-fixing a SW.
- The waterfall is a simple SW development model which is based on a sequence of steps very easy to follow. However, by adopting this model, SW development process requires more time and effort.
- Specification phase settles the baseline requirements which must be covered in the SW through technical implementation.
- Implementation constitutes the detailed abstraction of the SW which is better illustrated with the hierarchy and flow diagrams besides of its public function specification.
- Verification phase is intended to check that proper SW implementation has been done and requirements are fulfilled. However, verification is also resource-consuming and can adopt a more pragmatic approach by validating the SW results against reference data.

About developed SW tools: GRPP and GSPA

- GRPP and GSPA are user-oriented tools which maintain a friendly usage only requiring a common configuration file. In addition, they alert about configuration mistakes, input issues and processing warnings.
- The wide GRPP/GSPA configuration allows for flexibility and different executions. However, the user must have theory knowledge regarding each processing parameter since otherwise, it could lead to undesired results.
- The GRPP SPP algorithms do not encompass high complexity implementation. However, this effort is significantly increased when adding custom user configuration and different GNSS.
- GRPP can act as white box tool since it dumps most its internal data. This also accounts for user-customized data exploitation.
- GRPP has proven to be verified when processing GPS-SPS and GALILEO-OS (at least C/A and E1 signals) by accomplishing similar positioning results compared to other available GNSS processing tools i.e. RTKLIB.
- GSPA fulfills its reporting requirements apart from digesting all GRPP outputs in order to produce quality plots which have proven to summarize efficiently all the processing information.
- Ubuntu OS and Perl programming languages are fitted for developing SW products from scratch and have allowed a faster, flexible and organized implementation.

5.2 Regarding Analysis Campaign

Recalling the analysis campaign carried out, its main objective has been to assess individually signal-service accuracy and integrity performances with real data of GPS-SPS and GALILEO-OS. The expected results were stipulated in Table 4.1 expecting better performances in GPS than in GALILEO.

The campaign data was gathered from 5 IGS stations, part of the MGEX project. The data was arranged in 3 different dates: Date 1 set the same UTC processing time window in order to test global coverage, Date 2 set a different date for having the best SV availability and Date 3 was configured to encounter critical ionosphere phenomena. The selected signal-services to study have been GPS-SPS C/A and L2C; and GALILEO-OS E1 and E5a/E5b.

This campaign arrangement led to 60 GRPP+GSPA executions which were automatized with scripting skills. The configuration used for it, was kept basic only differing in the ephemerid time-out threshold among GPS and GALILEO, apart from the discarded SV in on GALILEO side. Campaign launching process was done iteratively until all executions were available. The results firstly reveled that several GALILEO scenarios (and some of GPS-L2C) had significant lacks of valid position status as expected.

Accuracy results show an overall picture of GPS-SPS offering better accuracy than GALILEO-OS as it was expected. However, it must be pointed out some exceptions where GALILEO is performing better than L2C. Date 1 and 2 have obtained nominal accuracy values which exceed expectations with C/A signals and meeting expected results for L2C, E1; with some exception on the GALILEO side. Date 3 shows accuracy degraded performances as expected, meaning that accuracy is increasing in order to bound the higher error due to the abnormal ionosphere phenomena.

Regarding integrity results, again for nominal conditions on Date 1 and 2, GPS-SPS seems to offer better integrity performances than GALILEO (especially SA), due to the higher number of SV in orbit. Although in some cases GPS is presenting more MI, rather than GALILEO which seems to be trading off less MI events with less SA. This observation is specially revealing in Date 3 where GPS integrity performances are severely degraded with HMI events, not as GALILEO which are mainly degraded by dropped SA.

Finally, GPSA plots have revealed campaign features like OWMG outdated reference, SV geometry impact on positioning error or MAJU high TEC consequences in vertical integrity. Probably without the added value of GSPA plots, these observations would have never been explored.

About campaign usefulness

- Sole single-frequency signal service performance measurement with real data is highly relevant in the context on a multi-GNSS and multi-frequency environment where each individual signal-service needs to work accordingly to its requirements.

- The most relevant GNSS positioning performance from a user perspective is the system accuracy but integrity is equally meaningful since its measuring the representativeness of the system solution against its real position.

- New generation GNSS services need to be evaluated and compared with real data respect the legacy services. In the EU, this attention is focused over GALILEO compared to GPS positioning solutions.

- GNSS performance campaigns should be studied in different locations and under different phenomena. This work has showed that very different results can be obtained in different locations and different times.

About IGS-MGEX data source and Trimble Planner

- IGS comprises a wide open-access GNSS data and product archive. This service is significantly useful for scientific research and algorithm testing.

- The MGEX project has proven to be essential for accessing GNSS legacy and non-legacy measurements and navigation data. Thanks to its receiver network, necessary GPS and GALILEO data has been acquired.

- Trimble GNSS Planner came in handy thanks to its configuration and displays. This has been very useful for planning the campaign, especially for setting fair GALILEO SV availability windows and for encountering ionosphere abnormal phenomena.

About GPS-SPS and GALILEO-OS meeting the expected performances results

- GPS-SPS using C/A signal has proven to exceed expectations regarding accuracy performance, being most of the times between 3-4 meters, even in abnormal conditions. Regarding integrity, the expected results are met but a few exceptions regarding high MI and SA losses under abnormal conditions must be pointed out.

- GPS-SPS using L2C signal meets accuracy requirements under nominal conditions (sometimes by a narrow margin) and these are exceeded during some abnormal ionosphere events. Regarding integrity under nominal conditions, L2C signals meets the criteria in some scenarios whilst in some other SA losses and high MI are taken place. Integrity under non-nominal conditions is severely affected presenting high occurrences of HMI events.

- GALILEO-OS using E1 signal seems to meet the expected accuracy results, sometimes even under abnormal conditions. Though most of the times integrity results are met, this service is showing in many cases SA losses and high MI occurrences. Nonetheless, integrity under abnormal conditions is keeping the same performance levels as in nominal conditions except in KOKV station.

- GALILEO-OS using E5a/E5b does not meet in most cases accuracy criteria under nominal conditions, not even accomplishing its own system definition requirements, especially in KOKV station. In the counterpart, integrity seems to be maintained with few MI occurrences trading off SA under 50%, discarding KOKV issues.

About performance comparison among GPS-SPS and GALILEO-OS

- GPS C/A signal seems to offer better positioning performances than GPS L2C signal. This is mainly due to the fewer GPS SV broadcasting L2C signal which leads to a worse SV geometry disposition and fewer observation redundancy.

- GALILEO E1 signal offers most of the time better performances than E5a/E5b signal. However, this may be due to processing issues encountered with E5a/E5b signal or GALILEO issues broadcasting E5a/E5b signals as showed in discarded satellite E24.

- GALILEO E1 signal has worse accuracy and integrity performances when compared to GPS C/A signal. This is caused by GALILEO constellation incompletion, although it shall be remarked that

GPS-SPS defines better accuracy requirements than GALILEO-OS. The only case when GALILEO E1 seems to perform better is when alarming under abnormal ionosphere conditions, whereas GPS maintains SA at the expense of increasing MI events.

- GALILEO E1 and GPS L2C signals are more similar in terms of accuracy with slightly more cases of L2C performing better than E1. These similarities are caused by the more balanced SV availability among E1 and L2C signals. For integrity performance, both signals do also offer similar performances with again, E1 trading-off SA by fewer MI events under critical ionosphere conditions; while L2C maintains higher SA but at the expense of increasing dramatically MI and HMI occurrences.

About measured performances extrapolation

Extrapolating the SPP algorithms presented in this thesis into a receiver implementation, the following presumptions can be adopted regarding GPS-SPS and GALILEO-OS performances under nominal conditions:

- GPS C/A can provide a fair accuracy under 7 meters in the horizontal domain and 11 meters in the vertical domain. This positioning service can be trusted accounting for a maximum of 20% MI events and more than 95% of SA.

- GPS L2C can provide an accuracy around 7 meters in the horizontal domain and 11 meters in the vertical domain. This positioning service can be trusted accounting for higher MI events than the 20% and SA around 95%.

- GALILEO E1 can provide accuracy around 7 meters in the horizontal domain and 11 meters in the vertical domain. This positioning service can be trusted accounting for higher MI events than the 30% and SA around 80% with even greater drops.

- GALILEO E5a/E5b cannot provide a fair accuracy of 7 meters in the horizontal domain and 11 meters in the vertical domain. However, the positioning solution integrity can be trusted with fewer MI than the 30% and a dropped SA under the 80% in most cases.

- The aforementioned performances cannot be truly trusted under ionosphere abnormal conditions since accuracy is increased in order to bound the higher observation error and integrity may suffer from severe degradations, especially with poor SV geometry disposition.

About detailed campaign results

- Minimum geometry of 5 SV is not enough to ensuring fair accuracy and integrity. Optimal results are obtained when having at least 3 DoF, hence 8 SV are required for warranty nominal positioning performances.

- SV geometry affects significantly to the positioning performances. As a matter of fact, accuracy and integrity performances are dramatically affected when measured through bad SV geometry dispositions.

- Precise reference definition is essential in order to measure properly integrity performance. ITRF realizations must be reviewed since reference station coordinates may have been displaced in areas of high tectonic plate activity.

- KOKV results with E5b signal may evidencing a GRPP feature which needs to be improved. This is the algorithm for GALILEO ephemerid selection.

- On top of that, GPS ephemerid selection is fairly achieved with a sole time-out threshold which can be set to 1.5 hours. For GALILEO, this is more complex matter since ephemerids are separated by data source (F/NAV and I/NAV) and normally broadcasted every 10 minutes.

- Severe HMI events can take place during critical ionosphere phenomena such as high TEC and scintillation. They mostly occur in weak SV geometry observations.

- Ionosphere critical events can degrade accuracy, but this is necessary in order to cover the actual error due to the abnormal phenomena. This is accomplished with fair SV availability and geometry disposition i.e. at least 8 SV observed.

- Multi-GNSS solutions present a clear advantage over single-service approaches, since more SV will be available. Nonetheless, only services with homogeneous performances should be combined. Otherwise, a worst outcome than in the sole service case could be produced.

About GRPP+GSPA usage

- GRPP and GSPA has proven its usage through a real user-oriented application. Not only GRPP+GSPA is able to measure positioning performances, but with the proper automatization, it is useful to carry out a performance study campaign with over 60 executions.

- GRPP output information and its arrangement through GSPA have proven its user-oriented potential. Many deductions and information can be extracted by only observing a few plots.

5.3 Regarding Thesis Purpose

The last conclusions will be related to the project purposes listed in at the introduction in section 1.1. Note that their intention is to close out the entire work and to highlight what abilities has the student been able to apply in the context of the master's degree.

As a reminder, the listed thesis purposes were related to:

- **Develop GNSS SW tools**. A summary regarding the activities carried out for this purpose is available at the beginning of section 5.1.

- **Assess GNSS positioning performances** using the SW tools developed in the context of this work. The performance assessment is summarized in section 5.2.

- **Apply the knowledge gained** through the master's degree in Geomatics and Geo-information. The theory framework of chapter settles the technical background studied whereas methodology and analysis chapters also illustrate several skills learnt during the master's courses.

Additionally, these conclusions will remark other relevant aspects. For instance, the applied skills which have not been studied but have complemented the master's aptitudes. Finally, the closing observations regarding the possible impact which this thesis may have in the social benefit or the scientific community will be highlighted. These are key aspects for technical disciplines, such as the geomatics, to be valued and recognized.

About GNSS SW development objective

- Regarding the development of GNSS algorithms by the student, it can be pointed that this objective has been accomplished satisfactorily. The clearest evidence is the developed GRPP+GSPA SW.

- Moreover, the SW development phase has been addressed by adopting a waterfall lifecycle process. This process has shown that, despite that it adds significant effort, their organizational advantages are worth it in order to develop more professional SW products.

- On top of that, thanks to the lifecycle applied, the student has carried properly the SW activities which can be encountered in a real enterprise scenario.

- Not only this SW has helped to fulfill the thesis purposes, but it has contributed to form settled tool which will hopefully have transcendence to other users.

About GNSS positioning performance assessment objective

- Regarding the assessment of GNSS positioning performances, it can be concluded that this objective has been successfully fulfilled.

- Apart from accuracy, integrity performance has been introduced and effectively measured, This performance has added a significant value from the user's perspective since it has illustrated the correctness of the GNSS positioning solution.

- In addition, performances have also been measured under nominal and abnormal conditions illustrating how GNSS solutions can range in terms of positioning error.

- On top of that, performances have also been measured through a world-wide network thanks to IGS and MGEX services. This has enabled GPS-SPS and GALILEO-OS performance extrapolation.

About applied master's degree knowledge

- Regarding the knowledge gained through the master's degree in geomatics and geo-information, it can be stated that several disciplines and skills have been applied to this thesis:
  - Firstly, spatial geodesy techniques regarding GNSS measurement processing have been settled through the academical framework and successfully applied in the thesis methodology under a practical application scope.
  - Secondly, programming skills have been the core of this project. Not only for the SW produced but also for the automatization of the campaign executions.
  - Lastly, the computer programming skills have been taken to a higher level. Going from the paradigm of private script development to the user-oriented SW production.

About contribution to the social benefit and scientific community

- It can be pointed that this master thesis work has a clear potential for contributing to the social benefit and the scientific community. The evidences for this rely on the methodology and the analysis phases:
  - On the one hand, the assessment of positioning performances has a direct impact on the social benefit as it has been showed by the GNSS market sector. This niche has exponentially grown in the last years and seems to maintain this tendency thanks to the positioning applications which can be derived from it.
  - On the other hand, the developed approach of GRPP and GSPA will constitute a contribution to the GNSS scientific community. In the near future, the first tool version will be available in a free-access repository for anyone to download and execute it.

5.4 Future Evolutions

Last but no the least, several future evolutions regarding developed SW and positioning performance exploration will be enumerated. It shall be pointed that these modifications can be divided in current or short-term improvements, and enhancements or long-term evolutions of GRPP+GSPA.

The items mentioned hereafter will be incorporated in future versions of GRPP and GSPA, tough it cannot be assured its due date because of its altruist nature. Hopefully, as more users make use of the tool, some of them could decide to join the project and contribute to its development.

Short-Term Additions

- Firstly, the **ephemerid selection algorithm** should be improved as concluded in section 5.2. It has been noted that a single time-out threshold may work properly when processing GPS but other GNSS like GALILEO require a more sophisticated approach.

- Secondly, in order to account for a more user-friendly usage GRPP and GPSA should incorporate:

  - **User manual** for GRPP and GSPA. This feature is essential for users to understand and being able to execute the tool and interpret their results.

  - **Basic configuration file**. The current configuration is only useful for advanced users since the technical background of each parameter should be known. This is an important aspect since most of the users would like to see a default configuration for some options e.g. LSQ convergence threshold.

  - Another relevant aspect is to offer an **automated tool installation**. Current GRPP and GSPA are dependent of PDL and Chart::Gnuplot libraries and its dedicated environments. These dependencies need to be manually configured and this can be tedious for many non-experienced users.

- Regarding GRPP functionalities, the following improvements could be introduced in the upcoming versions:

  - **NeQuick algorithm** for GALILEO ionosphere correction. In fact, this feature was planned to be included in the preliminary version of GRPP presented in this thesis. However, for the sake of simplicity, NeQuick was kept out the scope due to its implementation complexity.

  - **Dual signal processing**. It would mean a significant enhancement for GRPP to estimate the receiver position combining, for instance, GPS and GALILEO pseudorange measurements. This could also lead to study performances with multi-GNSS services.

  - **Support further GNSS**. GLONASS, BEIDOU and even SBAS will add a significant value to GRPP and will enable performance study on these systems.

- On top of that, GSPA could also account for further functionalities:

  - Preliminary position plots of GSPA only account when the receiver is in static mode. They should also cover **receiver kinematic scenarios**.

- So far, GPSA plots and numeric results are outputted in a directory with no arrangement. This should be improved for a better user experience, arranging the plots and results in a settled format such as **PDF or HTML**.

Long-Term Evolutions

- Several new features and modules could be added in order to improve tool's functionality:
  - **Carrier phase measurement processing module** could be added for higher precision applications. On the flip side, as more precision is obtained, more implementations are required such as time and reference system transformations e.g. receiver coordinates obtained in WGS84 and transformed to ITRS.
  - A **Precise Point Positioning (PPP) module** should be incorporated. This will increase dramatically the tool's value since current GNSS research activities are focused on PPP techniques due to its advantages for sole-receiver absolute positioning with sub-metric accuracy.
  - **Further corrections** and error root cause mitigation could be added such as cycle slip detection or multipath extenuation.
- Another interesting feature for a more versatile usage is the alternative to input certain parameters using precise products:
  - **Precise orbit SP3 files** could be read in order to account for a more accurate SV frame. For instance, this could be used for focusing only on receiver error sources.
  - **Precise receiver and SV clocks** products could be read as well. This could enable to fix the receiver clock bias and only estimate its position components.
  - **IONEX files** for having precise information regarding ionosphere corrections. This may be used for focusing in the troposphere correction and its extrapolation for measuring weather parameters such as water vapor.
- In addition, the tool could also support **different GNSS data sources** and not only RINEX format. Some examples could be RTCM and even real-time protocols.
- Finally, a total user-friendly experience will be offered by developing a **dedicated Graphical User Interface** (GUI) for configuring and launching the tool.

Chapter 6: Acronyms

6 Acronym List

Table 6.1 – Acronym List.

Acronym	Stands for
A/S	Anti-Spoofing
AL	Alert Limit
ASCII	American Standard Code for Information Exchange
AltBOC	Alternate Binary Offset Carrier
BGD	Broadcast Group Delay
BOC	Binary Offset Carrier
BPSK	Binary Phase Shift Keying
BR	Bibliography Reference
C/A	Coarse Acquisition
CDMA	Code Division Multiple Access
CFG	Configuration
CRINEX	Compressed RINEX
CS	Commercial Service
CTP	Conventional Terrestrial Pole
DoD	Department of Defense
DOP	Dilution of Precision
ECEF	Earth Centered, Earth Fixed
EGNOS	European Geostationary Navigation Overlay Service
ENU	Easting, Northing and Upping
ENV	Environment
ESA	European Space Agency
ETSIGCT	Escuela Técnica Superior de Ingeniería en Geodesia Cartografía y Topografía
F/NAV	Freely Navigation Message
FOC	Full Operational Capability
FUN	Functional
GAL	GALILEO
GGSP	Galileo Geodetic Service Provider
GIOVE	GALILEO In Orbit Validation
GLONASS	GLObal NAvigation Satellite System
GNSS	Global Navigation Satellite System/Service
GPS	Global Positioning System
GPST	GPS Time
GRPP	GNSS RINEX Post-Processing
GSPA	GNSS Service Performance Analyzer
GST	GALILEO System Time
GTRF	GALILEO Terrestrial Reference Frame
GUI	Graphical User Interface
HAL	Horizontal Alert Limit
HMI	Hazardous Misleading Information

HW	Hardware
I/NAV	Integrity Navigation Message
ICD	Interface Control Document
IERS	International Earth Rotation Service
IGS	International GNSS Service
IOC	Initial Operational Capability
IOV	In-Orbit Validation
ITRF	International Terrestrial Reference Frame
ITRS	International Terrestrial Reference System
LoC	Line of Code
LoS	Line Of Sight
LR	Link Reference
LSQ	Least Squares
MGEX	Multi-GNSS Experimental Service
MI	Misleading Information
NAV	Navigation Message
NAVSTAR	Navigation System With Ranging and Timing
OS	Open Service / Operative System
PDL	Perl Data Language
PIDS	Preliminary Item Design Specification
PPP	Precise Point Positioning
PPS	Precise Positioning Service
PRN	Pseudo-Random Noise
PRS	Public Regulated Service
REQ	Requirement
RINEX	Receiver Independent Exchange Format
RMS	Root Mean Square
RMSE	Root Mean Squared Error
RTCM	Radio Technical Commission for Maritime Services
RTK	Real Time Kinematic
S/A	Selective Availability
SA	System Availability
SAR	Search and Rescue
SBAS	Space Based Augmentation System
SIS	Signal In Space
SLR	Satellite Laser Ranging
SoL	Safety of Life
SPP	Standard Point Positioning
SPS	Standard Positioning Service
STDOUT	Standard Output
STDERR	Standard Error
SV	Space Vehicle
SW	Software

TAI	International Atomic Time
TBC	To be Completed
TBD	To be Determined
TEC	Total Electron Content
TECU	Total Electron Content Unit
TGD	Total Group Delay
ToE	Time of Ephemerids
ToW	Time of Week
TRS	Terrestrial Reference System
UPV	Universidad Politécnica de Valencia
UT	Universal Time
UTC	Universal Coordinated Time
VAL	Vertical Alert Limit
VLBI	Very Long Base Interferometry
WAAS	Wide Area Augmentation System
WGS84	World Geodetic System 1984
WLSQ	Weighted Least Squares

Chapter 7: References

7 References

This chapter lists all the references used for the thesis development. The references are divided in bibliography references (publications, articles, books…) and media links (websites). Each reference includes a marker named BR or LR for a better and more concise citation along the document.

7.1 Bibliography

Table 7.1 – Bibliography References.

Marker	Author/Reference	Document	Publisher	Issue
[BR.1]	Sanz Subirana, J.; Juan Zornoza, J.M.; Hernández Pajares, M.	ESA GNSS Data Processing. Vol I: Fundamentals and Algorithms.	ESA Communications.	2013
[BR.2]	Hoffman-Wellenhof, B.; Lichtenegger, H.; Wasle, E.	GNSS Global Navigation Satellite Systems. GPS, GLONASS, Galileo and more.	SpringerWienNewYork.	2008
[BR.3]	Seeber G.	Satellite Geodesy.	Walter de Gruyter.	2003
[BR.4]	Kaplan, E. D.; Hegarty, C. J.	Understanding GPS. Principles and Applications.	Artech House.	2006
[BR.5]	Berné Valero, J. L.; Anquela Julián, A. B.; Garrido Villén, N.	GNSS. GPS: Fundamentos y Aplicaciones en Geomática.	Editorial UPV.	2014
[BR.6]	Leick, A.; Rapoport, L.; Tatarnikov, D.	GPS Satellite Surveying.	Wiley.	2015
[BR.7]	Toho Diessongo, H.; Bock, H.; Schüler, T.; Junker, S.; Kiroe, A.; Hein, G. H.	Exploiting the Galileo E5 Wideband Signal for Improved Single-Frequency Precise Positioning.	Inside GNSS.	2012
[BR.8]	RINEX-V303	RINEX. The Receiver Independent Exchange Format. Version 3.03.	International GNSS Service (IGS), RINEX Working Group and Radio Technical Commission for Maritime Services Special Committee 104 (RTCM-SC104)	2015
[BR.9]	Moreno Monge, B.	Development of Algorithms for the GNSS data processing: their application to the Modernized GPS and Galileo Scenarios. Doctoral Thesis.	Universidad Complutense de Madrid.	2011
[BR.10]	Montenbruck, O.; Steigenberger, P.; Prange, L.; Deng, Z.; Zhao, Q.; Perosanz, F.; Romero, I.; Noll, C.; Stürze, A.; Weber, G.; Schmid, R.; MacLeod, K.; Schaer, S.	The Multi-GNSS Experiment (MGEX) of the International GNSS Service (IGS) – Achievements, Prospects and Challenges	Advances in Space Research 59(7):1671-1697.	2017

[BR.11]	Montenbruck, O.; Steigenberger, P.; Khachikyan, R.; Weber, G.; Langley, R.B.; Mervart, L.; Hugentobler, U.	IGS-MGEX: Preparing the Ground for Multi-Constellation GNSS Science.	Inside GNSS.	2014
[BR.12]	GNSS-MR-2017	GNSS Market Report.	European GNSS Agency.	2017
[BR.13]	GNSS-UTR-2018	GNSS User Technology Report.	European GNSS Agency.	2018
[BR.14]	GAL-OS-IONO-SF	European GNSS (Galileo) Open Service - Ionospheric Correction Algorithm for Galileo Single-Frequency Users.	European Commission.	2016
[BR.15]	IS-GPS-200	Navstar GPS Space Segment/Navigation User Interfaces.	Global Positioning Systems Directorate.	2013
[BR.16]	GAL-OS-SDD	Galileo Open Service Definition Document.	European Commission.	2016
[BR.17]	GAL-OS-SIS-ICD	Galileo Open Service Signal in Space Interface Control Document.	European Commission.	2016
[BR.18]	GPS-SPS-PS	GPS Standard Positioning Service Performance Standard	Global Positioning Systems Directorate.	2008

7.2 Media Links

Table 7.2 – Link References.

Marker	Title-Link
[LR.1]	Navipedia - Klobuchar Ionosphere Model
[LR.2]	Navipedia - The SBAS Integrity Concept Standardized by ICAO.
[LR.3]	SOPAC Hatanaka Format.
[LR.4]	Wikipedia – Waterfall Model (SW Development)
[LR.5]	Ubuntu MATE
[LR.6]	Perl
[LR.7]	Perl Hash
[LR.8]	CPAN
[LR.9]	Gnuplot
[LR.10]	Chart::Gnuplot
[LR.11]	RTKLIB: An Open Source Program Package for GNSS Positioning
[LR.12]	Trimble GNSS Planner
[LR.13]	NOOA, Ionosphere Scintillation

Chapter 8: Annexes

8 Annexes

This chapter contains the project annexes. These are additional information which could not be included within the document sections.

A.1 SW Tool: GRPP+GSPA Source Code Repository

GRPP, GSPA and common configuration parser source code is available under Github control repository in the following hyperlink.

Additionally, the following figures have been extracted from the aforementioned link. They stand for code metrics since the creation of the repository until 03/07/2019. They can be used as an information source which evidences GRPP and GSPA development and evolution. Further additions/deletions and commit details can be consulted in the previous link.

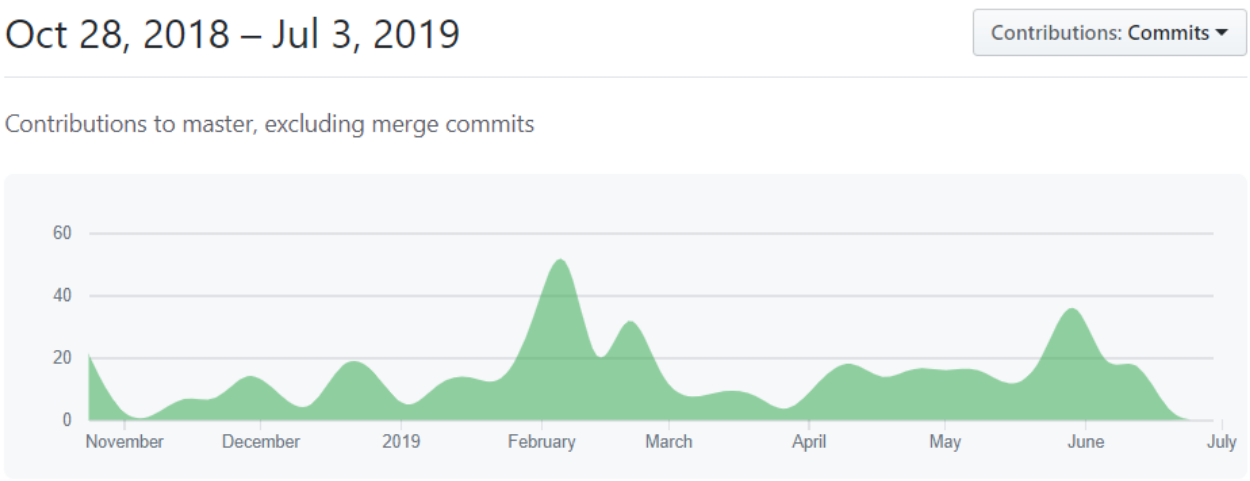

Figure 8.1 – Source code contributions. Source: github.com/ppinto94/TFM-SourceCode.

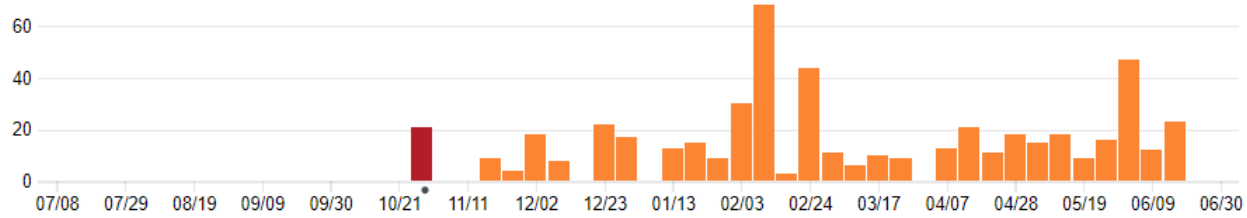

Figure 8.2 – Source code commits per week. Source: github.com/ppinto94/TFM-SourceCode.

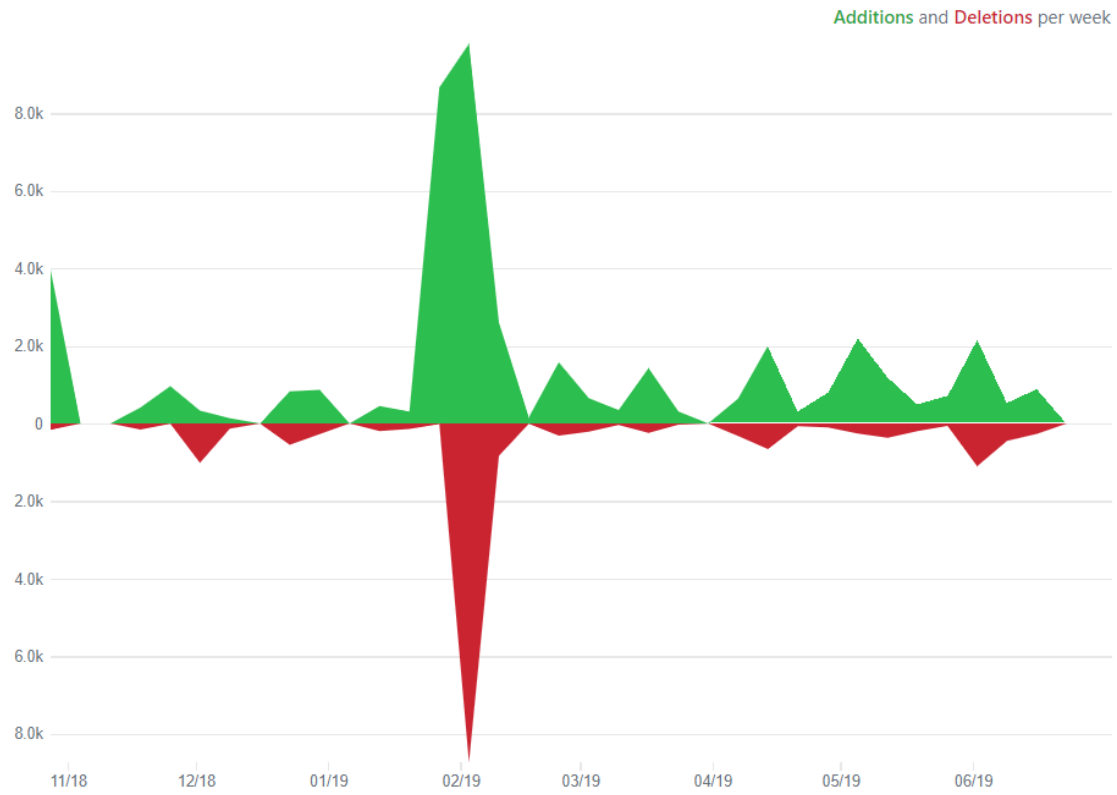

Figure 8.3 – Source code additions and deletions per week. Source: github.com/ppinto94/TFM-SourceCode.

A.2 SW Tool: GRPP/GSPA User Configuration File

The following raw text extracts show a common user configuration file which would be used as unique input for both GRPP and GSPA.

Example #1

The following configuration file launches GRPP processing using GPS C/A observations for CEBR station on 13/05/2019. This file was used for the GPS C/A performance verification stage presented in section 3.3. As it can be seen, both static and integrity modes are activated and CEBR ITRF coordinates have been set as the position reference.

```
# ========================================================================== #
# CONFIGURATION FILE:

# -------------------------------------------------------------------------- #
# Inputs/Outputs:

# Tool verbosity:
Verbosity  :  TRUE

# Execution label:
Processing Tag  :  "CEBR-Demo"

# Constellation selection:
Satellite Systems : G

# Inputs:
RINEX Observation path     :  /home/ppinto/WorkArea/demo/rnx/CEBR00ESP_R_20191330000_01D_30S_MO.rnx
RINEX Navigation GPS path  :  /home/ppinto/WorkArea/demo/rnx/CEBR00ESP_R_20191330000_01D_GN.rnx
RINEX Navigation GAL path  :  /home/ppinto/WorkArea/demo/rnx/CEBR00ESP_R_20191330000_01D_EN.rnx

# Outputs:
GRPP Output Path  :  /home/ppinto/WorkArea/demo/grpp/GPS-CA/
GSPA Output Path  :  /home/ppinto/WorkArea/demo/gspa/GPS-CA/
Log File          :  /home/ppinto/WorkArea/demo/gps_ca_grpp+gspa.log

# -------------------------------------------------------------------------- #
# Processing parameters:

# Time parameters:
Ini Epoch [GPS]     :  2019/05/13 00:00:00
End Epoch [GPS]     :  2019/05/13 23:59:59
Interval [seconds]  :  30

# Observations:
GPS Signal Observation    :  C1C
GAL Signal Observation    :  None

# Observation expected precision:
GPS Mean Observation Error [m]  :  3.0
GAL Mean Observation Error [m]  :  None

# Satellite mask:
Satellite Mask [degrees]   :  10
GPS Satellites to Discard  :  G04
GAL Satellites to Discard  :  None

# Satellite Navigation:
Ephemerid Time Threshold [h]  :  1.7

# Error source models:
Ionosphere Model GPS  :  Klobuchar
```

```
Ionosphere Model GAL   :  None
Troposphere Model      :  Saastamoinen

# Elipsoid:
Elipsoid Model  :  wgs84

# Position estimation convergence:
LSQ Maximum Number Iterations  :  3
LSQ Convergence Threshold      :  0.0005

# ------------------------------------------------------------------------ #
# Accuracy configuration:

Vertical Sigma Scale Factor (1D)    :  1.96
Horizontal Sigma Scale Factor (2D)  :  2.45

# Gaussian distribution critical values and associated probabilities:
# +================+======================+======================+
# |   Sigma factor |    Probability 1D (%) |   Probability 2D (%) |
# +================+======================+======================+
# |           1.00 |                 68.3 |                 39.3 | -> default
# +----------------+----------------------+----------------------+
# |           1.96 |                 95.0 |                  TBD |
# +----------------+----------------------+----------------------+
# |           2.00 |                 95.4 |                 86.5 |
# +----------------+----------------------+----------------------+
# |           2.45 |                 98.6 |                 95.0 |
# +----------------+----------------------+----------------------+
# |           3.00 |                 99.7 |                 98.9 |
# +----------------+----------------------+----------------------+

# ------------------------------------------------------------------------ #
# Static Mode Configuration:

Static Mode     :  TRUE
Reference Mode  :  IGS
# Reference IGS station marker name:
IGS Reference Station  :  CEBR

# Manual coordinates:
Reference ECEF X, Y, Z  :  None

# ------------------------------------------------------------------------ #
# Intergrity Mode Configuration:

Integrity Mode : TRUE

Vertical Alert Limit    :  30
Horizontal Alert Limit  :  15

# ------------------------------------------------------------------------ #
# Data dumper configuration:

# Delimiter for output files:
Delimiter  :  ","

# Data formats:
Epoch Format  :  gps
Angle Format  :  deg

# Sigma factor for receiver position:
Sigma Scale Factor  :  1

# END OF CONFIGURATION FILE
# ======================================================================== #
```

Example #2

This configuration examples executes GRPP with GALILEO E1 pseudorange observations. The processing takes place on 18/12/2018 between 00:00 and 07:00 UTC for accounting fair SV availability. Also note that eccentric GALILEO SV E14 and E18 are discarded. As in the previous example, this configuration was using for launching GRPP during its validation as explained in section 3.3. Note that the configuration has set static and integrity modes setting KOKV ITRF coordinates as the position reference.

```
# ========================================================================== #
# CONFIGURATION FILE:

# -------------------------------------------------------------------------- #
# Inputs/Outputs:

# Tool verbosity:
Verbosity  :  TRUE

# Execution identification:
Processing Tag  :  "KOKV Demo"

# Constellation selection:
Satellite Systems : E

# Inputs:
RINEX Observation path     :  /home/ppinto/WorkArea/demo/rnx/KOKV00USA_R_20183520000_01D_30S_MO.rnx
RINEX Navigation GPS path  :  /home/ppinto/WorkArea/demo/rnx/HKSL00HKG_R_20183520000_01D_GN.rnx
RINEX Navigation GAL path  :  /home/ppinto/WorkArea/demo/rnx/KOKV00USA_R_20183520000_01D_EN.rnx

# Outputs:
GRPP Output Path  :  /home/ppinto/WorkArea/demo/grpp/GAL-E1/
GSPA Output Path  :  /home/ppinto/WorkArea/demo/gspa/GAL-E1/
Log File          :  /home/ppinto/WorkArea/demo/gal_e1_grpp+gspa.log

# -------------------------------------------------------------------------- #
# Processing parameters:

# Time parameters:
Ini Epoch [GPS]     :  2018/12/18 00:00:01
End Epoch [GPS]     :  2018/12/18 07:00:00
Interval [seconds]  :  30

# Observations:
GPS Signal Observation    :  None
GAL Signal Observation    :  C1X

# Observation expected precision:
GPS Mean Observation Error [m]  :  None
GAL Mean Observation Error [m]  :  3.0

# Satellite mask:
Satellite Mask [degrees]   :  10
GPS Satellites to Discard  :  None
GAL Satellites to Discard  :  E14, E18

# Satellite Navigation:
Ephemerid Time Threshold [h]  :  1.7

# Error source models:
Ionosphere Model GPS  :  None
Ionosphere Model GAL  :  Klobuchar
Troposphere Model     :  Saastamoinen

# Elipsoid:
Elipsoid Model  :  wgs84
```

```
# Position estimation convergence:
LSQ Maximum Number Iterations  :  3
LSQ Convergence Threshold      :  0.0005

# ------------------------------------------------------------------------ #
# Accuracy configuration:

Vertical Sigma Scale Factor (1D)    :  1.96
Horizontal Sigma Scale Factor (2D)  :  2.45

# Gaussian distribution critical values and associated probabilities:
# +================+======================+======================+
# |   Sigma factor |    Probability 1D (%) |   Probability 2D (%) |
# +================+======================+======================+
# |           1.00 |                 68.3 |                 39.3 | -> default
# +----------------+----------------------+----------------------+
# |           1.96 |                 95.0 |                 ???? |
# +----------------+----------------------+----------------------+
# |           2.00 |                 95.4 |                 86.5 |
# +----------------+----------------------+----------------------+
# |           2.45 |                 98.6 |                 95.0 |
# +----------------+----------------------+----------------------+
# |           3.00 |                 99.7 |                 98.9 |
# +----------------+----------------------+----------------------+

# ------------------------------------------------------------------------ #
# Static Mode Configuration:

Static Mode     :  TRUE
Reference Mode  :  IGS

# Reference IGS station marker name:
IGS Reference Station  :  KOKV

# Manual coordinates:
Reference ECEF X, Y, Z  :  None

# ------------------------------------------------------------------------ #
# Intergrity Mode Configuration:

Integrity Mode : TRUE

Vertical Alert Limit    :  30
Horizontal Alert Limit  :  15

# ------------------------------------------------------------------------ #
# Data dumper configuration:

# Delimiter for output files:
Delimiter  :  ","

# Data formats:
Epoch Format  :  gps
Angle Format  :  deg

# Sigma factor for receiver position:
Sigma Scale Factor  :  1

# END OF CONFIGURATION FILE
# ======================================================================== #
```

A.3 SW Tool: Budget Estimation

Despite that the developed SW tool is intended to be open-source and free of charge, an emulation under a real commercial situation has been carried out. The purpose behind is to demonstrate that the student has gained skills for managing a SW project.

From the student's own experience, the SW development budget estimation is based on the following items:

- Total SW Lines of Code (LoC).
- Dedicated Human Resources to the project.

Note that SW companies do not require a high amount of material resources. Only computer machines, physical premises and other minor items are necessary. These are also known as the passive costs, which are added to a project's budget in order to account for the company maintenance. However, the scope of this budget will be limited to the active costs, the aforementioned items.

The strategy followed to calculate the SW cost is based on the time and effort which must be dedicated by the whole team (human resources) in order to specify, implement and verify the SW. The size of the SW will be based in its overall LoC which are encompassed in Table 8.1.

Table 8.1 – Developed SW LoC per module and package.

SW Lines of Code					
SW root path	**Directories**	**Module**	**LoC**	**LoC/Module**	
$SRC_ROOT/	**GRPP/**	DataDumper.pm	2356	7225	**GRPP/**
		ErrorSource.pm	327		
		MainRoutine.pl	735		
		NeQuickMode.pm	666		
		RecPosition.pm	1308		
		RinexReader.pm	1139		
		SatPosition.pm	694		
	GSPA/	CommonUtil.pm	129	3515	**GSPA/**
		MainSoleService.pl	513		
		PlotLSQInformation.pm	523		
		PlotPosPerformance.pm	951		
		PlotSatErrorSource.pm	403		
		PlotSatObservation.pm	491		
		ReportPerformances.pm	505		
	lib/	Geodetic.pm	309	1081	**lib/**
		MyMath.pm	187		
		MyPrint.pm	187		
		MyUtil.pm	196		
		TimeGNSS.pm	202		
	env/	Enviroments.pm	72	111	**env/**
		Enviroments.sh	39		
	./	GeneralConfiguration.pm	969	969	**GeneralConfiguration.pm**
		TOTAL	**12901**		**SW**

For this specific case, since the product is neither critical nor real-time, its Design Assurance Level can be classified as level E (shorted as DAL-E), meaning that no security implications are caused by SW failure. This leads to assume that approximately 30 LoC per day and worker can be treated. Please note that this metric is considering the LoC treatment in all the SW lifecycle phases: specification, implementation and verification.

Having more than 12K LoC implemented in the SW, this will mean that only one person would spend more than a year in developing this product (as a matter of fact he has). Consequently, 3 team players will be assigned to this project: 1 technical manager and 2 SW developer engineers.

In addition, the worker's salary must be specified. This is presented in Table 8.2. The salary information has been extracted from the Spanish Engineering Companies Convention published in the Official State's Bulletin on January 2017. The social contributions and taxes impositions have been estimated.

Table 8.2 – Human Resource Salary Table.

Human Resources Cost		
	Technical Manager	**Engineer/Developer**
Salary		
Base Salary	1 687.02 €	1 253.16 €
Contract Rewards	500.00 €	400.00 €
Convention Plus	144.26 €	144.26 €
Number of Pays	14	14
Taxes		
*Contribution Base	6.35%	6.35%
*IRPF	2.00%	2.00%
Total Salary		
Gross Salary	32 637.97 €	25 163.93 €
Net Salary	29 912.70 €	23 062.74 €
Salary/Hour		
Annual Labor Hours	1800	1800
Salary/Labor Hour	16.62 €	12.81 €

Finally, the total SW cost can be computed based in the total LoC and the hourly salary of each team player. This is encompassed in Table 8.3. The SW development cost is eventually estimated in approximately 54 000 €, with an industrial added benefit of the 15%. In addition, the SW would take more or less 6 months to be ready.

Note that this is the cost of developing the SW. As previously mentioned, passive costs should be added, and further activities expenses such as internal/external meetings should be considered. Moreover, it has been assumed that the 2 engineers will be 100% dedicated to the code activities, whilst the manager will have assigned a 50% (hence, engineers take grater SW workload), since he/she is assumed to have client meetings, discussions and other management activities.

Table 8.3 – SW tool production cost computation.

SW Cost Production			
***DAL-E LoC rate (per day and worker)**	30		
Total SW LoC	12901		
Work Assignment			
Team Player	Technical Manager	Engineer/Developer	Engineer/Developer
Num. Workers	1	1	1
Assigned Work	20.00%	40.00%	40.00%
Assigned LoC	2580	5160	5160
Dedicated Hours			
Required Days	86	172	172
Hours/Day	8	8	8
Total Hours	688	1376	1376
Work Cost			
Team Player salary per hour	16.62 €	12.81 €	12.81 €
Total cost per Team Player	11 434.18 €	17 631.55 €	17 631.55 €
		TOTAL	**46 697.29 €**
		TOTAL + Industrial Benefit (15%)	**53 701.88 €**

A.4 SW Tool: GRPP Interface Examples

This annex contains some examples of the hash interfaces designed for the developed SW tool. As a reminder, the hash-interface offers the advantage of storing the information in the machine's memory and the different modules can receive the hash reference as an input and access the data homogeneously. But, the hash-interface must be precisely defined.

All hash interfaces used in GRPP and GSPA are accessible in the source code repository. Refer to annex A.1 and inspect *tmp/DescriptiveICD.pl* file. The file is written in Perl language and it details each interface. Nonetheless, for its understanding is necessary to be familiar with Perl programming language.

If the reader is not familiarized with Perl, he/she can use the following code explanation as a guideline:

```
# This is a comment in Perl
# Perl most-used variables are classified in:
#  Scalar ($) -> holds any letter, number, strings and other variable references
#  Array  (@) -> holds a list of scalars
#  Hash   (%) -> creates a key-value pair relation of scalars

# These are some examples of Perl scalar variables:
my $number = 1;
my $string = "Hello World";
my $decimal = 2.0;
my $letter = 'c';

# These are some examples of Perl array variables:
# NOTE: arrays can only contain scalars
my @numbers = ($number, $decimal);
my @text    = ($string, $letter);
my @mix     = ($number, $string);

# This is an example of Perl hash variable:
# NOTE: key and values can only be scalar type
my $hash = ($number  => $string,
            $decimal => $letter);

# Perl allows to save and access variable references (memory addresses) using the backslash'\':
# NOTE: references are saved in a scalar variable
my $ref_scalar = \$number;
my $ref_array  = \@mix;
my $ref_hash   = \%hash;

# Perl references allow for a deeper structure definition. For instance:
my %struct = (NUMBER => $number,
              MIX    => $ref_array,
              ITEMS  => $ref_hash,
              ARRAY  => [0,1,2,3],
              HASH   => {a => 'A', b => 'B'});

# Note that '[]' stand for an array reference and '{}' for a hash reference.

# Consequently, hash structures can also be initialized in the following form:
my $ref_struct = {}; # hash initialization
   $ref_struct = \%struct;

# And hash content access is very straight forward:
print $ref_struct->{NUMBER};     # this will print "1"
print $ref_struct->{MIX}[1];     # this will print "Hello World"
print $ref_struct->{ITEMS}{2.0}; # this will print "c"
```

The following tables have been added for exemplifying the interfaces contained in the aforementioned file in a more pleasant manner. For the sake of clarity not all interface items have been kept. The examples represent:

- **Table 8.4** gathers hash-interface generic GRPP and GSPA configuration.
- **Table 8.5**. Processing computed data. This is the stored data for each epoch processed with GRPP.

Table 8.4 – Generic Configuration Hash-Interface Example.

Generic Configuration Hash Interface: %gen_conf			
Key	**Points to**	**Variable Type**	**Nature**
TAG	$processsing_tag	Scalar	Mandatory
SELECTED_SAT_SYS	@selected_sat_sys	Array	Mandatory
RINEX_OBS_PATH	$path_to_obs_file	Scalar	Mandatory
RINEX_NAV_PATH	%nav_rinex_paths	Hash	Mandatory
OUTPUT_PATH	%output_path_conf	Hash	Mandatory
LOG_FILE_PATH	$path_to_execution_log_file	Scalar	Mandatory
INI_EPOCH	$start_processing_epoch	Scalar	Mandatory
END_EPOCH	$end_processing_epoch	Scalar	Mandatory
INTERVAL	$processing_interval	Scalar	Mandatory
@selected_sat_sys			
0	$sat_sys	Scalar	Mandatory
…	$sat_sys	Scalar	Optional
%nav_rinex_paths			
G	$gps_nav_rinex_path	Scalar	Mandatory if 'G' in @selected_sat_sys
E	$gal_nav_rinex_path	Scalar	Mandatory if 'E' in @selected_sat_sys
%output_path_conf			
GRPP	$grpp_output_directory	Scalar	Mandatory
GSPA	$gspa_output_directory	Scalar	Mandatory

Table 8.5 – GRPP Observation Epoch Data Hash-Interface Example.

GRPP Observation Epoch Data Hash Interface: %obs_epoch			
Key	**Points to**	**Variable Type**	**Nature**
STATUS	$obs_epoch_status	Scalar	Mandatory
EPOCH	$gps_epoch	Scalar	Mandatory
NUM_SAT_INFO	%num_sat_hash	Hash	Mandatory
SAT_OBS	%sat_obs_hash	Hash	Mandatory
SAT_LOS	%line_of_sight_info	Hash	Mandatory
LSQ_INFO	@lsq_info	Array	Mandatory
SAT_POSITION	%sat_xyztc	Hash	Mandatory
REC_POSITION	%position_parameters	Hash	Mandatory
INTEGRITY_INFO	%integrity_info	Hash	Optional
%line_of_sight_info			
$sat_id	%rec_sat_los_data	Hash	Mandatory
…	%rec_sat_los_data	Hash	Optional

%rec_sat_los_data			
AZIMUT	$rec_to_sat_azimut	Scalar	Mandatory
ZENITAL	$rec_to_sat_zenital	Scalar	Mandatory
DISTANCE	$rec_to_sat_distance	Scalar	Mandatory
ELEVATION	$rec_to_sat_elevation	Scalar	Mandatory
IONO_CORR	$ionosphere_los_delay	Scalar	Optional
TROPO_CORR	$troposphere_los_delay	Scalar	Optional
ENU_VECTOR	@rec_to_sat_enu_vector	Array	Mandatory
ECEF_VECTOR	@rec_to_sat_ecef_vector	Array	Mandatory
@lsq_info			
0	%iteration_info	Hash	Mandatory
…	%iteration_info	Hash	Optional
%iteration_info			
STATUS	$boolean_status	Scalar	Mandatory
CONVERGENCE	$boolean_status	Scalar	Mandatory
NUM_OBSERVATION	$num_obs	Scalar	Mandatory
DEGREES_OF_FREEDOM	$num_obs - $num_parameter	Scalar	Mandatory
APX_PARAMETER	@rec_parameters	Array	Mandatory
PARAMETER_VECTOR	@rec_delta_parameters	Array	Mandatory
SAT_RESIDUALS	%sat_residuals	Hash	Mandatory
VARIANCE_ESTIMATOR	$variance_estimator	Scalar	Mandatory
%position_parameters			
STATUS	$boolean_status	Scalar	Mandatory
XYZ	@ecef_position	Array	Mandatory
CLK	$rec_clk_bias	Scalar	Mandatory
VAR_XYZ	@variance_ecef	Array	Mandatory
VAR_CLK	$rec_clk_variance	Scalar	Mandatory
VAR_ENU	@variance_enu	Array	Mandatory
%integrity_info			
HORIZONTAL	%integrity_info_domain	Hash	Mandatory
VERTICAL	%integrity_info_domain	Hash	Mandatory
%integrity_info_domain			
ERROR	$positioning_error	Scalar	Mandatory
PRECISION	$postioning_precision	Scalar	Mandatory
MI_FLAG	$misleading_info_flag	Scalar	Mandatory
HMI_FLAG	$hazardous_misleading_info_flag	Scalar	Mandatory
AVAIL_FLAG	$availability_boolean	Scalar	Mandatory

A.5 Performance Campaign: Data and Results Repository

From the following hyperlink a compressed .tar.gz file can be downloaded. This file archives the campaign data, configuration status and results as indicated in chapter 4.

Nonetheless, the hereafter table gathers each campaign station-date-signal execution status. The rest of the information such as accuracy and integrity performances results are included in a .csv and Microsoft Excel file, which are also accessible in the aforementioned link.

Table 8.6 – Campaign executions status.

Station	DATE_ID	Date	Sat Sys	Signal	Status	Epochs	Valid	%	Invalid	%
ABMF	DATE_1	20/02/2019	GPS	C/A	ok	481	481	100.0	0	0.0
ABMF	DATE_1	20/02/2019	GAL	E1	ok	481	447	92.9	34	7.1
ABMF	DATE_1	20/02/2019	GAL	E5b	ok	481	447	92.9	34	7.1
ABMF	DATE_1	20/02/2019	GPS	L2C	ok	481	481	100.0	0	0.0
KIRU	DATE_1	20/02/2019	GPS	C/A	ok	481	481	100.0	0	0.0
KIRU	DATE_1	20/02/2019	GAL	E1	ok	481	460	95.6	21	4.4
KIRU	DATE_1	20/02/2019	GAL	E5b	ok	481	460	95.6	21	4.4
KIRU	DATE_1	20/02/2019	GPS	L2C	ok	481	481	100.0	0	0.0
KOKV	DATE_1	20/02/2019	GPS	C/A	ok	481	481	100.0	0	0.0
KOKV	DATE_1	20/02/2019	GAL	E1	ok	481	318	66.1	163	33.9
KOKV	DATE_1	20/02/2019	GAL	E5b	ok	481	318	66.1	163	33.9
KOKV	DATE_1	20/02/2019	GPS	L2C	ok	481	473	98.3	8	1.7
OWMG	DATE_1	20/02/2019	GPS	C/A	ok	481	481	100.0	0	0.0
OWMG	DATE_1	20/02/2019	GAL	E1	ok	481	481	100.0	0	0.0
OWMG	DATE_1	20/02/2019	GAL	E5b	ok	481	439	91.3	42	8.7
OWMG	DATE_1	20/02/2019	GPS	L2C	ok	481	414	86.1	67	13.9
TASH	DATE_1	20/02/2019	GPS	C/A	ok	481	481	100.0	0	0.0
TASH	DATE_1	20/02/2019	GAL	E1	ok	481	300	62.4	181	37.6
TASH	DATE_1	20/02/2019	GAL	E5b	ok	481	308	64.0	173	36.0
TASH	DATE_1	20/02/2019	GPS	L2C	ok	481	472	98.1	9	1.9
ABMF	DATE_2	20/02/2019	GPS	C/A	ok	1620	1620	100.0	0	0.0
ABMF	DATE_2	20/02/2019	GAL	E1	ok	1620	1451	89.6	169	10.4
ABMF	DATE_2	20/02/2019	GAL	E5b	ok	1620	1276	78.8	344	21.2
ABMF	DATE_2	20/02/2019	GPS	L2C	ok	1620	1620	100.0	0	0.0
KIRU	DATE_2	29/04/2019	GPS	C/A	ok	961	961	100.0	0	0.0
KIRU	DATE_2	29/04/2019	GAL	E1	ok	961	939	97.7	22	2.3
KIRU	DATE_2	29/04/2019	GAL	E5b	ok	721	698	96.8	23	3.2
KIRU	DATE_2	29/04/2019	GPS	L2C	ok	961	922	95.9	39	4.1
KOKV	DATE_2	18/12/2018	GPS	C/A	ok	1081	1081	100.0	0	0.0
KOKV	DATE_2	18/12/2018	GAL	E1	ok	1081	835	77.2	246	22.8
KOKV	DATE_2	18/12/2018	GAL	E5b	ok	1081	834	77.2	247	22.8
KOKV	DATE_2	18/12/2018	GPS	L2C	ok	1081	985	91.1	96	8.9
OWMG	DATE_2	26/04/2019	GPS	C/A	ok	1201	1201	100.0	0	0.0

OWMG	DATE_2	26/04/2019	GAL	E1	**ok**	1201	1159	96.5	42	3.5
OWMG	DATE_2	26/04/2019	GAL	E5b	**ok**	1201	1109	92.3	92	7.7
OWMG	DATE_2	26/04/2019	GPS	L2C	**ok**	1201	1201	100.0	0	0.0
TASH	DATE_2	07/04/2019	GPS	C/A	**ok**	1201	1201	100.0	0	0.0
TASH	DATE_2	07/04/2019	GAL	E1	**ok**	1201	587	48.9	614	51.1
TASH	DATE_2	07/04/2019	GAL	E5b	**ok**	1201	587	48.9	614	51.1
TASH	DATE_2	07/04/2019	GPS	L2C	**ok**	1201	846	70.4	355	29.6
FAIR	DATE_3	26/08/2018	GPS	C/A	**ok**	401	401	100.0	0	0.0
FAIR	DATE_3	26/08/2018	GAL	E1	**ok**	401	203	50.6	198	49.4
FAIR	DATE_3	26/08/2018	GAL	E5b	**ok**	401	203	50.6	198	49.4
FAIR	DATE_3	26/08/2018	GPS	L2C	**ok**	401	401	100.0	0	0.0
KIRU	DATE_3	07/03/2019	GPS	C/A	**ok**	480	480	100.0	0	0.0
KIRU	DATE_3	07/03/2019	GAL	E1	**ok**	480	419	87.3	61	12.7
KIRU	DATE_3	07/03/2019	GAL	E5b	**ok**	480	403	84.0	77	16.0
KIRU	DATE_3	07/03/2019	GPS	L2C	**ok**	480	443	92.3	37	7.7
KOKV	DATE_3	16/04/2019	GPS	C/A	**ok**	720	660	91.7	60	8.3
KOKV	DATE_3	16/04/2019	GAL	E1	**ok**	720	468	65.0	252	35.0
KOKV	DATE_3	16/04/2019	GAL	E5b	**ok**	720	468	65.0	252	35.0
KOKV	DATE_3	16/04/2019	GPS	L2C	**ok**	720	553	76.8	167	23.2
KOUG	DATE_3	22/11/2018	GPS	C/A	**ok**	961	961	100.0	0	0.0
KOUG	DATE_3	22/11/2018	GAL	E1	**ok**	961	954	99.3	7	0.7
KOUG	DATE_3	22/11/2018	GAL	E5b	**ok**	961	954	99.3	7	0.7
KOUG	DATE_3	22/11/2018	GPS	L2C	**ok**	961	961	100.0	0	0.0
MAJU	DATE_3	10/04/2019	GPS	C/A	**ok**	1201	1201	100.0	0	0.0
MAJU	DATE_3	10/04/2019	GAL	E1	discard	1201	0	0.0	1201	100.0
MAJU	DATE_3	10/04/2019	GAL	E5b	discard	1201	0	0.0	1201	100.0
MAJU	DATE_3	10/04/2019	GPS	L2C	**ok**	1201	1152	95.9	49	4.1

A.6 Performance Campaign: IGS-MGEX Stations World Map

This annex contains a world map illustrating the geographical locations of the IGS-MGEX GNSS stations used for the positioning performance campaign study.

If the reader is using a hard copy of the document, the world map is saved in following page. In case that a digital copy is being used, the map can be found in .pdf format under the following hyperlink.

Visualizador de documentos

Turnitin Informe de Originalidad

Procesado el: 10-jul.-2019 12:29 p. m. CEST
Identificador: 1150715367
Número de palabras: 48490
Entregado: 1

48410958:TFM_Pinto.pdf Por Pablo Pinto Santos

Índice de similitud	Similitud según fuente	
5%	Internet Sources:	4%
	Publicaciones:	3%
	Trabajos del estudiante:	3%

incluir citas incluir bibliografía excluyendo las coincidencias < 5 de las palabras descargar imprimir

modo: ver informe en vista quickview (vista clásica) Change mode

1% match (Internet desde 12-jun.-2018)
http://www.navipedia.net

<1% match (Internet desde 06-nov.-2018)
https://kb.igs.org/hc/en-us/article_attachments/202583897/RINEX_303.pdf

<1% match (Internet desde 25-dic.-2017)
https://d-nb.info/1076512771/34

<1% match (Internet desde 29-jul.-2014)
http://www2.pv.infn.it

<1% match (Internet desde 29-ago.-2017)
http://orbi.ulg.ac.be

<1% match (Internet desde 07-feb.-2017)
http://scarlet.clarku.edu

<1% match (Internet desde 29-ene.-2016)
http://astro.ago.uni-lj.si

<1% match (trabajos de los estudiantes desde 25-ago.-2013)
Submitted to University of Newcastle upon Tyne on 2013-08-25

<1% match (Internet desde 16-ene.-2017)
http://epncb.oma.be

<1% match (publicaciones)
"GNSS — Global Navigation Satellite Systems", Springer Nature, 2008

<1% match (Internet desde 12-jun.-2018)
https://www.scribd.com/document/334539211/Fundamentals-of-Inertial-Navigation-Satellite-based-Positioning-and-Their-Integration

<1% match (Internet desde 22-ene.-2014)
http://gage.es

<1% match (publicaciones)
Lecture Notes in Electrical Engineering, 2016.

<1% match (Internet desde 02-jun.-2019)
http://ikee.lib.auth.gr

<1% match (Internet desde 16-abr.-2019)
http://www.eiseisokui.or.jp

<1% match (Internet desde 18-may.-2019)
https://hal.archives-ouvertes.fr/tel-01368049/document

<1% match (publicaciones)
"Springer Handbook of Global Navigation Satellite Systems", Springer Nature, 2017

<1% match (Internet desde 07-sept.-2017)
http://boris.unibe.ch

<1% match (Internet desde 24-oct.-2018)
http://athene-forschung.unibw.de

<1% match (Internet desde 04-ene.-2017)
http://researchbank.rmit.edu.au

<1% match (trabajos de los estudiantes desde 04-jun.-2008)
Submitted to University of Newcastle upon Tyne on 2008-06-04

<1% match (Internet desde 29-mar.-2016)
http://google.com.na

<1% match (Internet desde 24-nov.-2016)
https://www.hydro-international.com/content/news/hemisphere-gps-vector-gps-compass?output=pdf

<1% match (Internet desde 11-feb.-2019)
https://dspace.cc.tut.fi/dpub/bitstream/handle/123456789/27054/Kuismanen.pdf?isAllowed=y&sequence=1

<1% match (Internet desde 23-abr.-2019)
https://gssc.esa.int/navipedia/index.php/GNSS_Performances

<1% match (Internet desde 25-dic.-2017)
http://www.igs.org

<1% match (publicaciones)
Jan Wendel. "Back Matter", Walter de Gruyter GmbH, 2007

<1% match (trabajos de los estudiantes desde 18-ago.-2014)
Submitted to Cranfield University on 2014-08-18

<1% match (Internet desde 08-jun.-2017)
http://gnss.esri.com

<1% match (Internet desde 07-mar.-2015)
http://www.sokkia.com.tw

<1% match (Internet desde 04-ago.-2018)
http://citeseerx.ist.psu.edu

<1% match (Internet desde 01-dic.-2018)
https://es.scribd.com/document/177851511/Entire-GPS

<1% match (Internet desde 07-sept.-2017)
http://eprints.ucm.es

<1% match (Internet desde 25-nov.-2018)
https://gssc.esa.int/navipedia/GNSS_Book/ESA_GNSS-Book_TM-23_Vol_I.pdf

<1% match (Internet desde 27-dic.-2013)
http://www.navipedia.net

<1% match (publicaciones)
Jan Wendel. "Integrierte Navigationssysteme", Walter de Gruyter GmbH, 2007

<1% match (publicaciones)
"Satellite Navigation Systems", Aerospace Navigation Systems, 2016.

<1% match (publicaciones)
U. Engel. "A geolocation method using ToA and FoA measurements", 2009 6th Workshop on Positioning Navigation and Communication, 03/2009

<1% match (Internet desde 04-mar.-2016)
http://opus.bath.ac.uk

<1% match (Internet desde 11-mar.-2019)
https://www.gsc-europa.eu/system/files/galileo_documents/Galileo-OS-SIS-ICD.pdf

<1% match (Internet desde 01-abr.-2019)
http://dspace.vsb.cz

<1% match (trabajos de los estudiantes desde 06-nov.-2017)
Submitted to CVC Nigeria Consortium on 2017-11-06

<1% match (Internet desde 11-ago.-2017)
http://porto.polito.it

<1% match (Internet desde 16-ago.-2017)
http://www.navipedia.org

<1% match (trabajos de los estudiantes desde 10-dic.-2009)
Submitted to Brunel University on 2009-12-10

<1% match (Internet desde 22-mar.-2016)
http://epncb.oma.be

<1% match (Internet desde 22-sept.-2018)
https://hal.archives-ouvertes.fr/hal-00401029/file/bourda2009-proceedings.pdf

<1% match (publicaciones)
Dennis D. McCarthy, P. Kenneth Seidelmann. "Time - From Earth Rotation to Atomic Physics", Wiley, 2009

<1% match (publicaciones)
Akram Afifi, Ahmed El-Rabbany. "Un-differenced precise point positioning model using triple GNSS constellations", Cogent Geoscience, 2016

<1% match (publicaciones)
KotyÅ„ski, RafaÅ„, Karol KrÃ³l, Jacek Pniewski, and Oleg V. Angelsky. "<title>Spatial filtering of the light beam with a layered silver flat lens</title>", Proceedings of SPIE, 2008.

<1% match (trabajos de los estudiantes desde 18-jun.-2017)
Submitted to SIM Global Education on 2017-06-18

<1% match (trabajos de los estudiantes desde 22-ago.-2013)
Submitted to Middle East Technical University on 2013-08-22

<1% match (Internet desde 22-feb.-2018)
https://d-nb.info/1150852070/34

<1% match (Internet desde 11-mar.-2018)
https://link.springer.com/content/pdf/10.1007%2F978-3-7091-6199-9.pdf

<1% match (Internet desde 06-sept.-2017)
https://www.politesi.polimi.it/bitstream/10589/109823/3/L%27impiego%20del%20sistema%20EGNOS.pdf

<1% match (Internet desde 31-may.-2016)
http://oa.upm.es

<1% match (Internet desde 16-ene.-2017)
http://epncb.oma.be

<1% match (Internet desde 28-nov.-2014)
http://scholar.lib.vt.edu

<1% match (Internet desde 23-may.-2019)
https://link.springer.com/article/10.1007%2Fs10291-016-0566-5

<1% match (Internet desde 03-jun.-2019)
http://www.ijsrp.org

<1% match (Internet desde 03-ago.-2018)
http://blog.wsd.net

<1% match (Internet desde 17-jul.-2018)
https://repository.tudelft.nl/islandora/object/uuid:7fe64dde-7fb5-4392-8160-da6f7916dc6b/datastream/OBJ/download

<1% match (publicaciones)
Rosello, Josep, Pierluigi, Roland Weigand, Salvatore dAddio, Alberto Garcia, and Gustavo Lopez Risueno. "Next generation of ESA GNSS receivers for Earth Observation satellites", 30th AIAA International Communications Satellite System Conference (ICSSC), 2012.

<1% match (trabajos de los estudiantes desde 19-mar.-2012)
Submitted to Saint Michael's College on 2012-03-19

<1% match (trabajos de los estudiantes desde 16-mar.-2011)
Submitted to University of Florida on 2011-03-16

<1% match (Internet desde 29-ago.-2017)
https://minerva-access.unimelb.edu.au/bitstream/handle/11343/39356/67601_00003951_01_fraser_phd_thesis_2007.pdf?sequence=1

<1% match (Internet desde 29-ago.-2017)
https://minerva-access.unimelb.edu.au/bitstream/handle/11343/39223/67232_00003170_01_Neil_Brown_PhD_Thesis.pdf?sequence=1

<1% match (Internet desde 27-feb.-2019)
https://www.unavco.org/help/glossary/glossary.html

<1% match (Internet desde 21-mar.-2019)
https://b-ok.org/book/863361/3e3bd3

<1% match (Internet desde 12-oct.-2018)
http://eprints.nottingham.ac.uk

<1% match (trabajos de los estudiantes desde 13-jul.-2014)
Submitted to Utica College on 2014-07-13

<1% match (trabajos de los estudiantes desde 08-may.-2016)
Submitted to Institute of Technology Blanchardstown on 2016-05-08

<1% match (trabajos de los estudiantes desde 19-jun.-2014)
Submitted to Middle East Technical University on 2014-06-19

<1% match (Internet desde 30-oct.-2017)
http://docplayer.net

<1% match (Internet desde 05-sept.-2017)
http://www.ucalgary.ca

<1% match (Internet desde 16-jun.-2019)
http://www.mari-odu.org

<1% match (Internet desde 20-feb.-2014)
http://www.navcen.uscg.gov

<1% match (Internet desde 26-nov.-2017)
http://porto.polito.it

<1% match (Internet desde 26-ene.-2018)
https://documents.mx/download/link/guide-bernese

<1% match (Internet desde 26-feb.-2016)
http://diva-portal.org

<1% match (Internet desde 25-ago.-2018)
https://tel.archives-ouvertes.fr/tel-01695792/document

<1% match (Internet desde 16-abr.-2010)
http://www.geodetic.gov.hk

<1% match (Internet desde 05-mar.-2017)
https://publik.tuwien.ac.at/files/PubDat_228707.pdf

<1% match (Internet desde 16-nov.-2018)
https://opus4.kobv.de/opus4-fau/frontdoor/deliver/index/docId/954/file/AnnaMiskiewiczDissertation.pdf

<1% match (Internet desde 28-may.-2008)
http://comunidad.fotolibre.net

<1% match (publicaciones)
"China Satellite Navigation Conference (CSNC) 2019 Proceedings", Springer Science and Business Media LLC, 2019

<1% match (publicaciones)
Marco Porretta, Bernhard Kleine Schlarmann, Alexandre Ballereau, Massimo Crisci. "A Novel Uplink Scheduling Algorithm for the Galileo System", IEEE Transactions on Aerospace and Electronic Systems, 2018

<1% match (publicaciones)
"China Satellite Navigation Conference (CSNC) 2019 Proceedings", Springer Science and Business Media LLC, 2019

<1% match (publicaciones)
Carles Fernandez-Prades, Javier Arribas, Pau Closas. "Assessment of software-defined GNSS receivers", 2015 Second International Conference on Computer Science, Computer Engineering, and Social Media (CSCESM), 2015

<1% match (trabajos de los estudiantes desde 31-oct.-2018)
Submitted to Cranfield University on 2018-10-31

<1% match (trabajos de los estudiantes desde 18-ago.-2011)
Submitted to Jawaharlal Nehru Technological University on 2011-08-18

<1% match (trabajos de los estudiantes desde 08-sept.-2015)
Submitted to Kwame Nkrumah University of Science and Technology on 2015-09-08

<1% match (trabajos de los estudiantes desde 22-dic.-2016)
Submitted to Aston University on 2016-12-22

<1% match (trabajos de los estudiantes desde 07-nov.-2015)
Submitted to Aston University on 2015-11-07

<1% match (trabajos de los estudiantes desde 12-may.-2009)
Submitted to University of Newcastle upon Tyne on 2009-05-12

<1% match (trabajos de los estudiantes desde 24-abr.-2019)
Submitted to The Hong Kong Polytechnic University on 2019-04-24

<1% match (trabajos de los estudiantes desde 05-sept.-2006)
Submitted to Oakham School on 2006-09-05

<1% match (trabajos de los estudiantes desde 13-may.-2013)
Submitted to Colorado Technical University Online on 2013-05-13

<1% match (trabajos de los estudiantes desde 05-dic.-2018)
Submitted to University of Science and Technology on 2018-12-05

<1% match (trabajos de los estudiantes desde 28-abr.-2009)
Submitted to University of Southern California on 2009-04-28

<1% match (trabajos de los estudiantes desde 12-jun.-2013)
Submitted to Syracuse University on 2013-06-12

<1% match (trabajos de los estudiantes desde 14-jun.-2017)
Submitted to University of Pretoria on 2017-06-14

<1% match (trabajos de los estudiantes desde 15-ago.-2013)
Submitted to University of Birmingham on 2013-08-15

<1% match (trabajos de los estudiantes desde 25-sept.-2014)
Submitted to Symbiosis International University on 2014-09-25

<1% match (Internet desde 26-feb.-2017)
http://researchbank.rmit.edu.au

<1% match (Internet desde 10-ene.-2019)
http://www.anacniger.org

<1% match (Internet desde 05-mar.-2017)
https://publik.tuwien.ac.at/files/PubDat_228890.pdf

<1% match (Internet desde 16-nov.-2018)
http://eprints.nottingham.ac.uk

<1% match (Internet desde 18-dic.-2017)
https://d-nb.info/1052627730/34

<1% match (Internet desde 21-may.-2016)
http://porto.polito.it

<1% match (Internet desde 05-jun.-2017)
http://gnss.esri.com

<1% match (Internet desde 29-nov.-2017)
http://porto.polito.it

<1% match (Internet desde 13-may.-2019)
https://eprints.ucm.es/41977/1/T38592.pdf

<1% match (Internet desde 17-jul.-2010)
http://web.ist.utl.pt

<1% match (Internet desde 20-nov.-2018)
http://www.geethanjaliinstitutions.com

<1% match (Internet desde 07-nov.-2017)
https://helda.helsinki.fi/bitstream/handle/10138/224830/110MML15.pdf?sequence=1

<1% match (Internet desde 07-may.-2019)
https://polen.itu.edu.tr/bitstream/11527/940/1/8925.pdf

<1% match (Internet desde 18-ene.-2018)
http://www.mdpi.com

<1% match (Internet desde 03-ene.-2018)
http://www.mdpi.com

<1% match (Internet desde 01-sept.-2016)
http://www.science.gov

<1% match (Internet desde 27-jun.-2019)
https://www.ann-geophys.net/36/1227/2018/

<1% match (Internet desde 09-abr.-2019)
https://idus.us.es/xmlui/handle/11441/42635?show=full

<1% match (Internet desde 21-sept.-2018)
http://tuprints.ulb.tu-darmstadt.de

<1% match (Internet desde 11-sept.-2017)
https://communities.sas.com/t5/SAS-Procedures/earlier-dates-only-for-each-id/m-p/44658?nobounce=

<1% match (Internet desde 05-oct.-2016)
http://tdx.cat

<1% match (Internet desde 16-dic.-2015)
http://epic.awi.de

<1% match (Internet desde 05-mar.-2007)
http://www.frikis.net

<1% match (publicaciones)
Lecture Notes in Electrical Engineering, 2015.

<1% match (publicaciones)
"China Satellite Navigation Conference (CSNC) 2017 Proceedings: Volume III", Springer Science and Business Media LLC, 2017

<1% match (publicaciones)
Heikki Hurskainen, Jari Nurmi. "SystemC Model of an Interoperative GPS/Galileo Code Correlator Channel", 2006 IEEE Workshop on Signal Processing Systems Design and Implementation, 2006

<1% match (publicaciones)
Yidong Lou, Xianjie Li, Fu Zheng, Yang Liu, Hailin Guo. "Assessment and Impact on BDS Positioning Performance Analysis of Recent BDS IGSO-6 Satellite", Journal of Navigation, 2018

<1% match (publicaciones)
Li, Xingxing, Florian Zus, Cuixian Lu, Galina Dick, Tong Ning, Maorong Ge, Jens Wickert, and Harald Schuh. "Retrieving of atmospheric parameters from multi-GNSS in real-time: Validation with water vapor radiometer and numerical weather model : multi-GNSS atmospheric parameters", Journal of Geophysical Research Atmospheres, 2015.

<1% match (publicaciones)
G.A. Hajj, E.R. Kursinski, L.J. Romans, W.I. Bertiger, S.S. Leroy. "A technical description of atmospheric sounding by GPS occultation", Journal of Atmospheric and Solar-Terrestrial Physics, 2002

<1% match (trabajos de los estudiantes desde 12-abr.-2019)
Submitted to UWC ChangShu China on 2019-04-12

<1% match (trabajos de los estudiantes desde 05-may.-2010)
Submitted to Harper Adams University College on 2010-05-05

<1% match (trabajos de los estudiantes desde 28-sept.-2017)
Submitted to University of Bath on 2017-09-28

<1% match (trabajos de los estudiantes desde 28-ago.-2017)
Submitted to University of Nottingham on 2017-08-28

<1% match (trabajos de los estudiantes desde 19-mar.-2018)
Submitted to Aristotle University of Thessaloniki on 2018-03-19

<1% match (trabajos de los estudiantes desde 19-abr.-2009)
Submitted to Cranfield University on 2009-04-19

<1% match (trabajos de los estudiantes desde 01-feb.-2015)
Submitted to Cranfield University on 2015-02-01

<1% match (trabajos de los estudiantes desde 15-may.-2013)
Submitted to Tshwane University of Technology on 2013-05-15

<1% match (trabajos de los estudiantes desde 03-sept.-2015)
Submitted to University College London on 2015-09-03

<1% match (trabajos de los estudiantes desde 03-may.-2018)
Submitted to University of Newcastle upon Tyne on 2018-05-03

<1% match (trabajos de los estudiantes desde 13-abr.-2018)
Submitted to Kingston University on 2018-04-13

<1% match (trabajos de los estudiantes desde 18-may.-2009)
Submitted to University of Newcastle upon Tyne on 2009-05-18

<1% match (trabajos de los estudiantes desde 24-abr.-2006)

Submitted to Texas A&M University, College Station on 2006-04-24

<1% match (trabajos de los estudiantes desde 21-abr.-2015)
Submitted to 9561 on 2015-04-21

<1% match (trabajos de los estudiantes desde 29-feb.-2012)
Submitted to University of Wales central institutions on 2012-02-29

<1% match (trabajos de los estudiantes desde 22-dic.-2010)
Submitted to University of Malaya on 2010-12-22

<1% match (trabajos de los estudiantes desde 11-jul.-2008)
Submitted to University of Nottingham on 2008-07-11

<1% match (trabajos de los estudiantes desde 10-mar.-2010)
Submitted to Cranfield University on 2010-03-10

<1% match (trabajos de los estudiantes desde 27-jun.-2017)
Submitted to Indian Institute of Remote Sensing on 2017-06-27

<1% match (trabajos de los estudiantes desde 15-mar.-2011)
Submitted to University of Johannsburg on 2011-03-15

<1% match (trabajos de los estudiantes desde 19-abr.-2011)
Submitted to iGroup on 2011-04-19

<1% match (trabajos de los estudiantes desde 21-jun.-2010)
Submitted to Brunel University on 2010-06-21

<1% match (publicaciones)
Astrophysics and Space Science Library, 2016.

<1% match (publicaciones)
Bernhard Hofmann-Wellenhof, Herbert Lichtenegger, James Collins. "Global Positioning System", Springer Nature, 1992

<1% match (trabajos de los estudiantes desde 26-jul.-2018)
Submitted to Polytechnic of Turin on 2018-07-26

<1% match (publicaciones)
"IAG 150 Years", Springer Nature, 2016

<1% match (publicaciones)
Michel Capderou. "Handbook of Satellite Orbits", Springer Nature, 2014

<1% match (publicaciones)
Gethin Wyn Roberts. "Noise comparison of triple frequency GNSS carrier phase, doppler and pseudorange observables", Measurement, 2019

<1% match (publicaciones)
Kamil Krasuski, Janusz C´wiklak, Henryk Jafernik. "Aircraft positioning using PPP method in GLONASS system", Aircraft Engineering and Aerospace Technology, 2018

<1% match (trabajos de los estudiantes desde 18-mar.-2013)
Submitted to Bolton Institute of Higher Education on 2013-03-18

<1% match (trabajos de los estudiantes desde 20-jul.-2015)
Submitted to Yonsei University on 2015-07-20

<1% match (trabajos de los estudiantes desde 19-ago.-2011)
Submitted to Cranfield University on 2011-08-19

<1% match (trabajos de los estudiantes desde 14-may.-2007)
Submitted to University of Sunderland on 2007-05-14

<1% match (trabajos de los estudiantes desde 28-may.-2017)
Submitted to Univerza v Ljubljani on 2017-05-28

<1% match (trabajos de los estudiantes desde 26-ago.-2013)
Submitted to University of Surrey on 2013-08-26

FINAL MASTER THESIS Master’s Degree in Geomatics and Geo-information GNSS Open Service Case Study: Development of SW Tools for Assessing GPS and GALILEO Positioning Performances by Means of Post-Processing Single-Frequency Pseudorange Observations A contribution to available open source tools Author: Pablo Pinto Santos pabpinsa@topo.upv.es Mentor: Ángel Esteban Martín Furones aemartin@upvnet.upv.es Valencia, July of 2019 State of commitment: The presented document has been fully edited by the author; not being delivered as a previous academical work. All other external items have been properly referenced either on the text or in the bibliography section. Agradecimientos Sin duda alguna este trabajo es la historia de un fracaso y un éxito. Un fracaso, porque me acuerdo perfectamente

de que al terminar mi trabajo de final de grado de 134 páginas, allá en el 2016, me prometí que no me volvería a castigar de semejante manera. Con unas orgullosas 163 razones puedo concluir que siempre incumplo este tipo de promesas. Pero no puedo evitar sentirme orgulloso al mismo tiempo y considerar este trabajo también un éxito. Mañana justo se cumplirán dos años desde que empecé a trabajar como ingeniero en Madrid, y por decirlo de la manera más correcta posible, no es que haya sido precisamente de mi particular gozo (al menos de manera global y relativa). Esto se aplica especialmente a compaginar el trabajo con un máster. Ya las cosas iban justas solo teniendo una asignatura en el primer semestre, no me quería ni imaginar como sería con el trabajo final. No me equivocaba, trabajar 40 horas semanales y dedicarte hacer lo mismo otras 22 más es… bueno, hacerlo durante 1 añito y me decís que tal ;) Nunca he presumido de conocerme a mi mismo lo suficientemente bien -de hecho, seguramente ahora mismo conozca mejor la teoría de GNSS- pero si que tengo clara una cosa y es que yo saco lo mejor de mi cuando me empleo en algo que me apasiona, hasta el punto en el que no puedo hacer otra cosa (deberíais verme hacer algo que detesto o me aburre). Por lo que tuve que añadir esa pizca de "pasión" a este trabajo, ese ingrediente común que me acompañó y me motivó a estudiar Geomática y Topografía. Es entonces cuando decidí que había que hacer algo al respecto. Es entonces cuando decidí que nada me haría más feliz que mi trabajo tuviera algún tipo de trascendencia. Y es entonces cuando decidí que mi herramienta GNSS sería publicada de forma abierta para que otras personas pudieran aprovecharlo. Sinceramente creo que esto ha sido el corazón del éxito del que tan orgulloso me siento hoy… y también la razón de que se me haya ido la pinza y haya hecho un código yo solito de casi 13K líneas. ¿Y a quién agradezco este resultado? Por supuesto a mi familia por apoyarme y aconsejarme tan sabiamente durante el proceso: "Acaba esto antes de ponerte a otra cosa" me decían mis padres, posiblemente esta frase es mi salvación de que mis ambiciones me conduzcan del relativo orden al más inmediato caos. A mi hermano, porque existe este mutuo acuerdo no escrito en que yo aguante sus tonterías y él la mías, es sencillamente perfecto. Mención de honor para mi tutor, Ángel que ha aguantado mis correos kilométricos y hemos compartido la esperada revelación de que, a día de hoy, preferimos ir en un coche autónomo controlado por GPS que por GALILEO :) (aunque yo no me montaría en ninguno de los dos y él seguramente tampoco). Agradecer también a los profesores del máster y su insistencia en desarrollar aplicaciones con una orientación al usuario, porque esto ha contribuido en gran parte a la pizca de "pasión" que os estaba contando. Y gracias a mis personas más cercanas de siempre: Alexey, Pepe, Lluis, Sol, Reda, compis de GMV (y sus consejos para que GALILEO funcione) y a los que me estoy dejando por el camino. ¿Y después de esto qué? Es invertible preguntárselo. Pero acabo de entender que es completamente normal responder con un "no lo sé". La ciencia siempre mantiene desconocidas las respuestas a sus grandes preguntas. Parece que esta es una de ellas. Los últimos acontecimientos me han demostrado que hay que estar listo para el fracaso y que el futuro es caprichoso e incierto. Así que será mejor que disfrutemos del proceso, porque será lo último que recordemos al final del camino. "Busca lo que es relevante, no lo que es fácil o conveniente", esta frase de Jordan B. Peterson no puede venir mejor para el caso. Tengo la sensación de que se cierra una etapa y comienza otra nueva con una incertidumbre cuanto menos atractiva. No sé exactamente que vendrá después de esto, pero no será más de lo mismo… Table of Contents List of Figures

Abstract English Nowadays, as the number of GNSS services are increasing, it is necessary to study and evaluate with real data the enhanced capabilities which these positioning products can provide, and how they are evolving compared with their legacy services and its competitors. Among the emerging positioning services, it is noteworthy Europe's GALILEO system, which is close to reach its full operational capability, and is willing to fulfill competitive user level performances which can be used through its open service signals: E1, E5a and E5b. On the legacy side, the most remarkable constellation is USA's GPS, which has been achieving a positioning standard service with the C/A signal and a precise positioning service for military purposes with the P signal. In addition, GPS evolutions will provide a civilian service through more robust signals, such as the L5. The objective of this work is to compare open positioning services from GPS and GALILEO constellations by analyzing their accuracy and integrity performances obtained from a pre-planned campaign, taking as reference-data the IGS station network. The positioning methodology to be used is post-processing single-frequency pseudorange observations in static mode. For committing this purpose, the main workload is focused on developing a configurable and flexible SW tool which is able to batch the pseudorange observations provided by the spatial frame of the GPS and GALILEO satellites, in order to estimate the receiver's position by means of a Least Squares routine. Lately, these data will be inputted in other analysis tools, which will also be developed in the framework of this project, in order to summarize and display the obtained performances. Consequently, and supported by the obtained results, the conclusions regarding the evolution of the studied services will be drawn. Castellano Actualmente, mientras el número de servicios GNSS disponibles aumenta, resulta necesario evaluar con datos reales las mejoras que ofrecen los nuevos productos de posicionamiento, y cuál es su desempeño y evolución respecto de sus servicios antecesores y el de sus competidores. Entre los servicios de posicionamiento emergentes, resulta de especial interés el proporcionado por la constelación Europea de GALILEO, la cual está cerca de alcanzar su completa capacidad operacional, y que resulta prometedora en cuanto a sus requisitos de prestaciones a nivel usuario, que pueden obtenerse mediante el uso de las señales de su servicio abierto: E1, E5a y E5b. De entre los sistemas ya existentes, el más destacado es el proporcionado por la constelación Estadounidense de GPS, el cual ha estado permitiendo con la señal C/A un servicio de posicionamiento estándar y un servicio de posicionamiento preciso con la seña P para fines militares. Adicionalmente las evoluciones del sistema GPS planean transmitir un servicio

civil con señales más robustas, como puede ser la L5. El objetivo de este trabajo es comparar los servicios abiertos de posicionamiento de las constelaciones de GPS y GALILEO, mediante el análisis de sus prestaciones de precisión e integridad obtenidas de una campaña de observación, dónde los datos de referencia a usar son la red de estaciones del IGS. La metodología de posicionamiento a implementar es el post-procesado de observables de pseudo-rango mono-frecuencia en modo estático. Para alcanzar este objetivo, el esfuerzo principal estará enfocado en el desarrollo de una herramienta SW totalmente configurable por el usuario, que sea capaz de procesar los observables de pseudorango proporcionados por el marco de referencia espacial que forman los satélites de GPS y GALILEO, para posteriormente obtener las posiciones del receptor por medio de un algoritmo de estimación por mínimos cuadrados. Los resultados que se obtengan de este procesamiento serán transmitidos a otras herramientas de análisis, las cuales se desarrollarán también en el marco de este proyecto, con la finalidad de resumir y presentar de manera gráfica las prestaciones obtenidas de la campaña. Finalmente, con el soporte de estos resultados, se expondrán las conclusiones sobre el desempeño y la evolución de los servicios anteriormente comentados. Valencià Actualment, mentre el nombre de serveis GNSS disponibles augmenta, cal avaluar amb dades reals les millores que ofereixen els nous productes de posicionament, i quin és el seu acompliment i evolució respecte dels seus serveis antecessors i el dels seus competidors. Entre els serveis de posicionament emergents, resulta d'especial interès el proporcionat per la constel·lació Europea de GALILEO, la qual està a prop d'arribar a la seva completa capacitat operacional, i que resulta prometedora quant als seus requisits de prestacions a nivell usuari, que poden obtenir-se mitjançant l'ús dels senyals del seu servei obert: E1, E5a i E5b. D'entre els sistemes ja existents, el més destacat és el proporcionat per la constel·lació Nord-americana de GPS, el qual ha estat permetent amb el senyal C / A un servei de posicionament estàndard i un servei de posicionament precís amb el senyal P per a fins militars. A més a les evolucions del sistema GPS planegen transmetre un servei civil amb senyals més robustes, com pot ser la L5. L'objectiu d'aquest treball és comparar els serveis oberts de posicionament de les constel·lacions de GPS i GALILEO, mitjançant l'anàlisi de les seves prestacions de precisió i integritat obtingudes d'una campanya d'observació, on les dades de referència a utilitzar són la xarxa d'estacions del IGS. La metodologia de posicionament a implementar és el post-processat d'observables de pseudo-rang mono-freqüència en manera estàtica. Per assolir aquest objectiu, l'esforç principal estarà enfocat en el desenvolupament d'una eina SW totalment configura-ble per l'usuari, que sigui capaç de processar els observables de pseudo-rang proporcionats pel marc de referència espacial que formen els satèl·lits de GPS i GALILEO, per posteriorment obtenir les posicions del receptor per mitjà d'un algoritme d'estimació per mínims quadrats. Els resultats que s'obtinguin d'aquest processament seran transmesos a altres eines d'anàlisi, les quals es desenvoluparan també en el marc d'aquest projecte, amb la finalitat de resumir i presentar de manera gràfica les prestacions obtingudes de la campanya. Finalment, amb el suport d'aquests resultats, s'exposaran les conclusions sobre l'acompliment i l'evolució dels serveis anteriorment comentats. Chapter 1: Introduction 1 Introduction The current document presents the memorandum of the Final Master's Degree Thesis in Geomatics and Geo-information belonging to the student Pablo Pinto Santos of the Superior Technical School in Geodesy, Cartography and Land Surveying Engineering (ETSIGCT) of the Polytechnic University of Valencia (UPV). The thesis has been mentored by Professor Ángel Esteban Martín Furones, belonging to the Department of Cartography, Geodesy and Photogrammetry Engineering of the UPV. The memorandum is divided in 8 chapters where each contains a major aspect e.g. methodology, analysis, references, conclusions etc. The chapters are not independent, but they maintain a relation. At the beginning of each chapter, a general contextualization will be detailed in order to enclose this work as a whole. This first chapter is devoted to introduce the master thesis conducted by the student, its scope/motivation and its main objectives to be achieved; as well as to provide a document outline which summarizes the project phases. 1.1 Thesis Scope This master thesis is under the scope of Geomatics engineering. Geomatics involves all the disciplines which deal with data subjected to be geo-referenced by applying new information technologies. It could be said that geo-positioning is the common feature which determines the quality of the geospatial information. In other words, location determination is at stake when enabling geo-information applications such as GIS, mapping or surveying data collection. Traditionally, coordinate determination was performed by land surveying techniques thanks to the local reference frames supported by the nations. However, with the raise of space exploration, other positioning methods were born. This is the case of Global Navigation Satellite Systems (GNSS) which provide global and continuous navigation services to the users. Nowadays, GNSS has practically replaced classical positioning methods and is the main technology used for geo-referencing data, either by direct methods i.e. GNSS surveying antenna; or by indirect means e.g. GNSS locates a sensor which gathers metric data. According to the master's disciplines, this master thesis will be focused in the Spatial Geodesy field. More specifically, Geodesy is the science which is devoted to determining the earth's shape and the position of its nearby objects. The "spatial" word is added for indicating that these purposes are achieved by space- based techniques. Currently, there are several spatial geodesy techniques but, GNSS is indisputably among the most relevant due to its application, economic and social outreach. GNSS State of the Art The GNSS field has suffered from an exponential growth in the last years. From technological solutions based on single-service and single-frequency (with intended civilian positioning degradation by the system e.g. GPS Anti-Spoofing), to the current multi-GNSS and multi-frequency implementations, thanks to the latest global systems i.e.: GALILEO and BEIDOU; and the modernization of the existing ones i.e.: GPS and GLONASS. Unquestionably, the tendency in the GNSS sector is focused on developing multi-GNSS/frequency products since they allow for higher accuracy services which, not only fulfill traditional professional applications, but they also have allocated their benefits in the mass market. For instance: driverless cars or augmented reality products (see GNSS User Technology Report: [BR.13]). On the professional side, non-absolute techniques such as Real Time Kinematic (RTK) are used for centimetric positioning, whilst absolute and real-time Precise Point Positioning (PPP) has increased and is the most sounded technology under the GNSS scientific research. On the mass market side, a division is observed. Sigle-Frequency combined with Standard Point Positioning (SPP) offers economical and energy low-cost advantages, meanwhile dual-frequency, plus multi-GNSS, plus sensor fusion implementation enables the highest accuracy but at a greater expense. Either way, both methods are proven to meet user accuracy requirements. However, the arise of security and safety standards which must be guaranteed in Safety of Life applications (SoL) still requires further work in order to accomplish other performances, mainly: integrity, continuity and availability. These performances may seem achievable on paper with simulations, but reality shows that very few experiments have been performed with real data scenarios. Under the pragmatic nature of the GNSS state of the art review, this thesis will be focused in assessing accuracy and integrity performances with real data, using mass-market single-frequency SPP, for both legacy and new

generation systems i.e. GPS and GALILEO. Besides, the individual performance assessment of each system is also an essential background in order to combine and produce multi-GNSS or multi-frequency solutions as it will be concluded. Academical Implications Moreover, and since this thesis is also framed under the termination of the aforementioned master's degree, it is expected that the student will demonstrate the knowledge and technical skills gained through this academic stage. The master is intended not only in expanding the geomatic fields but also in the student's ability to produce dedicated applications for their social, scientific and economic exploitation. Henceforth, across this memorandum the theoretical basis regarding the GNSS positioning techniques used will be settled. Then, the methodology for implementing the dedicated algorithms will be explained i.e. software developed tool. Afterwards, a practical analysis application using the exposed methodology will be carried out i.e. the positioning performance study campaign. And finally, the conclusions regarding all the work phases and the project as whole will be enumerated. Added Values In addition, it should be mentioned that this thesis is also devoted to present an open-source GNSS tool contribution to the user community (hence, the thesis subtitle). The tool's preliminary intention was to fulfill the needs for the analysis stage. However, its design was taken in advantage and adapted for a user- end usage. It is expected that this approach will add more value and transcendence to the work performed. As a final point, it is noteworthy to mention that the SW tool and many other features of this project are also due to the student's gained know-how of his professional experience in the GNSS technological sector. This has led to combine other skills producing better results and work methods, as it will be shown in the following pages of this work. 1.1 Thesis Purpose Having introduced the scope of this work, its purpose can be defined accordingly. For the sake of simplicity, this is divided in a sequence of main objectives. Each objective encloses a major work feature i.e.: methodology, analysis and synthesis of the master's degree aptitudes. The following three main objectives are listed: • Development of GNSS Software (SW) tools. The tools will be focusing on single-frequency SPP algorithms by means of processing GNSS pseudoranges measurements and navigation data in post- processing mode with the receiver being in static mode. • Positioning performance assessment of GPS Standard Positioning Service (SPS) and GALILEO Open Service (OS) with real data. The target performances to measure will be user- domain accuracy and integrity. • Demonstrate the knowledge and skills gained during the master's degree are properly applied. This will be illustrated emulating a professional application. The end-objective is to perform an individual and original work in order to present it in a university courtroom. The first two objectives are covered in dedicated thesis chapters: Chapter 2 and Chapter 3 respectively. The third objective is assessed in all the phases, from the writing of this introduction until the conclusion enumeration. Performance Specification Further performance specification is needed at this stage. GNSS, as any other technique, is not free of error. Several phenomena affect the uncertainty of the solution, as it will be explained in the theory framework (chapter 2). By now, it is enough to understand that GNSS positioning always involves an error which its magnitude varies randomly (at least in theory). Commonly, the performances measured in the user domain are related with the real positioning error. This is the case for accuracy and integrity: • Accuracy is the performance which provides the positioning error magnitude by taking advantage of the redundancy during the GNSS observation (more measurements than parameters to be estimated). • Integrity is the correctness or the trust which can be placed in the system position solution for being representative of the real error. Both performances are deeply explained in sections 2.6.1 and 2.6.2. The reader is encouraged to read these sections is he/she is not familiar with the terminology (especially for integrity performance). GPS-SPS and GALILEO-OS stipulate its system user domain requirements. This is done in its definition documents: GPS-SPS-PD [BR.18] and GALILEO-OS-SDD [BR.16]. These requirements are presented in Table 2.6 for GPS, and in Table 2.7 for GALILEO. Table 1.1 – Stipulated Positioning Error Requirements for GPS-SPS and GALILEO-OS. Single-Frequency SPP Service GPS-SPS and GALILEO-OS Coverage Global Accuracy (95%) Horizontal 7 m Vertical 11 m However, the student's academical experience has showed that these values are kept very conservative since better performances are usually obtained. Thus, a more optimistic criteria for this thesis will be set according to the student's judgement. The error requirements for both GPS-SPA and GALILEO- OS are presented in Table 1.1. Eventually, the conclusions will remark if these requirements are properly accomplished, and in case they are not, which shall be used. Complementary Objectives Last but not the least, it is important to highlight a complementary objective to keep in mind regarding the added value of creating an open-source SW tool. Preliminarily, the first alternative was not to develop any SW but to take advantage of the already available free-of-charge GNSS processing tools. However, these tools did not fit the thesis expectations. As a result, it was decided to develop a dedicated SW with the motivation of fulfilling the specific project needs. But thanks to the encouragement provided by the master's degree in developing geomatic applications, and following with the GNSS open-service approach, the SW tool adopted a user-end motivation. Therefore, a complementary objective regarding the SW development process was born during the thesis development. This objective can be defined as the developed SW shall be available as an open-source tool for any user willing to make use of it. It is important to keep this objective in mind since all the stages of the thesis will somehow prove that this is being accomplished, as it will be detailed in each chapter. 1.2 Document Outline As previously mentioned, the memorandum is divided in 8 chapters attending to the main thesis stages: • Chapter 1 encompass the thesis introduction. It explains broadly the scope, motivation, main objectives and provides the specification of the expected positioning performances for GPS and GALILEO systems. • Chapter 2 serves as the theoretical framework. GNSS systems and algorithms used for the methodology and analysis phases are detailed in order to support the developed solutions for this project. • Chapter 3 presents the methodology used for the thesis, i.e. developed SW tool. It emphasizes the followed lifecycle approach for its specification, implementation and validation; rather than being a deep source code explanation. • Chapter 4 is devoted to explain the project analysis stage. This is the campaign for assessing GPS and GALILEO positioning performances. The scope, data arrangement and its results are presented and commented in this chapter. • Chapter 5 enumerates the conclusions based on the thesis purposes. In addition, enhancements and planned evolutions regarding the developed SW tool are also included for future work lines. • Chapter 6 lists the acronyms used through the document. • Chapter 7 includes the references which encompass the bibliography and media links used for the thesis development. • Chapter 8 holds the annexes. More specifically: ? SW tool items such as source code repository, budget estimation and internal interface examples. ? Analysis Campaign items like results repository and selected stations world map. Chapter 2: Theory Framework 2 Theory Framework A Global Navigation Satellite System (GNSS) is defined as a system composed of a satellite constellation which enables a 3D navigation service anywhere in the globe. For committing this purpose, the satellites are constantly emitting signals, so dedicated GNSS receivers can acquire them and determine their position by solving a triangulation geometric problem

which involves the distances retrieved from the satellite's signals. The GNSS term can also be referred as all the different systems which provide global navigation services. The oldest and most known is U.S. Global Positioning System (GPS). But there are several others such as the Russian GLObal Navigation Satellite System (GLONASS), Europe's own system GALILEO or the Chinese system COMPASS/BEIDOU. The following sections of this chapter are devoted to explain the GNSS systems and positioning techniques for establishing the knowledge basis used through this work. Beware that if the reader is familiar with GNSS terminology, this chapter can be skipped. The rest of the chapters will usually refer to this framework, so the reader can review the theory concepts whenever needed. 2.1 GNSS Based Positioning For an intuitive approach on GNSS positioning, it shall be pointed that for any position determination two concepts must be defined: • Reference System. • Reference Frame. A reference system is a theoretical concept which establishes a universal reference by defining parameters, hypothesis and constants. In geodesy, a Terrestrial Reference System (TRS) is commonly defined as 3 perpendicular right-hand axes where their intersection is centered on the earth's center of masses and their movement is fixed relative to the earth' s rotation, denoting an ECEF (Earth Centered, Earth Fixed) reference system. In addition, approximate models of the earth are defined as part of the reference system as well. On the one hand a revolution ellipsoid is defined for a geometric approximation as shown in Figure 2.1. On the other hand, a Geoid is defined as a physical approximation since it represents a constant geopotential surface. Figure 2.1 – ECEF reference system definition and geodetic ellipsoid. Source: Sanz Subirana et al. 2013. The different TRS are defined with continuous GNSS observations and other geodesy techniques such as VLBI, SLR or gravitational measures. A reference system could be enough to determine the three coordinates of any point: X, Y and Z; which are the perpendicular distances to the axes (or geodetic coordinates: latitude φ, longitude λ and ellipsoidal height h). However, in a practical sense is hard to achieve such thing, since the reference system is just a theoretical definition and not a physical materialization. Therefore, a reference frame which provides reference coordinates is needed, so any other point can be placed on the reference system by observing this frame. Classically, the reference frames were a network of monuments build up on the earth's surface (see Figure 2.2). These points were defined with very precise coordinates by astronomical observations and network adjustments, meaning that fair precision could only be achieved locally and not globally. With the rise of space exploration in the 1970's and the launch of satellites orbiting the earth, a new reference frame concept is borne, and this is the primary characterization of a GNSS: the satellite constellation acts as the reference frame. Figure 2.2 – Geodetic monument and geodetic network example. Source: Wikipedia.org. So, satellite coordinates are known, and any user can measure the distance to the satellites in order to triangulate its position. Unfortunately, this is a complex matter because: • A precise ranging satellite-user determination of at-least 3 satellites is essential. • A precise method is needed for knowing the satellite coordinates at any time, since they are moving relative to the earth at a high speed (approximately 5 km/s). The satellite's signal is intended to solve these issues. The signal is an electromagnetic wave that is being generated by an atomic clock onboard the satellites. The signal is allocated on the L band of the microwave spectrum with a nominal frequency of 10.23 MHz. This also allows to modulate information onto the signal itself. The information transmitted by the GNSS signals is the navigation message (the so-called ephemerids) which contain the Keplerian parameters, so the satellite coordinates can be computed by applying orbital mechanics. GNSS users make use of receivers in order to decode the information transmitted by the signal. In addition, the signal travels at the speed of light, thus the travel time among the satellites and the user is directly derived into a range measurement for the receiver. This enables a precise notion of the reference frame and the range measurements to it. However, the signal transmission time requires a very precise timing system. Note that the signal travels at the speed of light (299800 km/h), meaning that an ambiguity of 10-5 seconds is translated into an uncertainty of 300 meters in the position solution. As previously mentioned, satellites are equipped with high precision atomic clocks. These clocks rely on the frequency needed for transitioning energy levels in the atoms of a stable element such as Hydrogen. Nevertheless, for a fair timing synchronization, user receivers should be equipped with atomic clock as well. But this is not cost-effective. Instead, the receivers use quartz clocks, which are much cheaper, and take advantage of observing an additional satellite in order to estimate the offset among the receiver's clock and the reference time system defined by the constellation. This leads to have at least 4 satellites in view as shown in Figure 2.3 in order to obtain a position solution. This constraint is essential for the constellation design as it will be specified in section 2.2.1. Figure 2.3 – Minimum GNSS satellite configuration for positioning. Source: mobacommunity.com Summing up, the GNSS basic positioning principles have been covered by an intuitive approach. The following key points are highlighted: • For any positioning method a reference system and a reference frame need to be precisely defined. • For GNSS positioning, the satellite constellation defines the reference frame. • Satellite coordinates are precisely determined thanks to the orbital information broadcasted in the signal. • In addition, the signal's time of travel is used as the primary range measurement, but this needs high timing accuracy. • Precise timing is achieved by the atomic clocks onboard the satellites which in addition generate the signal. • GNSS receivers can estimate its position X, Y, Z and its receiver clock offset by observing at least four satellites. No to mention that GNSS positioning is far more complex when achieving metric precision. But this will be issued in the upcoming sections of this chapter. 2.2 GNSS Architecture A GNSS is primarily composed of the satellite constellation, the space segment and their broadcasted signals, but this is not enough for maintaining a reliable and continuous service. A GNSS generally consist of two more segments: the control (or ground) segment and the user segment. 2. 2 .1 Space Segment As previously mentioned, the GNSS space segment is the satellite constellation composed of the different Space Vehicles (SV). The main goal of the SV is to transmit the signals and to store and broadcast their navigation message uplinked from the control segment. In addition, the constellation must ensure that at least 4 satellites are in view from anywhere on the earth to maintain global coverage. GNSS SV are placed in Medium Earth Orbit (MEO) at about 20000 km over the earth. They have an approximate revolution period of 12 hours, meaning that a SV is in view two times per sidereal day. Their inclination over the equator's plane oscillates among 60º and 50º, and their orbits are nearly circular. With this orbital configuration, a GNSS constellation needs of at least 21 satellites for ensuring global coverage, although it is common for systems to maintain more than 24 satellites which are used as backup SV. Figure 2.4 – GNSS satellite constellation. Source: Navipedia.net. SV by themselves are complex engineering pieces and have various mechanisms which allow them to be in orbit, communicate with the control segment and broadcast their signals. Nevertheless, their most critical component is the atomic clock which is the signal generator and precise time instrument. As pointed in section 2.1, these clocks are made of a stable element such as Rubidium, Cesium or Hydrogen. 2.2.2 Signal in Space Atomic clocks onboard the SV, generate the Signal In Space

(SIS) service. This is done by inducing atomic jumps in the stable element which generates an electromagnetic wave with a very precise nominal frequency. This frequency is allocated in the L band of the microwave spectrum. As all the electromagnetic waves, the signal travels at the speed of light in the void. The SIS is just an energy propagation and does not provide any information. However, the signal can be easily modulated in order to carry the SV's navigation message and ranging code. Consequently, the main signal components are: • Carrier wave is defined as the wave which "carries" the information. • Ranging code is also referred as the Pseudo-Random Noise (PRN) which is a sequence of zeros and ones for the receiver to determine the travel time of the signal. • Navigation data is the binary coded message which contains the orbital parameters of the SV, its clock corrections, almanacs and other useful information. The Ranging code and navigation data are modulated over the carrier wave with a lower frequency rate. This creates a certain bandwidth which is used for multiplexing the signal and take advantage of broadcasting different data at the same time. There are three types of modulation based on the wave property to vary as shown in Figure 2.5: • Amplitude Modulation (AM) • Frequency Modulation (FM) • Phase Modulation (PM) The common way for modulating GNSS SIS is the phase modulation. Except for GLONASS, which uses frequency modulation. Figure 2.5 – Carrier wave modulation methods. Source: Hoffman et al. 2008. 2.2. 3 Control Segment The control segment is comprised of the facilities, systems and operators which are constantly monitoring the space segment. It is also referred as the ground segment and its main objectives are: • Control SV health status and configuration. • Compute, predict and validate the SV ephemeris (navigation message). Maintain the time reference with the SV's clocks and ground atomic clocks. • Uplink the ephemerids to each SV. • Resolve SV anomalies. Usually control segments are composed of master control centers and remote tracking stations but the architecture differs on each system (GPS, GALILEO…). For more information about ground control segments, refer to [BR.1] or [BR.2]. 2.2.4 User Segment The user segment encompasses all the GNSS receivers which provide positioning and accurate timing. This is achieved by receiving the carrier signal and demodulating its information, so they can estimate the pseudoranges (and other observables) and compute the SV position, to finally determine the user position by solving navigation equations. Nowadays there is a wide variety of GNSS receivers which can range from complex surveying antennas with up to 400 channels, to minimalistic receivers which are usually allocated on smartphones and watches. In any case a GNSS receiver is composed of: • • • Antenna with preamplification. Radio frequency section. Micro-processor and memory data for storage. • An intermediate-precision oscillator e.g. quartz clock. 2.3 GNSS Systems It was early mentioned that GNSS can also be referred as the different systems which deliver navigation services. At the issue date of this document, the fully operational and autonomous systems are the U.S. GPS and the Russian GLONASS. There are several others in development, such as the Chinese system BEIDOU or Europe's own system GALILEO, which are expected to reach their Full Operational Capability (FOC) phase in the upcoming years. In addition, GNSS also englobes the Space Based Augmentation Services (SBAS) such as U.S Wide Area Augmentation System (WAAS) and the European Navigation Overlay System (EGNOS). Although these systems do not provide an autonomous and global positioning service but enhance precision and integrity broadcasting wide area corrections. The following sections describe the GNSS segments and services used for this master thesis purpose i.e. GPS and GALILEO. For other GNSS specifications such as GLONASS, BEIDOU or SBAS, refer to [BR.1]. 2.3.1 GPS "The NAVSTAR Global Positioning System (GPS) is an all-weather, space based navigation system under development by the Department of Defense (DoD) to satisfy the requirements for the military forces to accurately determine their position, velocity, and time in a common reference system, anywhere on or near the earth on a continuous basis" (Hoffman et al 2008, [BR.2]). "Since the DoD is the initiator of GPS, the primary goals were military ones. But the US Congress, with guidance from the President, directed the DoD to promote its civil use […]. However, the real impact of the originally military GPS occurred in 1983, when the US President offered free civilian access after the incident of the Korean Airlines Flight 007" (Hoffman et al. 2008, [BR.2]). Furthermore, On May of 2000, U.S president Bill Clinton announced the de-activation of Selective-Availability (S/A), a feature that was causing a positioning precision degradation of ten times. GPS program was started in the 1960's and after several tests, the Initial Operational Capability (IOC) was announced in 1993 when 24 SV were available for navigation. Later, on 1995, FOC was declared after validating the systems for military performances. GPS Space Segment NAVSTAR (Navigation System With Ranging and Timing) is the GPS satellite constellation. NAVSTAR is arranged with 24 SV slots divided in 6 orbital planes with 55º of inclination at an approximate altitude of 20200km with an eccentricity of 0.02. NAVSTAR satellites are divided into different blocks based on the time they were launched and its evolutions: • Block I was formed by 11 development satellites launched between 1978 and 1985. • Block II and IIA were formed by 28 operational satellites launched from 1989 and some of them are still operating nowadays. • Block IIR, IIR-M and IIF were formed by replacement operational satellites. "Block IIR satellites are capable of autonomously determining their orbits and generating their own navigation messages" (Sanz Subirana et al. 2013, [BR.1]). Block IIR-M included some modernizations such as new military code and a more robust civilian signals (L2C and L5). • Block III will be formed by future satellites which will include enhancements such as interoperability with other GNSS and jamming protection. This block will broadcast the fourth civilian signal (L1C). GPS Services and Signals GPS has a SIS legacy service which is based on two carrier waves in the L band denoted as L1 and L2. They both are derived from a nominal frequency of 10.23MHz: $L1 = 154\ r\ 10.23\ LAr = 1575.420\ LAr\ L2 = 120\ r\ 10.23\ LAr = 1227.600\ LAr$ On these two carrier waves, two codes and one navigation message are modulated using Binary Shift Keying Technique (BPSK): • Coarse/Acquisition (C/A) code has a chipping rate of 1. 023 Mbps which is translated in on a chip length of 293.1 m. C/A code is only modulated over L1 and purposely omitted from L2 in order to deny full precision to civilian users. • Precise Code (P) is dedicated to military means and other authorized users. Its chipping rate is 10 Mbps (chip width of 29.31 m). Unlike C/A, P code is modulated over both carrier waves, L1 and L2, thus enabling military receivers to take advantage of dual-frequency solutions. • Navigation message: is modulated on L1 and L2 as well, carrying the SV ephemerids as specified in section 2.2.2. The main legacy services provided by GPS are derived from the aforementioned codes: • Standard Positioning Service (SPS) is based on C/A code which is only provided on L1. Is open service and free of charge. Although S/A was applied in C/A, it was completely removed on 2008 and it will not be included in the next GPS evolutions. • Precise Positioning Service (PPS) provides a more precise service than SPS with P code modulated over L1 and L2. P code is subjected to Anti-Spoofing, resulting in the Y code, in order to restrict system availability to nonmilitary users. Additionally, GPS has a service modernization which includes new civilian and an additional military signal (the M code). L2C is open use and was introduced in block IIR-M. The code is modulated using BPSK on L2 carrier and broadcasted at a higher power, "making reception easier under trees and even indoors" (Saenz Subirana

et al. 2013, [BR.1]). • L5C is open service and was introduced in block IIF. This signal is provided onto the new carrier frequency, the L5 (1173.45 MHz = 115 x 10.23 MHz), and has a modulation that meets Safety of Life (SoL) requirements, a better multipath performance and robustness against interferences. • L1C will enter service with block III. It will be open service and its main purpose is to provide interoperability with other GNSS such as GALILEO and to improve positioning in urban areas thanks to its MBOC modulation. Figure 2.6 depicts GPS signal spectra meanwhile Table 2.1 provides a technical summary of the mentioned services. Figure 2.6 – GPS signal spectra allocation before and after modernization. Source: Sanz Subirana et al. 2013. Table 2.1 – GPS signal service specifications. Link Carrier Freq. [MHz] Code Modulation Code Rate [Mcps] Data Rate [bps] Service C/A P BPSK 1. 023 10.23 50 50 Civil Military L1 1575.420 M BOC 5.115 N/A Military L2 1227.600 L1C-I data L1C-Q pilot P L2C M MBOC BPSK BOC 1.023 10.23 1.023 50 - 50 25 N/A Civil Military Civil Military L5 1176 .450 L5-I data L5-Q pilot BPSK 1.023 50 - Civil 2.3.2 GALILEO In the 1980's the European Union understood the economic, social and technologic importance of satellite-based navigation. On 1999, they started to develop its own and independent GNSS called GALILEO. Unlike GPS, GALILEO's primary premise is to be civil-use oriented and it will ensure interoperability with other GNSS: "In its paper concerning the involvement of Europe in a new generation of satellite navigation service, the European Commission (1999) recommended Galileo to be an open, global system, fully compatible with GPS but independent from it. The key parameters of Galileo have been identified to be the independence of any other system while maintaining interoperability, global availability, and high level of service reliability, thus implementing integrity information." (Hoffman et al. 2008, [BR.2]). The main reasons for European Union countries to start its own GNSS rely on GPS (and other systems) lack of compliance with the following requirements: • Other GNSS do not satisfy aviation standards for accuracy, integrity and continuity. • GPS and GLONASS are under military control and their availability can be trimmed in case of conflict. • They do not provide a legal guarantee nor a legal frame in case of a system failure. GALILEO system is still under development by the European Space Agency (ESA) and managed through the European Commission (EC). Nonetheless, GALILEO is not the only European satellite-navigation project. As mentioned earlier, EGNOS is the European SBAS which was developed in the frame of GALILEO and has acted as its cornerstone. EGNOS's is nowadays operative and it will be a key system in the future for providing maximum integrity to airborne users along with GALILEO. It is noteworthy to point out that GALILEO is a promising system to the GNSS ecosystem. On the one hand, each satellite is equipped with two maser hydrogen passive atomic clocks, with better long-term and short-term stability, which provide a better accuracy and timing than other GNSS. On the other hand, GALILEO will have the capability of transmitting real-time integrity information. This is achieved by broadcasting maximum error in the SIS domain: SISE (Signal In Space Error). GALILEO Space Segment The GALILEO constellation in FOC, will consist in 27 SV allocated on MEO (23 222 km), arranged in 3 orbital planes with 56º of inclination and with an orbit eccentricity of 0.002. The satellites will have a period of 14 hours, repeating their geometry every 10 days. "This constellation guarantees, under nominal operation, a maximum of six satellites in view from any point on the Earth's surface at any time, with an elevation above the horizon of more than 10º" (Sanz Subirana et al. 2013, [BR.1]). In addition, "this satellite disposition will ensure a better coverage in northern latitudes" (Berné Valero et al. 2014, [BR.5]). The GALILEO space segment has been evolving as specified in the following milestones: • Experimental Phase. Two experimental SV were launched between 2005 and 2008: GIOVE-A and GIOVE-B (GIOVE stands for GALILEO In Orbit Validation). They served several purposes such as: ensuring GALILEO frequency fillings, validate the technologies to be used in the operational SV and develop user equipment. • In Orbit Validation Phase. Four more SV were launched (2 on October 2011 and other 2 on October 2012) for qualifying the control and user segments through validation tests and operations. These four satellites were allocated in the first and second orbital planes and were the first operational GALILEO SV. • Full Operational Capability Phase. On the issue date of this document, there are 26 GALILEO SV in orbit: 22 of them marked as USABLE and the other 4 mark as NOT USABLE for testing or maintenance reasons. Consequently, FOC is unlikely to be reached as expected by 2020, although is viable to be declared in the upcoming years with 30 SV (27 operational plus 3 backup). GALILEO Services and Signals "Europe has chosen a service-oriented approach for the design of GALILEO" (Hoffman et al. 2008, [BR.2]). GALILEO will transmit 10 navigation signals in the same frequency bands as GPS, denoted: E1, E5a, E5b and E6. The signals were designed to serve the different services which are based in a variety of needs: • Open Service (OS). It is free of charge to users worldwide and it is provided by three different signals (E1, E5a and E5b). Is the equivalent to GPS's SPS as "Single-frequency receivers will provide similar performances as GPS C/A" (Sanz Subirana et al. 2013, [BR.1]). • Public Regulated Service (PRS). This service is provided with two signals and two navigation messages, which allows for higher continuity performance and introduces robustness against jamming and spoofing. However, it is only available to security authorities e.g.: police or military, with a controlled access and under governmental control. • Commercial Service (CS). It is reserved for commercial purposes. It is broadcasted with two additional signals protected with encryption and two higher rate navigation messages. • Search and Rescue Service (SAR). This service complements the COSPAS-SARSAT rescue service by adding an up-link signal in order to inform users that its emergency situation has been notified. • Safety of Life Service (SoL). The service is already offered by EGNOS to airborne users which require critical safety standards. On FOC, GALILEO will improve this service along with the future versions of EGNOS. These services are provided through 4 dedicated signals: • E1 is allocated on the E1 (homologous of L1) band and supports the OS, PRS, CS and SoL with three signal components: ? E1-A is dedicated to PRS and hence is encrypted. ? E1-B is open service and stands for the data channel which contains unencrypted integrity information and encrypted commercial data. ? E1-C is the pilot or data less of the open service component. • E6 is encrypted in the E6 band and dedicated exclusively to the CS and PRS. As E1 signal, it is composed of three components: ? E6-A is only accessible to PRS users. ? E6-B is the data channel for the CS. The higher E6 data rate (500 bps) allows for the modulation additional commercial information. ? E6-C is the pilot channel for the CS broadcasting the ranging code. • E5a is allocated on the E5 band (homologous of L5) and only supports GALILEO's OS. The signal allows basic navigation and timing. It is composed of: ? E5a-I, the data channel which includes navigation data. ? E5a-Q, the pilot channel which encompass unencrypted ranging code. • E5b, like E5a, is allocated on the E5 band. However, it supports SoL and CS besides of OS. It is also comprised of two components: ? E5b-I, the data channel, includes unencrypted integrity data and encrypted commercial information. ? E5b-Q, the pilot channel, includes ranging code available to all users. An additional signal can be created as a result of combining E5a and E5b using the Alternate Binary Offset Carrier (AltBOC) modulation technique. The resulting signal is denoted as E5 and can be processed as a whole with a proper user implementation. This signal is encouraging for many applications since it has proved, at least with

simulated data, a very enhanced positioning accuracy with low multi-path and tracking noise performances (see [BR.7]). Figure 2.7 depicts the GALILEO's signal spectra and Table 2.2 summarizes the signal specification and supported services. Figure 2.7 – GALILEO signal spectra allocation. Source: San Subirana et al. 2013. Table 2.2 – GALILEO signal service specifications. Band Carrier Freq. [MHz] Channel E1-A data Modulatio n BOC Code Rate [Mcps] 2.5575 Data Rate [bps] N/A Service PRS E1 1575.420 E1-B data E1-C pilot MBOC 1.023 125 - OS, CS, SoL E6 1278.750 E6- A data E6- B data E6 -C pilot BOC BPSK 5. 115 N/A 500 - PRS CS E5a 1176.450 E5a-I data E5a-Q pilot BPSK 10. 23 25 - OS E5b 1207.140 E5b-I data E5b-Q pilot BPSK 10. 23 125 - OS, CS, SoL 2.4 GNSS Reference Frames GNSS positioning relies on the accurate definition of the spatial reference frame formed by the satellite constellation and the synchronization against the time scale. In the following sections, the theory regarding the time and coordinates frames will be exposed and detailed for GPS and GALILEO systems. 2.4.1 Time Scales Time scales have been always defined upon periodic cycles. Therefore, the first systems used natural phenomena as the earth's rotation or celestial mechanics in order to stablish time frames. These are known as Universal Time (UT) and Sidereal Time. Both use the earth's rotation as a reference, UT sets the reference against the Sun and the Sidereal Time against the Aries Point (vernal equinox). However, these references are not uniform and accurate enough for achieving high synchronization demands. As technology evolved, more accurate time frames could be defined. International Atomic Time (TAI) was introduced and it is based on the transitions between atomic energy levels. TAI and UT accumulate drift over time. Eventually, Universal Time Coordinated (UTC) was defined in order to be aligned within a certain margin from UT. UTC is based on an atomic reference composed of 250 Caesium and Hydrogen clocks distributed in 65 laboratories around the world. The following relations between TAI, UTC and UT are met: $LAA = LLA + 1r \times m$; (2.1) $LLA = LL + cLL$; $|cLL| < 0.9r$ (2.2) As deduced from equation (2.1), UTC is maintained from TAI plus a number of leap seconds denoted as m. The number of leap seconds is not constant and is provided periodically by the International Earth Rotation and Reference System Service (IERS); e.g. 1 Jan 1999 n = 32 seconds. Equation (2.2), points that UT and UTC realizations are kept within 0.9 seconds. GPS Time Simplified as GPST, is a continuous atomic time scale with no leap seconds. GPST is constantly maintained by the GPS control segment by means of its atomic clocks onboard the GPS SV and those on the ground segment. The GPST's origin started at 0 hours UTC, January the 6th of 1980, meaning that at that time GPST = 0 seconds. Since the number of leap seconds at GPST's origin was 19 seconds, the following relation among UTC and GPST can be deduced: $ALLL - LLA = m - 19r$; (2.3) GALILEO Time Like GPST, GALILEO System Time (GST) is a continuous time scale based on the atomic references from the GALILEO's space and ground segments. In addition, GST is kept synchronized with TAI below 50ns. GST origin was set at 0 hours UTC August the 22th of 1999. 2.4.2 Spatial Reference Systems As explained in section 2.1, the usual reference system used for framing a GNSS navigation solution is a TRS, also referred as an ECEF. More specifically, and as showed at the beginning of this chapter in Figure 2.1, the TRS: • Has its origin on the Earth's center of masses. • Its Z-axis is aligned with the Earth's rotation movement as defined by the Conventional Terrestial Pole. • Its X-axis is aligned with the intersection among the equatorial plane and the Greenwich meridian (perpendicular to the Z-axis) • Its Y-axis is right hand perpendicularly defined against the Z and X axes. The international definition of the TRS is known as the International Reference System (ITRS). Along the mentioned TRS characteristics, ITRS's ellipsoid is the GRS80 model (Geocentric Reference System 1980). ITRS realization is the International Terrestrial Reference Frame (ITRF), a set of ground stations around the globe which its coordinates are precisely and periodically determined by spatial geodesy techniques such as VLBI, SLR or GNSS. These realizations are denoted as ITRFyy, where yy stands for the last two-year digits of the data used to determine the solution. Usually, GNSS reference systems and frames tend to be closely aligned with ITRS and ITRF respectively. GPS Reference System Since NAVSTAR origins, GPS has used its own World Geodetic System, the so-called WGS-84, developed by the U.S. DoD. Its initial implementation was derived from a set of observations from first GPS satellites (Transit SV). However, further WGS-84 refinements have used ITRF solutions like ITRF92 and ITRF94. WGS-84 uses its own ellipsoid definition. Since WGS-84 was defined as GPS reference system: "GPS broadcast ephemerids are linked to the position of the satellite antenna phase center in the WGS84 reference frame. Thus, the user's receiver coordinates will be expressed in the same ECEF frame." (Sanz Subirana et al. 2013, [BR .1]). GALILEO Reference System The GALILEO Terrestial Reference Frame (GTRF) was established by the GALILEO Geodetic Service Provider (GGSP). Its first realization was produced from GPS observation since it was needed for the GALILEO satellite IOV phase. Consequently, future GTRF versions will use both GALILEO and GPS measurements. Like GPS system, the user coordinates will be provided against GTRF if GALILEO ephemerids are used. GTRF is required to be maintained against ITRF with no more than 3 cm of difference. Therefore, the difference among GTRF, WGS84 or ITRF are not significant for applications which require metric precision: "For navigation purposes and most user requirements, the agreement between ITRF, GTRF, and WGS-84 is sufficient and no coordinate transformations have to be applied. For geosciences, surveying, and other high-accuracy applications, an appropriate transformation has to be applied." (Hoffman et al. 2008, [BR.2]). 2.5 GNSS Standard Point Positioning The GNSS single-frequency pseudorange positioning method, commonly referred as Standard Point Positioning (SPP), has been intuitionally introduced in section 2.1. However, this technique requires several modelling techniques since there are a lot of error sources affecting the positioning accuracy such as atmospheric disturbance, instrumental delays, clock synchronization or satellite orbits uncertainty determination among the most relevant. In the upcoming subsections, a more detailed explanation of the techniques concerning pseudorange positioning will be covered. In addition, algorithms used in this project will be detailed. Note that the subsections were written for GPS and GALILEO systems. For other GNSS and further processing techniques, refer to the bibliography references: [BR.4], [BR.6] or [BR.3]. 2.5.1 Geometric Range Modelling GNSS signal contains a ranging code pseudo-randomly generated which is referred as the PRN. This is just a bit sequence different for each operational SV. Recalling section 2.2.2, the primary GNSS raw measurement is the signal' s time of transmission between the SV's antenna and the receiver' s antenna, denoted as ΔL. This observation is obtained by correlating the PRN broadcasted by the SV and the replica generated in the receiver. The maximum correlation peak is the observed ΔL as shown in Figure 2 .8. Figure 2 .8 – PRN correlation among SV and Receiver. Source: Sanz Subirana et al. 2013. If ΔL is multiplied by the signal's speed propagation, the speed of light (c = 299792458 m/r), the pseudorange (L) is obtained as shown in the following equation: $LRRRcc = c \times \Delta L$; (2.4) The pseudorange is the apparent range between the SV and the receiver. Nonetheless, this range is critically affected by several error sources. The most significant is the disagreement among satellite's time scale rRR, receiver's time scale $rRcc$ and the time reference scale L (e.g. GPST). The pseudorange obtained from a ranging code L (e.g. GPS C/A) at a given carrier frequency c (e.g. GPS L1) can be expressed accounting for the

different time scales as: $LRe = c \times (LRcc(rr) - LRR(rc))$; (2.5) Where rr is the pseudorange reception time expressed in the receiver' s time scale and rc is the pseudorange emission time expressed in the SV's time scale. Referring this expression to the reference time scale L, equation (2.6) is adopted: $LRe = \pi + c \times (\delta RRec - \delta RRV)$; (2.6) π denotes the actual range between the SV and the receiver. $\delta RRec$ and δRRV denote respectively the receiver and satellite clock offsets (or clock biases) against the time reference scale L. Common SPP algorithms, compute from satellite ephemerids the SV's clock bias and estimate the receiver's clock bias along with its position solution. The following most significant error sources in the pseudorange measurements account for signal's propagation though the atmosphere. In GNSS, the atmospheric errors are split in two types: • Ionosphere delay. This delay occurs at approximately 350 km over the earth's surface caused by the Total Electron Content (TEC) re-distribution on the upper atmosphere due to the ionization by several phenomena like Sun's rays. This is translated in a positive delay on the pseudorange directly related to the signal's carrier frequency (dispersive medium). This delay can vary between 5 m and even 30 m, but fortunately, most of it can be easily modelled with deterministic algorithms for single- frequency GNSS users. • Troposphere delay. This delay occurs at approximately 60 km from the earth's surface. It is mainly caused by the temperature, pressure and water vapor variations in the first layers of the atmosphere and usually split in the hydrostatic and wet components. Unlike Ionosphere delay, the troposphere delay is a non-dispersive medium and cannot be related to any of the signal' s properties. This causes troposphere effect to be difficultly estimated. Nevertheless, 90% of the delay comes from the hydrostatic component which causes an approximate positive delay of 10 m in the positioning solution. Dedicated algorithms used in this project for ionosphere and troposphere delays are detailed in section 2.5.3. Ionosphere delay, troposphere delay and other error sources affecting the range observation (δR) can be added to equation (2.6) resulting in the basic pseudorange expression: $LRe = \pi + c \times (\delta RRec - \delta RRV) + \Delta iRlell + \Delta rrll + \delta R$; (2.7) Equation (2.7) shows the best possible range observation between the SV and the receiver. Therefore, this equation will be combined, with at least other four equations, in order to estimate the receiver's position by an algorithm which minimizes the positioning error i.e. the Least Squares (LSQ) method. This will be mathematically assessed in section 2.5.4. Several other error sources can be added to this expression such as instrumental delays or multipath effects. However, for metric precision, which is achieved in SPP, the pointed error sources are enough, and the rest affect fewer to have a significant impact on positioning performances. Nonetheless, further information about pseudorange measurement modelling can be consulted in [BR.1]. 2.5.2 Satellite Orbit and Clock Modelling Recalling section 2.2.1, SV constitute the reference frame of a GNSS solution and therefore their coordinates must be precisely estimated for an accurate positioning service. Orbital and satellite's clock correction parameters are transmitted in the navigation message. The orbital parameters are the Keplerian elements derived from classical orbital mechanics. According to Newton's theory, the movement between two bodies can be defined by their gravity attractive forces: $A(m1 + m2)\, r\ddot{} + r3 \times r = 0$; (2.8) Where r is the relative position vector, m terms denote the two object masses and A is the universal gravity constant ($A = 6.674 \times 10{-}11\ NKlc22$). The satellite's orbit can be expressed as follows by integrating equation (2.8): $r(r) = r(r0, W, c, i, \Omega, \omega, \tau)$; (2.9) Arguments: r, W, c, i, Ω, ω, τ are the Keplerian elements illustrated in Figure 2.9. More specifically: • Ω is the ascending node, the geocentric angle between the ascending node direction and the Aries point direction. • i is the inclination of the orbit against the equatorial plane. • ω is the perigee's argument, which is the angle between the ascending node and perigee directions measured along the orbital plane. • W is the orbit's semi-major axis. • c is the orbit eccentricity, the ratio between its semi-major axis and semi-minor axis. • $r0$ is the perigee passing time, when the satellite is closest to the earth. Figure 2.9 – SV Orbital Parameters (Keplerian Elements). Source: San Subirana et al. 2013. The orbital position of a satellite can be obtained at any epoch (r), using the so-called orbital anomalies (see Figure 2.10): • True Anomaly $\boldsymbol{V(r)}$ is the geocentric angle between the perigee direction and the satellite direction. • Eccentric Anomaly $\boldsymbol{E(r)}$ is the angle among the perigee and an imaginary point obtained from drawing a line which is normal to the major axis and crosses through the satellite, intersecting a circle with W radius. • Mean Anomaly $\boldsymbol{M(\ r)}$ is a mathematical abstraction related to mean angular motion (areolar velocity). For satellite's clock correction, the ephemerids provide this information with three coefficients ($W0$, $W1$, $W2$), modelling a second-degree polynomial at a given reference epoch. This reference epoch is denoted as Time Of Ephemerids (ToE), which is transmitted in the ephemerids as well. Therefore, for computing the satellite's clock correction at any epoch r, the following expression shall be applied: $rc = W0 + W1(r - LmA) + W2(r - LmA)2$; (2.10) Figure 2.10 – Orbital Anomalies. Source: Sanz Subirana et al. 2013. Satellite Position and Clock Correction at Emission Time Table 2.3, shows the Keplerian elements and the satellite clock parameters broadcasted in the navigation message of any GPS or GALILEO SV. Table 2.3 – Navigation message. Broadcasted parameters. Parameter $\boldsymbol{TnE\ a0\ a0\ a0\ \sqrt{a}\ e\ \Delta n\ M0\ \omega\ i0\ \Omega0\ i\ \Omega\ Crc, Crr\ Crc, Crr\ Cic, Cir}$ Definition Satellite Clock Parameters Time of ephemerids. Reference epoch in seconds within the week (ToW format). SV clock offset against system's reference time scale (e.g. GPST) SV clock rate SV clock drift rate Orbital Parameters Square root of the semi-major axis Orbital plane eccentricity Mean motion difference Mean anomaly at ToE Argument of perigee SV inclination at ToE Longitude of the ascending node at the beginning of the week Rate of inclination Rate of node's right ascension Cosine and sine Latitude argument corrections Cosine and sine orbital radius corrections Cosine and sine inclination correction In order to compute the SV coordinates using the broadcast ephemerids, the following algorithm based on GAL-OS-SIS-ICD/2016 ([BR.17]) and IS-GPS-200J/2018 ([BR.15]) is presented. "An accuracy of about 5 m (RMS) is achieved for GPS satellites with S/A off" (Sanz Subirana et al. 2013, [BR.1]). 1. Solve by two iterations the emission time rc , by applying the following expression: $rc{=}rr{-}(c){-}\ rc{-}LmA$; L 2. Where rr is the reception time by the receiver in ToW format, L is the SV-Receiver pseudorange measurement, c denotes the speed of light and rc stands for SV's clock correction. rc is set to 0 in the first iteration and is computed by applying equation (2.10), where $rc = r - LmA$. In addition, Emission time (computed in ToW format) must be protected against interpolation jumps by applying: $rc = rc - 604800r$; $ic\ rc > 302400r$; $rc = rc + 604800r$; $ic\ rc < -302400r$; 3. Having computed the time parameters, the satellite's coordinates are computed from the Keplerian elements. Firstly, compute SV's orbit mean motion parameter: $m{=}\ \sqrt{}\ {+}\Delta l$; $\lambda\ W$ 4. Where $\lambda = 3.986004418 \times 1014$, is the geocentric gravitational constant. The mean anomaly is found as: $L = L0 + m \times rc$; 5. Eccentric anomaly can be iteratively computed (e.g. 10 iterations), where $A = L$,in the first iteration: $A = L + c \times \sin(A)$; (2.11) (2.12) (2.13) (2.14) (2.15) 6. And true anomaly is: $\sqrt{}1{-}\ c2{\times}\sin(A)\ r = \text{atan}(\ \cos(A) - c\ )$; (2.16) 7. The argument of latitude is found as: 8. The orbital correction terms are computed as follows: $\phi 0 = r + r$; (2.17) $\delta r = Arr \times \sin(2\phi 0) + Arc * \cos(2\phi 0)$; $\delta r = Arr \times \sin(2\phi 0) + Arc * \cos(2\phi 0)$; (2.18) $\delta i = Air \times \sin(2\phi 0) + Aic * \cos(2\phi 0)$; 9. Argument of latitude, orbit radius and inclination are corrected by the following expressions: $\phi = \phi 0 + \delta r$; $r = W\ (1 - c \times \cos(\ A)) + \delta r$; $i = i0$

+ δi + $\dot{i}$ × rc; 10. The corrected longitude of the ascending node along the orbital plane parameters are defined: $\Omega = \Omega 0 + (\Omega - \Omega c) \times rc - \Omega c \times LmA$; $rll = r \times \cos(\phi)$; $rll = r \times \sin(\phi)$; 11. Where Ωc = 7.2921151467 × 10−5 is the earth's angular speed (earth's rotation speed). Finally, satellite ECEF coordinates are obtained as: $WrXr = rll - \cos(\Omega) - rll \times \cos(i) \times \sin(\Omega)$; $WrXr = rll - \sin(\Omega) - rll \times \cos(i) \times \cos(\Omega)$; $WrXr = rll \times \sin(i)$; 12. Last but not the least, two additional corrections are necessary in order to obtain SV's clock bias. The first one stands for the relativistic effect correction. The second one should only be applied to single-frequency users and accounts for the group delay: $\delta RRV = rc + \Delta Rrcl - \Delta Bc2B$; $\sqrt{\lambda} \times W\ c2\ c1\ 2\ c1\ \Delta Rrcl = -2 \times c2 \times c \times \sin(A)$; $\Delta BB = (c2) \times \Delta BB$; Where $c1$ is the Spatial filtering of the light beam with a layered silver flat lens", Proceedings of SPIE, 2008.">carrier frequency for Spatial filtering of the light beam with a layered silver flat lens", Proceedings of SPIE, 2008.">the signal which Spatial filtering of the light beam with a layered silver flat lens", Proceedings of SPIE, 2008.">the group delay is broadcasted and $c2$ the Spatial filtering of the light beam with a layered silver flat lens", Proceedings of SPIE, 2008.">carrier frequency for Spatial filtering of the light beam with a layered silver flat lens", Proceedings of SPIE, 2008.">the signal which Spatial filtering of the light beam with a layered silver flat lens", Proceedings of SPIE, 2008.">the group delay correction is computed. GPS broadcast its group delay in the navigation message for L1 carrier frequency. GALILEO, with OS navigation data, broadcast the group delay for E1-E5a and E1-E5b frequency combinations (refer to [BR.17]). (2.19) (2.20) (2.21) (2.22) Satellite Position at Reception Time The previous method has introduced the algorithm for computing the SV coordinates at the time when the satellite's antenna produces the signal. However, for the user is not useful to have these coordinates at emission time but at reception time because it is a common reference for all other SV measurement. Therefore, SV coordinates must be propagated at reception time knowing the signal transmission time. Moreover, the coordinates are tied to an ECEF frame (fixed to earth's rotation). Thus, the SV coordinate propagation will be translated in a rotation over the Z axis which lasts as much as the signal transmission time. The following algorithm retrieved from Sanz Subirana et al. 2013 ([BR.1]) is presented for this work: 1. SV ECEF coordinates are provided at emission time as: $WcRR\ rcRR = (WcRR\ )$; $WcRR$ 2. In addition, an approximate receiver position must be provided in order to compute the transmission time: $W0Rec\ r0Rec = (\ W0Rec\ )$; $W0Rec$ 3. Compute the signal's transmission time using a geometric approach (no pseudorange measurement is needed): $\Delta LRRcRc = \| rcRR - r0\ Rec \| \ c$; 4. Propagate the earth fixed SV coordinates at emission time (rc) to reception time (rr) using the transmission time. Firstly, compute the earth's rotation angle lapsed during the transmission time: $\theta rrer = \Delta LRRcRc \times \Omega c$; 5. Where Ωc = 7.2921151467 × 10−5 is the earth's angular speed. Finally, apply a Z- axis rotation matrix with $\theta rrer$ over the SV coordinates at emission time: $WrRR\ \cos(\theta rrer)\ \sin(\theta rrer)\ rrRR = LX(\theta rrer) \cdot rcRR = (WrRR\ )$; $LX(\theta rrer) = (-\sin(\theta rrer)\ \cos(\theta rrer)\ WrRR\ 0\ 0\ 0\ 0)$; 1 (2.23) (2.24) (2.25) (2.26) (2.27) 2.5.3 Atmospheric Effects Modelling As previously explained, atmospheric effects on GNSS positioning are divided in two major components, the Ionosphere delay and the Troposphere delay. Is not the intention of this project to present a detailed explanation of this phenomena on GNSS measurements but to present the algorithms used to mitigate them. In order to find out more about Ionosphere and Troposphere effects, please refer to the following references: [BR.1] and [BR.5]. Several ionosphere and troposphere models for error estimation are developed in the GNSS bibliography for single-frequency users. Ionosphere models usually rely on the provision of ionosphere coefficients for modelling the delay. The coefficients are used to estimate the Slant TEC contained in the SV -Receiver Line Of Sight (LoS) and then mapped to Vertical TEC in the receiver's zenith. These coefficients are provided through the navigation messages. Both GPS and GALILEO broadcast their own ionosphere coefficients. Nominally, GPS coefficients are used in the Klobuchar model and GALILEO coefficients in the NeQuick model. • Klobuchar Model. This model was dedicated for GPS receivers and assumes that the highest TEC is located at an altitude of 350 km and it presents a daily periodicity with a maximum peak at midday and a lowest peak at midnight. The highest amplitude is represented as a cosine function of the geo- magnetic latitude and the GPS α and α coefficients; modelled by a third-degree polynomial function as illustrated in Figure 2.11. "Klobuchar's model does not remove completely the ionosphere delay and several authors point that the model compensates for the 60% to 70% during night time and 70% and 90% during day time" (Berné Valero et al. 2014, [BR.5]). • NeQuick Model. This model was dedicated for GALILEO single-frequency receivers using the broadcasted GALILEO ionosphere coefficients in the navigation message. NeQuick is far more complex than Klobuchar's model, but more accurate in return. NeQuick is based on the numerical integration of the TEC in the signal's propagation along the LoS, based on the local time and the solar activity in the receiver's latitude. The detailed NeQuick algorithm is completely described in [BR.14]. Figure 2.11 – World Ionosphere delay map extracted from TEC measurements and Klobuchar's model ionosphere amplitude modelling. Source: Sanz Subirana et al. 2013. Troposphere delay relies on the angle in which the signal is received respect the user's horizon, (satellite elevation). Then, the slant delay is mapped in the zenithal direction of the receiver position. Troposphere delay also depends on the receiver's altitude and weather parameters. These weather parameters are normally modelled, since it is difficult to derive them from ground measurements. The most used models are Hopfield and Saastamoinen: • Hopfield Model. This model was developed using experimental data obtained from long-term observations on the troposphere. The model splits the root cause of the delay in two components: a wet component and a dry one. Dry component can be easily derived from dry gas laws meanwhile wet component is much more difficult to model. • Saastamoinen Model. This model establishes that the delay can be derived from the gas laws. The empiric formulae require the atmospheric pressure, the water vapor content and the temperature as inputs. Saastamoinen model provides the functions to estimate these three parameters based on the user's height. Moreover, a mapping function is introduced for a more refined model which depends on the height and the SV elevation. For this project, Klobuchar and Saastamoinen models have been used for estimating the ionosphere and troposphere delay on the developed single-frequency positioning solution. The algorithms for both models are presented hereafter. Klobuchar Ionosphere Model Klobuchar's model for estimating ionosphere delay of a specific signal L carried in the frequency c, needs the following inputs: • $\alpha 0$, $\alpha 1$, $\alpha 2$ and $\alpha 3$: ionosphere coefficients retrieved from GPS navigation message. • $\alpha 0$, $\alpha 1$, $\alpha 2$ and $\alpha 3$: ionosphere coefficients retrieved from GPS navigation message. • φRcc and λRcc : approximate receiver geodetic coordinates both in semicircles (1 semicircle = π radians). • $ArRRRcc$ and $ArRRRcc$: the SV-Receiver elevation over the receiver's horizon in semicircles and azimuth in radians. • rr: epoch seconds within GPS time of week. The following algorithm has been extracted from [LR.1]: 1. Calculate the Earth-center angle: $0.0137\ \psi = ArRRcRc + 0.11 - 0.22$; (2.28) 2. Compute the latitude and longitude of the Ionospheric Pierce Point (IPP): $\phi i = \varphi Rcc + \psi \times \cos(ArRRRcc)$; $\phi i = \{-00..441166;;\ iicc\ \phi\phi ii >< 0-.041.4616$; $\psi \times \sin(ArRRcRc)$ (2.29) $\lambda i = \lambda Rcc + \cos(\phi i)$; 3. Find the geomagnetic latitude of the IPP: $\phi l = \phi i + 0.064 \times \cos(\lambda i - 1.617)$; 4. Find the local

time at the IPP: (2.30) $rBPP$ = 43200 × λi + rr; $rBPP$ = {$rBPPrBP$−P 8+6480604;00ic; irc≥r 8<64000 ; (2.31) 5. Compute the ionosphere delay amplitude, period and phase: 3 Ai = ∑ αl × ϕll ; Ai = 0 ic Ai < 0; l=0 3 (2.32) Li = ∑ αl × ϕll ; Li = 72000 ic Li < 72000; l=0 2π × (r − 50400) Wi = Li ; 6. Compute the slant factor: A = 1 + 16 × (0.53 − $ArRRRcc$)3; 7. Compute the ionosphere time delay and transform it to meters: Δ $Rilel1l$= { [5 × 10 −9 + Ai × (1 − Wi2 $W24i$4 2 +)] × A; ic |Wi| ≤ 1.57 ; Δ$Rilel1l$[m] = Δ$iRlel1l$[r] ∗ c; 5 × 10−9 × A; ic |Wi| < 1.57 8. Finally, ionosphere delay is given on frequency c1 (i.e. GPS L1). Transformation between the target carrier frequency c = c2 is given by: 2 Δ $Rilel2l$= (c1) × Δ Re1 c $illl$; 2 (2.33) (2.34) (2.35) Saastamoinen Troposphere Model The following algorithm has been retrieved from Moreno Monge 2011 ([BR.9]). Saastamoinen's troposphere model only needs as inputs the approximate receiver's height and the SV-Receiver zenital angle: • $hRcc$: approximate receiver height in kilometers. • $WcRRRcc$: the SV-Receiver zenital angle respect to the receiver's zenith in radians. In addition, Table 2.4 gives the interpolation table for the height dependent B mapping parameter to be applied in the model's basic correction. The saastamoinen delay is computed as follows: 0.002277 1255 Δ$rrll$ = cos($WcRRRcc$) ×[m+(L + 0.05) × crl − A × tan2($WcRRcRc$)] + cL; Where L stands for temperature in Kelvin degrees, m denotes pressure in millibars, crl is the partial pressure of water vapor, A is interpolated from Table 2.4 based on the input height and cL shall be extracted from Table 5.5 of Hoffman et.al 2008 ([BR.2]). L, m and crl are found as: • m = 1013.25 × (1 − 0.000065 × $hRcc$)5.225; • L = 291.15 − 0.0065 × $hRcc$; • A = 50 × c−0.0006396×$hRec$; • crl = (A × 0.01) × c−37.2465+0.213166−(0.000256908×R2); Table 2.4 – Saastamoinen B mapping parameter interpolation table. Height (km) B (mb) 0.0 1.156 (2.36) (2.37) 0.5 1.079 1.0 1.006 1.5 0.938 2.0 0.874 2.5 0.813 3.0 0.757 4.0 0.654 5.0 0.563 2.5.4 Least Squares Estimation for Standard Point Positioning The aim of single-frequency code based- based point positioning, hereafter SPP, is to determine the receiver ECEF coordinates: (W, W, W)Rcc and its clock bias: $\delta RRec$. Recalling section 2.1, this involves a triangulation geometric problem involving at least four SV in view with known coordinates (computed from the broadcasted ephemerids as specified in section 2.5.2): (W, W, W)RRi and the pseudoranges retrieved from them: $LRRRRcic$. Linear Equation System Since the pseudoranges are noisy, the corrections must account for several error sources as postulated in equation (2.7). π is the actual range between the SV and the receiver expressed as: π $RRRcci$ = √($WRRi$ − $WRcc$)2 + ($WRRi$ − $WRcc$)2 + ($WRRi$ − $WRcc$)2; (2.38) This induces a non-linear system whose actual resolution is based on linearizing (2.38) from an approximate position of the receiver: (W0, W0, W0)Rcc. The approximate SV-Receiver range is denoted as $m0RRRcic$. From the arrangement of equation (2.7) the following one is derived: $LRRRRcic$ − $ARRRcci$ ≅ $\pi RRRcci$ + c × $\delta RRec$; (2.39) Where $ARRcRci$ = c × $\delta RRVi$ + Δ$Rilell$ + Δ$rrll$; and the linearization of (2.38) introducing $m0RRRcci$ gives: π $RRRcci$ = $m0RRRcic$ $W0Remc$0−$RRRcWicRRi$ + $W0Rec$ − $WRRi$ $W0Rec$ − $WRRi$ cr + m0 $RRRcci$ cr + m0 $RRRcic$ cr; (2.40) With cr = $WRcc$ − $W0Rec$, cr = $WRcc$ − $W0Rec$ and cr = $WRcc$ − $W0Rec$. And substituting (2.40) in (2.39), finally gives: $LRRRRcic$ − $ARRcRci$ − $m0RRRcic$ $W0Remc$0−$RRRcWicRRi$ = $W0Rec$ − $WRRi$ $W0Rec$ − $WRRi$ cr + $m0RRRcic$ cr + RRi cr c × δRec; (2.41) $m0Rcc$ Which is the desired linear expression of equation (2.39). Equation (2.41) can be expressed in matrix notation with m observed satellites as: $W0Rec$ − WRR1 $W0Rec$ − WRR1 $W0Rec$ − WRR1 ($LRRRRc$1c − $ARRcR$1c − $m0RRRc$1c ⋯ $LRRRRcnc$ − $ARRRcnc$ − $m0RRRcnc$)= $m0RRRc$1c $W0Rec$ − $WRRn$ $W0Rec$ − $WRRn$ $W0Rec$ − $WRRn$ ⋯ $m0RRRc$1c ⋯ $m0RRRc$1c ⋯ ($m0RRRcnc$ $m0RRRcnc$ $m0RRRcnc$ c cr (cr cr); (2.42) c $c\delta R$ Rec) Once cr, cr, cr and $c\delta RRec$are obtained, the receiver position is obtained along with its clock bias $\delta RRec$: $WRcc$ $W0Rec$ cr ($WRcc$ $W0Rec$ cr $WRcc$) = $W0Rec$ + (cr) ; (2.43) $\delta RRec$ (δ0$RRec$) $c\delta RRec$ This procedure could be done iteratively on each epoch, thus having a more precise approximate position on each iteration. This will improve the final receiver solution till a certain threshold is accomplished or a maximum number of iterations is reached. "In a GNSS static observation a fair estimation has converged in the third iteration. More than 4 or 5 iterations induce the risk of losing statistical reliability." (Berné Valero et al. 2014, [BR.5]). Weighted Least Squares Estimation The equation system presented in (2.42) with 4 SV (m = 4), will define a compatible system where only one possible parameter solution could be computed. However, this is not the optimal case since more SV pseudorange observations will provide redundancy to the solution. Furthermore, previous linear models have been presented neglecting the measurement residuals encompassed in δR from equation (2.7). In the case of m = 4, the solution could not give any accuracy estimation and no positioning performances could be assessed. Consequently, the minimum SPP case is when m ≥ 5, creating a un-determined compatible system, where the best solution possible is the one which minimizes δR (the observation residuals). This scenario leads to adopt a Least Squares method. More specifically, a Weighted Least Squares method (WLSQ) since the pseudorange measurement quality vary as function of the SV elevation. Several bibliography references deeply explain the WLSQ algorithm. However, a brief introduction is presented hereafter based on Berné Valero et al. 2014 ([BR.5]), using its mathematical notation: • The WLSQ algorithm is evolved from the one developed by Gauss-Makarov. This enumerates the following assumptions: - Stochastic model: the observations, for this issue the pseudoranges, follow a normal distribution free of systematic errors. Where LR denotes the observations and r02 the a priori variance estimator, typically set as 1: L∼L(LR, r02); - Functional model: establishes the mathematical relations between the observations and the parameters to be retrieved: A(W, A) = 0; • W are the parameters to be estimated through WLSQ and A the corrected observations. Following with the LSQ definition: W = WX + cW; A = LR + r; • From the previous expression it can be pointed, firstly, that the parameters are expressed as the sum of the approximate parameters (WX) plus the estimated parameter corrections (cW). Secondly, the corrected observations are expressed as the sum of the raw observation (LR) plus its associated residual (r). • Expressing equation (2.45) as a linear system: ∂A ∂A A(W, A) = A(WX, LR) + ∂W cW + ∂A cA = 0; - A(WX, LR) is denoted as the independent term vector: W. - ∂B is denoted as the parameter design matrix: A. ∂X - ∂B ∂B is denoted as the observation design matrix: A. - cA = r is the vector containing the observation residuals. • The residual vector accomplishes a normal distribution with 0 mean and a theoretical variance (r2): r ∼L(0, r02L); L = L−1; • L stands for the cofactor matrix, L the weight matrix which details the expected variance of the observations. • Equation (2. 47) can be expressed in matrix notation as: A(W, A) = AW + Ar − W = 0; • This model solution implies the WLSQ basic assumption of minimizing the residuals: Ω = $rRLr$ = $mimimrm$; Master's Degree in Geomatics and Geo-information: Final Master Thesis - Pablo Pinto Santos (2.44) (2.45) (2.46) (2.47) (2.48) (2.49) (2.50) Now that WLSQ has been introduced, the algorithm will be specified for the GNSS SPP case exposed at the beginning: • By taking the indirect observation reduction (A = −A), expression (2.49) is equivalent to equation (2.42) adding the observations residuals (r = δR): - W = AW − r; - W =($LRRRRc$1c − $ARRRc$1c − $m0$ RR1 ⋯ Rcc $LRRRRcnc$ − $ARRcRnc$ − $m0RRRcnc$); $X0Rec$ −XRV1 $X0Rec$ −XRV1 $X0Rec$ −XRV1 - A= $l0$ $RRVec$1 ⋯ $l0$ $RRVec$1 ⋯ $l0$ $RRVec$1 ⋯ $X0Rec$ −X RVn $X0Rec$−$XRVn$ $X0Rec$−$XRVn$ ($l0$ $RRVecn$ $l0RRVenc$ $l0RRVenc$ cr - W=(cr cr) ; $c\delta RRec$ δR1 - r = ( ); … δRl • • • • c ; c) For the weight matrix (L), the diagonal terms are arranged according to the following expression extracted from Moreno

Monge 2011 ([BR.9]). Ar is the satellite observation elevation and cR is the expected mean error of signal L. This allows for a better fit when processing different GNSS signals: Li = sin2($ArRRcRci$) $cR2$; If the minimum condition (2.50) is applied to the system in (2.51), the following expression is obtained: (AR $\cdot L\cdot A)\cdot r = AR \cdot L\cdot W$; The steps to reach the aforementioned expression are detailed in Berné Valero et al. 2014 ([BR.5]). Specified for our SPP case, of 4 parameters (m = 4) to be estimated and m SV retrieved pseudoranges, the matrixes are dimensioned as: - A [m × 4] , holding the design terms for each observation and parameter: e.g. $X0Rec-XRVi$ $l0Rec$ RVi - W [4 × 1], holding the parameters to be estimated: cr, cr , cr and $c\delta RRec$ (2.51) (2.52) (2.53) - W [m × 1], holding the independent terms: LR $RRRc1c - ARRcR1c - m0$ $RR1$ Rcc - r [m × 1], holding the residuals for each SV observed pseudorange: $\delta R1$ - L [m × m], holding the weights of each observation: $LRRi$ = 21 σRVi • From expression (2.53), the parameter solution, the residual vector, the ex-post covariance matrix (σrr) and ex-post variance estimator ($\sigma 02$) can be deduced: - $W = (AR \cdot L \cdot A)-1 \cdot L \cdot W$; - $L = (AR \cdot L \cdot A)-1$; - $r = A \cdot W - W$; - $\sigma 02 = rlR-Plr$; m = 4; - $\sigma rr = \sigma 02 \times L$; (2.54) (2.55) (2.56) (2.57) (2.58) Finally, equations (2.54) to (2.58) shall be applied in every observation epoch r. Consequently, the position parameters and its associated errors can be postulated as: • $W(r)Rcc = [W0Rec + cr](r) \pm \sigma(r)r \rightarrow 68\%$; • $W(r)Rcc = [W0Rec + cr](r) \pm \sigma(r)r \rightarrow 68\%$; • $W(r)Rcc = [W0Rec + cr](r) \pm \sigma(r)r \rightarrow 68\%$; (2.59) • $\delta(r)RRcc = [\delta 0RRec + c\delta RRcc](r) \pm \sigma(r)\delta RRec \rightarrow 68\%$ Note that sigma parameters σr, σr, σr and $\sigma\delta R$ are extracted from square-rooting the diagonal elements in σrr. Since these uncertainties follow a normal distribution, the sigma values will be representative in the 68% of the cases when a new measurement is done over the population. This is the also the area covered by ± 1 × σ as shown in Figure 2.12. If more reliability is needed, sigma values shall be multiplied by a scaling factor e.g. ± 3 × σ for a 99.7%. Figure 2.12 – Gaussian distribution area covered by sigma critical values. Source: Wikipedia.org. Furthermore, since the priori variance estimator was set to 1 ($r02$ = 1), the ex-post value shall be close to it ($\sigma 02 \cong 1$) for a good-natured WLSQ estimation: • If $\sigma 02 > 1$, the actual errors are greater than those postulated in L (weight terms). • If $\sigma 02 < 1$, the actual errors are smaller than those postulated in L (weight terms). • If $\sigma 02 \gg 1$, this is an indicator of a bad-fitted estimation. Most likely root causes for this behavior are: ? Bad error source mitigation (systematic errors not removed). ? Bad a-priori variance observation estimation. ? Wrong functional model. 2.5.5 Receiver Position Solution and Precision So far, GNSS positions have been referred to an ECEF frame with three coordinates: W , W and W . However, from a user's perspective this is not intuitive because is hard for him to determine where the positioning error is located. Therefore, it is more proper to express the receiver position in a local reference system centered on a reference position close to the user. Easting ci , Northing mi and Upping ri are the new components (hereafter denoted as ENU) which stand for the local increment of the receiver position solution (Wi , Wi , Wi) → (φi , λi , hi) and its reference (WR , WR , WR) → (φR , λR , hR) . The method for transforming among ECEF and ENU coordinates is by applying a rotation matrix $LBBBNBRB$ over the user's geodetic position (φ, λ): $-\sin(\varphi)$ $-\sin(\varphi$ $)\cos(\lambda)$ $\cos(\varphi)\cos(\lambda)$ $LBBBB(\varphi,\lambda)=($ $\cos(\lambda)$ $-\sin(\varphi)\sin(\lambda)$ $\cos(\varphi)\sin(\lambda));$ (2.60) 0 $\cos(\varphi)$ rim (φ) In order to obtain the ENU increments against the reference on the receiver solution, the following formula shall be applied: ci (mi) = $LBBBNBRB(\varphi R, \lambda R) \cdot (Wi - WR)$; $Wi - WR$ (2.61) ri $Wi - WR$ Note that expression (2.61) could be applied on the accuracy indicators, the sigma parameters estimated on equation (2.59), in order to translate them in the ENU frame: (σli) = $LBBBNBRB(\varphi i, \lambda i) \cdot (\sigma Xi)$; σci σXi (2.62) σri σXi The sigma values obtained from WSLQ solution on equation (2.59) and those on equation (2.62), can be adopted in order to obtain the following precision indicators: • $\sigma B = \sqrt{\sigma X2i + \sigma X2i + \sigma X2i} + c \times \sigma\delta 2Rec$; • $\sigma P = \sqrt{\sigma X2i + \sigma X2i + \sigma X2i} = \sqrt{\sigma c2i + \sigma l2i + \sigma r2i}$; (2.63) (2.64) • $\sigma R = \sqrt{c} \times \sigma\delta 2Rec$; • $\sigma B = \sqrt{\sigma c2i + \sigma l2i}$; • $\sigma R = \sqrt{\sigma r2i}$; (2.65) (2.66) (2.67) Respectively, these terms denote the geometric, position, time, horizontal and vertical accuracies at 1 sigma level (reliability of 68%). As previously specified, the most significant precision indicators from a user perspective are σB, σR and sometimes σR along with its ENU components ci, mi and ri. 2.6 GNSS Positioning Performances The services provided by GNSS are usually assessed through navigation or positioning performances which measure the service's quality in a certain aspect, commonly based on the service's provided overall accuracy. However, the growth of GNSS applications in several demanding fields has caused new performances to be defined. This is the case for maritime and civil aviation fields where an unwarned large solution error can seriously increase the risk of an accident possibly causing injuries, large economic losses or even deaths. Furthermore, aviation users for instance, require the system to ensure fair performances during a large period of time with no interruption e.g. in the approach to landing phase. Consequently, and in addition to accuracy performance, integrity, continuity and availability performances are introduced: • Accuracy (or Precision) is the error bound provided by the system's algorithms for the estimated position at a given epoch. The precision is a statistical value meaning that the navigation or position solution must have enough redundancy to provide this information fairly. • Integrity is the reliability which can be placed on the system's solution. In the positioning paradigm, integrity measures if the position accuracy is representative of the actual error. Integrity is also referred as the probability of a system to provide misleading solutions e.g. phenomena which can lead to aircraft accidents. • Continuity is the system's ability to perform under a certain accuracy and integrity without interruption. It is measured as the probability in which the system performances will be maintained for the duration of an operation. • Availability: is the percentage of time in which the system accomplishes accuracy, integrity and continuity performances. It also represents the probability of finding a system to be available for a certain time period. In the following subsections a deeper explanation about accuracy and integrity concepts related to GNSS positioning is done along with the specifications on these for both GPS-SPS and GALILEO-OS. On the one hand, continuity will be out of the scope of this project since it is more related with real time systems rather than post-processing ones. On the other hand, availability will not be strictly defined in this work. In return, availability will denote the percentage of time in which stipulated GPS and GALILEO precision does not over-bound the user's required accuracy. 2.6.1 GNSS Positioning Accuracy Performance In GNSS, the measured accuracy stands for the uncertainty on the parameter estimation provided by a redundant system solution. The obtained accuracy is highly dependent on the following terms: • Statistical nature of the measurement errors. As explained in equation (2.48) , these errors should follow a white noise patter (random gaussian distribution) with 0 mean and expected $r02L$ variance. • Satellite geometry. This is a critical effect which can cause a bad precision performance as intuitively show in Figure 2.13, where a bad geometric arrangement can lead to a wider positioning error. The SV geometry is usually denoted as Dilution Of Precission (DOP). In most of the cases, a GNSS observation with more than 8 SV is more than enough for ensuring a good DOP whereas an observation with 5 SV is potentially dangerous of having a weaker geometry. Eventually, a fair SV geometry will depend on the SV disposition over the user's sky at the observation epoch. The more the SV are uniformly spread, the better for the accuracy performance as illustrated in Figure 2.14. The satellite geometry issue is also the cause of why

the GNSS navigation solutions account for a higher error in the vertical domain than in the horizontal, since a better vertical solution will involve SV to be located beneath the ground. As adopted in section 2.5.5, equation (2.64) to (2.67), present the accuracy parameters from the user's perspective in the horizontal and vertical components. These sigma values are given for 1 sigma of reliance level, meaning that in the case of the vertical component, the accuracy is reliable at the 68%, but for the horizontal component this will be the 39% of the cases, since it is a two-dimension measurement. This percentage is the statistical probability, or the area covered by the gaussian distribution at $\pm 1\sigma$ critical values as it was shown in Figure 2.12. In order to have a higher reliability, horizontal and vertical sigma components shall be multiplied by a scale factor to cover a higher area (probability) on the normal distribution. Table 2.5 presents these scale factors for the of one-dimension and two-dimension distributions. For instance, to obtain an accuracy performance on both vertical and horizontal components with the 95% of reliability, their sigma values should be multiplied by 1.96 and 2.45 respectively. Figure 2.13 – Geometry range disposition affecting the solution precision. Source: Sanz Subirana et al. 2013. Figure 2.14 – Left: poor SV geometry configuration. Right: a much better SV geometry configuration. Source: Trimble GNSS Planner. Finally, a fine numerical indicator for the accuracy performance obtained through m observation epochs is the so-called Root Mean Squared (RMS) trace. Accuracy RMS can be computed for both horizontal and vertical components as well as for the 3D position component from ENU sigma parameters: • (2.68) $LLLR = \sqrt{l1}\ \sum li{=}1\ \sigma r2i = \sqrt{l1}\ \sum li{=}1\ \sigma R2$; • (2.69) $LLLB = \sqrt{l1}\ \sum li{=}1(\sigma c2i + \sigma l2i) = \sqrt{1l}\ \sum li{=}1\ \sigma B2$; • $LLLP = \sqrt{l1}\ \sum li{=}1(\sigma c2i + \sigma l2i + \sigma r2i) = \sqrt{l1}\ \sum li{=}1\ \sigma P2$; (2.70) Table 2.5 – Sigma scale factors for gaussian distributions. Scale Factor Probability (%) for 1-D Probability (%) for 2-D 1 68.3 39.3 1.96 95.00 TBD 2.00 95.40 86.50 2.45 98.57 95.00 3.00 99.70 98.90 GPS and GALILEO Accuracy Requirements Table 2.6 displays the accuracy requirements for GPS SPS, using SPP techniques with C/A signal. The values based on the 95% of probability level and extracted from Hoffman et al. 2013. The values presented are very conservative since they are assuming the worst-case positioning scenario. "Furthermore, the SPS performance is usually much better than the specification. "Conley et al. (2006: p. 362) mention average values for a 20-site network of 7.1m horizontal error and 11.4m vertical error but stress the large number of possible GPS receiver configurations and integrations and the various environmental conditions" (Hoffman et al 2008, [BR.2]). In contrast, some other authors set other accuracy values (Kelly 2006): 8 and 60 meters on the horizontal and vertical components respectively for 95% of probability. For any other concerns regarding GPS SPS accuracy performance, please refer to [BR.1]. Table 2.6 – GPS Standard Positioning Service accuracy requirements. Satellite-Only Service GPS Standard Positioning Service Coverage Global Accuracy (95%) for single-frequency SPP Horizontal 13m Vertical 22m Timing accuracy (95%) 40ns For GALILEO system, Table 2.7 shows the Open Service accuracy performances obtained with E1 signal. The accuracy requirements have been extracted as well from Hoffman et al. 2008 ([BR.2]). "Since always the worst-case situation is considered, the service availability has to be considered the critical parameter in the performance definition […]. Galileo single-frequency receivers will provide a performance comparable to GPS C/A-code receivers." (Hoffman et al. 2008, [BR.2]). Refer to this reference for the exact definition of this parameters for GALILEO system. Table 2.7 – GALILEO Open Service accuracy requirements. Satellite-Only Service GALILEO Open Service Coverage Global Accuracy (95%) for single-frequency SPP Horizontal 15m/24m Vertical 35m Timing accuracy (95%) 30ns 2.6.2 GNSS Positioning Integrity Performance Under the scope of GNSS positioning, "Integrity is the measure of the trust that can be placed in the correctness of the information supplied by a navigation system" (Navipedia, [LR.2]). Some real time GNSS like SBAS are able broadcast their own integrity messages by providing alarms to users whenever the system is not suitable for navigation. This requires an Alert Limit (AL) definition. For the GNSS static positioning case, integrity compliance can be measured by having the receiver's reference coordinates so the actual error can be determined and compared with the solution's accuracy. If the accuracy (also called Protection Limit) over-bounds the AL threshold, the system shall warn the user, hence providing integrity. Note that the tradeoff between the AL definition and the nominal accuracy is essential to define a system which accomplishes integrity performance. Several scenarios can raise among different integrity phenomena. Firstly, true negative and false positives integrity events can occur, being the second ones the most feared. These are also known as Misleading Information events. Meanwhile, true negative phenomena will only flag the system as not available and thus losing availability performance on the way. In order to illustrate these concepts, Figure 2.15 shows the integrity events for the vertical component through time and Figure 2.16 presents the same for the horizontal component on 4 different situations. Summing up, the following integrity events can be defined: • Misleading Information (MI) events occur when the system's accuracy is passed by the actual position error, but this is kept within AL. • Hazardous Misleading Information (HMI) events occur when the AL is exceeded without the system being able to notice this to the user. In other words, system's accuracy is below the AL but not the position error. • System Availability (SA) is flagged as valid whenever the accuracy is within the AL and vice-versa. As a conclusion, ideal cases will occur whenever the actual positioning error is covered by the system's accuracy, providing fair SA. The worst-case scenario would be when a high number of HMI events are taken place. As an advance for the integrity assessment on this work, horizontal and vertical AL (HAL and VAL) can be placed by adopting the required system's accuracy performances (e.g. Table 2.6 for GPS case and Table 2.7 for GALILEO case). Consequently, and if the reference receiver coordinates are known, the percentage of MI, HMI and SA epochs could be computed through an observation campaign. Finally, note that if the assumed statistical nature of the measurement errors is met, the measured SA should be very similar to the gaussian reliance level stipulated. For instance, if GPS horizontal accuracy is 13 meters at the 95%, SA shall be close to 95% for a reliable solution estimation. Figure 2.15 – Integrity events on vertical domain. Source: Figure 2.16 – Integrity events on horizontal domain. Navipedia.net. Source: Navipedia.net GPS and GALILEO Integrity Requirements On the one hand, GPS does not provide integrity performance requirements, at least on its SPS. On the other hand, one the reasons that brought GALILEO to be developed was the provision of integrity against the legacy GNSS. Unfortunately, at the time being, the integrity GALILEO service is being redefined and therefore no integrity requirements can be stipulated for its OS. Nonetheless, integrity on GNSS solutions can be measured and relatively compared between different services. 2.7 GNSS Data Formats Even though it has been discussed the necessary data for GNSS SPP single frequency algorithms, it has not been pointed yet in which format this information can be provided. Real time pseudoranges and navigation data are transmitted through the SV's signal, and with the proper receiver implementation, they can be decoded. Eventually, the receiver stores the data with the manufacturer's format. However, under the scope of this project, since several data sources from different receivers will be treated; it is imperative for the GNSS data to be receiver independent. In addition, the analysis study will be done in post-processing mode, meaning that no real-time implementations are needed. In this context the RINEX

(Receiver INdependent Exchange) format is introduced. The RINEX format was originally designed by the University of Bern for a better exchange of GPS data during the first large European Reference Frame (EUREF 89) realization. This was assessed with a plain text (or ASCCI) structured file which gathered the pseudoranges and carrier frequency observations related to a common timestamp (observation epoch). Due to the useful nature of this format, RINEX evolutions were translated in several file types which enclose different GNSS information as follows: • Observation file contains all the GNSS measurements sources (not only pseudoranges but carrier phase or doppler) referred to the epochs in which the receiver has observed them. • Navigation file gathers the broadcasted ephemerids data as transmitted by the SV navigation channel. They can also contain useful information like coefficients for ionosphere modelling. • Meteorological file contains the station's atmospheric data like pressure, temperature or relative humidity. In addition to the aforementioned types, several other spin-off standards are based on RINEX concept as well, such as SINEX (station precise coordinate information), IONEX (ionosphere accurate data) or SP3 (SV precise position). Legacy RINEX encompass version 1 and version 2. Version 2 has been widely used and many SW products only accept this format. However, a more modern RINEX version 3 is available and enables several benefits like a better signal source identification and the enhanced use of the latest GNSS like GALILEO. The RINEX data exchange versatility is also based on a name convention format. Tough RINEX files can be named without this convention, it is highly recommended. This is especially relevant in RINEX version 3 in order to access useful information, like RINEX file type, source constellation, receiver marker name, etc. The naming convention is deeply explained in RINEX documents [BR.8]. Since RINEX are plain text based format (.rnx extension for RINEX version 3), large observation files can occupy high portions of disk space. Thus, it is usual to encounter RINEX files compressed in Hatanaka format, denoting CRINEX files (.crx extension). The decompression of this format can be done straight forward with the binaries provided by Yuri Hatanaka in [LR.3]. In general terms RINEX files are arranged in a file header and a file body. They both are fixed structured form, meaning that no length dependents fields are allowed. This enables RINEX parsers to take advantage of template reading formats. Examples of observation and navigation RINEX files are presented in the hereafter file extracts. Further information about RINEX standard can be consulted in [BR.8]. • RINEX V3 Observation file extract: 3.02 OBSERVATION DATA M (MIXED) RINEX VERSION / TYPE NetR9 5. 22 Receiver Operator 20190115 000000 UTC COMMENT gfzrnx-1.05-6775 HEADER EDIT 20190116 012648 UTC PGM / RUN BY / DATE YEBE MARKER NAME 13420M001 MARKER NUMBER GEODETIC MARKER TYPE Area de Geodesia Instituto Geografico Nacional OBSERVER / AGENCY 5536R50061 TRIMBLE NETR9 5. 22 REC # / TYPE / VERS 0180418 TRM29659.00 NONE ANT # / TYPE 4848724.9050 -261632.4930 4123093.9010 APPROX POSITION XYZ 0.0000 0.0000 0.0000 ANTENNA: DELTA H/E/N G 12 C1C L1C S1C C2W L2W S2W C2L L2L S2L C5X L5X S5X SYS / # / OBS TYPES R 12 C1C L1C S1C C1P L1P S1P C2C L2C S2C C2P L2P S2P SYS / # / OBS TYPES 30.000 INTERVAL 2019 1 15 0 0 0.0000000 GPS TIME OF FIRST OBS G L2X -0.25000 SYS / PHASE SHIFT R L1P 0.25000 SYS / PHASE SHIFT R L2C -0.25000 SYS / PHASE SHIFT DBHZ SIGNAL STRENGTH UNIT 24 R01 1 R02 -4 R03 5 R04 6 R05 1 R06 -4 R07 5 R08 6 GLONASS SLOT / FRQ # R09 -2 R10 -7 R11 0 R12 -1 R13 -2 R14 -7 R15 0 R16 -1 GLONASS SLOT / FRQ # R17 4 R18 -3 R19 3 R20 2 R21 4 R22 -3 R23 3 R24 2 GLONASS SLOT / FRQ # GLONASS COD/PHS/BIS END OF HEADER > 2019 1 15 0 0 0.0000000 0 13 .000000002000 R2 22650554.75805 120867759.49215 30.800 22650564.92206 94008232.29106 38.500 22650564.81306 94008233.28006 39.700 G10 22654444.02307 119050059.30307 44.900 22654450.29705 92766187.39705 33.900 22654450.08206 92766169.40406 41.600 22654445.18005 88900871.14605 33.800 • RINEX V3 Navigation file extract: 3.02 N: GNSS NAV DATA G: GPS NAV DATA RINEX VERSION / TYPE NetR9 5. 22 Receiver Operator 20190115 000000 UTC PGM / RUN BY / DATE GPSA .7451D-08 -.1490D-07 -.5960D-07 .1192D-06 IONOSPHERIC CORR GPSB .8806D+05 -.4915D+05 -.1966D+06 .3277D+06 IONOSPHERIC CORR GPUT .0000000000D+00 .355271368D-14 319488 2036 TIME SYSTEM CORR 18 18 1929 7 LEAP SECONDS END OF HEADER G10 2019 01 15 00 00 00 .135467387736D-03 -.648014975013D-11 .000000000000D+00 .260000000000D+02 -.340625000000D+02 -.169314444065D-05 .422777992208D-02 .172800000000D+06 -.670552253723D-07 .440579833061D+00 -.521540641785D-07 .460840624433D-08 .690296292305D-05 .282394335255D+01 .515366102409D+04 .962418025762D+00 .247093750000D+03 -.278465880730D+01 -.806105006081D-08 .392873507616D -10 .100000000000D+01 .203600000000D +04 .000000000000D+00 .240000000000D+01 .000000000000D+00 .186264514923D-08 .260000000000D+02 .168966000000D +06 .400000000000D+01 Chapter 3: Methodology 3 Methodology: Software Tool development For committing the work purposes defined in chapter 1, it has been decided to develop a dedicated Software tool (hereafter simplified as SW) flexible enough for processing different GNSS pseudorange measurements in post-processing mode and using single-frequency SPP algorithms introduced in chapter 2. Currently, there are already several open source tools for GNSS measurement processing, such as RTKLIB, gLAB or GAMP. As a matter of fact, the first alternative for this work was to use them to measure the target GPS and GALILEO performances. However, our own experience with these tools demonstrated a lack of flexibility and completeness from a user perspective. Some of them did not support all GPS-SPS and GALILEO-OS signals, whereas some others required of an extensive input and output treatment in order to assess integrity performance or process only E5b signal. On topo of that, the black- box nature of these tools made difficult to know the specific processing details which were taking place, like the ionosphere model. Consequently, the feasibility of this approach was considered not to be as time-consuming as developing our own SW solution, which in return has produced a fair and flexible tool. Taking advantage of this alternative, it was then decided that the developed SW will establish a preliminary version of a new open source tool which, apart from contributing to the GNSS community, will hopefully fill the gap that was initially encountered with the other tools. Nonetheless, the added value of making a user-oriented product implied to carry out a premeditated SW development process for producing a quality solution which will satisfy the different user needs. Note that this situation is very different from developing a single script, where is user-limited and solves one specific problem. In contrast, this case requires a precise definition of functional, performance and user necessities; along with a warranty that the SW works accordingly. As a result, it was necessary to adopt a SW engineering process for its development. The SW engineering paradigm is based on a lifecycle workflow which implies the definition, design, implementation, verification, documentation and bug-fixing of a SW product. In the context of this project, the lifecycle adopted has been the waterfall kind (see [LR.4]), a logic ordered sequence of steps. Tough the settled waterfall model has not been strictly followed, the main steps of the SW development have been: • SW tool specification and definition. This phase is intended to explain the nature and the high-level concept of the solution to be developed. • SW tool architecture and algorithm design. This accounts for the detailed architecture

and algorithm decomposition adopted in order to accomplish the SW specifications. • SW tool performance verification. This phase verifies that the SW is compliant with the specifications by defining test cases which validate the SW features. The upcoming sections of this chapter are dedicated to explain more deeply these steps in order to reveal the functional nature but also the complexity encompassed in the SW tool. Please, note that it is not the intention of this chapter to completely assess the SW lifecycle or to be a user manual, but to illustrate and summarize it for a better understanding of the thesis methodology. Note: In spite of the fact that the developed SW tool is open-source and free of charge, a budget estimation is available in annex A.3 emulating the production cost in a commercial contract scenario. 3.1 Specification and Definition The first logic step when developing a SW solution is to define what the SW shall do, to whom is oriented, in which context is to be used and many other aspects. Once the main goal of the SW has been settled, this is abstracted in high level diagrams and a set of preliminary design items. These features are then decomposed in low level SW features, such as requirements and detailed design diagrams; so the detailed architecture and algorithm implementation can be performed. The Preliminary Item Design Specifications (PIDS) adopted for this project SW are summarized in Table 3.1. In a real commercial scenario, these items would be provided by the costumer in order to specify its needs on the SW contract. Table 3.1 – Preliminary Item Design Specifications for the SW tool. Code Preliminary Item Design Specification PIDS-01 The SW shall post-process GNSS pseudorange measurements and navigation data for single-frequency SPP services. PIDS-02 The SW shall support GPS Standard Positioning Service and GALILEO Open Services. PIDS-03 PIDS-04 The SW shall measure both accuracy and integrity performances whenever the receiver is in static mode. The pseudoranges and navigation data shall be provided as inputs with a GNSS- receiver independent format. PIDS-05 PIDS-06 PIDS-07 The accuracy and integrity performance results shall be provided in both numerical and graphical formats. The SW shall be open source, free of charge and user oriented. The SW shall enable different processing configurations which are specified by the user. 3.1. 1 High Level Architecture From Table 3. 1, a high-level architecture diagram can be drawn in order to illustrate the SW main batch sequence. This is displayed on Figure 3.1. Figure 3.1 – SW tool high level architecture, first decomposition. Figure 3.1, represents the SW highest architecture possible. However, from PIDS a lower SW architecture can be decomposed as illustrated in Figure 3.2. Figure 3.2 – SW tool high level architecture, second decomposition. On the one hand, the processing module will oversee the GNSS data processing and will measure the accuracy and integrity performances. On the other hand, the report module will use the processing module outputs to show and summarize them with a proper display method. On top of that, processing and report modules will have a user configuration-dependent behavior and this configuration will be common for both modules. Note that the architecture presented encompass all the specified PIDS. Furthermore, it is already adopting a modulated solution by splitting the SW in a processing and report modules, allowing for a more flexible and independent implementation. Further decomposition of both modules is done in section 3.2. Lastly, both processing and report modules will be eventually maintained and executed as separated tools. This will allow more flexibility since, for instance, the user may only want to run the processing module and treat by his own the processing outputs. Expected Inputs and Outputs The high-level architecture has been defined. However, the definition phase should account as well for the input and output specification. From the high-level architecture presented, the following inputs and outputs can be enumerated: • Inputs ? User-Configuration encompass the user-specified processing parameters. These parameters will be specified in the SW's requirements, but they account for the different settings of the GNSS SPP algorithms, like pseudorange signal or the satellite mask. The configuration will be inserted as a plain text file and will allow the tool for a more flexible nature. ? GNSS Data stands for the raw pseudoranges, the navigation data and any other necessary inputs. Since the SW is not real-time and must accept measurements from any receiver, the best possible standard to adopt is the settled RINEX version 3 format (refer to section 2.7). • Outputs ? Processing outputs will be raw numeric outputs from the SPP algorithms implemented in the processing module. For instance, they will cover satellite positions computed from the broadcasted ephemeris, Receiver-SV ionospheric correction, observations residuals from WLSQ estimation, etc. These outputs will be arranged in delimited plain text files with a column and row arrangement. For instance, rows could hold the observation epochs and columns the accuracy indicators. ? Results and Reports will summarize the processing outputs in numerical and graphical formats in order to display the obtained positioning performances. Besides accuracy and integrity indicators, they should also provide useful processing information like satellite availability or LSQ routine estimation results, although this has not been specified in PIDS. Results and reports will be provided in plain text file format (ASCII coded) and image plots (e.g. .png extension). 3.1.2 Requirements The SW requirements are a detailed abstraction of the PIDS and therefore can be traced to them. They are not user demands but engineering criteria which shall be accomplish by the SW. These criteria must be precisely and unambiguously defined, not allowing for assumption presumption. Eventually, requirements are the SW baseline or main reference for all its lifecycle. Due to the nature of this project commitment, it has been decided to split the SW requirements in three kinds for a better understanding: • Environment Requirements. They refer to SW and even Hardware (HW) external components specification for the development, maintenance and execution support. • User Configuration Requirements. They encompass the required parameters customization by the user which allow for a different SW processing configuration. • Functional Requirements. They depict the several functionalities which the SW shall fulfill. They are subdivided for each module: ? Processing Module Functional Requirements ? Report Module Functional Requirements Environment Requirements This requirement type stands for the environments specifications where the tool is going to be developed and executed. Since our SW tool has an open-source and free of charge approach, its programming language and target Operative System (OS) should have these characteristics as well. On the HW side, the SW is expected to be executed on a common user machine e.g. personal laptop. Environment requirements are arranged in Table 3.2. Table 3.2 – SW environment requirements. Requirement ID Description Related PID REQ-ENV-1 The SW shall be developed by open source and free of charge programming languages. PIDS-06 REQ-ENV-2 The SW shall be developed and supported on an open source and free of charge operating system. PIDS-06 REQ-ENV-3 The SW execution shall be supported on a computer machine with the following minimum specifications: • Processor - dual core @ 2.4 GHz (i5 or i7 Intel processor or equivalent AMD) PIDS-06 • • • • • • RAM - 4 GB Hard Drive - 320 GB 5400 RPM hard drive Wireless (for laptops) - 802.11g/n (WPA2 support required) Monitor - 19" LCD - desktop only Operating System – Open Source Linux Distro (Ubuntu, Fedora, RedHat, …) Backup Device - External hard drive and/or USB Flash Drive User Configuration Requirements The user configuration requirements specify all the parameters which can be changed manually by the user in order to allow for different processing customization. The needed parameters have been identified thanks to the theorical framework

presented in chapter 2. Nonetheless some tests during the SW development revealed that further configuration was needed. The configuration requirements are detailed in Table 3.3. Table 3.3 – SW user configuration requirements. Requirement ID Description PID Trace REQ-CFG-4 Main Configuration The SW shall require as input the GNSS system configuration among GPS or GALILEO systems. PIDS-07 REQ-CFG-5 The SW shall require as input the receiver static mode configuration among activated or de-activated. PIDS-07 REQ-CFG-6 The SW shall require as input the receiver integrity mode configuration among activated or de-activated if the receiver static mode has been set as "activated". PIDS-07 REQ-CFG-7 Input/Output Configuration The SW shall require as input the path of a RINEX version 3 observation file. PIDS-07 REQ-CFG-8 The SW shall require as input the path of a RINEX version 3 GPS navigation file if GPS system has been selected or if Klobuchar ionospheric model has been selected. PIDS-07 REQ-CFG-9 The SW shall require as input the path of a RINEX version 3 GALILEO navigation file if GALILEO system has been selected. PIDS-07 REQ-CFG-10 The SW shall require as input the processing output path configuration. PIDS-07 Processing Configuration REQ-CFG-11 The SW shall require as input the initial and end epoch configuration. PIDS-07 REQ-CFG-12 The SW shall require as input the interval time stamp configuration. PIDS-07 REQ-CFG-13 The SW shall require as input the RINEX version 3 GPS pseudorange observation code among C/A or L2C signals if GPS has been selected. PIDS-07 REQ-CFG-14 The SW shall require as input the RINEX version 3 GALILEO pseudorange observation code among E1, E5a or E5b signals, if GALILEO system has been selected. PIDS-07 REQ-CFG-15 The SW shall require as input the Receiver-SV mask configuration. PIDS-07 REQ-CFG-16 The SW shall require as input the excluded PRN configuration for GPS and GALILEO systems. PIDS-07 REQ-CFG-17 The SW shall require as input the ephemerids time-out threshold configuration. PIDS-07 Atmosphere Modelling Configuration REQ-CFG-18 The SW shall require as input the ionosphere model configuration among Klobuchar or Null (no correction) models for each GPS and GALILEO systems. PIDS-07 REQ-CFG-19 The SW shall require as input the troposphere model configuration among Saastamoinen or Null (no correction) models. PIDS-07 Position Estimation Configuration REQ-CFG-20 The SW shall require as input the mean expected measurement error configuration for GPS observations weighting, if GPS system has been selected. PIDS-07 REQ-CFG-21 The SW shall require as input the mean expected measurement error configuration for GALILEO observation weighting, if GALILEO system has been selected. PIDS-07 REQ-CFG-22 The SW shall require as input the delta displacement convergence threshold configuration for WLSQ estimation. PIDS-07 REQ-CFG-23 The SW shall require as input the maximum allowed number of iterations configuration for WLSQ estimation. PIDS-07 Integrity Mode Configuration REQ-CFG-24 The SW shall require as input the receiver static reference position in WGS84 ECEF coordinates when both static and integrity modes have been activated. PIDS-07 REQ-CFG-25 The SW shall require as input the horizontal AL and sigma scale factor configuration if integrity mode has been activated. PIDS-07 REQ-CFG-26 The SW shall require as input the vertical AL and sigma scale factor configuration if integrity mode has been activated. PIDS-07 Functional Processing Requirements These requirements depict the functionality features of the processing module. They mostly account for the algorithms to be implemented but also on how the different user configuration must be allocated from a processing perspective. Processing module functional requirements are listed in Table 3.4. Table 3.4 – SW processing module functional requirements. Requirement ID Description PID Trace Generic Features REQ-FUN-27 The SW processing module shall support pseudorange measurements and navigation data for GPS and GALILEO systems. PIDS-02 REQ-FUN-28 The SW processing module shall support WGS84 and GRS80 ellipsoid models. PIDS-01 Supported Inputs REQ-FUN-29 The SW processing module shall support and read a user-specified single RINEX version 3 multi-GNSS observation file. PIDS-04 PIDS-07 REQ-FUN-30 The SW processing module shall support and read a user-specified single RINEX version 3 GPS navigation file. PIDS-04 PIDS-07 REQ-FUN-31 The SW processing module shall support and read a user-specified single RINEX version 3 GALILEO navigation file. PIDS-04 PIDS-07 Output Formatting REQ-FUN-32 The SW processing module shall provide its processing information, warnings and errors in a dedicated plain text log file and in the terminal STDOUT. PIDS-06 PIDS-07 REQ-FUN-33 The SW processing module shall provide its processing outputs on a user-specified directory. PIDS-05 PIDS-07 Measurement Processing REQ-FUN-34 The SW processing module shall process only the pseudorange measurements which fall between a user-specified initial and end epochs. PIDS-01 PIDS-07 REQ-FUN-35 The SW processing module shall process the pseudorange measurements every user-specified interval stamp. PIDS-01 PIDS-07 REQ-FUN-36 The SW processing module shall process the user-specified GPS-SPS pseudorange measurements among C/A or L2C signals. PIDS-01 PIDS-02 PIDS-07 REQ-FUN-37 The SW processing module shall process the user-specified GALILEO- OS pseudorange measurements among E1, E5a or E5b signals. PIDS-01 PIDS-02 PIDS-07 REQ-FUN-38 The SW processing module shall not process measurements from observed SV which are below a user-specified elevation mask. PIDS-01 PIDS-07 REQ-FUN-39 The SW processing module shall not process measurements from user- specified GPS PRN numbers. PIDS-01 PIDS-07 REQ-FUN-40 The SW processing module shall not process measurements from user- specified GALILEO PRN numbers. PIDS-01 PIDS-07 Ephemerids Processing REQ-FUN-41 The SW processing module shall accept the satellite system PRN ephemerids, coming from the RINEX navigation file, which do not exceed a user-specified time-out threshold on each observed SV. PIDS-01 PIDS-07 REQ-FUN-42 The SW processing module shall compute for every observed SV its ECEF coordinates in WGS84 at the time reception of each processing epoch by implementing the broadcast ephemerids satellite coordinate computation algorithms specified in section 2.5.2. PIDS-01 REQ-FUN-43 The SW processing module shall compute for every observed SV its clock bias against GPST at the emission time of each processing epoch, by implementing the broadcast ephemerids satellite clock correction computation algorithm specified in section 2.5.2, taking into account the selected signal carrier frequency. PIDS-01 Atmosphere Error Modelling REQ-FUN-44 The SW processing module shall implement Klobuchar's ionosphere correction model specified in section 2.5.3, taking into account selected signal carrier frequency, for every processing epoch and on each SV- Receiver LoS, using the alpha and beta ionospheric coefficients provided by GPS navigation message. PIDS-01 REQ-FUN-45 The SW processing module shall be able of not applying ionosphere correction model in every processing epoch. PIDS-01 REQ-FUN-46 The SW processing module shall implement Saastamoinen's troposphere correction model specified in section 2.5.3, for every processing epoch and for each SV-Receiver LoS. PIDS-01 REQ-FUN-47 The SW processing module shall be able of not applying troposphere correction model in every processing epoch. Receiver Parameter Estimation PIDS-01 REQ-FUN-48 The SW processing module shall estimate the receiver position ECEF coordinates in WGS84 and its clock bias against GPST time scale for every processing epoch by implementing the algorithms specified in section 2.5.4. PIDS-01 REQ-FUN-49 The SW processing module shall set the weight terms for GPS measurements with the user-specified observation mean error as indicated in equation (2.52). PIDS-01 PIDS-07 REQ-FUN-50 The SW

processing module shall set the weight terms for GALILEO measurements with the user-specified observation mean error as indicated in equation (2.52). PIDS-01 PIDS-07 REQ-FUN-51 The SW processing module shall stop estimating the receiver position solution, on every processing epoch, if a user-specified delta displacement threshold is reached respect to the previous iteration of the same processing epoch. PIDS-01 PIDS-07 REQ-FUN-52 The SW processing module shall stop estimating the receiver position solution, on every processing epoch, if a user-specified maximum number of iterations is reached in the same processing epoch. PIDS-01 PIDS-07 Performance Indicators REQ-FUN-53 The SW processing module shall estimate the positioning accuracy indicators from WLSQ routine and provide them as specified in section 2.5.5 for each processing epoch. PIDS-01 PIDS-03 REQ-FUN-54 The SW processing module shall flag for the horizontal domain the integrity MI, HMI and SA events on each processing epoch if the integrity mode is activated. PIDS-03 REQ-FUN-55 The SW processing module shall flag for the vertical domain the integrity MI, HMI and SA events on each processing epoch if the integrity mode is activated. PIDS-03 Functional Report Requirements Finally, report module requirements listed in Table 3.5 specify the functional aspects of the user-end results and plots. Although from PIDS decomposition, only positioning performance reports are needed, the report module will also provide further information depicted from processing outputs, such as observation residuals or satellite availability among many others. This has been worthy for illustrating GNSS processing concepts and for many other reasons like bug detection and mitigation during the SW development. Table 3.5 – SW report module functional requirements. Requirement ID Description PID Trace Output Formatting REQ-FUN-56 The SW report module shall provide its report results on a user- specified directory. PIDS-05 REQ-FUN-57 The SW processing module shall provide its processing information, warnings and errors in a dedicated plain text log file and in the terminal STDOUT. PIDS-05 Numeric Reports REQ-FUN-58 The SW report module shall provide in a plain text format the measured accuracy RMSE for horizontal, vertical and position domains as specified in section 2.6.1. PIDS-05 REQ-FUN-59 The SW report module shall provide in a plain text format the mean position error against its reference for horizontal, vertical and position domains (ENU components) if static mode is activated. PIDS-05 REQ-FUN-60 The SW report module shall provide in a plain text format the integrity performance indicators: MI, HMI and SA cases; for the horizontal and vertical domains if both static and integrity modes are activated. PIDS-05 Graphical Reports REQ-FUN-61 The SW report module shall display in a 2D plot the horizontal receiver positions errors against its reference, Easting and Northing components, of each processing epoch if static mode is activated. PIDS-05 REQ-FUN-62 The SW report module shall display in a 2D plot the vertical receiver position errors against its reference, Upping component, of each processing epoch if static mode is activated. PIDS-05 REQ-FUN-63 REQ-FUN-64 The SW report module shall display in a 2D plot the measured accuracies in the horizontal, vertical and position domains (ENU components) of each processing epoch. The SW report module shall display in a 2D plot the integrity performance information: system accuracy, system error, AL, MI, HMI and SA; of each processing epoch, for the horizontal and vertical domains and if both static and integrity modes are activated. PIDS-05 PIDS-05 3.2 Architecture and Algorithm Design Once the SW features have been precisely defined, the detailed design regarding the architecture and algorithm composition can be assessed. But first, some detailed technical implementations need to be specified. These generic details stand for the Operative System (OS) and the programming language used for developing and executing the SW. Note that these two features will be conditioned from the environment requirements specified in the previous section of this chapter. • Operative System. The free of charge and open source paradigm is indisputably the Linux kernel- based OS. Therefore, the SW has been developed under Ubuntu MATE distro, Long Term Support version 16.04 (more information on Ubuntu MATE official website [LR.5]). Nonetheless, the SW could be run on any Linux distro OS as far it has the required programming language environments. • Programming Language. The chosen programming language for the SW development has been the Practical Extraction and Reporting Language, or Perl for short, version 5.26 (more information on Perl official website [LR.6]). In addition, the processing module will use the Perl Data Language (PDL) extension for matrix algebra and other math operations, and the report module will take advantage of Gnuplot language, version 5.2 (see web link [LR.9]) in order to produce the graphical displays. Figure 3.3 – Ubuntu MATE distro icon. Source: Figure 3.4 – Perl programming language icon. Source: ubuntu-mate.org perl.org The many advantages of choosing Ubuntu and Perl environments counteract the fewer drawbacks which came along in this project's context: • On the one hand, Ubuntu and Perl are compliant with the environment requirements specified in section 3.1.2, since they are both open source and free of charge. In addition, Ubuntu MATE OS HW requirements cover the ones specified in REQ-ENV-3. • On the other hand, Perl programming language is an interpreted programming language which allows dynamic memory treatment. Thus, tedious memory initialization is not needed but can be done "on the run" while the algorithm is executing. This combined with its hash data structure, makes Perl a very appealing choice for an efficient SW interface modulation. In the computer science context, a hash is a structure which builds a direct relation among two variables. A Perl hash is composed as a list of keys-value pairs which can only be scalar variable types: characters, string or numbers. However, scalars can also hold variable and code references (memory addresses) allowing Perl hashes to build complex structures which can contain arrays or subsequent hashes (see [LR.7]). Indeed, extrapolating the hash concept to the SW paradigm, a hash can act as input/output interface in order to be used by the SW modules. This also allows for accessing data "on-the-fly" and not depending of a long-list of input/output interface. However, a hash-based SW requires of a detailed definition of the interfaces for the algorithms to access the data homogeneously. The Perl hash-interfaces of the SW are exemplified in annex A.4. By having specified this implementation approach, the high-level architecture presented in section 3.1.1 can be further depicted with the aforementioned hash-interface elements as shown in Figure 3.5. Note that an extra SW item has been added, the Configuration Parser module. This will be in charge of reading the user configuration and translate it into a generic configuration interface which can be used by the processing and report modules. Figure 3.5 – Processing flow diagram. Furthermore, Perl programs can be composed of package modules (.pm extension) or script files (.pl extension). Packages are divided in Perl functions or subroutines, meanwhile Perl scripts can contain subroutines, but they execute a main routine. The packages can be loaded in a Perl scripts in order to execute its subroutines. However not all subroutines are imported by default, in the package exportation properties, a list of exported subroutines must be specified. These exported features are known as public subroutines whereas package items which are not exported are the private subroutines. The following subsections contain each of the SW Perl modules architecture and public subroutine specification. Please note that not all SW features are covered in this section since deeper SW specification is out of scope of the project's methodology explanation. Nevertheless, SW details can be explored by source code inspection (refer to annex A.1). 3.2.1 User Configuration Module It can be deduced from Figure 3.5 that a

user configuration parser is needed in order to create a common configuration interface. This module is available in the source code as a single Perl package named GeneralConfiguration.pm. The module's purpose is to read the user's configuration file (see example in annex A.2) with the processing parameters specified in section 3.1.2, and translate them into a hash which follows the common- configuration hash-interface. In addition, configuration module also exports constant information such as GNSS signal frequencies or satellite system RINEX codes. Module Architecture The Configuration modules is made of a single Perl package and therefore no detailed architecture diagram is presented. Public Subroutine Specification The configuration module exports the following public subroutines: • LoadConfiguration is in charge of reading the configuration file provided by the user and build the common-configuration hash-interface (see an interface example in annex A.4). The subroutine basically loads the input file in memory and parses it by taking advantage of the Perl built-in regular expression functionalities. The parsed parameters are then saved in the configuration hash. The subroutine also makes consistency checks while reading the parameters e.g. checks that the configured satellite mask is a numeric parameter. If the parameters are not properly set, the subroutine will raise an error indicating the erroneous configured parameter and its cause (see Terminal Demo 1). This subroutine implements all the User Configuration Requirements (REQ-CFG-4 to REQ-CFG-26). Terminal Demo 1 – Wrong user configuration example. # Troposphere model has been configured wrong in the following configuration file: ppinto@ppinto-UbuntuVM:~/WorkArea/cfg$ grep Troposphere tst/wrong_parameters.cfg Troposphere Model : Jaastamoinen # When LoadConfiguration subroutine is called, it raises a configuration error and the execution is aborted: ppinto@ppinto-UbuntuVM:~/WorkArea/cfg$ $GRPP tst/wrong_parameters.cfg *** 2019/06/05 18:54:56 *** ERROR:30405 *** *** - Troposphere model 'Jaastamoinen' is not supported *** - Supported models are: none, saastamoinen *** 2019/06/05 18:54:56 *** ERROR:30405 *** at /home/ppinto/WorkArea/src/GeneralConfiguration.pm line 659. Configuration file loading error at /home/ppinto/WorkArea/src/GNSS_RINEX_Post-Processing//MainRoutine.pl line 85. • CheckConfigurationFile this subroutine makes simple checks on the provided configuration file. The checks are not made over the configured parameters but on the file itself. It checks that the file exists, has plain text format and has user reading permissions. This subroutine is called when the processing or report modules receive a raw configuration file before parsing it. 3.2.2 Processing Module: GNSS RINEX Post-Processing The processing module constitutes the core element of the SW since it processes the RINEX data using single-frequency pseudorange SPP algorithms presented in chapter 2. Consequently, the module has been named: GNSS RINEX Post-Processing, hereafter GRPP. Module Architecture It can be deduced from functional processing requirements in section 3.1.2 that GRPP is likely to present a certain complexity. Therefore, SW decomposition is essential in order to depict its architecture into simpler elements. GRPP architecture approach is package-oriented which encompass the following Perl packages: • RinexReader.pm encompass the subroutines which read the RINEX files and store their information in internal GRPP observation and navigation hash-interfaces. • SatPosition.pm holds the implemented algorithms for estimating the satellite position and clock bias using the navigation data retrieved from RinexReader package. • RecPosition.pm encompass the algorithms for estimating the user's receiver position and clock bias at the processing epochs using the observation data retrieved from RinexReader package and the satellite positions from SatPosition package. • ErrorSource.pm constitutes the subroutines for modeling the error sources in the pseudorange observations. So far, the package only supports atmosphere error modelling since satellite clock modelling is done in SatPosition package. • DataDumper.pm holds the subroutines for dumping the computed data through all the other modules. The processing data is passed through a GRPP internal observation-data hash-interface. The package hierarchy is presented in Figure 3.6. Note that not all packages are independent, but they maintain a hierarchical relation. For instance, RecPosition needs to import ErrorSource for estimating the atmosphere corrections in each LoS when building the pseudorange equations for the WLSQ algorithm. Also note that all GRPP packages load the GeneralConfiguration module and a Library Perl Module. This library stands for a recopilation of common subroutines and constants used throughout all SW modules. It consists of several individual packages: MyUtil.pm, MyPrint.pm, MyMath.pm, TimeGNSS.pm and Geodetic.pm. For instance, MyMath package includes the WLSQ algorithm whilst TimeGNSS encapsulates all the conversion time functions for GNSS time scale management. More details about library module can be found by code inspection (refer to annex A.1). Figure 3.6 – GRPP architecture hierarchy diagram. Public Subroutine Specification GRPP tool uses the following public subroutines exported by each of the packages. For the sake of clarity, not all subroutines have been included, only the most relevant: • RinexReader: ? ReadObservationRinexV3 reads a RINEX version 3 observation file, as specified in REQ-FUN- 29. The retrieved data is stored in a hash which follows the observation-data hash-interface (exemplified in annex A.4). The subroutine also checks that the configured observations are present on the file and only stores the observations which fall in the time configuration specified by the user (see REQ-FUN-34 and REQ-FUN-35). ? ReadNavigationRinex reads a RINEX version 2 or 3 navigation file as specified in REQ-FUN- 30 and REQ-FUN-31. The navigation data is stored as well in hash which follows a navigation- data hash-interface. Technically, the sub can only read GPS and GALILEO navigation files since the data is arranged differently for each system (for instance, GLONASS has its own arrangement). In order to solve this, the ephemerids block subroutines are called by reference depending on the treated satellite. In addition, the reading takes in consideration the navigation data sources. For GPS this is always the same but for GALILEO it can vary depending on the signal service (see [BR.8]). • SatPosition: ? ComputeSatPosition computes the position and clock bias of each observed SV on each processing epoch by implementing the algorithms specified in REQ-FUN-42 and REQ-FUN-43. Nonetheless, the SV must select valid ephemerids from the navigation-data hash before proceeding to the computation. The ephemerid selection criteria is based on REQ-FUN-41. Furthermore, since navigation data reading for GPS and GALILEO was different, the SV position computation and ephemerids selection take this into account. Specifically, they account for the GALILEO data source when selecting the ephemerids, and the different ephemerid arrangement when computing the SV clock bias correction. • RecPosition: ? ComputeRecPosition estimates the receiver position and its clock bias along with its associated accuracy by implementing the functional requirements: from REQ-FUN-48 to REQ-FUN-52. This involves that the WLSQ routine stops iterating when it reaches a maximum number of iterations or when the position solution has converged. Moreover, the subroutine also discards those observed SV which fall below the configured mask as indicated in REQ-FUN-38. Finally, and if both static and integrity modes have been activated, the integrity performance indicators are computed as specified in REQ-FUN-54 and REQ-FUN-55. • ErrorSource: ? NullIonoDelay and NullTropoDelay they return zero delay estimation for ionosphere and troposphere corrections. These subroutines fulfill REQ-FUN-45 and REQ-FUN-47. • ? ? ComputeIonoKlobucharDelay estimates the ionosphere delay through Klobuchar's model for the selected signal carrier frequency. This subroutine

fulfills REQ-FUN-44. ComputeTropoSaastamoinenDelay estimates the troposphere delay through Saastamoinen's model. The subroutine fulfills REQ-FUN-46. DataDumper: ? DumpRecPosition writes the receiver position solution and clock bias for each observation epoch. The receiver position is outputted in ECEF and geodetic coordinates along with its sigma values. In addition, and if the static mode has been activated, the receiver ENU components and its accuracy indicators are also outputted. Table 3.6 – Receiver position raw output. # > Receiver marker 'CEBR' adjusted coordinates. # > Reference system for ECEF coordinates : WGS84 # > Reference coordinates from static mode 'igs' #ECEF_X ECEF_Y ECEF_Z GEO_Lat GEO_Lon 4846664.92 -370195.201 4116929.52 40.45342914 -4.36785259 EpochGPS Status NumObs ECEF_X … Sigma_X … Sigma_E 1241740800 1 9 4846665.771 … 0.858 … 0.669 1241740830 1 9 4846666.002 … 0.793 … 0.619 … … … … … … … … … GEO_Lat … 40.4534217 … 40.4534213 … … … REF_IE … 0.355 … 0.333 … … … … … … ? DumpSatPosition writes the satellite positions and its clock bias computed from its navigation data for each observation epoch. The satellite coordinates are given in both ECEF and geodetic formats. ? DumpNumValidSat outputs the satellite availability metrics on each observation epoch. These metrics are: number of observed satellites, number of satellites with no-null observation, number of satellites with valid navigation position and number of satellites to enter in WLSQ routine. Table 3.7 – Number of valid SV raw output. # > Satellite system 'G' number of valid satellites. # > Selected observation for G -> C1C EpochGPS AvailSat ValidObs ValidNav ValidLSQ 1241740800 10 9 9 9 1241740830 10 9 9 9 … … … … … ? DumpInfoBySat outputs satellite related information such its estimated residuals from WLSQ algorithm, or its computed ionosphere delay. It also outputs the satellite observed azimuth and elevation. Table 3.8 – Residuals per SV raw output. # > Receiver-Satellite 'G' LSQ residuals. # > Configured mean_obs_err for 'G' -> 3.000 # > Resiudals are refered to last LSQ iteration EpochGPS Status NumIterLSQ G01 G02 … G19 G22 … G32 1241740800 1 3 0.991 -0.747 … -0.657 -1.191 … NaN 1241740830 1 3 0.568 -0.293 … -0.759 -0.845 … NaN … … … … … … … … … … … ? DumpLSQReportByEpoch writes the WLSQ information per observation epoch. This is: number of parameters, number of observations, degrees of freedom, ex-post standard deviation estimator, convergence status and, the approximate and estimated parameters. Table 3.9 – WLSQ report raw output. # > Least Squares Report by observation epoch. EpochGPS Iter 1241740800 1241740830 3 3 Status 1 1 Convergence NumObs Parameter DegOfFree StdDevEstimator ApxX 0 0 9 9 4 4 5 5 0.1 0.1 4846664.918 4846665.771 … … … dX 0.448 -0.174 … … … … … … … … … … … … … … … … … ? DumpEpochSigma writes the accuracy indicators specified in section 2.6.1 per observation epoch. The sigma values are in essence the accuracy indicators. By default, no sigma scale factor is applied. Table 3.10 – Accuracy report raw output. # > Accuracy (sigma) report. # > Reference ECEF frame : WGS84 # > Reference ENU frame : Local receiver position EpochGPS Status SigmaG SigmaP SigmaT SigmaH SigmaV 1241740800 1 1.378 1.164 0.736 0.894 0.916 1241740830 1 1.273 1.076 0.680 0.827 0.845 … … … … … … … ? DumpIntergrityInfo writes the integrity indicators specified in section 2.6.2 along with their precision (with the configured sigma scale factor) and actual error. The information is split for vertical and horizontal domains. The outputs are only available when both static and integrity modes have been activated. Table 3.11 – Vertical integrity report raw output. # > Vertical integrity information. # > 'Status' refers to receiver position estimation # > Created : 2019/06/14 19:56:08 EpochGPS Status SigmaScaleFactor AlertLimit Error Precision 1241740800 1 1.96 30 0.374 1.796 1241740830 1 1.96 30 0.643 1.658 … … … … … … … MI HMI 0 0 0 0 … … Available 1 1 … Module Execution In order to maintain GRPP as a single tool and with a user-friendly usage, GRPP is orchestrated by a single Perl script, which is called in order to run the module as a whole: • MainRoutine.pl manages GRPP public subroutines in order to run the tool with the user configuration. The main routine is subdivided in three steps: ? Configuration Loading imports GeneralConfiguration package, check and loads the user configuration parameters. ? Data Processing manages the processing routine by reading the RINEX data, computing the satellite positions and finally computing the receiver positions. ? Data Dumping creates the GRPP outputs by dumping the processed data pushed in the GRPP internal hashes. In addition, it dumps in binary format the common-configuration and observation-data hashes for other Perl scripts to recover them if needed. GRPP package and public subroutine arrangement by MainRoutine can be illustrated by its processing flow diagram in Figure 3.7. In Figure 3.7, the GRPP hash-interface flow is better understood. Note that: • RinexReader package is in charge of initializing the observation data hash and then this is received and updated by SatPosition and RecPosition. • SatPosition also initializes and fills navigation data hash which contains all the SV ephemerids. • Navigation data hash is transmitted to RecPosition in order to retrieve the ionosphere coefficients if needed by the input configuration. • ErrorSource is plugged into RecPosition for importing the ionosphere and troposphere correction subroutines. • All packages make use of the configuration hash-interface and thus, the user cannot execute their public subroutines without it. Figure 3.7 – GRPP architecture flow diagram. Finally, to illustrate how a user would run GRPP, a Linux terminal example is contained in Terminal Demo 2. This example launches GRPP for GALILEO-OS E1 verification case (see section 3.3.2). The only input received by GRPP is the user configuration file (see annex A.2). When launching GRPP MainRoutine, the scripts starts to print useful information to the user like: • Configuration brief. • Which part of the tool is being executed. • Any processing warnings such as a processing epoch with invalid solution status or a SV with no selected ephemerids. • Receiver position summary containing ECEF coordinates and its standard deviation accuracies, along with the percentage of valid and invalid solution status. • Where the outputs have been allocated. • The time which took to execute the public subroutines and the entire GRPP processing. Terminal Demo 2 – GRPP launching example for GALILEO-OS E1 on KOKV IGS station. ppinto@ppinto-UbuntuVM:~/WorkArea/demo$ $GRPP cfg/KOKV_GAL-E1.cfg # ## # # > Welcome to GNSS Rinex Post-Processing tool # # ## # # Script was called from : '/home/ppinto/Drive/tmp/MASTER/TFM/src/GNSS_RINEX_Post-Processing/MainRoutine.pl' # Configuration file used : '/home/ppinto/Drive/tmp/MASTER/TFM/demo/cfg/KOKV_GAL-E1.cfg' # == # # > Configuration brief of 'KOKV Demo' # # == # # > Selected Satellyte Systems and Observation # # ····· # # - GALILEO (E) -> E1 (C1X) # > Satellite Mask configuration # # ····· # # - Elevation threshold = 10 [deg] # - Discarded GALILEO satellites : E14, E18 # > Error Source Models # # ····· # # - Troposphere model : Saastamoinen # -

GALILEO Ionosphere model : Klobuchar # > Rinex Input files # # ····· # # - Observation Rinex : KOKV00USA_R_20183520000_01D_30S_MO.rnx # - GALILEO Navigation Rinex : KOKV00USA_R_20183520000_01D_EN.rnx # > Processing time window # # ····· # # - Start time = 2018/12/18 00:00:01 (GPS time = 1229126401) # - End time = 2018/12/18 07:00:00 (GPS time = 1229151600) # - Interval = 30 [sec] # - Number of epochs = 840 # > Static Mode Configuration # # ····· # # - Static mode : IGS # - IGS station : KOKV # - Reference ECEF (X, Y, Z) = -5543838.239 -2054586.439 2387810.121 # - Reference Geodetic (lat, lon, h) = 22.1262643 -159.6649309 1167.360 # ==========# # > Data Processing routine has started # # ==========# # > Reading Observation Rinex... # # ····· # # > Computing satellite positions... # # ····· # # > Computing receiver positions... # # ····· # *** 2019/06/16 18:57:32 *** WARNING:90305 *** at /home/ppinto/WorkArea/src/GNSS_RINEX_Post-Processing/RecPosition.pm line 275. # > Receiver position summary: # # Observation epoch : 2018/12/18 00:00:30 -> Status = OK # | X | Y | Z = -5543833.009 | -2054584.615 | 2387809.444 | # | sX | sY | sZ = 16.535 | 4.522 | 4.848 | # Observation epoch : 2018/12/18 00:01:00 -> Status = OK # | X | Y | Z = -5543837.207 | -2054585.560 | 2387810.140 | # | sX | sY | sZ = 15.490 | 4.251 | 4.557 | # Observation epoch : 2018/12/18 00:01:30 -> Status = OK # | X | Y | Z = -5543836.577 | -2054585.698 | 2387810.395 | # | sX | sY | sZ = 15.583 | 4.291 | 4.601 | # Observation epoch : 2018/12/18 00:02:00 -> Status = OK # | X | Y | Z = -5543836.364 | -2054585.624 | 2387809.881 | # | sX | sY | sZ = 15.583 | 4.307 | 4.618 | # [...] # Observation epoch : 2018/12/18 06:58:30 -> Status = OK # | X | Y | Z = -5543834.811 | -2054581.220 | 2387809.224 | # | sX | sY | sZ = 6.166 | 2.664 | 2.253 | # Observation epoch : 2018/12/18 06:59:00 -> Status = OK # | X | Y | Z = -5543834.128 | -2054581.138 | 2387808.424 | # | sX | sY | sZ = 5.206 | 2.250 | 1.898 | # Observation epoch : 2018/12/18 06:59:30 -> Status = OK # | X | Y | Z = -5543836.136 | -2054582.119 | 2387809.629 | # | sX | sY | sZ = 7.895 | 3.415 | 2.871 | # Observation epoch : 2018/12/18 07:00:00 -> Status = OK # | X | Y | Z = -5543835.016 | -2054581.957 | 2387809.450 | # | sX | sY | sZ = 7.576 | 3.279 | 2.749 | # > Receiver position status summary: # # # >>> 840 (100%) epochs processed 839 (99%) epochs with valid status 1 (0%) epochs with invalid status # # > Data processing time lapses: # # ····· # # > Elapsed time for reading observation RINEX = 1.90 seconds # # > Elapsed time for computing satellite positions = 0.72 seconds # # > Elapsed time for computing receiver positions = 8.66 seconds # # ==========# # > Data Dumping routine has started # # ==========# # > Dumping satellite observation data... # # ····· # # - Gathered satellite observations # - Number of valid satellites # - Satellite navigation positions # > Dumping satellite line of sight related data... # # ····· # # - Elevation by satellite # - Azimut by satellite # - Line of sight information # > Dumping satellite error modelling related data... # # ····· # # - Ionosphere delay by satellite # - Troposphere delay by satellite # - LSQ residuals by satellite # > Dumping LSQ related data... # # ····· # # - LSQ report by performed iteration per epoch # - LSQ report per observation epoch (last performed iteration) # > Dumping receiver position related data... # # ····· # # - Receiver position solutions in ECEF and ENU frames per epoch # - Dilution Of Precision in ECEF and ENU frames per epoch # > Dumping integrity related data... # # ····· # # - Vertical integrity information # - Horizontal integrity information # > Dumping raw configuration and data hashes... # # ····· # # - Raw general configuration perl hash : "$ref_gen_conf" # - Raw observation data perl hash : "$ref_obs_data" # > Data dumping time lapses: # # ····· # # > Elapsed time for dumping satellite observation data = 0.52 seconds # # > Elapsed time for dumping line of sight related data = 0.35 seconds # # > Elapsed time for dumping satellite error modeling data = # > Elapsed time for dumping least squares related data = # > Elapsed time for dumping receiver position related data = # > Elapsed time for dumping integrity related data = # > Elapsed time for dumping raw configuration and data hash = 0.32 seconds 0. 16 seconds 0. 11 seconds 0. 05 seconds 0. 48 seconds # # # # # # ==========# # > GNSS Rinex Post-Processing routine is over for 'KOKV Demo' # # ==========# # Results are available at : /home/ppinto/WorkArea/demo/grpp/GAL-E1/ # Log file is available at : /home/ppinto/WorkArea/demo/gal_e1_grpp+gspa.log # > Elapsed time for GRPP script = 13.30 seconds # # ##########

3.2.3 Report Module: GNSS Service Performance Analyzer Although GRPP outputs can be interpreted by the user, the amount of information produced by the module is such that it requires significant time and effort to summarize it. Furthermore, GRPP only produces numeric information, and for instance, performance analysis is much easier assessed with plots. Therefore, the report module purpose is two-fold, in order to fill GRPP gaps. Since the end objective of this work is to analyze the different GNSS service positioning performances, the report module has been named as: GNSS Service Performance Analyzer, hereafter donated as GSPA. Still, GSPA not only provides accuracy and integrity performance information but reports most of the data produced by GRPP. Consequently, the GSPA architecture is arranged with the same logic as the GRPP DataDumper package, meaning at the same time that GSPA is dependent from GRPP outputs. Module Architecture The Perl packages which encompass GSPA are showed in Figure 3.8: • ReportPerformances.pm is in charge of providing the positioning performances numeric results as specified in REQ-FUN-58, REQ-FUN-59 and REQ-FUN-60. PlotSatObservation.pm generates the plots which illustrate satellite availability, elevation and geometry during the observation time window. • PlotSatErrorSource.pm shows the modelled error for each SV at each observation epoch like the ionosphere delay or the residual error from WLSQ. • PlotLSQInformation.pm reports in graphical

format the WLSQ routine information. • PlotPosPerformance.pm outputs the plots which account for the positioning accuracy and integrity performances. Furthermore, it displays the positioning solution and the receiver clock bias estimation. • CommonUtil.pm is a package imported by all other GSPA packages. It contains generic functionalities which widely account for the treatment of the data extracted from GRPP outputs. Figure 3.8 – GSPA architecture hierarchy diagram. As previously mentioned, plot packages take advantage of an external library, since Perl built-in features do not offer graphical displays. This Perl library is the Chart::Gnuplot (version 2.23) and its basic functionality relies on arranging chart and dataset objects in order to build Gnuplot scripts, which are then called to generate the plots. The library is part of the Comprehensive Perl Archive Network (CPAN) project, a large collection or Perl SW and documentation that has grown over 24 years. For more information regarding Chart::Gnuplot or CPAN project, visit the following links: [LR.8] and [LR.10]. Public Subroutine Specification GSPA encapsulates the following public subroutines arranged by package (except for CommonUtil). An output file/figure comes along with each subroutine to illustrate the user-end result: • ReportPerformances.pm: ? ReportPostionAccuracy writes in a dedicated file the maximum, minimum and RMS statistics for the receiver vertical, horizontal, position and time domains as indicated in REQ-FUN-58. The file also reports the number of observations and how many of them have a valid position solution. # ---------- ---------- # # > Position accuracy report from CEBR on 2019/05/13 using GPS-C/A # # ---------- # # Component NumEpochs NumOkEpochs % SigmaFactor MinAcc RMSAcc MaxAcc >>> Vertical > Horizontal Position 2880 2880 100.0 3.14 0.06 4.46 16.10 Time 2880 2880 100.0 1.96 0.04 2.39 9.96 2880 2880 2880 100.0 2880 100.0 1.96 0.05 3.05 13.00 2.45 0.04 3.25 9.50 ? ReportPositionError provides the same information as the accuracy report using the real receiver local errors (ENU increments) against the configured reference, fulfilling REQ-FUN-59. # ---------- ---------- # # > Position actual error report from CEBR on 2019/05/13 using GPS-C/A # # ---------- ---------- # > # Component NumEpochs NumOkEpochs % > Vertical > Horizontal Position 2880 2880 2880 2880 100.0 2880 100.0 2880 100.0 MinErr -5.62 0.03 0.09 RMSErr 1.80 1.04 2.08 MaxErr 4.30 2.90 5.73 ? ReportPositionIntegrity reports in a dedicated file the number of observations epochs which were flagged with an integrity event for the receiver vertical and horizontal domains as indicated in REQ-FUN-60. # ---------- ---------- # # > Position integrity report from CEBR on 2019/05/13 using GPS-C/A # # ---------- ---------- # # Component NumEpochs NumOkEpochs % SigmaFactor AlertLimit MI % HMI % SA % > Vertical 2880 2880 100.0 1.96 30.00 660 22.9 0 0.0 2880 100.0 > Horizontal 2880 2880 100.0 2.45 15.00 67 2.3 0 0.0 2880 100.0 • PlotSatObservation.pm: ? PlotSatelliteAvailability shows the information dumped by DumpNumValidSat (GRPP DataDumper subroutine). Figure 3.9 – SV Availability plots for GPS and GALILEO. ? PlotSatelliteElevation illustrates for each SV its observed elevation against the receiver's horizon. The configured mask is presented as shaded grey area. One plot is generated for each GNSS (GPS/GALILEO). Figure 3.10 – SV elevation plots for GPS and GALILEO. ? PlotSatelliteSkyPath displays the SV paths as if the trails were drawn from the receiver's zenith perspective. The paths are colored to represent the observation epoch, thus depicting the SV geometry evolution. In addition, the configured satellite mask is drawn as a shaded grey area. SV falling below the mask, do not account for the receiver position estimation. Figure 3.11 – SV sky-path plots for GPS and GALILEO. • PlotSatErrorSource.pm: ? PlotSatelliteResiduals shows the estimated residuals from WLSQ algorithm of each SV (arranged in the Y axis). The residuals are colored with a bi-polar palette. The highest residuals are colored as either blue or red, whereas small residuals (the optimal situation) are colored with a lighter beige color. This illustrates where the errors are mainly focused. An optimal estimation should equally distribute the residuals among LoS. Figure 3.12 – SV residuals plot for GPS and GALILEO. ? PlotSatelliteIonosphereDelay the plot arrangement is similar as PlotSatelliteResidual differing in the palette type, being a color-value increase for a higher ionosphere delay. This plot should show that higher delays are encountered when the SV have lower elevation, because the slant signal path is greater than its zenital projection. ? PlotSatelliteTroposphereDelay displays the troposphere delay with the same format specified in PlotSatelliteIonosphereDelay. Figure 3.13 – SV ionosphere delay plot. Figure 3.14 – SV troposphere delay plot. • PlotLSQInformation.pm: ? PlotLSQEpochEstiamton generates two types of plots: - The first one summarizes the basic WLSQ information such as the number of iterations performed or the ex-post standard deviation indicator. Figure 3.15 – WLSQ overall report plots. - The second plot type encompass 4 different plots which illustrate each of the receiver parameters (X, Y, Z and clock bias) estimation evolution. The approximate and estimated values are showed in the first subplot. Besides, delta accumulated corrections for all iterations are displayed in the bottom subplot. Figure 3.16 – WLSQ specific parameter estimation report plots. PlotPosPerformance.pm: ? PlotReceiverPosition: outputs three types of plots. - The first plot type emulates a bullseye diagram where the hits are the obtained receiver positions in the horizontal domain. The position origin (0, 0) represents the configured reference position, therefore, the plot is representing the positioning errors committed. Three plots are generated where the positions are colored with its Upping component, horizontal accuracy and observation epoch. - The second plot type is a single chart with a multiplot arrangement in where the ENU components have individually plotted along with a grey line that represents the static reference. Each line is colored with its associated accuracy. In the optimal case, the highest deviations from the reference should be yellow-colored for a better integrity performance. - The last plot type shows the receiver clock bias evolution. The points are colored with the clock bias sigma as in the previous plot. Figure 3.17 – Receiver EN position plots. Figure 3.18 – Receiver ENU position and clock bias solution plots. ? PlotAccuracyPerformance displays the accuracy indicators as specified in REQ-FUN-63. The sigma values are split in two plots, one for the ECEF frame and other one for the ENU frame. Figure 3.19 – Accuracy report plots on ECEF and ENU frames. ? PlotIntegrityPerformance shows the integrity phenomena for the vertical and horizontal domains (arranged in two different plots). The plots were inspired in Figure 2.15 and colors have been added to them for a more intuitive information extraction. An desired integrity position solution occurs when the scaled precision does not over-pass the real error and the alert limit, having SA over most of the observation window. Figure 3.20 – Vertical and horizontal integrity report plots. Module Execution As adopted in GRPP, GSPA is orchestrated by a main Perl script, which is called in order to run GSPA module: • MainSoleService.pl organizes the public GSPA subroutines for running the module as a whole. Moreover, it also loads the user configuration by importing GeneralConfiguration package. The main routine is basically divided in the following steps: ? Plot reporting routine calls the public subroutines allocated in the plotting packages in order to generate the plot images. ? Performance reporting routine calls the subroutines exported by ReportPerformances package to provide the numeric results. Figure 3.21 – GSPA architecture flow diagram. As it can be seen in Figure 3. 21, the execution

flow of GSPA is simpler than GRPP. Each GPSA package uses the hash-interface configuration for running their subroutines and, unlike GRPP, no internal interfaces are needed. GSPA is launched calling the same user configuration file used for running GRPP previously. Otherwise, GRPP outputs will not be available and GSPA will run raising an execution error. GSPA execution is presented in Terminal Demo 3. The execution example is the one used for validating GRPP under GPS- SPS signals (see section 3.3.2). Like GRPP, GSPA also informs the user about which module is currently running and where the outputs will be located. Terminal Demo 3 – GSPA launching example for GPS-SPS C/A on CEBR station. ppinto@ppinto-UbuntuVM:~/WorkArea/demo$ $GSPA cfg/CEBR_GPS-CA.cfg # ## # # > Welcome to GNSS Service Performance Analyzer tool # # ## # # Script was called from : '/home/ppinto/WorkArea/src/GNSS_Service-Performance-Analyzer//MainSoleService.pl' # GRPP data loaded from : '/home/ppinto/Drive/tmp/MASTER/TFM/demo/grpp/GPS-CA' # Configuration loaded from : '/home/ppinto/Drive/tmp/MASTER/TFM/demo/cfg/CEBR_GPS-CA.cfg' # == # # > Plot reporting routine has started # # == # # > Ploting GPS satellite availability # # ····· # # > Ploting GPS observed elevation # # ····· # # > Ploting GPS sky-path # # ····· # # > Ploting GPS satellite residuals # # ····· # # > Ploting GPS satellite ionosphere delay # # ····· # # > Ploting GPS satellite troposphere delay # # ····· # # > Ploting LSQ estimation iformation # # ····· # # > Ploting receiver position solutions # # ····· # # > Ploting accuracy performance results # # ····· # # > Ploting integrity performance results # # ····· # # > Graphical report time lapses: # # ····· # # > Elapsed time for ploting satellite observation data # > Elapsed time for ploting satellite error source data # > Elapsed time for ploting LSQ estimation information = = = 1.87 seconds 2.55 seconds 1.15 seconds # # # # > Elapsed time for ploting positioning performance data = 3.61 seconds # # == # # > Performance reporting routine has started # # == # # > Reporting position accuracy performance # # ····· # # > Reporting position error performance # # ····· # # > Reporting position integrity performance # # ····· # # > Numerical report time lapses: # # ····· # # > Elapsed time for reporting accuracy performance = 0.06 seconds # # > Elapsed time for reporting error performance = 0.10 seconds # # > Elapsed time for reporting integrity performance = 0.08 seconds # # == # # > GNSS Service Performance Analyzer routine is over # # == # # Plots and reports are available at : '/home/ppinto/WorkArea/demo/gspa/GPS-CA/' # Log file is available at : '/home/ppinto/WorkArea/demo/gps_ca_grpp+gspa.log' # > Elapsed time for GSPA script = 9.44 seconds # # ## # 3.3 Performance Verification Verification in the context of a SW lifecycle is intended to demonstrate that the SW is compliant with its specification by means of testing. In other words, Verification designs, executes and checks that the SW fulfills its baseline requirements. In the technological industry, the Verification and Validation (V&V) phase depends on the SW complexity. Nonetheless in most cases, V&V is depicted in a Unitary Test phase, e.g. Perl subroutines are executed individually with controlled inputs and theirs outputs are cross-checked with those expected; and a System Test phase i.e. the entire SW is tested as a whole with different nominal and robustness scenarios. Eventually, the SW performances are also assessed by these verification methods. It can be remarked that performance criteria accomplishment is one of the best indicators (if not the best) of a SW being ready and validated. 3.3.1 Verification Scope The verification phase of a project can be very expensive and time-consuming. For SoL systems, V&V is crucial and mandatory in their contracts. However, considering the scope of this project, the developed SW is neither critical nor real-time, so no Unitary Test are really needed to demonstrate that each feature of GRPP and GSPA works accordingly. As instead, the positioning performance results are much more interesting from the academic perspective, since they will be used to study GPS and GALILEO navigation services. Note that GSPA will not be verified since GSPA does not compute performance indicators by itself. It only arranges those retrieved from GRPP outputs. Consequently, the verification of GRPP would be focused on assess the performances obtained with the SW tool. But, in order to compare GRPP performances, reference data must be stipulated from an outer source. As a result, it was decided to compare GRPP positioning results with those obtained with other GNSS post-processing tool. The discrepancies among both results will then determine if GRPP is successfully verified. The selected tool on where the trust of reference data is relying, has been RTKLIB, which is an open source program developed by T. Takasu for SPP with GNSS. It also includes several enhanced capabilities such as PPP algorithms for both real time and post-processing. It also supports RINEX data format, apart from other protocols. The program consists on a collection of application programs, one per tool functionality. The one which it has been used for the verification of this project has been RTKPOST – Post-Processing Analysis. For more information regarding RTKLIB, please refer to the following link [LR.11]. From both RTKLIB and GRPP, station receiver coordinates are computed in WGS-84 ECEF format. The vector difference can be computed straight forward with a simple subtraction and a root square trace: $cXXX = \sqrt{cX2 + c2X + c2X}$; (3.1) $(cX, cX, cX) = (WBRPP, WBRPP, WBRPP) - (WRRKKBB, WRRKKBB, WRRKKBB)$; Since this difference is obtained for several observation epochs, the RMS, maximum and minimum differences can be computed as representative statistical values: 1 l $LWrcXXX$ = max($cXXX$) ; $LimcXXX$ = min($cXXX$) ; $LLLcXXX = \sqrt{m} \sum ciX2XX$; (3.2) i=0 These values will be used as verification indicators which must fulfill the upcoming criterion for GRPP to be successfully validated. Otherwise, GRPP

specification and implementation should be reviewed and modified. 3.3.2 Verification Cases and Criteria Once the high-level scope of the verification has been set, the case specification and criteria are the next items to be detailed. Since the upcoming performance study campaign will be centered on GPS-SPS and GALILEO-OS, two verification cases can be created accordingly: • GPS-SPS Verification Case. RTKLIB and GRPP will be executed with RINEX data from the same station using only GPS C/A pseudorange signal. • GALILEO-OS Verification Case. RTKLIB and GRP will be executed with RINEX data from the same station using only GALILEO E1 pseudorange signal. Note that GPS-SPS or GALILEO-OS broadcast other free-access signals like L2C. However, RTKLIB does not support the processing of all of them and it was decided that C/A and E1 would represent fairly the verification performances. For both cases, it has been decided to use RINEX from IGS institution (International GNSS Service), who publishes daily data of their associated stations under a free-access repository. After a constellation availability study for GALILEO case, the selected stations have been CEBR and KOKV, located in the Iberia peninsula and Hawaii archipelago as showed in Figure 3.22. Figure 3.22 – IGS reference stations used for the performance verification. Regarding configuration of both tools: • RTKLIB has been configured in single mode, with a 10º mask, using broadcasted ephemerids (RINEX navigation files) for satellite position determination, Saastamonien troposphere correction and broadcasted ionosphere model (which it turned out to be Klobuchar's for both GPS and GALILEO executions). Observation RINEX files needed to be trimmed for the selected constellation and signal observation since RTKLIB does not allow the user to specifically select a single observation source. • GRPP was configured similarly as RTKLIB but setting directly the observation codes (C1C) for C/A and E1 pseudorange observations. Furthermore, some SV needed to be discarded (G04, E14 and E18) due to processing anomalies. Finally, the criterion was set accordingly to the accuracy performance requirements of GPS and GALILEO presented in section 2.6.1. As a remainder, these are the positioning error tolerances for the 95% of the cases. Since verification process is being assessed under nominal conditions, the tolerance threshold criteria will be defined as: • The maximum and minimum difference indicators presented in equation (3.2), shall not exceed 0.5 times the GNSS 3D position accuracy requirement for 95% confidence level. • The RMS difference indicator presented in equation (3.2), shall not exceed 0.2 times the GNSS 3D position accuracy requirement for 95% confidence level. Note that these values are arbitrary and may be further discussed. However, they are acting as a verification tolerance indicator. Beware that there will always be differences among GRPP and RTKLIB, the magnitude on these should be around the GNSS system's precision but, assuming fair system performances, they should never be higher than the worst-case accuracy threshold. In this case, the thresholds have been lowered to the 50% and 20% in order to account for the nominal conditions presented in the verification cases. As a summary, the verification information for both services is detailed in Table 3.12. Table 3.12 – Verification case specification and criteria. GPS-SPS GALILEO-OS Measurement Source C/A pseudorange E1 pseudorange Station CEBR (Iberia Peninsula) KOKV (Hawaii Archipelago) Date 13/05/2019 18/12/2018 Processing Window Whole day From 00:00 to 07:00 Difference Threshold Criteria 5 meters for RMS ±13 m for max/min 8 m for RMS ±19 m for max/min 3.3.3 Verification Results and Reports For producing the verification results, ECEF coordinates obtained with RTKLIB and GRPP were arranged in a spreadsheet and then, their differences were computed as specified in equation (3.1). In addition, plots representing the differences for each coordinate component were drawn. Lastly, the reference position for each station was also incorporated to the plots in order to discard possible gross-singular errors produced by RTKLIB or GRPP. GPS-SPS using C/A signal For GPS-SPS C/A verification case, differences range to a maximum of 5 meters which is the most-known precision when using GPS C/A signal with SPP algorithms. In addition, Figure 3.23 shows a kind-of random pattern in the coordinate differences, probably due to the SV-ephemerid different criteria selection among GRPP and RTKLIB. Therefore, and since verification indicators in Table 3.13 are compliant whit those postulated in section 3.3.2, GRPP can be successfully verified when processing GPS-SPS pseudorange signals. Table 3.13 – Verification difference indicators for GPS-SPS C/A case. Comparison Statistics for GPS-SPS C/A (GRPP – RTKLIB) Diff. X Diff. Y Diff. Z Diff. XYZ (3D) Min -0.9 -1.4 -0.9 0.2 RMS 1.5 0.4 1.2 2.0 Max 4.1 0.9 3.9 4.9 GRPP / RTKLIB Differences in ECEF coordinates 5.00 4.00 3.00 2.00 1.00 0.00 -1.00 -2.00 Diff_X Diff_Y Diff_Z Figure 3.23 – GRPP vs RTKLIB differences using GPS-SPS C/A. GALILEO-OS using E1 signal Unfortunately, for GALILEO verification case, the difference indicator values presented in Table 3.14 do not accomplish the threshold criteria, especially on the maximum difference. By looking at the differences in the ECEF coordinates displayed in Figure 3.24, it can be seen how the discrepancy among GRPP and RTKLIB is concentrated on a few epochs in the ECEF X component. A closer look to this coordinate obtained with both tools, and displaying its station (KOKV) static reference, is showed in Figure 3.25. Table 3.14 – Verification difference indicators for GALILEO-OS E1 case. Comparison Statistics for GALILEO-E1 (GRPP – RTKL IB) Diff. X Diff. Y Diff. Z Diff. XYZ (3D) Min -15.2 -5.2 -5.4 0.5 RMS 7.1 2.6 3.2 8.2 Max 23.4 5.1 6.3 24.2 Figure 3.25 is illustrating that the highest difference seems to be due by an RTKLIB outlier. Note that RTKLIB result is uneven with the real station X coordinate. Also, note that in the remaining observations epochs, the differences are within the expected range. At this point, it can be assured that these discrepancies are caused by an unexpected behavior in RTKLIB. We could think of a GALILEO system failure as well, but GRPP results are fairly aligned to the reference using the same processing data and no GALILEO issues were published for that date. Eventually, it was decided to re-compute the verification indicators excluding the observation epochs presenting this anomaly. 30.00 25.00 20.00 15.00 10.00 5.00 0.00 -5.00 -10.00 -15.00 -20.00 GRPP / RTKLIB Differences in ECEF coordinates -5543810.00 -5543820.00 -5543830.00 -5543840.00 -5543850.00 -5543860.00 -5543870.00 Diff_X Diff_Y Diff_Z Figure 3.24 – GRPP vs RTKLIB differences using GALILEO-OS E1. ECEF X Coordinate RTKLIB_X GRPP_X REF_X Figure 3.25 – ECEF X coordinate against its real value, obtained with RTKLIB and GRPP using GALILEO-OS E1. Difference indicators in Table 3.15 are now compliant with the threshold criteria defined in section 3.3.2. Moreover, the differences observed in the ECEF coordinates are also within the expected GALILEO precision. Thus, it can be conluded that GRPP is also successfully verified for GALILEO-OS pseudorange signal processing. However, it must be remarked that indicators are compliant with a very narrow margin, beign almost at the threshold value. This is probably caused by a poor GALILEO SV geometry, causing a worse accuracy performance as disscussed in section 2.6.1. Note that at that time (18/12/2018) GALILEO constellation was not in FOC, having 20 SV which were operating with a reliable status. As a metter of fact, the RTKLIB anomaly previously observed was located on a time window when only the minum number of SV were observed (this is 5 SV). GSPA satellite availability plots for this execution were presented in section 3.2. 3 (Figure 3. 9 and Figure 3. 11). Also note in Figure 3.15, where GPS and GALILEO WLSQ estimations can be comapred, the difference among degrees of freedom: GPS has in most epochs at least 3 DoF whereas this situation in GALILEO is exceptional. This leaves no doubt about GPS and GALILEO verification performance differences, as it will be concluded too

in the upcoming analysis chapter. Table 3.15 – Verification difference indicators for GALILEO-OS E1 without RTKLIB outlier. Comparison Statistics for GALILEO-E1 (GRPP – RTKLIB) Diff. X Diff. Y Diff. Z Diff. XYZ (3D) Min -15.2 -5.2 -5.4 0.5 RMS 6.7 2.6 3.3 7.9 Max 5.9 5.1 6.3 17.1 10.00 5.00 0.00 -5.00 -10.00 -15.00 -20.00 GRPP / RTKLIB Differences in ECEF coordinates Diff_X Diff_Y Diff_Z Figure 3.26 – GRPP vs RTKLIB differences using GALILEO-OS E1 without RTKLIB outlier. Chapter 4: Analysis 4 Analysis: Positioning Performance Study Campaign As introduced in chapter 1, the main academic objective is to apply the knowledge acquired in chapter 2 and the methodology developed in chapter 3 in a GNSS study-case. This is encompassed in this forth analysis chapter, where the effort is focused on the positioning performance assessment of GPS-SPS and GALILEO-OS with real data. In other words, the analysis chapter presents the committed positioning performance campaign with GRPP and GSPA SW. Along this chapter, the major campaign features and results will be detailed and commented in order to later assess the project conclusions (refer to chapter 5). The following sections are focused in the most relevant campaign items: starting by its purpose and scope, passing through the planification and ending up with the performance results obtained. For the sake of clarity, not all detailed campaign results are available in the document (like every single GSPA plot). If any detailed campaign result is wished to be consulted, a dedicated free-access repository is available for this purpose. Please refer to annex 0. 4.1 Motivation and Description The importance of GNSS products, from a civilian-end perspective, rely on their economic potential and their market reach. Over 8 million of devices are expected to incorporate GNSS antennas and navigation solutions by 2020 (see European GNSS market report [BR.12]). This potential relies in the provision of an enough-accurate position with a global and continuous service. Therefore, the positioning performances are directly related with the GNSS solutions benefit and the investment for a GNSS to be improved and evolved. Moreover, the GNSS ecosystem has evolved from a single/dual constellation usage (traditionally GPS and GLONASS) to a multi-GNSS constellation environment with the rise of BEIDOU, GALILEO and the rest of local navigation services such as EGNOS or WAAS (see section 2.3). Although nowadays the GNSS receiver market tendency is indisputably focused on a multi-frequency solution, is still of interest to develop single-frequency SPP algorithms. Needless to point that these have the easiest implementation and lowest cost approach (hence a huge market reach, as mentioned in section 1.1), but they also lead to study single-constellation and single-service performances. Eventually, it does not matter how complex is the GNSS and service combination if a sole service or constellation is not performing as expected in the reality. This is the core interest of studying performances individually and the reason being for using real data in the assessment. Seeing that navigation accuracy is the most valuable performance from a user perspective, this performance will be assessed in the campaign by presenting the accuracy results obtained with GRPP and reported by GSPA. As a reminder of section 2.6.1, accuracy is the error bound of a solution which is provided thanks to the observation redundancy. Normally the user trusts the navigation algorithm's accuracy, not even wondering if the solution is being representative of its actual error. In order to fill this gap, not only accuracy is considered but also its solution integrity. Recalling section 2.6.2, integrity indicates how reliable a systems navigation solution is. Integrity will also be measured from GSPA reports. Finally, and as stated in the project's title, accuracy and integrity positioning performances will be study for both GPS-SPS and GALILEO-OS (under nominal and singular conditions) using single-frequency SPP methodology presented in chapter 3. 4.1.1 Main Objectives As previously mentioned, this master thesis work had initially a main objective which it turned out to be complemented by an additional one. The main settled objective was to study the positioning performances of GNSS free-access services. But on the run, a dedicated GNSS processing SW was borne for committing this intention, forming then a baseline version for a new open-source tool contribution to the GNSS user community. Consequently, it can be said that the campaign's reason being serves the preliminary objective, but it goes beyond that. The actual campaign purpose is two-fold: • Assess accuracy and integrity performances for both GPS-SPS and GALILEO-OS signal services, by means of processing its data with GRPP+GSPA SW. • Demonstrate GRPP+GSPA potential in a real study-case in order to further validate it as a user- oriented tool. The first objective will be assessed numerically by comparing the performances obtained with GPS and GALILEO services on both receiver vertical and horizontal domains. The second objective will be assessed with a more subjective approach by illustrating GRPP+GSPA results along the campaign presentation (section 4.3). 4.1.2 Expected Results In order to introduce the expected campaign results, it is noteworthy to have a clear picture of the status of both GPS and GALILEO systems. The campaign has been performed over observation dates between August 2018 to April 2019. At that time, GPS satellite constellation was operating in FOC with over 30 SV in healthy conditions. Therefore GPS-SPS status can be expected to be nominal with very few and ground-segment notified anomalies. However, GALILEO has not acquired at the time being FOC. On August 2018, 20 SV were orbiting the earth, 3 of them with an unhealthy status: E14 and E18 (due orbit eccentricity); and E22, which was removed from active service until further notice. On November 2018, 4 new SV entered service accounting for a total of 21 SV operating in nominal conditions. The incompletion of GALILEO satellite constellation is a key fact to consider since not as many satellites as GPS-SV would be available. Obviously, this will be affecting the SV-observation geometry, degrading at the same time GALILEO performances. Having stated the aforementioned conditions, the following campaign expected results can be listed according to each target performance: • Accuracy is expected to meet the requirements stipulated in section 1.1, with worse vertical domain performance. Although these requirements are in fact more demanding compared to those in section 2.6.1, the expectations are kept optimistic since it is usual to obtain better performances under nominal conditions. Nonetheless, GALILEO status will lead to worse accuracy performances compared to those in GPS; but in any case, they should not be worse than those stipulated by its own system definition document (refer to [BR.16]). • Integrity cannot possibly be compared with any reference criteria. However, it can be presumed that better integrity results are expected in the horizontal domain rather than in the vertical one. In addition, GPS-SPS integrity outcomes will be better than those on GALILEO, demonstrating that fair integrity performance requires a good SV observation geometry. Finally, if accuracy performances have been accomplished as expected, SA should be close to the 95% and MI should not overpass the 30% whereas HMI shall be very few (less than 7%), unless in special scenario conditions. Expected campaign positioning performances are schematically presented in Table 4.1. Table 4.1 – Expected performance campaign results. Performance Domain GPS-SPS GALILEO-OS Horizontal Meet criteria of Table 1.1. Expected even better results. Meet criteria of Table 1.1. If not, at least meet worst case requirements in Table 2.7. Accuracy Vertical Meet criteria of Table 1.1. Assumed worse performance than horizontal domain. Meet criteria of Table 1.1. If not, meet at least the worst-case requirements in Table 2.7. Assumed a worse performance than horizontal domain. Horizontal Expect more than 95% of SA with a maximum of 20% MI and 5% HMI under nominal conditions. Expect in most cases SA dropped under

95% (70% minimum) with more than 20% MI and 5% HMI under nominal conditions. Integrity Vertical Expect around 95% of SA with a maximum of 30% of MI and 5% HMI under nominal conditions. Expect in most cases SA dropped under 95% (50% minimum) with slightly more than 30% of MI and 5% of HMI under nominal conditions. Apart from assess performances in nominal conditions, the campaign will also include scenarios where non-nominal conditions are taken place. These will be ionosphere critical phenomena (refer to section 4.2.2). Positioning performances will also be measured in these cases, but since the behavior under abnormal phenomena is non-deterministic, no expected results will be stipulated. As instead, the obtained results will serve as comparison among normal and abnormal situations. This will add further vale to the analysis phase and will also illustrate how accuracy and integrity unfold under critical circumstances. 4.2 Data Arrangement For committing the proposed performance study campaign, a data-source and a preliminary planification was essential. Regarding the data source, it was already used in section 3.3 the IGS station network for the GRPP+GSPA performance verification. For the campaign it has not been different since IGS provides the widest free- of-charge GNSS data collection. More specifically, it has been taken in advantage the Multi-GNSS Experimental Service (hereafter denoted as MGEX) which is a pilot project of IGS institution. The IGS-MGEX is a dedicated service to track, collect and analyze all possible GNSS signal services. Of course, this includes the legacy and non-legacy GNSS like GPS and GALILEO. Over a four-year period, MGEX has been gathering GNSS data from their tracking stations and publishing them in open repositories, along with processed GNSS products such as precise SV positions. For more information regarding MGEX, please refer to the bibliography references: [BR.10] and [BR.11]. From MGEX service, a set of stations will be selected, and then different observation dates will also be determined in order to gather a data archive in where to study the positioning performances. This will be detailed in the upcoming sections: 4.2.1 and 4.2.2. The downloaded data has been GRPP inputs: RINEX observation and navigation files. Figure 4.1 – IGS MGEX available tracking stations. Source: igs.org Regarding preliminary planification and prior to the data download, it was necessary to select those stations and dates with a fair GPS and GALILEO constellation availability. For committing this purpose Trimble GNSS Planner was used (see [LR.12]). This planner is web-based and uses the almanac data of the GNSS constellations for building an observation report. In addition, it also displays the SV anomalies and even the ionosphere TEC and critical phenomena like scintillation. The Trimble GNSS planner was especially helpful for planning GALILEO processing windows since without this tool, more tedious approaches would have been necessary, turning the campaign in a much more time-consuming process. 4.2.1 Selected Stations The IGS MGEX stations selected for the performance campaign are identified by its four-letter combination and listed in Table 4 .2. The location of these stations can be geographically consulted in the world map of annex A.6. Table 4.2 – Detailed information of selected stations for campaign. Station City Country Agenc y Lat Long Height (m) Receiver ABMF Les Abymes Guadeloupe IGN 16.26231 N 61.52753 W -25.0 LEICA GR25 FAIR Fairbanks USA JPL 64.97800 N 147.49924 W 319.2 JAVAD TRE_G3TH DELTA KIRU Kiruna Sweden ESOC 67.85730 N 20.96840 E 391.1 SEPT POLARX4 KOKV Kokee Park USA JPL 22.12626 N 159.66493 W 1167.5 JAVAD TRE_G3TH DELTA KOUG MAJU Kourou Rita, Majuro French Guiana Marshall Islands CNES GA 5.09847 N 7.11914 N 52.63975 W 171.36453 E 107.2 33.9 SEPT POLARX5TR SEPT POLARX4TR OWMG Owenga New Zealand CNES 44.02430 S 176.36880 W 21.6 TRIMBLE NETR9 TASH Tashkent Uzbekistan GFZ 41.32805 N 69.29557 E 439.7 JAVAD TRE_G3TH DELTA Eight stations have been selected according to five different geographical areas. These areas were not randomly selected. As contrary, they were carefully chosen in order to study the GPS and GALILEO performances over different locations. Note that the stations are spread in different latitudes and longitudes for accounting different phenomena which may affect the GNSS measurement processing. Station Precise Reference It was already explained in section 2.5.4 that in order to measure integrity performance the reference station coordinates shall be precisely defined. The precise coordinates of the aforementioned stations were extracted from the ITRF realizations (refer to section 2.4.2 for ITRF definition). The campaign station precise coordinates are presented in Table 4.3. Note that the these ECEF coordinates are given in ITRS whereas GRPP results are outputted in WGS84. However, both references are so closely aligned that the difference between them is insignificant, considering the accuracy magnitude expected in the campaign, as so it happens with the different ITRF realizations. Last but not the least, GRPP SW loads the precise coordinates defined in Table 4.3 by reading a dedicated data file containing all the stations coordinates. Afterwards, GRPP loads the reference of the configured station for the static and integrity modes. The data file is stored under a dat directory in the GRPP+GSPA repository (refer to annex A.1). Table 4.3 – Campaign stations precise ITRF coordinates. Station ECEF X [m] ECEF Y [m] ECEF Z [m] ITRF realization ABMF 2919785.720 -5383745.056 1774604.712 ITRF14 KIRU 2251420.712 862817.279 5885476.769 ITRF14 KOKV -5543838.239 -2054586.439 2387810.121 ITRF14 OWMG -4584393.742 -290932.452 -4410048.404 ITRF96 TASH 1695945.059 4487138.593 4190140.719 ITRF14 FAIR -2281621.697 -1453595.838 5756961.799 ITRF14 KOUG 3855263.343 -5049731.993 563040.402 ITRF14 MAJU -6257572.259 950332.805 785215.297 ITRF14 4.2.2 Selected Dates Once target IGS stations were defined, the next step was to select the observation dates of each location. By making different date arrangements. It was concluded that three dates would be enough to cover the positioning performance analysis. These three dates are dedicated to study different scenarios which may affect differently to the GNSS measurement processing and SV availability: • Date #1 will be set as the same UTC time processing window for all stations. Since the stations are world-wide spread, this date will test if the GNSS has indeed global coverage. • Date #2 sets a different time in each campaign station in order to encounter good SV availability. This date will test both GPS and GALILEO free-access services with the best possible constellation availability. • Date #3 also sets a different UTC dates for each station. But unlike Date #2, the dates have been selected according to ionosphere critical events such as high TEC or scintillation phenomena. Summing up, it could be stated that Date #1 and Date #2 test the performances under nominal conditions and Date #3 under singular conditions. The detailed time setting for each station-date pair is listed in Table 4.4. Note in Table 4.4 that stations for Date #1 and Date #2 are the same whereas Date #3 includes different ones. The initial objective was to maintain the same stations for all dates. However, issues for selecting time windows with critical ionosphere conditions were found and hence, different stations were set. Once again, for selecting the dates presented in Table 4.4 Trimble GNSS planner was quite useful (as a matter of fact, several GSPA plots were inspired by those found in this tool). On the one hand, the SV availability plots helped to determine those dates with fair GALILEO constellation availability for Date #2. On the other hand, ionosphere information displayed in this tool was essential in order to identify the time windows for Date #3 as showed in Figure 4.2. Table 4.4 – Selected station-date pair for campaign. Station ABMF KIRU KOKV OWMG TASH ABMF KIRU KOKV OWMG TASH FAIR KIRU KOKV KOUG MAJU Date ID Date #1 Date #2 Date #3 Date Day of year Processing start time

Processing end time 20/02/2019 51 6:00 10:00 20/02/2019 51 6:00 10:00 20/02/2019 51 6:00 10:00 20/02/2019 51 6:00 10:00 20/02/2019 51 6:00 10:00 20/02/2019 51 6:00 10:00 29/04/2019 119 13:00 21:00 18/12/2018 352 0:00 9:00 26/04/2019 116 8:00 18:00 07/04/2019 97 7:20 17:20 26/08/2018 238 6:20 9:40 07/03/2019 66 20:00 23:59 16/04/2019 106 18:00 23:59 22/11/2018 326 14:00 22:00 10/04/2019 100 1:00 11:00 Figure 4.2 – Ionosphere conditions over MAJU and FAIR stations for Date #3 analysis. Each critical ionosphere phenomena for each station is listed in Table 4.5. High TEC values are usually found in equatorial latitudes, not as scintillation events, which are more singular and located in high latitudes. Scintillation is known for being a rapid electron density change in the ionosphere layers which affects electro-magnetic waves severely. Find more information about this phenomenon on [LR.13]. Table 4.5 – Date #3 critical ionosphere phenomena on each station. Station Critical Ionosphere Phenomenon Observations FAIR Moderate-Severe Scintillation Between 8:00 and 10:00 UTC KIRU Moderate Scintillation At around 22:00 UTC KOKV Moderate TEC Maximum of 40 TECU KOUG Moderate TEC Maximum of 35 TECU MAJU High TEC Maximum of 95 TECU 4.2.3 Selected Signals As a recap of GNSS systems services explained in section 2.3, GPS and GALILEO encompass different free-access service which are provided by different carrier frequencies, ranging codes and navigation data. For GPS-SPS, the signals offered nowadays are C/A, L2C, L5C and L1C (refer to theory section 2.3.1 for a deeper specification). For the campaign realization, it has been selected: • Legacy C/A signal. • New-generation L2C signal. L5C and L1C wanted to be incorporated but eventually were discarded due to the few SV available broadcasting these signals. Also note that worse performances may be obtained with L2C since not all SV incorporate this ranging code. Regarding GALILEO, available signals encompassing the OS are E1, E5a and E5b (refer to section 2. 3.2 for a more detailed explanation). For the campaign study, it has been decided to process GRPP with: • E1 signal • E5a/E5b signals (depending on station receiver signal disposition). It would have been very interesting to incorporate E5 signal (combination of E5a and E5b through AltBOC modulation) since this signal-service seems to offer very promising performances in the simulations (refer to [BR.7]). However, the algorithm implementation was far-too complex and finally it was decided to leave this signal out of the campaign's scope. Eventually, it was concluded to launch the campaign processing with 4 different free-access GNSS signals. These are listed in Table 4.6 along with its expected pseudorange domain errors. A relevant technical detail related with the expected errors in Table 4.6 needs to be highlighted. Remember from GRPP specification (see REQ-FUN-49 and REQ-FUN-50) that the expected observation error is configured by the user and used by GRPP in order to account for the ponderation performed when estimating the receiver position parameters. The criteria followed for the campaign GRPP configuration has been to configure the 1% of the chip length of each signal observation. The chip length is defined as the longitude of each ranging code bit as shown in Figure 4.3. The chip length can be directly computed knowing the number of bits which form the code sequence and its chipping rate (refer to [BR.2] for formulae definition). Consequently, signal's chipping rate is indirectly proportional to the expected pseudorange error e.g. E1 against E5a/E5b specifications. Note that, the higher the chipping rate, the more precise ranging code correlation is achieved but wider bandwidths are needed. Table 4.6 – Selected signal-service observations and expected error in the pseudorange domain. System GPS GPS GALILEO GALILEO Service SPS SPS OS OS Carrier Signal Frequency [MHz] C/A 1575.42 L2C 1227.6 E1 1575.42 E5a/E5b 1176.45 / 1207.14 Chipping rate [Mbps] 1.023 1.023 1.023 10.23 Chip length [m] 293.05 293.05 293.05 29.30 Expected precision [m] 3.0 3.0 3.0 0.3 Figure 4.3 – Chip length illustration along with signal's bandwidth. Source: Hoffman et al. 2008. 4.3 Obtained Results Having stated the data arrangement for the campaign analysis, the observation and navigation RINEX files were downloaded and archived in an Ubuntu MATE virtual machine. Then the whole campaign launch process was assessed by automatizing its routine with Perl and Bash scripts (these can be consulted in the dedicated campaign repository of annex 0). The campaign is formed by 5 stations on 3 observation dates and 4 signal executions. This is translated in 60 GRPP+GSPA executions to be carried out for the campaign. Once again, script automatization came in handy for its management. Configuration Brief A small mention about GRPP+GSPA configuration needs to be added before presenting the campaign results. Since 60 executions were needed, 60 configuration files were necessary too. It would have been very tedious to configure each of them individually. Therefore, the configuration for the campaign was assessed by using 4 configurations templates (one for each signal). These are available in the campaign repository. The configuration was kept with a basic profile. For both GPS-SPS and GALILEO-OS: • Satellite mask of 10º. • Klobuchar model for ionosphere correction. • Saastamoinen model for troposphere correction. • Expected observation error according to Table 4.6. • Maximum of 4 iterations on LSQ routine and a convergence threshold of 0.0001 m. • Accuracy scale factors to account for the 95% of reliability in both vertical and horizontal domains. • Static mode with station references set according to the precise coordinates defined in Table 4.3. • Integrity mode with stipulated alert limits according to our own accuracy requirements in Table 1.1. The configuration differing among GPS and GALILEO was the ephemerids time-out threshold and the discarded SV: • Ephemerid time threshold: ? For GPS 1.5 hours ? For GALILEO 0.5 hours This is due to different navigation data layout in the RINEX format. On GPS side, the ephemerids block among each SV are spaced more or less by two hours, whereas on GALILEO case they are normally separated 10 minutes (though it can be more). Eventually, this specific configuration was needed in order to do not use timed-out navigation data. • Discarded SV: ? None for GPS ? E14, E18 and E24 (not in all scenarios) for GALILEO As previously commented, E14 and E18 are the two SV with a higher eccentricity due to launching issues. In addition, E24 was ripped of some E5a/E5b processing since residual plots showed significant noise in the first campaign iterations for this SV. 4.3.1 Campaign Processing Status For successfully launching the whole campaign, one iteration was not enough. As a matter of fact, 6 trials were necessary due to input data processing issues, such as GPS navigation files which did not include Klobuchar ionosphere coefficients. Nevertheless, 97% of the executions were successfully launched. Among all campaign executions, not all epochs had a valid position status. The campaign scenario status is exemplified in Table 4.7 and completely included in annex 0 (Table 8.6). Is not a surprise that GALILEO scenarios account for fewer valid processing status than GPS cases due to the announced lack of SV availability. Additionally, it can be observed that GPS C/A status for Date #1 and Date #2 are very similar, but this is not the case for GALILEO. When the same processing time window is set (as in Date 1) for an incomplete constellation, availability lacks in a global network are logically encountered. Table 4.7 – Campaign executions status extract. Station Date System Signal Epochs Valid Epochs Invalid Epochs Valid % Invalid % ABMF DATE_1 GPS C/A 481 481 0 100.0 0.0 OWMG DATE_2 GPS L2C 1201 1201 0 100.0 0.0 KOUG DATE_3 GAL E1 961 954 7 99.3 0.7 KIRU DATE_2 GAL E5b 721 698 23 96.8 3.2 MAJU DATE_3 GPS L2C 1201 1152 49 95.9 4.1 TASH DATE_2 GPS L2C 1201 846 355 70.4 29.6 KOKV DATE_1 GAL E1 481 318 163 66.1 33.9 TASH DATE_1 GAL E5b 481 308 173 64.0 36.0 FAIR DATE_3 GAL E1 401 203 198 50.6 49.4 TASH DATE_2 GAL E5b 1201 587 614 48.9 51.1

Unfortunately, two executions out of the 60 performed needed to be discarded. These two are the GALILEO scenarios in MAJU station on Date #3. Available GSPA plots seem to show a total lack of observed SV. Nonetheless, the root cause should be further investigated. Henceforth, these executions will not be included in the campaign results. 4.3.2 Accuracy Results Regarding accuracy performance campaign results, these have been arranged by campaign date. On each date, two figures are available which account for each GPS-SPS and GALILEO-OS. Inside each figure, the accuracy RMS indicators are available for each station, horizontal/vertical domain and system signal combination. Minor comments for each graph will be included. More important, accuracy issues and expected performance results will be highlighted and later discussed in section 4.3.4. Date #1 Vertical and Horizntal Accuracy RMS on Date #1 for GPS-SPS 11.0 10.0 9.0 8.0 RMS [m] 7.0 6.0 5.0 4.0 3.0 2.0 1.0 0.0 ABMF KIRU KOKV OWMG TASH HRMS C/A 3.8 2.2 3.4 2.9 2.2 VRMS C/A 4.6 2.5 3.3 2.4 3.0 HRMS L2C 3.2 5.9 6.4 2.3 6.4 VRMS L2C 3.8 6.2 6.1 2.1 8.1 Figure 4.4 – Campaign accuracy results on Date #1 for GPS-SPS. Vertical and Horizntal Accuracy RMS on Date #1 for GALILEO-OS 11.0 10.0 9.0 8.0 RMS [m] 7.0 6.0 5.0 4.0 3.0 2.0 1.0 0.0 ABMF KIRU KOKV OWMG TASH HRMS E1 5.3 7.0 4.6 6.1 5.6 VRMS E1 6.8 10.0 4.7 4.9 8.1 HRMS E5a/E5b 10.3 6.8 29.2 5.8 5.3 VRMS E5a/E5b 12.9 9.7 29.7 4.1 8.0 Figure 4.5 – Campaign accuracy results on Date #1 for GALILEO-OS. From Figure 4.4 and Figure 4.5 a better performance on the GPS side is immediately deduced. In fact, GPS accuracy performance is quite good specially for C/A signal not as for L2C due to the fewer SV available broadcasting this signal. All GPS performances fall within the expected results from section 4.1.2. Some GSPA plots examples with fair performances are sowed in page 120. For GALILEO results, a worse performance than in GPS cases is observed but this was expected due to the constellation incompletion. However, the performances of both signals meet the expected results criteria except for KOKV case. KOKV accuracy results can only be accepted with the requirements listed in Table 2.7. The KOKV issue is later assessed in page 123. Also note that performance among GALILEO in each station is more heterogenous. This is caused by the stations and time window selection. Since GALILEO has less than 24 SV, global coverage cannot be reached, hence having an impact in the accuracy performance. Date #2 Vertical and Horizntal Accuracy RMS on Date #2 for GPS-SPS 11.0 10.0 9.0 8.0 RMS [m] 7.0 6.0 5.0 4.0 3.0 2.0 1.0 0.0 ABMF KIRU KOKV OWMG TASH HRMS C/A 2.5 2.0 3.7 2.6 2.1 VRMS C/A 3.0 2.9 3.6 2.5 3.5 HRMS L2C 2.8 3.5 7.1 1.8 3.1 VRMS L2C 3.3 5.7 6.2 1.8 4.2 Figure 4.6 – Campaign accuracy results on Date #2 for GPS-SPS. Vertical and Horizntal Accuracy RMS on Date #2 for GALILEO-OS 11.0 10.0 9.0 RMS [m] 8.0 7.0 6.0 5.0 4.0 3.0 2.0 1.0 0.0 ABMF KIRU KOKV OWMG TASH HRMS E1 6.4 6.1 7.2 4.3 4.6 VRMS E1 8.5 10.4 8.2 4.6 7.2 HRMS E5a/E5b 10.3 5.9 28.9 12.7 5.1 VRMS E5a/E5b 13.4 7.0 28.1 11.6 7.6 Figure 4.7 – Campaign accuracy results on Date #2 for GALILEO-OS. Again and as expected, a better performance is accomplished in GPS side by looking at Figure 4.6 and Figure 4.7. GPS-SPS accuracies accomplish the expected results exceeding expectations in most cases. Date #2 was supposed to have fair constellation availability conditions. Consequently, better performances compared to those in Date #1 should be encountered. This seems to be the case for GPS (by a very narrow margin) but for GALILEO only a few instances of signal E1 present a significant improvement while some others are even worse. Most probably, the E14, E18 and E24 SV were included in the preliminary planning and then discarded for the campaign processing, eventually resulting in a worse observation geometry than the one predicted. GALILEO E1 scenarios are accomplish (tough in the limit) the expected results. However, some E5a/E5b executions seem to be problematic (again, especially in KOKV). Date #3 Vertical and Horizntal Accuracy RMS on Date #3 for GPS-SPS 11.0 10.0 9.0 8.0 RMS [m] 7.0 6.0 5.0 4.0 3.0 2.0 1.0 0.0 FAIR KIRU KOKV KOUG MAJU HRMS C/A 2.7 2.5 4.1 2.8 2.4 VRMS C/A 2.9 3.2 4.0 3.4 3.3 HRMS L2C 3.6 5.9 10.6 4.9 3.6 VRMS L2C 3.7 10.4 9.3 6.5 5.1 Figure 4.8 – Campaign accuracy results on Date #3 for GPS-SPS. Vertical and Horizntal Accuracy RMS on Date #3 for GALILEO-OS 11.0 10.0 9.0 RMS [m] 8.0 7.0 6.0 5.0 4.0 3.0 2.0 1.0 0.0 FAIR KIRU KOKV KOUG HRMS E1 14.7 4.6 6.6 17.2 VRMS E1 11.4 5.7 7.2 22.6 HRMS E5a/E5b 14.8 6.5 44.9 17.9 VRMS E5a/E5b 11.5 7.2 49.1 23.0 Figure 4.9 – Campaign accuracy results on Date #3 for GALILEO-OS. In the scenarios where non-nominal conditions are encountered, performances suffer from degradation as expected (see Figure 4.8 and Figure 4.9). Beware that for Date #3 is not as important meeting the expected results but to compare them with the ones obtained under nominal conditions. Nonetheless, GPS services are fulfilling the expected results even in critical conditions, especially for C/A signal where performances stay the same. Nonetheless, significant performance degradation does happen for L2C signal, meaning that ionosphere phenomena effects are projected through weaker SV constellation geometries. This statement is confirmed too by observing GALILEO performances where FAIR and KOUG cases seem to have a very bad constellation disposition. Is quite surprising that GALILEO performances stay nominal on KIRU and KOKV-E1 cases performing even better than in L2C homologous occurrences. 4.3.3 Integrity Results For integrity performance, results have also been arranged by processing date. For each date, percentages regarding integrity events (MI, HMI and SA) are represented on four figures. Each figure stands for the combination among the signals and the receiver local components (vertical and horizontal domains). Like accuracy results, minor comments are included for each date and most relevant results are highlighted and then detailed in section 4.3.4. Date #1 Horizontal Integrity Indicators on Date #1 for GPS-SPS 100.0 90.0 80.0 70.0 60.0 50.0 40.0 30.0 20.0 10.0 0.0 ABMF -C/A KIRU -C/A KOKV -C/A OWMG- C/A TASH -C/A ABMF -L2C KIRU -L2C KOKV -L2C OWMG- L2C TASH-L2C Horizontal HMI Horizontal MI Horizontal SA 0.0 0.0 0.0 0.0 2.5 3.5 100.0 100.0 99.2 0.0 0.0 0.0 0.0 0.0 0.6 2.3 4.4 14.3 4.9 100.0 100.0 100.0 74.2 72.9 0.0 9.2 100.0 0.0 5.5 74.6 Figure 4.10 – Campaign horizontal integrity results on Date #1 for GPS-SPS. Vertical Integrity Indicators on Date #1 for GPS-SPS 100.0 90.0 80.0 70.0 60.0 50.0 40.0 30.0 20.0 10.0 0.0 ABMF -C/A KIRU -C/A KOKV -C/A OWMG- TASH -C/A ABMF -L2C KIRU -L2C KOKV -L2C C/A OWMG- L2C TASH-L2C Vertical HMI Vertical MI Vertical SA 0.0 0.0 0.0 1.2 12.7 11.2 100.0 100.0 100.0 0.0 0.0 0.0 0.0 0.2 91.3 11.0 26.8 12.5 8.5 100.0 100.0 100.0 99.8 95.6 0.0 98.6 100.0 3.4 10.4 93.4 Figure 4.11 – Campaign vertical integrity results on Date #1 for GPS-SPS. For GPS integrity performance under Date #1 nominal conditions (Figure 4.10 and Figure 4.11), C/ A integrity performances on both vertical and horizontal domains are outstanding and exceed the expected results, except for OWMG. In fact, seems like OWMG has vertical integrity issues for both signal-services, meaning that the root cause may be related with the site instead of the signal. The most suspicious fact for this is OWMG precise coordinates ITRF realization which it turns to be the oldest (see Table 4.3). For L2C integrity performances these are bit odd and do not perform as well as C/A. Nonetheless this is due to the fewer SV available. Surprisingly, L2C vertical performances accomplish more SA trading off higher MI cases (compare L2C KOKV and TASH cases among vertical and horizontal components). Horizontal Integrity Indicators on Date #2 for GALILEO-OS 100.0 90.0 80.0 70.0 60.0 50.0 40.0 30.0 20.0 10.0 0.0 ABMF-E1 KIRU-E1 KOKV-E1 OWMG-E1 TASH-E1 ABMF-E5b KIRU-E5b KOKV-E5b OWMG- E5b TASH-E5b Horizontal HMI Horizontal MI Horizontal SA 0.0 0.0 0.0 0.0 0.0 0.0 0.0 16.4 36.2 0.0 34.9 2.7 21.3 21.3 3.0 0.0

81.4 72.4 91.2 67.6 75.3 41.6 75.9 16.4 0.0 2.7 81.5 0.0 34.7 80.2 Figure 4.12 – Campaign horizontal integrity results on Date #1 for GALILEO-OS. Vertical Integrity Indicators on Date #1 for GALILEO-OS 100.0 90.0 80.0 70.0 60.0 50.0 40.0 30.0 20.0 10.0 0.0 ABMF-E1 KIRU-E1 KOKV-E1 OWMG-E1 TASH-E1 ABMF-E5b KIRU-E5b KOKV-E5b OWMG- E5b TASH-E5b Vertical HMI Vertical MI Vertical SA 0.0 0.0 0.0 0.0 0.0 0.0 0.0 18.9 52.8 0.0 35.8 32.4 5.7 3.1 0.4 7.5 87.5 79.3 97.5 100.0 82.7 65.3 84.8 26.4 0.0 86.8 100.0 0.0 11.4 83.4 Figure 4.13 – Campaign vertical integrity results on Date #1 for GALILEO-OS For GALILEO, integrity performances are much more degraded compare to those obtained with GPS as expected (Figure 4.12 and Figure 4.13). It can be deduced a severe SA lost specially in the horizontal domain. High MI events (higher than 20%) are more often encounter in the vertical than in the horizontal domain. Also note that KOKV is manifesting its processing issue with high HMI cases. It can be stated that expected performances are accomplished by a very narrow margin, except for ABMF and KOKV E5b executions. In addition, note again the OWMG precise coordinate definition issue. Date #2 Horizontal Integrity Indicators on Date #2 for GPS-SPS 100.0 90.0 80.0 70.0 60.0 50.0 40.0 30.0 20.0 10.0 0.0 ABMF -C/A KIRU -C/A KOKV -C/A OWMG- TASH -C/A ABMF -L2C KIRU -L2C KOKV -L2C C/A OWMG- L2C Horizontal HMI Horizontal MI Horizontal SA 0.0 0.0 0.0 28.0 2.4 1.6 100.0 100.0 99.5 0.0 0.0 0.0 0.3 0.4 15.1 9.2 37.1 19.5 13.9 100.0 100.0 99.9 95.4 77.2 0.0 67.8 100.0 0.0 35.5 97.4 Figure 4.14 – Campaign horizontal integrity results on Date #2 for GPS-SPS. Vertical Integrity Indicators on Date #2 for GPS-SPS 100.0 90.0 80.0 70.0 60.0 50.0 40.0 30.0 20.0 10.0 0.0 ABMF -C/A KIRU -C/A KOKV -C/A OWMG- C/A TASH -C/A ABMF -L2C KIRU -L2C KOKV -L2C OWMG- L2C Vertical HMI Vertical MI Vertical SA 0.0 0.0 0.0 30.3 20.4 9.5 100.0 100.0 100.0 0.0 0.0 0.0 2.8 0.4 66.6 66.5 41.1 32.4 29.4 100.0 99.3 99.9 95.0 93.6 0.0 61.9 100.0 0.6 72.9 97.8 Figure 4.15 – Campaign vertical integrity results on Date #2 for GPS-SPS. On Date #2 for GPS-SPS (Figure 4.14 and Figure 4.15), similar results as those obtained previously under nominal conditions in Date #1 are obtained. At least for SA and HMI indicators but not for MI where expected results are not met in most cases even with C/A signal. This situation is especially relevant in ABMF, KIRU and TASH stations. Regarding OWMG this is not relevant since we have already commented the potential issue with this station. Furthermore, KOKV seems to present a horizontal L2C SA lost, probably due to the SV observation availability. The SA is improved in the vertical domain but at the expense of increasing MI cases over 20%. Horizontal Integrity Indicators on Date #2 for GALILEO-OS 100.0 90.0 80.0 70.0 60.0 50.0 40.0 30.0 20.0 10.0 0.0 ABMF-E1 KIRU-E1 KOKV-E1 OWMG-E1 TASH-E1 ABMF-E5b KIRU-E5b KOKV-E5b OWMG- E5b TASH-E5b Horizontal HMI Horizontal MI Horizontal SA 0.0 0.0 0.0 0.0 0.0 0.0 6.0 14.0 4.8 12.5 21.9 10.2 15.4 3.7 1.7 68.4 84.3 76.0 90.7 92.5 44.5 88.7 8.3 0.3 0.8 42.8 0.0 12.8 88.9 Figure 4.16 – Campaign horizontal integrity results on Date #2 for GALILEO-OS. Vertical Integrity Indicators on Date #2 for GALILEO-OS 100.0 90.0 80.0 70.0 60.0 50.0 40.0 30.0 20.0 10.0 0.0 ABMF-E1 KIRU-E1 KOKV-E1 OWMG-E1 TASH-E1 ABMF-E5b KIRU-E5b KOKV-E5b OWMG- E5b TASH-E5b Vertical HMI Vertical MI Vertical SA 0.0 0.0 0.6 1.4 0.0 0.7 0.0 3.2 27.4 6.5 32.0 29.8 39.9 19.5 11.2 2.8 76.7 93.0 84.1 97.2 95.7 60.1 97.0 18.2 3.5 18.1 63.5 0.0 47.9 94.0 Figure 4.17 – Campaign vertical integrity results on Date #2 for GALILEO-OS. For GALILEO integrity results on Date #2, it can be deduced that expected performances are met specially for SA indicator (Figure 4.16 and Figure 4.17). Once again KOKV and OWMG present processing issues. Obviously, GPS performances are far better, but for Date #2 the difference is not as big as in Date #1. This may be due to the date selection nature: Date #1 was set as the same UTC processing window for both GPS and GALILEO whereas Date #2 epochs were selected based on the best SV availability scenario. Date #3 100.0 90.0 80.0 70.0 60.0 50.0 40.0 30.0 20.0 10.0 0.0 Horizontal HMI Horizontal MI Horizontal SA 100.0 90.0 80.0 70.0 60.0 50.0 40.0 30.0 20.0 10.0 0.0 Vertical HMI Vertical MI Vertical SA Horizontal Integrity Indicators on Date #3 for GPS-SPS FAIR -C/A KIRU -C/A KOKV -C/A KOUG -C/A MAJU -C/A FAIR -L2C KIRU -L2C KOKV -L2C KOUG-L2C MAJU-L2C 0.0 0.0 0.0 0.0 0.0 0.0 0.9 0.4 0.0 0.0 2.5 3.5 23.3 21.0 21.1 3.0 9.9 25.7 29.8 15.3 100.0 100.0 97.0 100.0 100.0 100.0 83.5 47.0 89.6 95.4 Figure 4.18 – Campaign horizontal integrity results on Date #3 for GPS-SPS. Vertical Integrity Indicators on Date #3 for GPS-SPS FAIR -C/A KIRU -C/A KOKV -C/A KOUG -C/A MAJU -C/A FAIR -L2C KIRU -L2C KOKV -L2C KOUG-L2C MAJU-L2C 0.0 0.0 0.3 0.0 1.0 0.0 2.7 32.7 2.3 45.0 4.0 25.8 73.5 58.0 66.1 14.0 22.8 16.6 70.0 36.5 100.0 100.0 100.0 100.0 100.0 100.0 79.7 77.4 91.4 98.4 Figure 4.19 – Campaign vertical integrity results on Date #3 for GPS-SPS. As expected, Figure 4.18 and Figure 4.19 demonstrate that integrity performances are severely affected when facing abnormal ionosphere conditions. Despite that for GPS horizontal performances stay more or less the same, for the vertical domain these suffer from dramatic increase in either MI or HMI. Obviously, this is the expected behavior since ionosphere delay affects the receiver's zenithal component. The only remarkable exception is FAIR station which is not so affected by the scintillation. It shall be remarked that the vertical MI cases are significant in C/A signal while HMI cases for L2C are extreme for KOKV and MAJU executions. As in accuracy, seems like integrity performance degradation is largely projected through weaker SV geometries (differences in SV observation availability among C/A and L2C). Horizontal Integrity Indicators on Date #3 for GALILEO-OS 100.0 90.0 80.0 70.0 60.0 50.0 40.0 30.0 20.0 10.0 0.0 FAIR-E1 KIRU-E1 KOKV-E1 KOUG-E1 FAIR-E5b KIRU-E5b KOKV-E5b Horizontal HMI Horizontal MI Horizontal SA 0.0 5.9 51.2 0.0 1.2 91.6 0.0 34.6 77.8 0.0 15.8 56.4 0.0 3.4 48.8 0.0 2.0 71.2 16.0 2.1 22.2 Figure 4.20 – Campaign horizontal integrity results on Date #3 for GALILEO-OS. Vertical Integrity Indicators on Date #3 for GALILEO-OS 100.0 90.0 80.0 70.0 60.0 50.0 40.0 30.0 20.0 10.0 0.0 Vertical HMI Vertical MI Vertical SA KOUG-E5b 0.2 3.1 19.3 FAIR-E1 KIRU-E1 KOKV-E1 KOUG-E1 FAIR-E5b KIRU-E5b KOKV-E5b 0.0 0.0 28.6 6.1 0.0 0.2 20.3 12.8 18.4 34.2 19.4 20.7 2.0 7.9 56.2 95.0 89.1 76.7 57.1 91.6 31.2 Figure 4.21 – Campaign vertical integrity results on Date #3 for GALILEO-OS. KOUG-E5b 2.7 2.4 34.5 For GALILEO integrity outcomes on non-nominal conditions (Figure 4.20 and Figure 4.21), when comparing them to those obtained in the other dates (discarding pesky KOKV case), the performances are degraded specially in the vertical domain as expected. But compared to those obtained on the same date with GPS, a few interesting facts can be enumerated. Firstly, a worse SA indicator is clearly observed in GALILEO side most probably due to the fewer SV availability. Secondly, MI and HMI indicators are much better than those in GPS. It can be assumed that even with the lack of observed SV, GALILEO presents better alarming performances which are achieved by trading-off SA on the way. Finally, it is important to recall that MAJU station was discarded due to GALILEO processing issues. It would have been very interesting these results sine MAJU station seems to hold the worst integrity outcome in the whole campaign. 4.3.4 Detailed Results For this section, major campaign results aspects commented on section 4.3.2 and 4.3.3 are presented and detailed with GSPA output plots in order to better depict the performance analysis. If any further detailed results need to be consulted these are accessible through the campaign repository (refer to annex 0). Fair Performances Status Figure 4.22 shows the positioning errors and the horizontal integrity performance obtained with C/A signal. This is a clear example of GPS-SPS exceeding the expected performances under nominal

conditions. A random position pattern can be observed in the polar plot with a slightly biased upping component estimation, but only reaching 4 m as maximum, which is quite good for this service. Furthermore, the error white noise patter corresponds to the LSQ hypothesis detailed in equation (2.44), therefore is not a surprise that horizontal integrity is accomplished with 100% of SA and only a few MI cases. Figure 4.22 – GPS C/A expected performances under nominal conditions. On Figure 4.23 and Figure 4.24, positioning performances obtained with GALILEO-OS signals are displayed. They key aspect on both graphs is that most of the solutions are centered and do follow a random pattern distribution around the reference, but some positions are far away from it. However, it can be deduced that these anomalous solutions are mainly due to the SV availability. Figure 4.23 comes along the WLSQ report which indicates a very few DoF. Figure 4.24 is complemented with the SV availability plot which in most cases, the number of valid SV is not greater than 7. Figure 4.23 – GALILEO E1 expected performances under nominal conditions (accounting for fewer SV). Figure 4.24 – GALILEO E5b expected performances under nominal conditions (accounting for fewer SV). Last but not the least, Figure 4.25 is a good example of fair performances, but this time obtained under non-nominal circumstances. Seems like L2C signal is not affected by the scintillation event in FAIR on Date #2. However, a few MI cases in the vertical domain occur just when the abnormal event was reported (see Table 4.5). This means that eventually L2C signal is affected but probably due to its fair SV geometry disposition its performances are not severely degraded. Figure 4.25 – GPS L2C fair performances under non-nominal conditions. Constellation Geometry Disposition Figure 4.26 – SV geometry affecting GALILEO-E1 positioning results. GSPA sky plot and its color palette applied to the observation epoch have turned to be very useful for analyzing the SV geometry impact on the positioning performances as showed in Figure 4.26 and Figure 4.27. On Figure 4.26, apart from a NW bias in the position solution, it can be seen how the cloud is also spread in the SW to NE direction. This is due to the SV geometry observed next to it. Note that the SV geometry is mainly aligned in all processing epochs in the NW-SE direction, thus "letting the solution to be free" in the complementary direction (SW-NE). This behavior is better depicted in Figure 4.27. Note that, for instance, solutions around 8:00 AM (colored in green) have a fair SV geometry and thus a centered and non-biased solution at the reference is obtained. As opposite, solution obtained at 9:00 AM (colored in red) has a SV geometry aligned in the E-W direction, thus producing a North-biased positioning estimation. Figure 4.27 – SV geometry affection on GPS-C/A positioning results. Unexpected Processing Issues Figure 4.28 – GALILEO-E5b KOKV processing issue illustration. Figure 4.28 illustrates the so commented issues encountered in KOKV when processing GALILEO E5b signal. It can be immediately deduced some kind of error correlated with time, not presenting a random pattern as expected and exemplified previously in the fair performances instances. Also note that the residuals are especially high (15 meters) for E31 and E04, but with such a few SV it could not be possible to discard them. Possible explanations for this behavior could be: • KOKV receiver issues. This is assumed since all issues are always encountered in this station. However, reviewing receiver models in Table 4.2, this is the same than TASH station. Nonetheless other phenomena like multipath could be taken place. • GRPP bug when processing E5b signal. This cause is also suspicious since GRPP has not been validated using this signal. It is believed that the root cause may be located at the navigation data selection since the errors showed in Figure 4.28 were obtained in other processing tests and they were due to incorrect clock parameters selection. However, this behavior is not observed in any other campaign scenario. Eventually, KOKV root cause issue should be further investigated and assessed in future campaign versions. Figure 4.29 – OWMG systematic positioning error and vertical integrity issue. Figure 4.30 – OWMG parameter estimation showing high correction over approximate position. Regarding OWMG issue mentioned in 4.3.3, Figure 4. 29 and Figure 4. 30 illustrate more information regarding the root cause problem. By looking at Figure 4.29, it can be pointed that integrity MI cases are due to a continuous precision against error overflow. The polar plot is also showing a biased positioning estimation, which do not seem to be due to signal anomalies but to the station reference coordinates. Indeed, by observing Figure 4.30, the approximate position is corrected in both X and Z ECEF components by around 6 meters. In conclusion, all these evidences seem to point that OWMG precise ITRF station coordinates need to be updated. Note that the time between the ITRF 1996 realization used as a reference (see Table 4.3) and the campaign processing year, is 23 years, which it turns to be a significant period of time for coordinates to have suffered from tectonic plate displacement, especially in the pacific area. Ionosphere Abnormal Phenomena Impacts Figure 4.31 – MAJU SV elevation and ionosphere correction under critical events. Figure 4.32 – MAJU positioning results and integrity performance under high TECU events. Figure 4.32 and Figure 4.33 show C/A performances over MAJU station under abnormal ionosphere conditions. It can be concluded from both figures that a total lack of integrity is encountered when SV have a lower elevation which is translated in a high ionosphere correction provided by Klobuchar's model, but not effectively mitigated. This was expected since Klobuchar estimates a complex mean such as the ionosphere by a cosine amplitude function (recall section 2.5.3). Note also in the polar plot on Figure 4.32 how the ionosphere is affecting the horizontal domain "spreading" the position solutions. Finally, an interesting phenomenon which has taken place over KIRU station during scintillation phenomena is depicted in Figure 4.33. Note that the "peak" in the polar plot is caused by a progressively augmentation of the accuracy (which by the way accomplishes integrity performance quite well). This peak can be placed when the scintillation event occurred (see Table 4.5, approximately at 22:00), thus evidencing that the event had a symbolic impact on the positioning solution. Figure 4.33 – FAIR ionosphere scintillation event and accuracy performance impact. Chapter 5: Conclusions 5 Conclusions Chapter 4 has presented the analysis campaign performed with the methodology explained in chapter 3. Both chapters were introduced by chapter 1 and supported by the theory frame in chapter 2. Consequently, the thesis conclusions are ready to be enumerated in this chapter. The conclusions cover the main aspects of the thesis which are not just a few. Therefore, this chapter has been divided in three main sections as follows: • Section 5.1 comprises the conclusions regarding the methodology techniques used, i.e. the SW tool development. • Section 5.2 lists the conclusions about the analysis phase i.e. the positioning performance study campaign. • Section 5.3 relates the main objectives presented in section 1.1 with the final thesis conclusions in order to determine their grade of accomplishment. These sections start with a brief recap of the procedures followed through-out the work and then the conclusions are enumerated. The conclusions may be also grouped in different subsections attending to their complexity. Finally, section 5.4 has been added in order to account for future work lines which may arise from this thesis. They are mainly focused in improvements and additions to the SW tool developed which will hopefully be implemented in future versions. 5.1 Regarding Methodology Techniques As a recap, the followed methodology has been to produce a dedicated SW tool for processing GNSS pseudorange measurements using single-frequency SPP algorithms in order to report accuracy and integrity performances for GPS-SPS and GALILEO-OS. Since it was decided that the SW will

constitute an open source tool contribution to the GNSS community, the development approach adopted was contextualized in a SW lifecycle waterfall model with three differentiated phases: specification, implementation and validation. This was necessary in order to produce a controlled user-oriented solution. Specification was defined by the SW PIDS and their abstraction into high-level concepts diagrams and baseline requirements to be implemented in the SW algorithms. Implementation was carried out by selecting Ubuntu MATE, and Perl as programming language. Perl hash data structure was used in advantage of settling common interfaces for connecting SW modules and packages. Eventually two main tools were produced: GRPP and GSPA. Finally, verification phase was assessed by performance comparison among GRPP and RTKLIB. The positioning results of both tools were compared and then analyzed against stipulated pass/fail criteria based on the GPS and GALILEO positioning requirements. GRPP finally showed to be compliant for processing GPS-SPS and GALILEO-OS signals. About SW lifecycle adopted • Lifecycles are essential for SW development. They guarantee an organized approach and a traced environment for documenting, evolving, maintaining and bug-fixing a SW. The waterfall is a simple SW development model which is based on a sequence of steps very easy to follow. However, by adopting this model, SW development process requires more time and effort. • Specification phase settles the baseline requirements which must be covered in the SW through technical implementation. • Implementation constitutes the detailed abstraction of the SW which is better illustrated with the hierarchy and flow diagrams besides of its public function specification. • Verification phase is intended to check that proper SW implementation has been done and requirements are fulfilled. However, verification is also resource-consuming and can adopt a more pragmatic approach by validating the SW results against reference data. About developed SW tools: GRPP and GSPA • GRPP and GSPA are user-oriented tools which maintain a friendly usage only requiring a common configuration file. In addition, they alert about configuration mistakes, input issues and processing warnings. • The wide GRPP/GSPA configuration allows for flexibility and different executions. However, the user must have theory knowledge regarding each processing parameter since otherwise, it could lead to undesired results. • The GRPP SPP algorithms do not encompass high complexity implementation. However, this effort is significantly increased when adding custom user configuration and different GNSS. • GRPP can act as white box tool since it dumps most its internal data. This also accounts for user- customized data exploitation. • GRPP has proven to be verified when processing GPS-SPS and GALILEO-OS (at least C/A and E1 signals) by accomplishing similar positioning results compared to other available GNSS processing tools i.e. RTKLIB. GSPA fulfills its reporting requirements apart from digesting all GRPP outputs in order to produce quality plots which have proven to summarize efficiently all the processing information. • Ubuntu OS and Perl programming languages are fitted for developing SW products from scratch and have allowed a faster, flexible and organized implementation. 5.2 Regarding Analysis Campaign Recalling the analysis campaign carried out, its main objective has been to assess individually signal-service accuracy and integrity performances with real data of GPS-SPS and GALILEO-OS. The expected results were stipulated in Table 4.1 expecting better performances in GPS than in GALILEO. The campaign data was gathered from 5 IGS stations, part of the MGEX project. The data was arranged in 3 different dates: Date 1 set the same UTC processing time window in order to test global coverage, Date 2 set a different date for having the best SV availability and Date 3 was configured to encounter critical ionosphere phenomena. The selected signal-services to study have been GPS-SPS C/A and L2C; and GALILEO- OS E1 and E5a/E5b. This campaign arrangement led to 60 GRPP+GSPA executions which were automatized with scripting skills. The configuration used for it, was kept basic only differing in the ephemerid time-out threshold among GPS and GALILEO, apart from the discarded SV in on GALILEO side. Campaign launching process was done iteratively until all executions were available. The results firstly reveled that several GALILEO scenarios (and some of GPS-L2C) had significant lacks of valid position status as expected. Accuracy results show an overall picture of GPS-SPS offering better accuracy than GALILEO-OS as it was expected. However, it must be pointed out some exceptions where GALILEO is performing better than L2C. Date 1 and 2 have obtained nominal accuracy values which exceed expectations with C/A signals and meeting expected results for L2C, E1; with some exception on the GALILEO side. Date 3 shows accuracy degraded performances as expected, meaning that accuracy is increasing in order to bound the higher error due to the abnormal ionosphere phenomena. Regarding integrity results, again for nominal conditions on Date 1 and 2, GPS-SPS seems to offer better integrity performances than GALILEO (especially SA), due to the higher number of SV in orbit. Although in some cases GPS is presenting more MI, rather than GALILEO which seems to be trading off less MI events with less SA. This observation is specially revealing in Date 3 where GPS integrity performances are severely degraded with HMI events, not as GALILEO which are mainly degraded by dropped SA. Finally, GPSA plots have revealed campaign features like OWMG outdated reference, SV geometry impact on positioning error or MAJU high TEC consequences in vertical integrity. Probably without the added value of GSPA plots, these observations would have never been explored. About campaign usefulness • Sole single-frequency signal service performance measurement with real data is highly relevant in the context on a multi-GNSS and multi-frequency environment where each individual signal-service needs to work accordingly to its requirements. The most relevant GNSS positioning performance from a user perspective is the system accuracy but integrity is equally meaningful since its measuring the representativeness of the system solution against its real position. New generation GNSS services need to be evaluated and compared with real data respect the legacy services. In the EU, this attention is focused over GALILEO compared to GPS positioning solutions. • GNSS performance campaigns should be studied in different locations and under different phenomena. This work has showed that very different results can be obtained in different locations and different times. About IGS-MGEX data source and Trimble Planner • IGS comprises a wide open-access GNSS data and product archive. This service is significantly useful for scientific research and algorithm testing. The MGEX project has proven to be essential for accessing GNSS legacy and non-legacy measurements and navigation data. Thanks to its receiver network, necessary GPS and GALILEO data has been acquired. • Trimble GNSS Planner came in handy thanks to its configuration and displays. This has been very useful for planning the campaign, especially for setting fair GALILEO SV availability windows and for encountering ionosphere abnormal phenomena. About GPS-SPS and GALILEO-OS meeting the expected performances results • GPS-SPS using C/A signal has proven to exceed expectations regarding accuracy performance, being most of the times between 3-4 meters, even in abnormal conditions. Regarding integrity, the expected results are met but a few exceptions regarding high MI and SA losses under abnormal conditions must be pointed out. • GPS-SPS using L2C signal meets accuracy requirements under nominal conditions (sometimes by a narrow margin) and these are exceeded during some abnormal ionosphere events. Regarding integrity under nominal conditions, L2C signals meets the criteria in some scenarios whilst in some other SA losses and high MI are taken place. Integrity under non-nominal conditions is severely affected presenting high

occurrences of HMI events. • GALILEO-OS using E1 signal seems to meet the expected accuracy results, sometimes even under abnormal conditions. Though most of the times integrity results are met, this service is showing in many cases SA losses and high MI occurrences. Nonetheless, integrity under abnormal conditions is keeping the same performance levels as in nominal conditions except in KOKV station. GALILEO-OS using E5a/E5b does not meet in most cases accuracy criteria under nominal conditions, not even accomplishing its own system definition requirements, especially in KOKV station. In the counterpart, integrity seems to be maintained with few MI occurrences trading off SA under 50%, discarding KOKV issues. About performance comparison among GPS-SPS and GALILEO-OS GPS C/A signal seems to offer better positioning performances than GPS L2C signal. This is mainly due to the fewer GPS SV broadcasting L2C signal which leads to a worse SV geometry disposition and fewer observation redundancy. GALILEO E1 signal offers most of the time better performances than E5a/E5b signal. However, this may be due to processing issues encountered with E5a/E5b signal or GALILEO issues broadcasting E5a/E5b signals as showed in discarded satellite E24. • GALILEO E1 signal has worse accuracy and integrity performances when compared to GPS C/A signal. This is caused by GALILEO constellation incompletion, although it shall be remarked that GPS-SPS defines better accuracy requirements than GALILEO-OS. The only case when GALILEO E1 seems to perform better is when alarming under abnormal ionosphere conditions, whereas GPS maintains SA at the expense of increasing MI events. GALILEO E1 and GPS L2C signals are more similar in terms of accuracy with slightly more cases of L2C performing better than E1. These similarities are caused by the more balanced SV availability among E1 and L2C signals. For integrity performance, both signals do also offer similar performances with again, E1 trading-off SA by fewer MI events under critical ionosphere conditions; while L2C maintains higher SA but at the expense of increasing dramatically MI and HMI occurrences. About measured performances extrapolation Extrapolating the SPP algorithms presented in this thesis into a receiver implementation, the following presumptions can be adopted regarding GPS-SPS and GALILEO-OS performances under nominal conditions: • GPS C/A can provide a fair accuracy under 7 meters in the horizontal domain and 11 meters in the vertical domain. This positioning service can be trusted accounting for a maximum of 20% MI events and more than 95% of SA. • GPS L2C can provide an accuracy around 7 meters in the horizontal domain and 11 meters in the vertical domain. This positioning service can be trusted accounting for higher MI events than the 20% and SA around 95%. • GALILEO E1 can provide accuracy around 7 meters in the horizontal domain and 11 meters in the vertical domain. This positioning service can be trusted accounting for higher MI events than the 30% and SA around 80% with even greater drops. • GALILEO E5a/E5b cannot provide a fair accuracy of 7 meters in the horizontal domain and 11 meters in the vertical domain. However, the positioning solution integrity can be trusted with fewer MI than the 30% and a dropped SA under the 80% in most cases. The aforementioned performances cannot be truly trusted under ionosphere abnormal conditions since accuracy is increased in order to bound the higher observation error and integrity may suffer from severe degradations, especially with poor SV geometry disposition. About detailed campaign results Minimum geometry of 5 SV is not enough to ensuring fair accuracy and integrity. Optimal results are obtained when having at least 3 DoF, hence 8 SV are required for warranty nominal positioning performances. • SV geometry affects significantly to the positioning performances. As a matter of fact, accuracy and integrity performances are dramatically affected when measured through bad SV geometry dispositions. • Precise reference definition is essential in order to measure properly integrity performance. ITRF realizations must be reviewed since reference station coordinates may have been displaced in areas of high tectonic plate activity. • KOKV results with E5b signal may evidencing a GRPP feature which needs to be improved. This is the algorithm for GALILEO ephemerid selection. On top of that, GPS ephemerid selection is fairly achieved with a sole time-out threshold which can be set to 1.5 hours. For GALILEO, this is more complex matter since ephemerids are separated by data source (F/NAV and I/NAV) and normally broadcasted every 10 minutes. • Severe HMI events can take place during critical ionosphere phenomena such as high TEC and scintillation. They mostly occur in weak SV geometry observations. • Ionosphere critical events can degrade accuracy, but this is necessary in order to cover the actual error due to the abnormal phenomena. This is accomplished with fair SV availability and geometry disposition i.e. at least 8 SV observed. • Multi-GNSS solutions present a clear advantage over single-service approaches, since more SV will be available. Nonetheless, only services with homogeneous performances should be combined. Otherwise, a worst outcome than in the sole service case could be produced. About GRPP+GSPA usage • GRPP and GSPA has proven its usage through a real user-oriented application. Not only GRPP+GSPA is able to measure positioning performances, but with the proper automatization, it is useful to carry out a performance study campaign with over 60 executions. • GRPP output information and its arrangement through GSPA have proven its user-oriented potential. Many deductions and information can be extracted by only observing a few plots. 5.3 Regarding Thesis Purpose The last conclusions will be related to the project purposes listed in at the introduction in section 1.1. Note that their intention is to close out the entire work and to highlight what abilities has the student been able to apply in the context of the master's degree. As a reminder, the listed thesis purposes were related to: • Develop GNSS SW tools. A summary regarding the activities carried out for this purpose is available at the beginning of section 5.1. • Assess GNSS positioning performances using the SW tools developed in the context of this work. The performance assessment is summarized in section 5.2. • Apply the knowledge gained through the master's degree in Geomatics and Geo-information. The theory framework of chapter settles the technical background studied whereas methodology and analysis chapters also illustrate several skills learnt during the master's courses. Additionally, these conclusions will remark other relevant aspects. For instance, the applied skills which have not been studied but have complemented the master's aptitudes. Finally, the closing observations regarding the possible impact which this thesis may have in the social benefit or the scientific community will be highlighted. These are key aspects for technical disciplines, such as the geomatics, to be valued and recognized. About GNSS SW development objective • Regarding the development of GNSS algorithms by the student, it can be pointed that this objective has been accomplished satisfactorily. The clearest evidence is the developed GRPP+GSPA SW. • Moreover, the SW development phase has been addressed by adopting a waterfall lifecycle process. This process has shown that, despite that it adds significant effort, their organizational advantages are worth it in order to develop more professional SW products. On top of that, thanks to the lifecycle applied, the student has carried properly the SW activities which can be encountered in a real enterprise scenario. Not only this SW has helped to fulfill the thesis purposes, but it has contributed to form settled tool which will hopefully have transcendence to other users. About GNSS positioning performance assessment objective • Regarding the assessment of GNSS positioning performances, it can be concluded that this objective has been successfully fulfilled. Apart from accuracy, integrity performance has been introduced and effectively

measured, This performance has added a significant value from the user's perspective since it has illustrated the correctness of the GNSS positioning solution. • In addition, performances have also been measured under nominal and abnormal conditions illustrating how GNSS solutions can range in terms of positioning error. • On top of that, performances have also been measured through a world-wide network thanks to IGS and MGEX services. This has enabled GPS-SPS and GALILEO-OS performance extrapolation. About applied master's degree knowledge • Regarding the knowledge gained through the master's degree in geomatics and geo-information, it can be stated that several disciplines and skills have been applied to this thesis: ? Firstly, spatial geodesy techniques regarding GNSS measurement processing have been settled through the academical framework and successfully applied in the thesis methodology under a practical application scope. ? Secondly, programming skills have been the core of this project. Not only for the SW produced but also for the automatization of the campaign executions. ? Lastly, the computer programming skills have been taken to a higher level. Going from the paradigm of private script development to the user-oriented SW production. About contribution to the social benefit and scientific community • It can be pointed that this master thesis work has a clear potential for contributing to the social benefit and the scientific community. The evidences for this rely on the methodology and the analysis phases: ? On the one hand, the assessment of positioning performances has a direct impact on the social benefit as it has been showed by the GNSS market sector. This niche has exponentially grown in the last years and seems to maintain this tendency thanks to the positioning applications which can be derived from it. ? On the other hand, the developed approach of GRPP and GSPA will constitute a contribution to the GNSS scientific community. In the near future, the first tool version will be available in a free- access repository for anyone to download and execute it. 5.4 Future Evolutions Last but no the least, several future evolutions regarding developed SW and positioning performance exploration will be enumerated. It shall be pointed that these modifications can be divided in current or short-term improvements, and enhancements or long-term evolutions of GRPP+GSPA. The items mentioned hereafter will be incorporated in future versions of GRPP and GSPA, tough it cannot be assured its due date because of its altruist nature. Hopefully, as more users make use of the tool, some of them could decide to join the project and contribute to its development. Short-Term Additions • Firstly, the ephemerid selection algorithm should be improved as concluded in section 5.2. It has been noted that a single time-out threshold may work properly when processing GPS but other GNSS like GALILEO require a more sophisticated approach. • Secondly, in order to account for a more user-friendly usage GRPP and GPSA should incorporate: • ? ? ? User manual for GRPP and GSPA. This feature is essential for users to understand and being able to execute the tool and interpret their results. Basic configuration file. The current configuration is only useful for advanced users since the technical background of each parameter should be known. This is an important aspect since most of the users would like to see a default configuration for some options e.g. LSQ convergence threshold. Another relevant aspect is to offer an automated tool installation. Current GRPP and GSPA are dependent of PDL and Chart::Gnuplot libraries and its dedicated environments. These dependencies need to be manually configured and this can be tedious for many non-experienced users. Regarding GRPP functionalities, the following improvements could be introduced in the upcoming versions: ? NeQuick algorithm for GALILEO ionosphere correction. In fact, this feature was planned to be included in the preliminary version of GRPP presented in this thesis. However, for the sake of simplicity, NeQuick was kept out the scope due to its implementation complexity. ? Dual signal processing. It would mean a significant enhancement for GRPP to estimate the receiver position combining, for instance, GPS and GALILEO pseudorange measurements. This could also lead to study performances with multi-GNSS services. ? Support further GNSS. GLONASS, BEIDOU and even SBAS will add a significant value to GRPP and will enable performance study on these systems. On top of that, GSPA could also account for further functionalities: ? Preliminary position plots of GSPA only account when the receiver is in static mode. They should also cover receiver kinematic scenarios. ? So far, GPSA plots and numeric results are outputted in a directory with no arrangement. This should be improved for a better user experience, arranging the plots and results in a settled format such as PDF or HTML. Long-Term Evolutions • Several new features and modules could be added in order to improve tool's functionality: • • ? Carrier phase measurement processing module could be added for higher precision applications. On the flip side, as more precision is obtained, more implementations are required such as time and reference system transformations e.g. receiver coordinates obtained in WGS84 and transformed to ITRS. ? A Precise Point Positioning (PPP) module should be incorporated. This will increase dramatically the tool's value since current GNSS research activities are focused on PPP techniques due to its advantages for sole-receiver absolute positioning with sub-metric accuracy. ? Further corrections and error root cause mitigation could be added such as cycle slip detection or multipath extenuation. Another interesting feature for a more versatile usage is the alternative to input certain parameters using precise products: ? Precise orbit SP3 files could be read in order to account for a more accurate SV frame. For instance, this could be used for focusing only on receiver error sources. ? Precise receiver and SV clocks products could be read as well. This could enable to fix the receiver clock bias and only estimate its position components. ? IONEX files for having precise information regarding ionosphere corrections. This may be used for focusing in the troposphere correction and its extrapolation for measuring weather parameters such as water vapor. In addition, the tool could also support different GNSS data sources and not only RINEX format. Some examples could be RTCM and even real-time protocols. Finally, a total user-friendly experience will be offered by developing a dedicated Graphical User Interface (GUI) for configuring and launching the tool. Chapter 6: Acronyms 6 Acronym List Table 6.1 – Acronym List. Acronym Stands for A/S Anti-Spoofing AL Alert Limit ASCII American Standard Code for Information Exchange AltBOC Alternate Binary Offset Carrier BGD Broadcast Group Delay BOC Binary Offset Carrier BPSK Binary Phase Shift Keying BR Bibliography Reference C/A Coarse Acquisition CDMA Code Division Multiple Access CFG Configuration CRINEX Compressed RINEX CS Commercial Service CTP Conventional Terrestrial Pole DoD Department of Defense DOP Dilution of Precision ECEF Earth Centered, Earth Fixed EGNOS European Geostationary Navigation Overlay Service ENU Easting, Northing and Upping ENV Environment ESA European Space Agency ETSIGCT Escuela Técnica Superior de Ingeniería en Geodesia Cartografía y Topografía F/NAV Freely Navigation Message FOC Full Operational Capability FUN Functional GAL GALILEO GGSP Galileo Geodetic Service Provider GIOVE GALILEO In Orbit Validation GLONASS GLObal NAvigation Satellite System GNSS Global Navigation Satellite System/ Service GPS Global Positioning System GPST GPS Time GRPP GNSS RINEX Post-Processing GSPA GNSS Service Performance Analyzer GST GALILEO System Time GTRF GALILEO Terrestrial Reference Frame GUI Graphical User Interface HAL Horizontal Alert Limit HMI Hazardous Misleading Information HW Hardware I/NAV Integrity Navigation Message ICD Interface Control Document IERS International Earth Rotation Service IGS International GNSS Service IOC Initial Operational Capability IOV In-Orbit Validation ITRF International

Terrestrial Reference Frame ITRS International Terrestrial Reference System LoC Line of Code LoS Line Of Sight LR Link Reference LSQ Least Squares MGEX Multi-GNSS Experimental Service MI Misleading Information NAV Navigation Message NAVSTAR Navigation System With Ranging and Timing OS Open Service / Operative System PDL Perl Data Language PIDS Preliminary Item Design Specification PPP Precise Point Positioning PPS Precise Positioning Service PRN Pseudo-Random Noise PRS Public Regulated Service REQ Requirement RINEX Receiver Independent Exchange Format RMS Root Mean Square RMSE Root Mean Squared Error RTCM Radio Technical Commission for Maritime Services RTK Real Time Kinematic S/A Selective Availability SA System Availability SAR Search and Rescue SBAS Space Based Augmentation System SIS Signal In Space SLR Satellite Laser Ranging SoL Safety of Life SPP Standard Point Positioning SPS Standard Positioning Service STDOUT Standard Output STDERR Standard Error SV Space Vehicle SW Software TAI International Atomic Time TBC To be Completed TBD To be Determined TEC Total Electron Content TECU Total Electron Content Unit TGD Total Group Delay ToE Time of Ephemerids ToW Time of Week TRS Terrestrial Reference System UPV Universidad Politécnica de Valencia UT Universal Time UTC Universal Coordinated Time VAL Vertical Alert Limit VLBI Very Long Base Interferometry WAAS Wide Area Augmentation System WGS84 World Geodetic System 1984 WLSQ Weighted Least Squares Chapter 7: References 7 References This chapter lists all the references used for the thesis development. The references are divided in bibliography references (publications, articles, books…) and media links (websites). Each reference includes a marker named BR or LR for a better and more concise citation along the document. 7.1 Bibliography Table 7.1 – Bibliography References. Marker Author/Reference Document Publisher Issue [BR.1] Sanz Subirana, J.; Juan Zornoza, J.M.; Hernández Pajares, M. ESA GNSS Data Processing. Vol I: Fundamentals and Algorithms. ESA Communications. 2013 [BR.2] Hoffman-Wellenhof, B.; Lichtenegger, H.; Wasle, E. GNSS Global Navigation Satellite Systems. GPS, GLONASS, Galileo and more. SpringerWienNewYork. 2008 [BR.3] Seeber G. Satellite Geodesy. Walter de Gruyter. 2003 [BR.4] Kaplan, E. D.; Hegarty, C. J. Understanding GPS. Principles and Applications. Artech House. 2006 [BR.5] Berné Valero, J. L.; Anquela Julián, A. B.; Garrido Villén, N. GNSS. GPS: Fundamentos y Aplicaciones en Geomática. Editorial UPV. 2014 [BR.6] Leick, A.; Rapoport, L.; Tatarnikov, D. GPS Satellite Surveying. Wiley. 2015 [BR.7] Toho Diessongo, H.; Bock, H.; Schüler, T.; Junker, S.; Kiroe, A.; Hein, G. H. Exploiting the Galileo E5 Wideband Signal for Improved Single-Frequency Precise Positioning. Inside GNSS. 2012 [BR.8] [BR.9] [BR.10] RINEX-V303 Moreno Monge, B. Montenbruck, O.; Steigenberger, P.; Prange, L.; Deng, Z.; Zhao, Q.; Perosanz, F.; Romero, I.; Noll, C.; Stürze, A.; Weber, G.; Schmid, R.; MacLeod, K.; Schaer, S. RINEX. The Receiver Independent Exchange Format. Version 3.03. Development of Algorithms for the GNSS data processing: their application to the Modernized GPS and Galileo Scenarios. Doctoral Thesis. The Multi-GNSS Experiment (MGEX) of the International GNSS Service (IGS) – Achievements, Prospects and Challenges International GNSS Service (IGS), RINEX Working Group and Radio Technical Commission for Maritime Services Special Committee 104 (RTCM- SC104) Universidad Complutense de Madrid. Advances in Space Research 59(7):1671-1697. 2015 2011 2017 [BR.11] Montenbruck, O.; Steigenberger, P.; Khachikyan, R.; Weber, G.; Langley, R.B.; Mervart, L.; Hugentobler, U. IGS-MGEX: Preparing the Ground for Multi-Constellation GNSS Science. Inside GNSS. 2014 [BR.12] [BR.13] [BR.14] [BR.15] [BR.16] GNSS-MR-2017 GNSS-UTR-2018 GAL-OS-IONO-SF IS-GPS-200 GAL-OS-SDD GNSS Market Report. GNSS User Technology Report. European GNSS (Galileo) Open Service - Ionospheric Correction Algorithm for Galileo Single- Frequency Users. Navstar GPS Space Segment/Navigation User Interfaces. Galileo Open Service Definition Document. European GNSS Agency. European GNSS Agency. European Commission. Global Positioning Systems Directorate. European Commission. 2017 2018 2016 2013 2016 [BR.17] GAL-OS-SIS-ICD Galileo Open Service Signal in Space Interface Control Document. European Commission. 2016 [BR.18] GPS-SPS-PS GPS Standard Positioning Service Performance Standard Global Positioning Systems Directorate. 2008 7.2 Media Links Table 7.2 – Link References. Marker Title-Link [LR.1] Navipedia - Klobuchar Ionosphere Model [LR.2] Navipedia - The SBAS Integrity Concept Standardized by ICAO. [LR.3] SOPAC Hatanaka Format. [LR.4] Wikipedia – Waterfall Model (SW Development) [LR.5] Ubuntu MATE [LR.6] Perl [LR.7] Perl Hash [LR.8] CPAN [LR.9] Gnuplot [LR.10] Chart::Gnuplot [LR.11] RTKLIB: An Open Source Program Package for GNSS Positioning [LR.12] Trimble GNSS Planner [LR.13] NOOA, Ionosphere Scintillation Chapter 8: Annexes 8 Annexes This chapter contains the project annexes. These are additional information which could not be included within the document sections. A.1 SW Tool: GRPP+GSPA Source Code Repository GRPP, GSPA and common configuration parser source code is available under Github control repository in the following hyperlink. Additionally, the following figures have been extracted from the aforementioned link. They stand for code metrics since the creation of the repository until 03/07/2019. They can be used as an information source which evidences GRPP and GSPA development and evolution. Further additions/deletions and commit details can be consulted in the previous link. Figure 8.1 – Source code contributions. Source: github.com/ppinto94/TFM-SourceCode. Figure 8.2 – Source code commits per week. Source: github.com/ppinto94/TFM-SourceCode. Figure 8.3 – Source code additions and deletions per week. Source: github.com/ppinto94/TFM-SourceCode. A.2 SW Tool: GRPP/GSPA User Configuration File The following raw text extracts show a common user configuration file which would be used as unique input for both GRPP and GSPA. Example #1 The following configuration file launches GRPP processing using GPS C/A observations for CEBR station on 13/05/2019. This file was used for the GPS C/A performance verification stage presented in section 3.3. As it can be seen, both static and integrity modes are activated and CEBR ITRF coordinates have been set as the position reference. # ========== # # CONFIGURATION FILE: # ---------- # # Inputs/Outputs: # Tool verbosity: Verbosity : TRUE # Execution label: Processing Tag : "CEBR-Demo" # Constellation selection: Satellite Systems : G # Inputs: RINEX Observation path RINEX Navigation GPS path RINEX Navigation GAL path # Outputs: GRPP Output Path GSPA Output Path Log File : /home/ppinto/WorkArea/demo/rnx/CEBR00ESP_R_20191330000_01D_30S_MO.rnx : /home/ppinto/WorkArea/demo/rnx/CEBR00ESP_R_20191330000_01D_GN.rnx : /home/ppinto/WorkArea/demo/rnx/CEBR00ESP_R_20191330000_01D_EN.rnx : : : /home/ppinto/WorkArea/demo/grpp/GPS-CA/ /home/ppinto/WorkArea/demo/gspa/GPS-CA/ /home/ppinto/WorkArea/demo/gps_ca_grpp+gspa.log # ---------- ---------- # # Processing parameters: # Time parameters: Ini Epoch [GPS] : 2019/05/13 00:00:00 End Epoch [GPS] : 2019/05/13 23:59:59 Interval [seconds] : 30 # Observations: GPS Signal Observation : C1C GAL Signal Observation : None # Observation expected precision: GPS Mean Observation Error [m] : 3.0 GAL Mean Observation Error [m] : None # Satellite mask: Satellite Mask [degrees] : 10 GPS Satellites to Discard : G04 GAL Satellites to Discard : None # Satellite Navigation: Ephemerid Time Threshold [h] : 1.7 # Error source models: Ionosphere Model GPS : Klobuchar

Ionosphere Model GAL Troposphere Model : : None Saastamoinen # Elipsoid: Elipsoid Model : wgs84 # Position estimation convergence: LSQ Maximum Number Iterations : LSQ Convergence Threshold : 3 0.0005 # ---------- # # Accuracy configuration: Vertical Sigma Scale Factor (1D) Horizontal Sigma Scale Factor (2D) : : 1.96 2.45 # Gaussian distribution critical values and associated probabilities: # +==========+==========+==========+ # | Sigma factor | Probability 1D (%) | Probability 2D (%) | # +==========+==========+==========+ # | 1.00 | 68.3 | 39.3 | -> default # +----------+----------+----------+ # | 1.96 | 95.0 | TBD | # +----------+----------+----------+ # | 2.00 | 95.4 | 86.5 | # +----------+----------+----------+ # | 2.45 | 98.6 | 95.0 | # +----------+----------+----------+ # | 3.00 | 99.7 | 98.9 | # +----------+----------+----------+ # ---------- # # Static Mode Configuration: Static Mode : TRUE Reference Mode : IGS # Reference IGS station marker name: IGS Reference Station : CEBR # Manual coordinates: Reference ECEF X, Y, Z : None # ---------- # # Intergrity Mode Configuration: Integrity Mode : TRUE Vertical Alert Limit Horizontal Alert Limit : : 30 15 # ---------- # # Data dumper configuration: # Delimiter for output files: Delimiter : "," # Data formats: Epoch Format : Angle Format : gps deg # Sigma factor for receiver position: Sigma Scale Factor : 1 # END OF CONFIGURATION FILE #

==========

Example #2 This configuration examples executes GRPP with GALILEO E1 pseudorange observations. The processing takes place on 18/12/2018 between 00:00 and 07:00 UTC for accounting fair SV availability. Also note that eccentric GALILEO SV E14 and E18 are discarded. As in the previous example, this configuration was using for launching GRPP during its validation as explained in section 3.3. Note that the configuration has set static and integrity modes setting KOKV ITRF coordinates as the position reference.

==========

CONFIGURATION FILE: # ---------- # # Inputs/Outputs: # Tool verbosity: Verbosity : TRUE # Execution identification: Processing Tag : "KOKV Demo" # Constellation selection: Satellite Systems : E # Inputs: RINEX Observation path RINEX Navigation GPS path RINEX Navigation GAL path # Outputs: GRPP Output Path GSPA Output Path Log File : /home/ppinto/WorkArea/demo/rnx/KOKV00USA_R_20183520000_01D_30S_MO.rnx : /home/ppinto/WorkArea/demo/rnx/HKSL00HKG_R_20183520000_01D_GN.rnx : /home/ppinto/WorkArea/demo/rnx/KOKV00USA_R_20183520000_01D_EN.rnx : : : /home/ppinto/WorkArea/demo/grpp/GAL-E1/ /home/ppinto/WorkArea/demo/gspa/GAL-E1/ /home/ppinto/WorkArea/demo/gal_e1_grpp+gspa.log # ---------- # # Processing parameters: # Time parameters: Ini Epoch [GPS] : 2018/12/18 00:00:01 End Epoch [GPS] : 2018/12/18 07:00:00 Interval [seconds] : 30 # Observations: GPS Signal Observation : None GAL Signal Observation : C1X # Observation expected precision: GPS Mean Observation Error [m] : None GAL Mean Observation Error [m] : 3.0 # Satellite mask: Satellite Mask [degrees] : 10 GPS Satellites to Discard : None GAL Satellites to Discard : E14, E18 # Satellite Navigation: Ephemerid Time Threshold [h] : 1.7 # Error source models: Ionosphere Model GPS : Ionosphere Model GAL : Troposphere Model : None Klobuchar Saastamoinen # Elipsoid: Elipsoid Model : wgs84 # Position estimation convergence: LSQ Maximum Number Iterations : LSQ Convergence Threshold : 3 0.0005 # ---------- # # Accuracy configuration: Vertical Sigma Scale Factor (1D) Horizontal Sigma Scale Factor (2D) : : 1.96 2.45 # Gaussian distribution critical values and associated probabilities: # +==========+==========+==========+ # | Sigma factor | Probability 1D (%) | Probability 2D (%) | # +==========+==========+==========+ # | 1.00 | 68.3 | 39.3 | -> default # +----------+----------+----------+ # | 1.96 | 95.0 | ???? | # +----------+----------+----------+ # | 2.00 | 95.4 | 86.5 | # +----------+----------+----------+ # | 2.45 | 98.6 | 95.0 | # +----------+----------+----------+ # | 3.00 | 99.7 | 98.9 | # +----------+----------+----------+ # ---------- # # Static Mode Configuration: Static Mode : TRUE Reference Mode : IGS # Reference IGS station marker name: IGS Reference Station : KOKV # Manual coordinates: Reference ECEF X, Y, Z : None # ---------- # # Intergrity Mode Configuration: Integrity Mode : TRUE Vertical Alert Limit Horizontal Alert Limit : : 30 15 # ---------- # # Data dumper configuration: # Delimiter for output files: Delimiter : "," # Data formats: Epoch Format : Angle Format : gps deg # Sigma factor for receiver position: Sigma Scale Factor : 1 # END OF CONFIGURATION FILE

==========

A.3 SW Tool: Budget Estimation Despite that the developed SW tool is intended to be open-source and free of charge, an emulation under a real commercial situation has been carried out. The purpose behind is to demonstrate that the student has gained skills for managing a SW project. From the student's own experience, the SW development budget estimation is based on the following items: • Total SW Lines of Code (LoC). • Dedicated Human Resources to the project. Note that SW companies do not require a high amount of material resources. Only computer machines, physical premises and other minor items are necessary. These are also known as the passive costs, which are added to a project's budget in order to account for the company maintenance. However, the scope of this budget will be limited to the active costs, the aforementioned items. The strategy followed to calculate the SW cost is based on the time and effort which must be dedicated by the whole team (human resources) in order to specify, implement and verify the SW. The size of the SW will be based in its overall LoC which are encompassed in Table 8.1. Table 8.1 – Developed SW LoC per module and package. SW root path Directories Module SW Lines of Code LoC LoC/Module $SRC_ROOT/ GRPP/ DataDumper.pm 2356 7225 GRPP/ ErrorSource.pm 327 MainRoutine.pl 735 NeQuickMode.pm 666 RecPosition.pm 1308 RinexReader.pm 1139 SatPosition.pm 694 GSPA/ CommonUtil.pm 129 3515 GSPA/ MainSoleService.pl 513 PlotLSQInformation.pm 523 PlotPosPerformance.pm 951 PlotSatErrorSource.pm 403 PlotSatObservation.pm 491 ReportPerformances.pm 505 lib/ Geodetic.pm 309 1081 lib/ MyMath.pm 187 MyPrint.pm 187 MyUtil.pm 196 TimeGNSS.pm 202 env/ Enviroments.pm 72 111 env/ Enviroments.sh 39 ./ GeneralConfiguration.pm

969 969 GeneralConfiguration.pm TOTAL 12901 SW For this specific case, since the product is neither critical nor real-time, its Design Assurance Level can be classified as level E (shorted as DAL-E), meaning that no security implications are caused by SW failure. This leads to assume that approximately 30 LoC per day and worker can be treated. Please note that this metric is considering the LoC treatment in all the SW lifecycle phases: specification, implementation and verification. Having more than 12K LoC implemented in the SW, this will mean that only one person would spend more than a year in developing this product (as a matter of fact he has). Consequently, 3 team players will be assigned to this project: 1 technical manager and 2 SW developer engineers. In addition, the worker's salary must be specified. This is presented in Table 8.2. The salary information has been extracted from the Spanish Engineering Companies Convention published in the Official State's Bulletin on January 2017. The social contributions and taxes impositions have been estimated. Table 8.2 – Human Resource Salary Table. Human Resources Cost Technical Manager Engineer/Developer Salary Base Salary 1 687.02 € 1 253.16 € Contract Rewards 500.00 € 400.00 € Convention Plus 144.26 € 144.26 € Number of Pays 14 14 Taxes *Contribution Base 6.35% 6.35% *IRPF 2.00% 2.00% Total Salary Gross Salary 32 637.97 € 25 163.93 € Net Salary 29 912.70 € 23 062.74 € Salary/Hour Annual Labor Hours 1800 1800 Salary/Labor Hour 16.62 € 12.81 € Finally, the total SW cost can be computed based in the total LoC and the hourly salary of each team player. This is encompassed in Table 8.3. The SW development cost is eventually estimated in approximately 54 000 €, with an industrial added benefit of the 15%. In addition, the SW would take more or less 6 months to be ready. Note that this is the cost of developing the SW. As previously mentioned, passive costs should be added, and further activities expenses such as internal/external meetings should be considered. Moreover, it has been assumed that the 2 engineers will be 100% dedicated to the code activities, whilst the manager will have assigned a 50% (hence, engineers take grater SW workload), since he/she is assumed to have client meetings, discussions and other management activities. Table 8.3 – SW tool production cost computation. SW Cost Production *DAL-E LoC rate (per day and worker) 30 Total SW LoC 12901 Work Assignment Team Player Technical Manager Engineer/Developer Engineer/Developer Num. Workers 1 1 1 Assigned Work 20.00% 40.00% 40.00% Assigned LoC 2580 5160 5160 Dedicated Hours Required Days 86 172 172 Hours/Day 8 8 8 Total Hours 688 1376 1376 Work Cost Team Player salary per hour 16.62 € 12.81 € 12.81 € Total cost per Team Player 11 434.18 € 17 631.55 € 17 631.55 € TOTAL 46 697.29 € TOTAL + Industrial Benefit (15%) 53 701.88 € A.4 SW Tool: GRPP Interface Examples This annex contains some examples of the hash interfaces designed for the developed SW tool. As a reminder, the hash-interface offers the advantage of storing the information in the machine's memory and the different modules can receive the hash reference as an input and access the data homogeneously. But, the hash-interface must be precisely defined. All hash interfaces used in GRPP and GSPA are accessible in the source code repository. Refer to annex A.1 and inspect tmp/DescriptiveICD.pl file. The file is written in Perl language and it details each interface. Nonetheless, for its understanding is necessary to be familiar with Perl programming language. If the reader is not familiarized with Perl, he/she can use the following code explanation as a guideline: # This is a comment in Perl # Perl most-used variables are classified in: # Scalar ($) -> holds any letter, number, strings and other variable references # Array (@) -> holds a list of scalars # Hash (%) -> creates a key-value pair relation of scalars # These are some examples of Perl scalar variables: my $number = 1; my $string = "Hello World"; my $decimal = 2.0; my $letter = 'c'; # These are some examples of Perl array variables: # NOTE: arrays can only contain scalars my @numbers = ($number, $decimal); my @text = ($string, $letter); my @mix = ($number, $string); # This is an example of Perl hash variable: # NOTE: key and values can only be scalar type my $hash = ($number => $string, $decimal => $letter); # Perl allows to save and access variable references (memory addresses) using the backslash'\': # NOTE: references are saved in a scalar variable my $ref_scalar = \$number; my $ref_array = \@mix; my $ref_hash = \%hash; # Perl references allow for a deeper structure definition. For instance: my %struct = (NUMBER => $number, MIX => $ref_array, ITEMS => $ref_hash, ARRAY => [0,1,2,3], HASH => {a => 'A', b => 'B'}); # Note that '[]' stand for an array reference and '{}' for a hash reference. # Consequently, hash structures can also be initialized in the following form: my $ref_struct = {}; # hash initialization $ref_struct = \%struct; # And hash content access is very straight forward: print $ref_struct->{NUMBER}; # this will print "1" print $ref_struct->{MIX}[1]; # this will print "Hello World" print $ref_struct->{ITEMS}{2.0}; # this will print "c" The following tables have been added for exemplifying the interfaces contained in the aforementioned file in a more pleasant manner. For the sake of clarity not all interface items have been kept. The examples represent: • Table 8.4 gathers hash-interface generic GRPP and GSPA configuration. • Table 8.5. Processing computed data. This is the stored data for each epoch processed with GRPP. Table 8.4 – Generic Configuration Hash-Interface Example. Generic Configuration Hash Interfac e: %gen_conf Key Points to Variable Type Nature TAG $processsing_tag Scalar Mandatory SELECTED_SAT_SYS @selected_sat_sys Array Mandatory RINEX_OBS_PATH $path_to_obs_file Scalar Mandatory RINEX_NAV_PATH %nav_rinex_paths Hash Mandatory OUTPUT_PATH %output_path_conf Hash Mandatory LOG_FILE_PATH $path_to_execution_log_file Scalar Mandatory INI_EPOCH $start_processing_epoch Scalar Mandatory END_EPOCH $end_processing_epoch Scalar Mandatory INTERVAL $processing_interval Scalar Mandatory @selected_sat_sys 0 $sat_sys Scalar Mandatory … $sat_sys Scalar Optional %nav _rinex_paths G $gps_nav_rinex_path Scalar Mandatory if 'G' in @selected_sat_sys E $gal_nav_rinex_path Scalar Mandatory if 'E' in @selected_sat_sys %output_path_conf GRPP $grpp_output_directory Scalar Mandatory GSPA $gspa_output_directory Scalar Mandatory Table 8.5 – GRPP Observation Epoch Data Hash-Interface Example. GRPP Observation Epoch Data Hash Interface: %obs_epoch Key Points to Variable Type Nature STATUS $obs_epoch_status Scalar Mandatory EPOCH $gps_epoch Scalar Mandatory NUM_SAT_INFO %num_sat_hash Hash Mandatory SAT_OBS %sat_obs_hash Hash Mandatory SAT_LOS %line_of_sight_info Hash Mandatory LSQ_INFO @lsq_info Array Mandatory SAT_POSITION %sat_xyztc Hash Mandatory REC_POSITION %position_parameters Hash Mandatory INTEGRITY_INFO %integrity_info Hash Optional %line_of_sight_info $sat_id %rec_sat_los_data Hash Mandatory … %rec_sat_los_data Hash Optional %rec_sat_los_data AZIMUT $rec_to_sat_azimut Scalar Mandatory ZENITAL $rec_to_sat_zenital Scalar Mandatory DISTANCE $rec_to_sat_distance Scalar Mandatory ELEVATION $rec_to_sat_elevation Scalar Mandatory IONO_CORR $ionosphere_los_delay Scalar Optional TROPO_CORR $troposphere_los_delay Scalar Optional ENU_VECTOR @rec_to_sat_enu_vector Array Mandatory ECEF_VECTOR @rec_to_sat_ecef_vector Array Mandatory @lsq_info 0 %iteration_info Hash Mandatory … %iteration_info Hash Optional %iteration_info STATUS $boolean_status Scalar Mandatory CONVERGENCE $boolean_status Scalar Mandatory NUM_OBSERVATION $num_obs Scalar Mandatory DEGREES_OF_FREEDOM $num_obs - $num_parameter Scalar Mandatory APX_PARAMETER @rec_parameters Array Mandatory PARAMETER_VECTOR @rec_delta_parameters Array Mandatory

SAT_RESIDUALS %sat_residuals Hash Mandatory VARIANCE_ESTIMATOR $variance_estimator Scalar Mandatory %position_parameters STATUS $boolean_status Scalar Mandatory XYZ @ecef_position Array Mandatory CLK $rec_clk_bias Scalar Mandatory VAR_XYZ @variance_ecef Array Mandatory VAR_CLK $rec_clk_variance Scalar Mandatory VAR_ENU @variance_enu Array Mandatory %integrity_info HORIZONTAL %integrity_info_domain Hash Mandatory VERTICAL %integrity_info_domain Hash Mandatory %integrity_info_domain ERROR $positioning_error Scalar Mandatory PRECISION $postioning_precision Scalar Mandatory MI_FLAG $misleading_info_flag Scalar Mandatory HMI_FLAG $hazardous_misleading_info_flag Scalar Mandatory AVAIL_FLAG $availability_boolean Scalar Mandatory A.5 Performance Campaign: Data and Results Repository From the following hyperlink a compressed .tar.gz file can be downloaded. This file archives the campaign data, configuration status and results as indicated in chapter 4. Nonetheless, the hereafter table gathers each campaign station-date-signal execution status. The rest of the information such as accuracy and integrity performances results are included in a .csv and Microsoft Excel file, which are also accessible in the aforementioned link. Table 8.6 – Campaign executions status. Station DATE_ID Date Sat Sys Signal Status Epochs Valid % Invalid % ABMF DATE_1 20/02/2019 GPS C/A ok 481 481 100.0 0 0.0 ABMF DATE_1 20/02/2019 GAL E1 ok 481 447 92.9 34 7.1 ABMF DATE_1 20/02/2019 GAL E5b ok 481 447 92.9 34 7.1 ABMF DATE_1 20/02/2019 GPS L2C ok 481 481 100.0 0 0.0 KIRU DATE_1 20/02/2019 GPS C/A ok 481 481 100.0 0 0.0 KIRU DATE_1 20/02/2019 GAL E1 ok 481 460 95.6 21 4.4 KIRU DATE_1 20/02/2019 GAL E5b ok 481 460 95.6 21 4.4 KIRU DATE_1 20/02/2019 GPS L2C ok 481 481 100.0 0 0.0 KOKV DATE_1 20/02/2019 GPS C/A ok 481 481 100.0 0 0.0 KOKV DATE_1 20/02/2019 GAL E1 ok 481 318 66.1 163 33.9 KOKV DATE_1 20/02/2019 GAL E5b ok 481 318 66.1 163 33.9 KOKV DATE_1 20/02/2019 GPS L2C ok 481 473 98.3 8 1.7 OWMG DATE_1 20/02/2019 GPS C/A ok 481 481 100.0 0 0.0 OWMG DATE_1 20/02/2019 GAL E1 ok 481 481 100.0 0 0.0 OWMG DATE_1 20/02/2019 GAL E5b ok 481 439 91.3 42 8.7 OWMG DATE_1 20/02/2019 GPS L2C ok 481 414 86.1 67 13.9 TASH DATE_1 20/02/2019 GPS C/A ok 481 481 100.0 0 0.0 TASH DATE_1 20/02/2019 GAL E1 ok 481 300 62.4 181 37.6 TASH DATE_1 20/02/2019 GAL E5b ok 481 308 64.0 173 36.0 TASH DATE_1 20/02/2019 GPS L2C ok 481 472 98.1 9 1.9 ABMF DATE_2 20/02/2019 GPS C/A ok 1620 1620 100.0 0 0.0 ABMF DATE_2 20/02/2019 GAL E1 ok 1620 1451 89.6 169 10.4 ABMF DATE_2 20/02/2019 GAL E5b ok 1620 1276 78.8 344 21.2 ABMF DATE_2 20/02/2019 GPS L2C ok 1620 1620 100.0 0 0.0 KIRU DATE_2 29/04/2019 GPS C/A ok 961 961 100.0 0 0.0 KIRU DATE_2 29/04/2019 GAL E1 ok 961 939 97.7 22 2.3 KIRU DATE_2 29/04/2019 GAL E5b ok 721 698 96.8 23 3.2 KIRU DATE_2 29/04/2019 GPS L2C ok 961 922 95.9 39 4.1 KOKV DATE_2 18/12/2018 GPS C/A ok 1081 1081 100.0 0 0.0 KOKV DATE_2 18/12/2018 GAL E1 ok 1081 835 77.2 246 22.8 KOKV DATE_2 18/12/2018 GAL E5b ok 1081 834 77.2 247 22.8 KOKV DATE_2 18/12/2018 GPS L2C ok 1081 985 91.1 96 8.9 OWMG DATE_2 26/04/2019 GPS C/A ok 1201 1201 100.0 0 0.0 OWMG DATE_2 26/04/2019 GAL E1 ok 1201 1159 96.5 42 3.5 OWMG DATE_2 26/04/2019 GAL E5b ok 1201 1109 92.3 92 7.7 OWMG DATE_2 26/04/2019 GPS L2C ok 1201 1201 100.0 0 0.0 TASH DATE_2 07/04/2019 GPS C/A ok 1201 1201 100.0 0 0.0 TASH DATE_2 07/04/2019 GAL E1 ok 1201 587 48.9 614 51.1 TASH DATE_2 07/04/2019 GAL E5b ok 1201 587 48.9 614 51.1 TASH DATE_2 07/04/2019 GPS L2C ok 1201 846 70.4 355 29.6 FAIR DATE_3 26/08/2018 GPS C/A ok 401 401 100.0 0 0.0 FAIR DATE_3 26/08/2018 GAL E1 ok 401 203 50.6 198 49.4 FAIR DATE_3 26/08/2018 GAL E5b ok 401 203 50.6 198 49.4 FAIR DATE_3 26/08/2018 GPS L2C ok 401 401 100.0 0 0.0 KIRU DATE_3 07/03/2019 GPS C/A ok 480 480 100.0 0 0.0 KIRU DATE_3 07/03/2019 GAL E1 ok 480 419 87.3 61 12.7 KIRU DATE_3 07/03/2019 GAL E5b ok 480 403 84.0 77 16.0 KIRU DATE_3 07/03/2019 GPS L2C ok 480 443 92.3 37 7.7 KOKV DATE_3 16/04/2019 GPS C/A ok 720 660 91.7 60 8.3 KOKV DATE_3 16/04/2019 GAL E1 ok 720 468 65.0 252 35.0 KOKV DATE_3 16/04/2019 GAL E5b ok 720 468 65.0 252 35.0 KOKV DATE_3 16/04/2019 GPS L2C ok 720 553 76.8 167 23.2 KOUG DATE_3 22/11/2018 GPS C/A ok 961 961 100.0 0 0.0 KOUG DATE_3 22/11/2018 GAL E1 ok 961 954 99.3 7 0.7 KOUG DATE_3 22/11/2018 GAL E5b ok 961 954 99.3 7 0.7 KOUG DATE_3 22/11/2018 GPS L2C ok 961 961 100.0 0 0.0 MAJU DATE_3 10/04/2019 GPS C/A ok 1201 1201 100.0 0 0.0 MAJU DATE_3 10/04/2019 GAL E1 discard 1201 0 0.0 1201 100.0 MAJU DATE_3 10/04/2019 GAL E5b discard 1201 0 0.0 1201 100.0 MAJU DATE_3 10/04/2019 GPS L2C ok 1201 1152 95.9 49 4.1 A.6 Performance Campaign: IGS-MGEX Stations World Map This annex contains a world map illustrating the geographical locations of the IGS-MGEX GNSS stations used for the positioning performance campaign study. If the reader is using a hard copy of the document, the world map is saved in following page. In case that a digital copy is being used, the map can be found in .pdf format under the following hyperlink. • Master’s Degree in Geomatics and Geo-information: Final Master Thesis - Pablo Pinto Santos 6 Master’s Degree in Geomatics and Geo-information: Final Master Thesis - Pablo Pinto Santos 7 Master’s Degree in Geomatics and Geo-information: Final Master Thesis - Pablo Pinto Santos 8 Master’s Degree in Geomatics and Geo-information: Final Master Thesis - Pablo Pinto Santos 9 Master’s Degree in Geomatics and Geo-information: Final Master Thesis - Pablo Pinto Santos 10 Master’s Degree in Geomatics and Geo-information: Final Master Thesis - Pablo Pinto Santos 11 Master’s Degree in Geomatics and Geo-information: Final Master Thesis - Pablo Pinto Santos 12 Master’s Degree in Geomatics and Geo-information: Final Master Thesis - Pablo Pinto Santos 13 Master’s Degree in Geomatics and Geo-information: Final Master Thesis - Pablo Pinto Santos 14 Master’s Degree in Geomatics and Geo-information: Final Master Thesis - Pablo Pinto Santos 15 Master’s Degree in Geomatics and Geo-information: Final Master Thesis - Pablo Pinto Santos 18 Master’s Degree in Geomatics and Geo-information: Final Master Thesis - Pablo Pinto Santos 19 Master’s Degree in Geomatics and Geo-information: Final Master Thesis - Pablo Pinto Santos 20 Master’s Degree in Geomatics and Geo-information: Final Master Thesis - Pablo Pinto Santos 21 Master’s Degree in Geomatics and Geo-information: Final Master Thesis - Pablo Pinto Santos 22 Master’s Degree in Geomatics and Geo-information: Final Master Thesis - Pablo Pinto Santos 24 Master’s Degree in Geomatics and Geo-information: Final Master Thesis - Pablo Pinto Santos 25 Master’s Degree in Geomatics and Geo-information: Final Master Thesis - Pablo Pinto Santos 26 Master’s Degree in Geomatics and Geo-information: Final Master Thesis - Pablo Pinto Santos 27 Master’s Degree in Geomatics and Geo-information: Final Master Thesis - Pablo Pinto Santos 28 Master’s Degree in Geomatics and Geo-information: Final Master Thesis - Pablo Pinto Santos 29 Master’s Degree in Geomatics and Geo-information: Final Master Thesis - Pablo Pinto Santos 30 Master’s Degree in Geomatics and Geo-information: Final Master Thesis - Pablo Pinto Santos 31 Master’s Degree in Geomatics and Geo-information: Final Master Thesis - Pablo Pinto Santos 32 Master’s Degree in Geomatics and Geo-information: Final Master Thesis - Pablo Pinto Santos 33 Master’s Degree in Geomatics and Geo-information: Final Master Thesis - Pablo Pinto Santos 34 Master’s Degree in Geomatics and Geo-information: Final Master Thesis - Pablo Pinto Santos 35 Master’s Degree in Geomatics and Geo-information: Final Master Thesis - Pablo Pinto Santos 36 Master’s Degree in

Geomatics and Geo-information: Final Master Thesis - Pablo Pinto Santos 37 Master's Degree in
Geomatics and Geo-information: Final Master Thesis - Pablo Pinto Santos 38 Master's Degree in
Geomatics and Geo-information: Final Master Thesis - Pablo Pinto Santos 39 Master's Degree in
Geomatics and Geo-information: Final Master Thesis - Pablo Pinto Santos 40 Master's Degree in
Geomatics and Geo-information: Final Master Thesis - Pablo Pinto Santos 41 Master's Degree in
Geomatics and Geo-information: Final Master Thesis - Pablo Pinto Santos 42 Master's Degree in
Geomatics and Geo-information: Final Master Thesis - Pablo Pinto Santos 43 Master's Degree in
Geomatics and Geo-information: Final Master Thesis - Pablo Pinto Santos 44 Master's Degree in
Geomatics and Geo-information: Final Master Thesis - Pablo Pinto Santos 45 Master's Degree in
Geomatics and Geo-information: Final Master Thesis - Pablo Pinto Santos 46 Master's Degree in
Geomatics and Geo-information: Final Master Thesis - Pablo Pinto Santos 47 Master's Degree in
Geomatics and Geo-information: Final Master Thesis - Pablo Pinto Santos 48 Master's Degree in
Geomatics and Geo-information: Final Master Thesis - Pablo Pinto Santos 49 50 Master's Degree in
Geomatics and Geo-information: Final Master Thesis - Pablo Pinto Santos 51 Master's Degree in
Geomatics and Geo-information: Final Master Thesis - Pablo Pinto Santos 52 Master's Degree in
Geomatics and Geo-information: Final Master Thesis - Pablo Pinto Santos 53 Master's Degree in
Geomatics and Geo-information: Final Master Thesis - Pablo Pinto Santos 54 Master's Degree in
Geomatics and Geo-information: Final Master Thesis - Pablo Pinto Santos 55 Master's Degree in
Geomatics and Geo-information: Final Master Thesis - Pablo Pinto Santos 56 Master's Degree in
Geomatics and Geo-information: Final Master Thesis - Pablo Pinto Santos 57 Master's Degree in
Geomatics and Geo-information: Final Master Thesis - Pablo Pinto Santos 58 Master's Degree in
Geomatics and Geo-information: Final Master Thesis - Pablo Pinto Santos 59 Master's Degree in
Geomatics and Geo-information: Final Master Thesis - Pablo Pinto Santos 60 Master's Degree in
Geomatics and Geo-information: Final Master Thesis - Pablo Pinto Santos 61 Master's Degree in
Geomatics and Geo-information: Final Master Thesis - Pablo Pinto Santos 64 Master's Degree in
Geomatics and Geo-information: Final Master Thesis - Pablo Pinto Santos 65 Master's Degree in
Geomatics and Geo-information: Final Master Thesis - Pablo Pinto Santos 66 Master's Degree in
Geomatics and Geo-information: Final Master Thesis - Pablo Pinto Santos 67 Master's Degree in
Geomatics and Geo-information: Final Master Thesis - Pablo Pinto Santos 68 Master's Degree in
Geomatics and Geo-information: Final Master Thesis - Pablo Pinto Santos 69 Master's Degree in
Geomatics and Geo-information: Final Master Thesis - Pablo Pinto Santos 70 Master's Degree in
Geomatics and Geo-information: Final Master Thesis - Pablo Pinto Santos 71 Master's Degree in
Geomatics and Geo-information: Final Master Thesis - Pablo Pinto Santos 72 Master's Degree in
Geomatics and Geo-information: Final Master Thesis - Pablo Pinto Santos 73 Master's Degree in
Geomatics and Geo-information: Final Master Thesis - Pablo Pinto Santos 74 Master's Degree in
Geomatics and Geo-information: Final Master Thesis - Pablo Pinto Santos 75 Master's Degree in
Geomatics and Geo-information: Final Master Thesis - Pablo Pinto Santos 76 Master's Degree in
Geomatics and Geo-information: Final Master Thesis - Pablo Pinto Santos 77 Master's Degree in
Geomatics and Geo-information: Final Master Thesis - Pablo Pinto Santos 78 Master's Degree in
Geomatics and Geo-information: Final Master Thesis - Pablo Pinto Santos 79 Master's Degree in
Geomatics and Geo-information: Final Master Thesis - Pablo Pinto Santos 80 Master's Degree in
Geomatics and Geo-information: Final Master Thesis - Pablo Pinto Santos 81 Master's Degree in
Geomatics and Geo-information: Final Master Thesis - Pablo Pinto Santos 82 Master's Degree in
Geomatics and Geo-information: Final Master Thesis - Pablo Pinto Santos 83 Master's Degree in
Geomatics and Geo-information: Final Master Thesis - Pablo Pinto Santos 84 Master's Degree in
Geomatics and Geo-information: Final Master Thesis - Pablo Pinto Santos 85 Master's Degree in
Geomatics and Geo-information: Final Master Thesis - Pablo Pinto Santos 86 Master's Degree in
Geomatics and Geo-information: Final Master Thesis - Pablo Pinto Santos 87 Master's Degree in
Geomatics and Geo-information: Final Master Thesis - Pablo Pinto Santos 88 Master's Degree in
Geomatics and Geo-information: Final Master Thesis - Pablo Pinto Santos 89 Master's Degree in
Geomatics and Geo-information: Final Master Thesis - Pablo Pinto Santos 90 Master's Degree in
Geomatics and Geo-information: Final Master Thesis - Pablo Pinto Santos 91 Master's Degree in
Geomatics and Geo-information: Final Master Thesis - Pablo Pinto Santos 92 Master's Degree in
Geomatics and Geo-information: Final Master Thesis - Pablo Pinto Santos 93 Master's Degree in
Geomatics and Geo-information: Final Master Thesis - Pablo Pinto Santos 94 Master's Degree in
Geomatics and Geo-information: Final Master Thesis - Pablo Pinto Santos 95 Master's Degree in
Geomatics and Geo-information: Final Master Thesis - Pablo Pinto Santos 96 Master's Degree in
Geomatics and Geo-information: Final Master Thesis - Pablo Pinto Santos 97 Master's Degree in
Geomatics and Geo-information: Final Master Thesis - Pablo Pinto Santos 98 Master's Degree in
Geomatics and Geo-information: Final Master Thesis - Pablo Pinto Santos 100 Master's Degree in
Geomatics and Geo-information: Final Master Thesis - Pablo Pinto Santos 101 Master's Degree in
Geomatics and Geo-information: Final Master Thesis - Pablo Pinto Santos 102 Master's Degree in
Geomatics and Geo-information: Final Master Thesis - Pablo Pinto Santos 103 Master's Degree in
Geomatics and Geo-information: Final Master Thesis - Pablo Pinto Santos 104 Master's Degree in
Geomatics and Geo-information: Final Master Thesis - Pablo Pinto Santos 105 Master's Degree in
Geomatics and Geo-information: Final Master Thesis - Pablo Pinto Santos 106 Master's Degree in
Geomatics and Geo-information: Final Master Thesis - Pablo Pinto Santos 107 Master's Degree in
Geomatics and Geo-information: Final Master Thesis - Pablo Pinto Santos 108 Master's Degree in
Geomatics and Geo-information: Final Master Thesis - Pablo Pinto Santos 109 Master's Degree in
Geomatics and Geo-information: Final Master Thesis - Pablo Pinto Santos 110 Master's Degree in
Geomatics and Geo-information: Final Master Thesis - Pablo Pinto Santos 111 Master's Degree in
Geomatics and Geo-information: Final Master Thesis - Pablo Pinto Santos 112 Master's Degree in
Geomatics and Geo-information: Final Master Thesis - Pablo Pinto Santos 113 Master's Degree in
Geomatics and Geo-information: Final Master Thesis - Pablo Pinto Santos 114 Master's Degree in
Geomatics and Geo-information: Final Master Thesis - Pablo Pinto Santos 115 Master's Degree in
Geomatics and Geo-information: Final Master Thesis - Pablo Pinto Santos 116 Master's Degree in
Geomatics and Geo-information: Final Master Thesis - Pablo Pinto Santos 117 Master's Degree in
Geomatics and Geo-information: Final Master Thesis - Pablo Pinto Santos 118 Master's Degree in
Geomatics and Geo-information: Final Master Thesis - Pablo Pinto Santos 119 Master's Degree in
Geomatics and Geo-information: Final Master Thesis - Pablo Pinto Santos 120 Master's Degree in
Geomatics and Geo-information: Final Master Thesis - Pablo Pinto Santos 121 Master's Degree in
Geomatics and Geo-information: Final Master Thesis - Pablo Pinto Santos 122 Master's Degree in

Geomatics and Geo-information: Final Master Thesis - Pablo Pinto Santos 123 Master's Degree in
Geomatics and Geo-information: Final Master Thesis - Pablo Pinto Santos 124 Master's Degree in
Geomatics and Geo-information: Final Master Thesis - Pablo Pinto Santos 125 Master's Degree in
Geomatics and Geo-information: Final Master Thesis - Pablo Pinto Santos 126 Master's Degree in
Geomatics and Geo-information: Final Master Thesis - Pablo Pinto Santos 128 Master's Degree in
Geomatics and Geo-information: Final Master Thesis - Pablo Pinto Santos 129 Master's Degree in
Geomatics and Geo-information: Final Master Thesis - Pablo Pinto Santos 130 Master's Degree in
Geomatics and Geo-information: Final Master Thesis - Pablo Pinto Santos 131 Master's Degree in
Geomatics and Geo-information: Final Master Thesis - Pablo Pinto Santos 132 Master's Degree in
Geomatics and Geo-information: Final Master Thesis - Pablo Pinto Santos 133 Master's Degree in
Geomatics and Geo-information: Final Master Thesis - Pablo Pinto Santos 134 Master's Degree in
Geomatics and Geo-information: Final Master Thesis - Pablo Pinto Santos 135 Master's Degree in
Geomatics and Geo-information: Final Master Thesis - Pablo Pinto Santos 136 Master's Degree in
Geomatics and Geo-information: Final Master Thesis - Pablo Pinto Santos 137 Master's Degree in
Geomatics and Geo-information: Final Master Thesis - Pablo Pinto Santos 140 Master's Degree in
Geomatics and Geo-information: Final Master Thesis - Pablo Pinto Santos 141 Master's Degree in
Geomatics and Geo-information: Final Master Thesis - Pablo Pinto Santos 142 Master's Degree in
Geomatics and Geo-information: Final Master Thesis - Pablo Pinto Santos 144 Master's Degree in
Geomatics and Geo-information: Final Master Thesis - Pablo Pinto Santos 145 Master's Degree in
Geomatics and Geo-information: Final Master Thesis - Pablo Pinto Santos 148 Master's Degree in
Geomatics and Geo-information: Final Master Thesis - Pablo Pinto Santos 149 Master's Degree in
Geomatics and Geo-information: Final Master Thesis - Pablo Pinto Santos 150 Master's Degree in
Geomatics and Geo-information: Final Master Thesis - Pablo Pinto Santos 151 Master's Degree in
Geomatics and Geo-information: Final Master Thesis - Pablo Pinto Santos 152 Master's Degree in
Geomatics and Geo-information: Final Master Thesis - Pablo Pinto Santos 153 Master's Degree in
Geomatics and Geo-information: Final Master Thesis - Pablo Pinto Santos 154 Master's Degree in
Geomatics and Geo-information: Final Master Thesis - Pablo Pinto Santos 155 Master's Degree in
Geomatics and Geo-information: Final Master Thesis - Pablo Pinto Santos 156 Master's Degree in
Geomatics and Geo-information: Final Master Thesis - Pablo Pinto Santos 157 Master's Degree in
Geomatics and Geo-information: Final Master Thesis - Pablo Pinto Santos 158 Master's Degree in
Geomatics and Geo-information: Final Master Thesis - Pablo Pinto Santos 159 Master's Degree in
Geomatics and Geo-information: Final Master Thesis - Pablo Pinto Santos 160 Master's Degree in
Geomatics and Geo-information: Final Master Thesis - Pablo Pinto Santos 161 Master's Degree in
Geomatics and Geo-information: Final Master Thesis - Pablo Pinto Santos 162 Master's Degree in
Geomatics and Geo-information: Final Master Thesis - Pablo Pinto Santos 163